SYNTHESIS AND CHARACTERIZATION OF WHOLLY AROMATIC SEMICRYSTALLINE POLYIMIDES BASED UPON BIS(4-AMINOPHENOXY) BENZENES

by

Marvin Jerome Graham

Dissertation submitted to the Faculty of the

Virginia Polytechnic Institute and State University

in partial fulfillment of the requirements for the degree of

DOCTOR OF PHILOSOPHY

in

Chemistry

APPROVED

Dr. J. E. McGrath, Chairman

Dr. H. W. Gibson

Dr. J. S. Riffle

Dr. T. C. Ward

Dr. J. F. Wolfe

January, 1999

Blacksburg, Virginia

Synthesis and Characterization of Semicrystalline Wholly Aromatic Polyimides Based Upon Bis(4-aminophenoxy)benzenes

by

Marvin J. Graham

Abstract

Semicrystalline thermoplastic polyimides based upon bis(4-aminophenoxy)benzene and related "triphenyl ether" diamines were synthesized via the classical two step amic acid route. More specifically, polyimides were derived from para linked 1,4-bis(4-aminophenoxy)benzene, or TPEQ (triphenyl ether diamine- hydroquinone) and its meta isomer 1,3-bis(4-aminophenoxy)benzene, or TPER (triphenyl ether diamine-resorcinol). The reaction of these diamines with rigid or semi-rigid dianhydrides such as pyromellitic dianhydride (PMDA), biphenyl dianhydride (BPDA), and oxydiphthalic anhydride (ODPA) yields very thermally stable semi-crystalline polymers which have excellent resistance to organic liquids. Amorphous polyimides could be derived from hexafluoroisopropylidene-linked diphthalic anhydride (6FDA), but these systems were not extensively investigated. Importantly, molecular weight characterization of the semicrystalline systems at the soluble amic acid stage was successful by employing hydrodynamic volume calibrated, viscosity detector size exclusion chromatography (SEC). The experimental values were found to be within the targeted $<M_n>$ range of 20-30,000 g/mole. Polyimide powders derived from these ether diamines were prepared by solution imidization at 180°C, to afford about 70% imidized structures as judged by dynamic thermal gravimetric analysis (TGA), before crystallization/precipitation occurred. Relatively small particle sizes ranging from 2 to 25 μm in size were generated, which would be appropriate for thermoplastic polymer matrix composites prepared by powder processing. All specimens showed excellent thermooxidative stability, consistent with the aromatic imide structure.

The molecular design of the aromatic polyetherimide repeat unit was critical for the successful utilization of these semicrystalline high performance materials. The meta-linked TPER system when combined with the thermally stable s-biphenyl dianhydride (BPDA) produced a melting endotherm, T_m, at about 395°C, which was well within the thermal stability limitations of organic materials, i.e., less than or approximately 450°C. It was also demonstrated to be important to quantitatively endcap both ends of the chains at about 20-30,000 $<M_n>$ with non-reactive phthalimide groups to achieve appropriate melt viscosities and good melt stability. This was done by off-setting the stoichiometry in favor of the diamine, reacting with a calculated amount of phthalic anhydride and imidizing in bulk above the T_g (≈210°C) at 300°C. These considerations allowed for remarkable melt stability in nitrogen at 430°C for at least 45 minutes, and importantly, repeated recrystallizations from the melt to afford tough, ductile semicrystalline films with excellent solvent resistance. If the macromolecular chains were not properly endcapped, it was demonstrated that viscosity increased rapidly at 430°C, suggesting reactions such as transimidization involving terminal amine end groups with in-chain imide segments and/or other side reactions, which quickly inhibited recrystallization, probably by reducing molecular transport processes.

In contrast, polyimides based upon the more rigid para-linked TPEQ did not demonstrate melt or flow characteristics below 400°C, and degraded around the T_m at about 470°C! The less thermally stable TPEQ-ODPA based polyimide did melt around 409°C, and lower molecular weight samples, e.g., 10,000 M_n, recrystallized from the melt after short melt times, but cast films were brittle. It was hypothesized that the weak link may be the relatively electron rich arylene ether bond derived from the ODPA dianhydride.

Several alkylated derivatives of TPER were synthesized in good yield by the reactions of alkylated resorcinol precursors with p-fluoronitrobenzene to produce dinitro compounds, which were subsequently reduced. These model diamines were then used to synthesize polyimides by the classical two step route. As expected, few of the polyimides derived from BPDA and these diamines displayed melting transitions (T_m), probably because of poor chain packing. However, they could have potential as new thermally stable membrane materials. Several amorphous polyimides prepared from 1,3-bis(p-

aminophenoxy)-4-hexylbenzene were soluble in selected common organic solvents and could be cast into flexible films.

Keywords: Melt Stable Semicrystalline Poly(arylene ether imides), End Capping, Solvent Resistance, Bis(4-Aminophenoxy Benzene)

Acknowledgments

I would like to thank Dr. James E. McGrath for his efforts as my research advisor. The experience I had under him in the summer of 1992 was a major reason that I chose VPI, and his belief in me to be successful was also much appreciated.

I would also like to thank Dr. Garth L. Wilkes, Dr. Judy S. Riffle, Dr. Harry W. Gibson, Dr. T. C. Ward, Dr. J. F. Wolfe, and Dr. Neal Castagnoli for serving as members of my committee. I would like to thank Dr. Richey Davis for graciously allowing me the use of his laboratory facilities. In addition, I would like to thank Dr. Rich Gandour for his advice and interactions.

I would very much like to thank Dr. Srivatsan Srinivas for his collaboration with me and for his extensive thermal analysis in this research. Likewise I thank Slade Gardner for his rheological testing and discussion. I also would thank Varun Ratta for some later work on his behalf.

I would like to acknowledge all those in the chemistry department. Specifically, I thank Tom Glass for his aid in using the NMR facilities and Kim Harich for his mass spectrometry efforts.

I would also like to acknowledge the NSF secretarial staff of Laurie Good, Millie Ryan, Esther Brann, and Joyce Moser for their assistance and levity during my stay at VPI.

I would like to thank Dr. Saikumar Jayaraman and Dr. Stan Prybla for inviting me to work with them for a summer at BF Goodrich.

I wish to thank all those students and postdoctoral associates whom I have interacted in among the McGrath group. Among those are Dr. Martin Rogers, who served as my mentor during my SURP experience, Dr. Heather Brink, whose research efforts preceded my own, Drs. Limin Dong and Qing Ji, whose prowess in GPC is well established, and Dr. Amba Ayambem, who took over much of the research that I initiated. I would also like to thank Biao Tan, Dan Riley, Charles Tchatchoua, and Isaac Farr for their assistance.

I would like to thank my family for the support that they have given to me during my graduate studies.

Last, but definitely not least, I would like to thank God, by whom all things are possible.

Table of Contents

List of Figures

List of Tables

List of Schemes

Chapter 1: Introduction

Aromatic polyimides have enjoyed enormous acclaim and success as high performance polymeric materials. These polymers are distinguished by their extraordinary thermooxidative stability and excellent mechanical and electrical properties. As a result, polyimides have been widely employed as coatings, adhesives, and composite matrix resins in areas such as aerospace and electronics. While the original polyimides suffered through a multitude of problems, technological advances have been made in the field which have facilitated the use of these materials in the aforementioned industries as well as a number of other enterprises.

New diamine and dianhydride monomers have been steadily identified which have permitted the synthesis of polyimides of dramatically enhanced solubility and processability. The design of these monomers was such that flexible bridging groups, large side groups, or asymmetrical linkages would be encountered along the backbone of the largely aromatic polyimides. The transition temperatures of these polyimides were usually lowered as a result of such architectures, and these modifications were accomplished at the expense of the chemical and solvent resistance.

Semicrystalline thermoplastic polyimide materials can serve as a solution to the problem of poor solvent resistance. The development of a number of commercially available semicrystalline thermoplastics such as poly(ether ether ketone) (PEEK) would suggest success in the employment of semicrystalline polyimides. These polymers innately possess high levels of chemical and solvent resistance due to the presence of "physical" crosslinks as provided by the crystalline structure. In addition, the thermoplastic nature of these polyimides allows for rapid and sometimes repeatable processing. The semi-crystalline morphology and resultant solvent resistance can be problematic as far as synthesis and processing are concerned, yet the use of the two step route and the development of more recent technologies like powder prepregging can be adapted for successful exploitation. A drawback to these materials is that they frequently have high transition temperatures, sometimes approaching the onset of chemical or physical decomposition.

The research presented in this dissertation is concentrated on the synthesis and characterization of semicrystalline polyimides. More specifically, the polyimides of interest are derived from the isomeric ether diamines 1,3- and 1,4-bis(4-aminophenoxy)benzene, referred to henceforth as TPER and TPEQ, respectively.

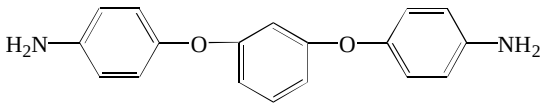

TPER

TPEQ

It has been established that the incorporation of flexible ether groups into the polyimide backbone can translate into reduced, but still attractive transition temperatures as well as tougher polymeric materials. The classical "two-step" polymerization method was employed to produce controlled molecular weight, phthalimide-endcapped polyimides. Both thermal and solution imidization techniques were utilized for cyclizing the polyamic acid to the end product. The polyimide powders synthesized by solution imidization techniques have been characterized by particle size and thermal analyses. More detailed thermal analyses were performed on selected samples prepared by thermal imidization. In addition, the degree of imidization is characterized for partially imidized polyimide powders prepared by the solution imidization technique.

A study involving the effect of endcapping on the melt stability of a TPER-based polyimide was undertaken. This involved the synthesis of amine, phthalimide ,and "partially" phthalimide polyimides of controlled molecular weights. These polyimides were subjected to similar melt treatments and thermal analyses in order to gauge the stabilities of the polymers to chemical and physical changes.

Novel diamines analogous to TPER were synthesized using alkylresorcinols as starting materials. Coupling these resorcinols with fluoronitrobenzene yields dinitro compounds which are readily reduced to the corresponding diamines. The diamines were subsequently polymerized to produce a series of polyimides. These polyimides were subjected to thermal analysis and solubility tests when applicable.

Among the areas of discussion in this dissertation is a literature review focusing on polyimide synthesis, molecular weight control, polyimide properties, semicrystalline polyimides, and alkylated polyimides. Following this review is a summary of the

experiments and analyses utilized in this research. The discussion of the results from this work is given, followed by the conclusions that were made concerning the research.

Chapter 2: Literature Review

2.1 Introduction

In the latter half of this century, there has been tremendous interest in the field of high performance polymers, and in particular, polyimides. These polymers consist primarily of in-chain heterocyclic imide functionalities that are usually obtained from the reaction of organic diamines with dianhydrides.

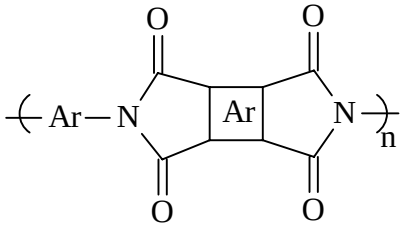

The interest in these materials stems primarily from their excellent thermal, mechanical, and electrical properties. In fact, the subject of polyimides has been extensively investigated throughout the literature.[1-8]

Although not intended to present a comprehensive review of the polyimide literature, this review will serve as a backdrop to the topics that will be discussed in the remainder of this dissertation. The initial part of this review will deal with methods of synthesizing polyimides and some important characterization methodologies. The next section will briefly discuss some aspects of polyimide molecular structure and how it relates to physical properties. The remaining sections will review some of the recent developments in semicrystalline polyimides, as well as pendant-alkyl containing polyimides.

2.2 Polyimide Synthesis

The first report of a polyimide in the literature arose from the work of Bogert and Renshaw.[9] They discovered that 4-aminophthalic anhydride self condensed to give an intractable polymeric material. Similarly, Brandt found out that upon reduction of 4-nitrophthalic anhydride an oligomeric substance is formed by the reaction of the nitro compound with the amine reduction product.[10]

Despite this early work, it was the efforts of Edwards and Robinson that sparked the belief that polyimides could be developed into viable commercial materials.[11-13] Their research focused on the reaction of aliphatic diamines with pyromellitic dianhydride (PMDA) using nylon salt-type chemistry to form insoluble yet melt processable polyimides. The subsequent use of aromatic diamines with PMDA would eventually lead to the development of the classical two-step route for synthesizing polyimides, the most noteworthy being DuPont's Kapton (Figure 2.2).[14-18] The two-step process was usually required because the final imide form was not sufficiently processable. Numerous other polyimide systems have evolved from this work, as well as different methods for successfully synthesizing these materials.

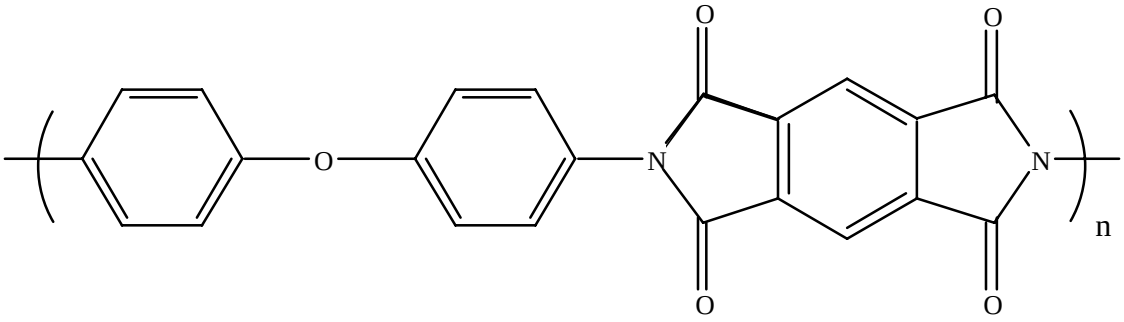

Figure 2.2: Chemical Repeat Unit of Kapton

2.2.1 Classical two-step polyimide synthesis

2.2.1.1 Polyamic acid synthesis

Aromatic polyimides are most commonly prepared via a two-step synthetic route. The first step involves the reaction of an aromatic diamine with an aromatic dianhydride to

form a polyamic acid. The polyamic acid can then undergo a cyclodehydration by thermally or chemically-mediated means to produce the polyimide shown in Scheme 2.2.1.1.1.

The formation of polyamic acid is accomplished via a low or ambient temperature nucleophilic substitution reaction of an aromatic diamine with an aromatic dianhydride, a proposed mechanism of which is shown in Scheme 2.2.1.1.2.[19-21] Amine attack of an anhydride carbonyl group occurs, followed by equilibration to an ionic ring-opened species in which the displaced carboxylate moiety is chemically attached to the product. Further equilibration yields the polyamic acid. Reverse reaction to the carboxylate is usually suppressed by the use of polar aprotic solvents such as N-methyl-pyrrolidone (NMP) or dimethylacetamide (DMAC). These solvents serve to effectively hydrogen bond to the amic acid, rendering the acid protons inert to transport to the amide group (Scheme 2.2.1.1.3).[22,23]

It has been recognized that the structure of the dianhydride has an influence on the rate of formation and stability of the polyamic acid, which is related to the dianhydride's ability to function as an electron acceptor.[24] Specifically, the reaction rate and facility increase proportionately with the electron affinity of the dianhydride. Some electron affinities are shown in Table 2.2.1.1.1. The dianhydrides that have strongly electron-withdrawing bridging groups are, in general, more reactive than those with electron-donating groups.

The reactivity of diamines in polyamic acid synthesis has been correlated to the basicities of the diamines.[25,26] It was demonstrated that for various diamines reacted with PMDA and benzophenone tetracarboxylic dianhydride (BTDA), faster reaction rates occurred with diamines of increased basicity. Examples of this tendency are shown in Table 2.2.1.1.2. Ando and coworkers have utilized ^{15}N NMR to characterize the electronic properties of various diamines,[27] and the chemical shift values of these diamines are shown in Table 2.2.1.1.3. The occurrence of lower chemical shifts correlates with the greater nucleophilicity and, thus, greater reactivity of those particular diamines.

As was expressed earlier, polyamic acid is usually prepared at low or ambient temperatures. The formation of polyamic acid is an exothermic reaction, so lowering the

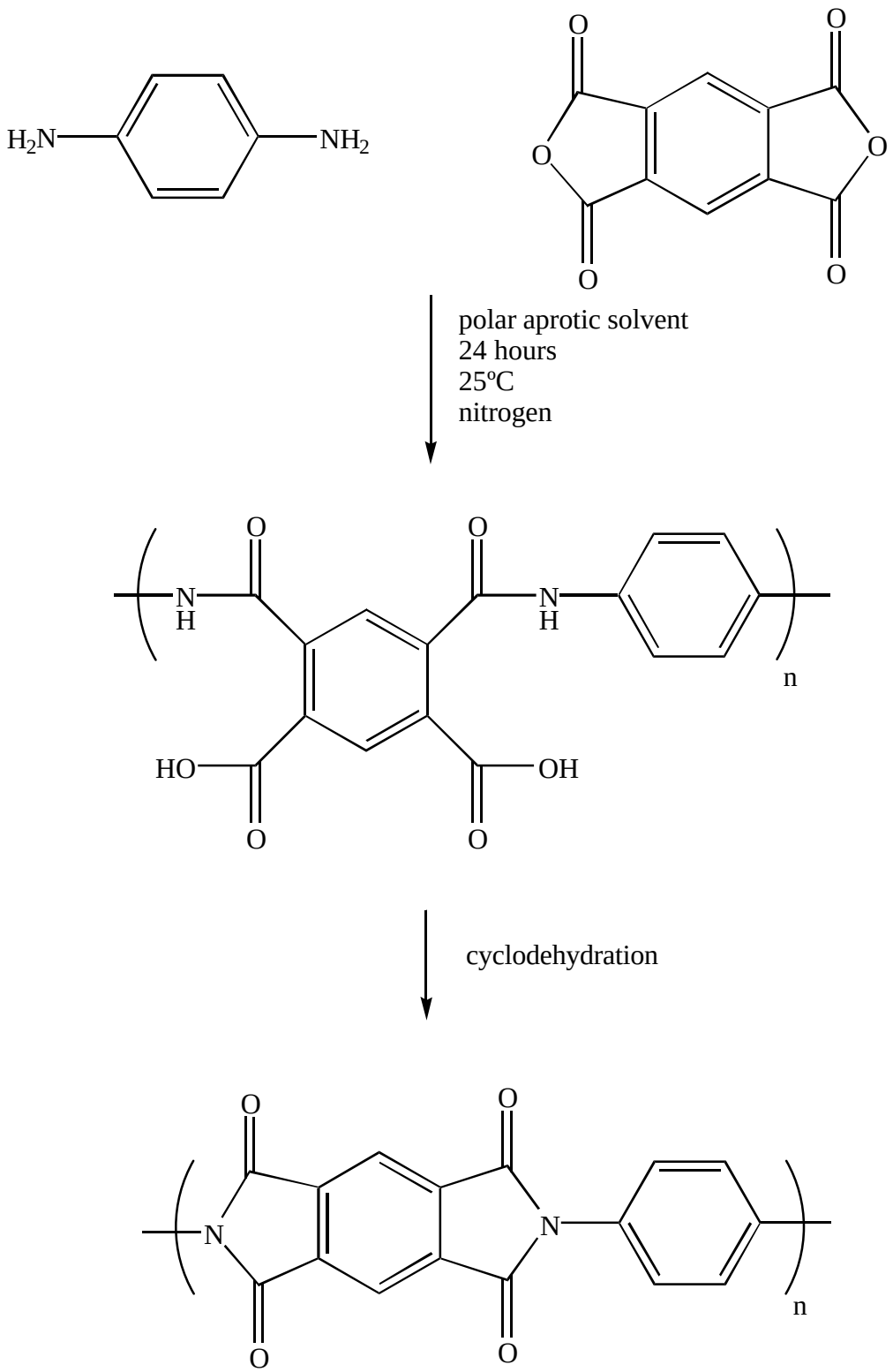

Scheme 2.2.1.1.1: Classical Two-Step Polyimide Synthesis

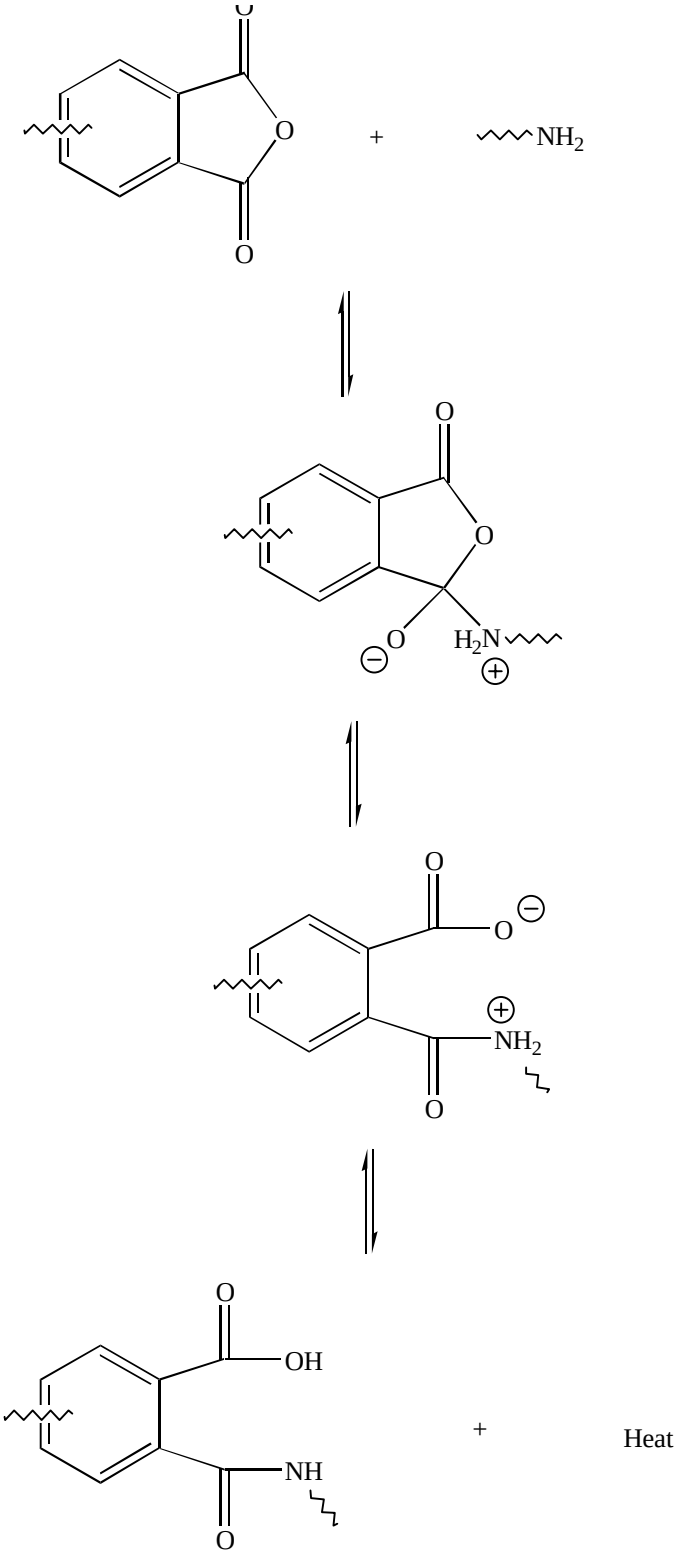

Scheme 2.2.1.1.2: Proposed Mechanism for Polyamic Acid Formation [19-21]

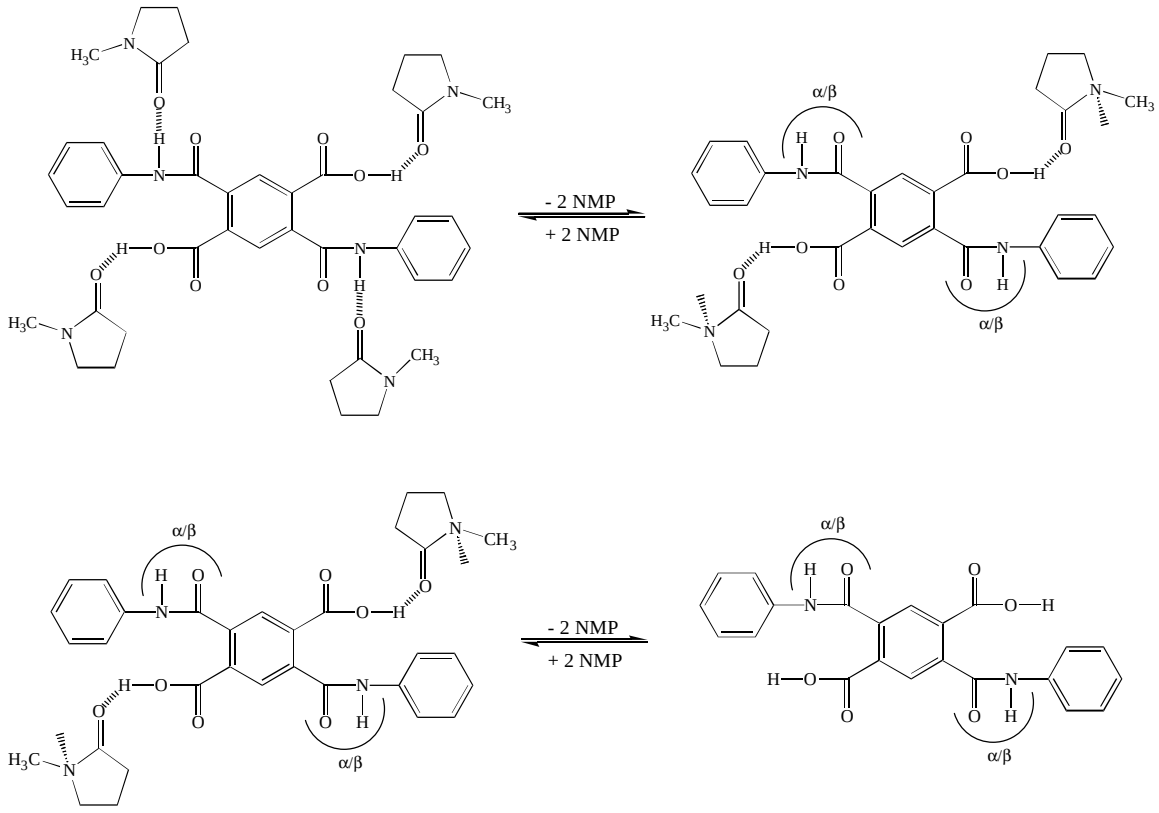

Scheme 2.2.1.1.3: Proposed NMP Solvent Complexation of Polyamic Acids[22,23]

Table 2.2.1.1.1: Electron Affinities of Selected Dianhydrides[4]

Dianhydride	Abbreviation	EA (eV)
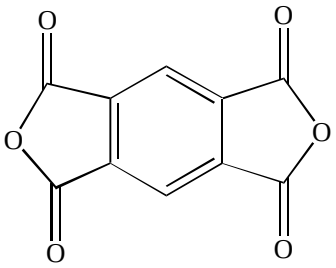	PMDA	1.90
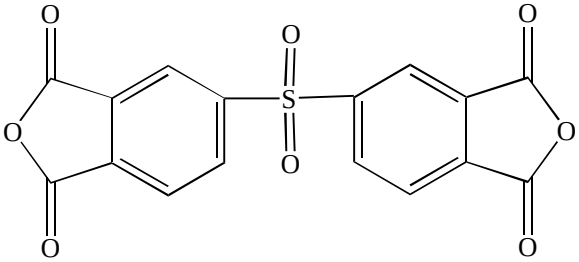	DSDA	1.57
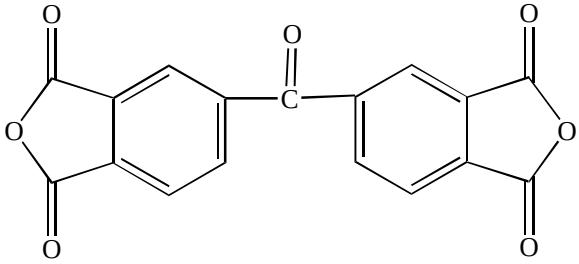	BTDA	1.55
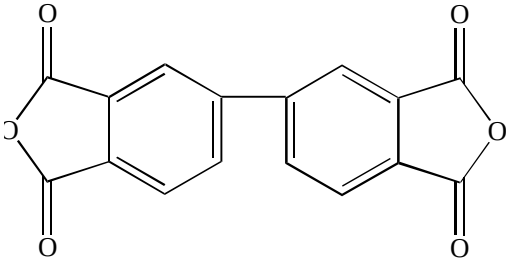	BPDA	1.38
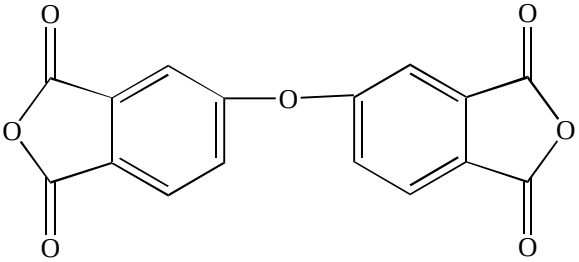	ODPA	1.30

Table 2.2.1.1.2: pK_a and Rate Constant Data of Selected Diamines for Reactions with PMDA and BTDA[4]

Diamine	pK_1 (H_2O)	PMDA k (l mol^{-1} sec^{-1})	BTDA k (l mol^{-1} sec^{-1})
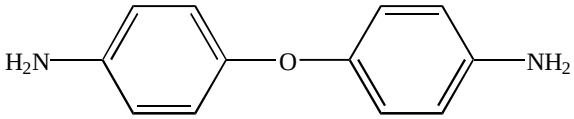	5.20	5.97	3.09
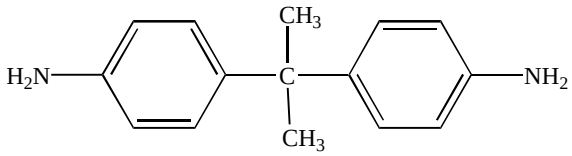		4.23	2.57
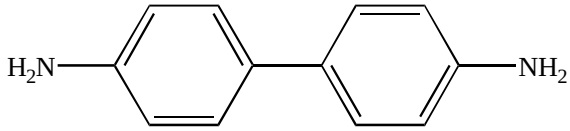	4.60	2.33	1.34
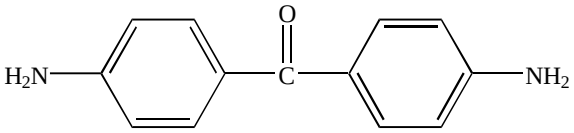	3.10	0.0074	-
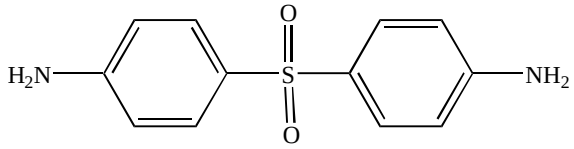	2.15	0.0022	0.0023

Table 2.2.1.1.3: ^{15}N NMR Chemical Shifts of Selected Diamines[27]

Diamine	Abbreviation	^{15}N Chemical Shift (ppm)
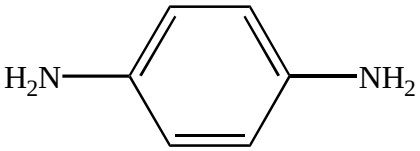	*p*-PD	53.8
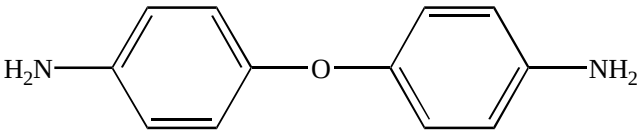	4,4'-ODA	57.9
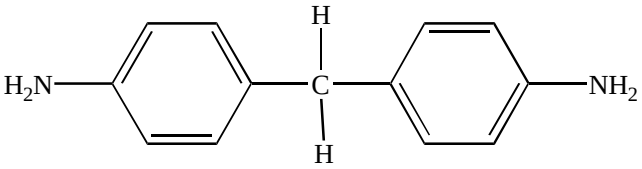	MDA	59.4
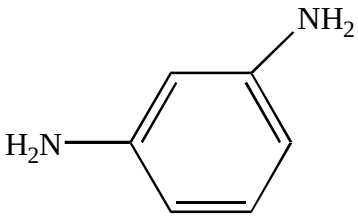	*m*-PD	60.8
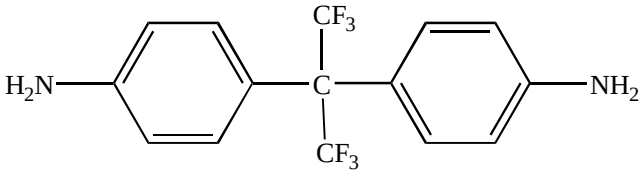	6F diamine	64.0
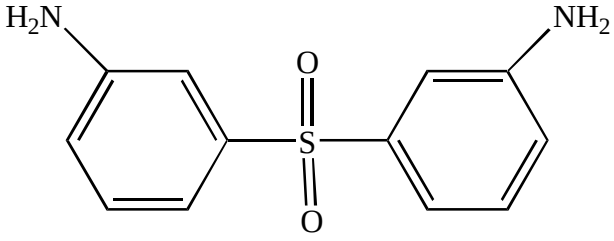	*m*-DDS	65.7

reaction temperature helps to drive the equilibrium process to favor the amic acid product. However, the use of polar aprotic solvents facilitates the reaction so that successful polymerization is achieved in ambient conditions. The presence of heat will drive the equilibration to the left, resulting in decreased molecular weight. In addition, synthesizing the polyamic acid at higher temperatures can lead to premature cyclization. This can result in reduced molecular weight due either to subsequent hydrolysis by water that is liberated upon cyclization,[19] or by precipitation of insoluble product of low molecular weight.[28]

Other reaction conditions such as monomer concentration or the order of monomer addition can impact on polyamic acid molecular weight. In general, dilute solutions of amic acids are less stable than more concentrated solutions.[1] This may be attributable to the presence of water or other impurities introduced by larger proportions of solvent, which could result in hydrolysis. Early reports suggested that high molecular weight polymer could only be achieved by the addition of solid dianhydride to a diamine solution.[29] More recently Volksen and Cotts reported that theoretical molecular weights could be attained experimentally by the use of dianhydride solution in the presence of very pure reactants and solvents.[30] Nevertheless, dianhydride addition to diamine solution is often required because of low solubility of the dianhydride. Rigorous reaction conditions, e.g., utilizing extremely dry solvents and an inert atmosphere, must be utilized for polyamic acid synthesis in order to minimize the occurrence of hydrolysis.

It has been established that a reduction in molecular weight can occur for polyamic acid solutions allowed to stand for long periods of time.[1] The depolymerization of amic acids has been mentioned as a source of weight average molecular weight (M_w) decrease. However, experiments with ODA-PMDA indicate that this decrease may be the result of having first achieved very high M_w, followed by equilibration, to yield a most probable molecular weight distribution (Figure 2.2.1.1.1).[31,32] This is evidenced by the fact that during this time period the number average molecular weight (M_n) remains constant (Figure 2.2.1.1.2). It should be pointed out that hydrolysis may also contribute to a reduction in M_w. Nevertheless, molecular weight decrease, for the most part, can be minimized by storing materials at near freezing temperatures (e.g., 5°C), which would, in

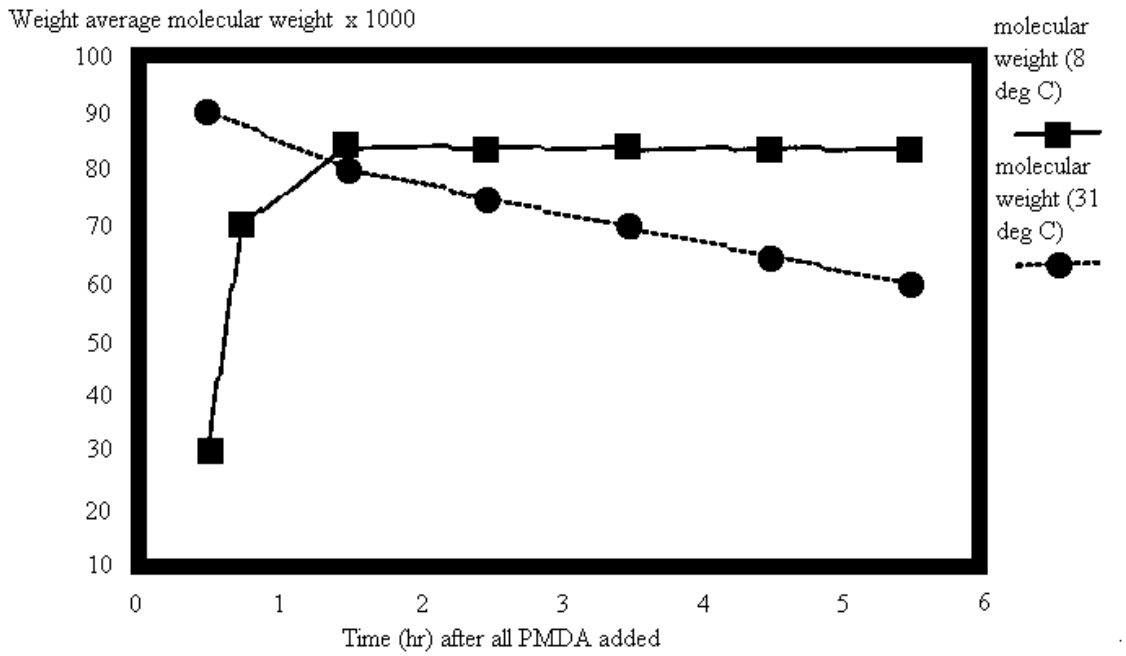

Figure 2.2.1.1.1: Weight Average Molecular Weight of PMDA/ODA Polyamic Acid as a Function of Time at 8 and 31°C[4]

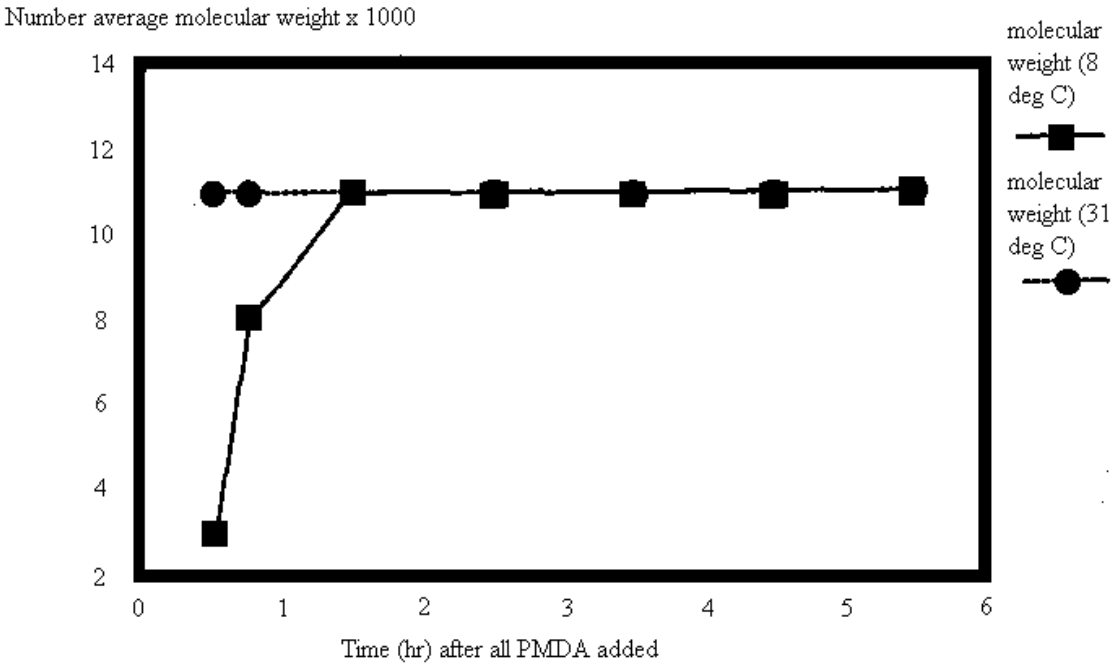

Figure 2.2.1.1.2: Number Average Molecular Weight of PMDA/ODA Polyamic Acid as a Function of Time at 8 and 31°C[4]

theory, favor equilibration to polyamic acid.

Synthesizing polyamic acids from more basic and nucleophilic aliphatic diamines has not been widely utilized due to complicating salt formation during the reaction and the lower stability of the aliphatic units. Despite these drawbacks, some recent trials have proved more successful,[33,34] primarily as a result of using NMP. Initial salt formation and/or gel formation were reported, but dissolution, homogeneity, and subsequent reactions were achieved over time.

2.2.1.2 Bulk (thermal) imidization

The most commonly used method of performing the cyclodehydration of polyamic acid to polyimide is by a bulk or thermal imidization.[18,19,35-39] The polyamic acid is processed as a cast film, coating, or spun fiber, and is then heated to 250 – 400°C to complete the cyclization to form the polyimide. Thermal imidization is probably the most cost-efficient and practical means for producing polyimides commercially.

Scientists at NASA developed one of the most efficient heat treatment methods for cyclodehydrating polyimides by bulk imidization to produce films,[40] which entails treating the cast polyamic acid for one hour each at 100, 200, and 300°C. When possible, the terminal cyclization temperature interval should exceed the T_g of polymer to ensure maximum conversion and solvent removal. Intractable polyimides are often processed in this manner.

The reaction mechanisms of bulk imidization processes are very complex in nature. Several techniques have been used to try to understand these reactions. The most common method of studying imidization is infrared spectroscopy analysis,[41,42] but other viable techniques including thermal analyses,[41,43] NMR,[44] microdielectrometry,[45] HPLC,[46] UV-visible spectroscopy,[44] and Raman spectroscopy.[47]

Mass spectrometry has also been utilized to study imidization.[48] This method, in fact, was used to determine that the majority of solvent is effectively removed after treatments at 150°C, after which cyclodehydration and additional solvent loss occurs between 150 to 250°C. This initial process has been identified as the rapid imidization

phase where cyclization occurs quickly,[36,49] which has been confirmed by Navarre.[41] Above 250°C, the final phase of imidization and solvent loss occurs as the glass transition is approached and/or exceeded. Up to this point, low polymer mobility, as well as the lack of residual solvent needed to effectively plasticize the polymer, both contribute to a slow final rate of cyclization.

Another explanation of solid-phase thermal imidization is that it is a physicochemical process of two stages.[50] The initial stage consists of the physical diffusion of the polyamic acid into various states, while the second stage encompasses the chemical formation of the imide ring. The overall process is influenced by choice and concentration of solvent, film thickness,[51] molecular mobility,[43,52] physical state of the amic acid,[50] degree of cyclization[35], and the presence of side reactions,[23,53] such as hydrolysis.

Molecular weight variations that result from converting a polyamic acid to a polyimide have been of interest in many laboratories. Most research undertaken in this area conclude that, for the most part, molecular weight retention is achieved upon complete cyclization to the polyimide.[30,31,54,55] However, changes in molecular weight have been witnessed during bulk imidization.

During imidization, there is a decrease in molecular weight, as characterized by the formation of anhydride and amine groups above 75°C.[50,56,57] More specifically, M_w experiences a decrease relative to M_n as demonstrated in a study on a thermally imidized soluble polyimide.[58] As temperature is increased, the anhydride reforms and reacts with the diamine to regenerate the initial molecular weight species.

Several side reactions as a result of thermal imidization have been proposed. Young and Chang indicated that the presence of reactive end groups can lead to increased molecular weight at elevated temperature,[59] which may be attributable to chain extension.

Other instances of side reactions have been proposed that may impact the solubility of polyimide systems. Among the more prevalent explanations is crosslinking by either intermolecular imide or imine formation.[53,60,61] Kim and coworkers discovered that imine formation and possible branching and/or crosslinking was evident in systems containing BTDA.[62] Diamidation has also been mentioned, but little experimental evidence exists

that strongly corroborates this phenomenon,[63] perhaps due to the tendency to recyclize to polyimide.[64] Nevertheless, accounts of several soluble polyimides obtained by bulk imidization contradict many of the crosslinking theories.[58,65-70]

2.2.1.3 Solution imidization

The appearance of soluble polyimides coincided with the development of solution imidization techniques. Using this method, fully imidized, high T_g soluble polyimides can be synthesized under relatively milder conditions than those needed for bulk imidizations. This is due to the added molecular mobility inherent in the solution state that allows for easier cyclodehydration of the polyamic acid.

Initial attempts to produce solution imidized polyimides were made by Vinogradova and coworkers in the early 1970's.[71] However, polymerization conducted in NMP at 200°C did not yield high molecular weight polyimides. This was likely a consequence of water of cyclization remaining in solution, which could cause hydrolysis.

This aspect of the reaction would eventually be overcome by work in the McGrath research group,[72-74] who added an azeotroping agent, such as o-dichlorobenzene (DCB), xylene, or cyclohexyl pyrrolidone to the existing polyamic acid solution to eliminate the water generated upon imidization. With the addition of an azeotroping agent, the imidization could be performed from 150 to 180°C to afford fully cyclized, high molecular weight polyimides, providing that the polyimides were soluble in the reaction solvent. Under these conditions, complete imidization could be achieved within 24 hours. Insoluble and/or crystalline polyimides would precipitate from solution, an occurrence that has actually been advantageously exploited in order to form submicron particles for composite fabrication. [75,183]

Polyimides prepared by solution imidization have the advantage of avoiding some of the side reactions that sometimes occur using bulk imidization at higher temperatures. In addition, it has been demonstrated that solution imidized polyimides were more soluble than those made by thermal imidization.[76] Furthermore, there is no likelihood of the formation of isoimide functionalities as those encountered when using chemical

imidization.

Kim and coworkers have thoroughly investigated the various mechanisms involved in solution imidization.[62] Their work concluded that in the early stages of imidization a decrease in intrinsic viscosity occurs, followed by an increase in viscosity with time. This is similar to what is experienced during bulk imidization.[58] Proton NMR also shows an increase in amine concentration in the early stages of the imidization, followed by a decrease with time. The amic acid concentration and intrinsic viscosity over time are summarized in Figure 2.2.1.3.1.

This study also revealed that amine and anhydride endgroups were formed during solution imidization. Moreover, the residual water generated from this process results in some hydrolysis, which is evidenced by the initial viscosity decrease. As the reaction proceeds, however, the endgroups react once again to regenerate the initial molecular weight species. The proposed mechanism for the solution imidization is given in Figure 2.2.1.3.2. The kinetics of the reaction are classified as an auto acid catalyzed second order process, in which a dependence on concentration is observed. The rate determining step was nucleophilic substitution of a carboxyl carbon by an amide nitrogen.

2.2.1.4 Chemical imidization

Cyclodehydration of polyamic acids can be accomplished at ambient temperature through the use of mixtures of acid anhydrides and tertiary amines as dehydrating agents.[38] Mixtures of acetic anhydride with pyridine or triethylamine are most often employed. However, the expense and problems associated with this reaction have made this a less attractive alternative for other imidization methods.

The mechanism of this particular reaction is shown in Figure 2.2.1.4.1,[77-79] which shows that when dehydrating agents are mixed with a polyamic acid, a mixed anhydride moiety is formed. It should be noted that the acetate functionality present serves as an improved leaving group in comparison to the proton it replaces. Thus, the imidization can

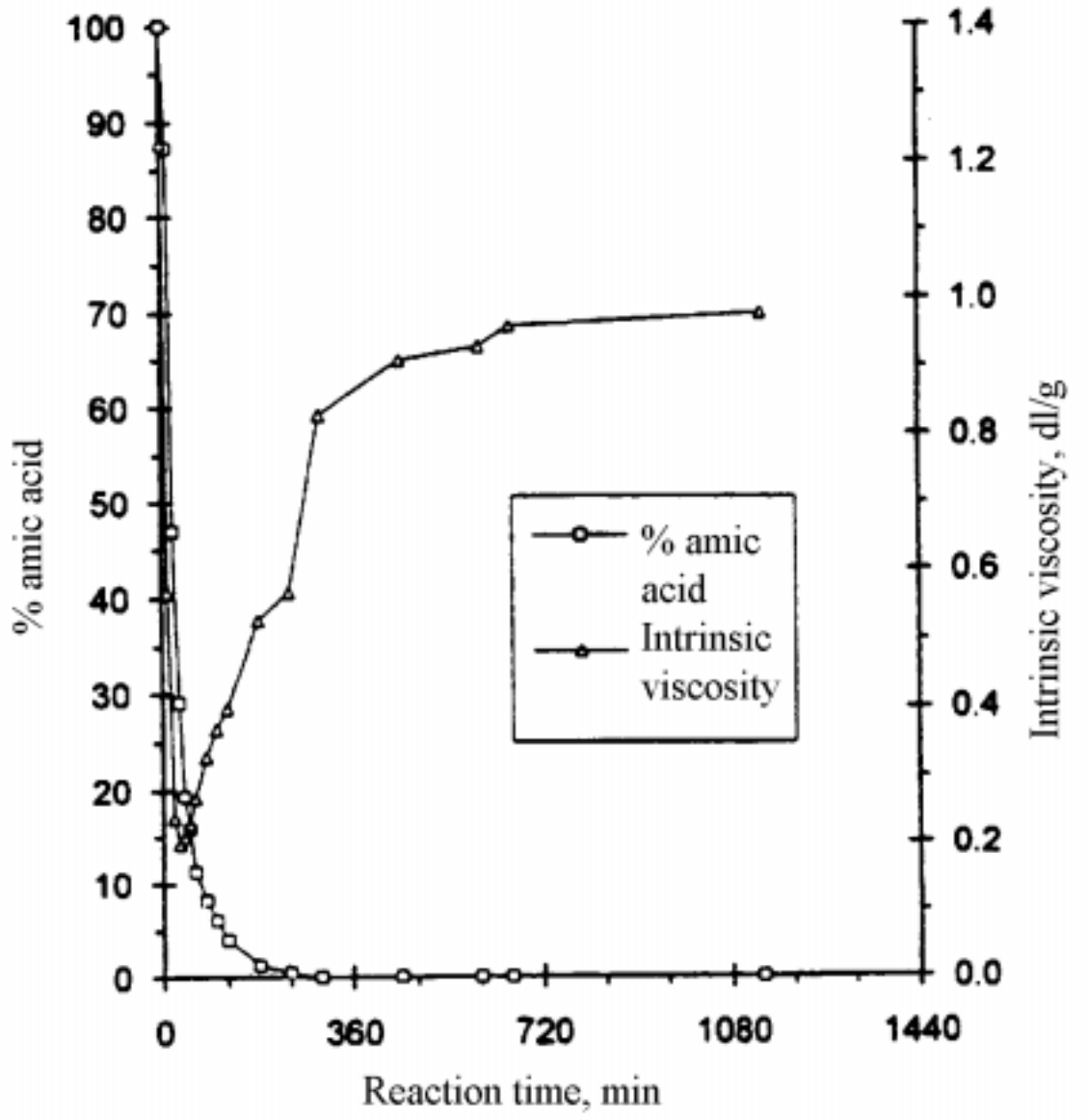

Figure 2.2.1.3.1: Amic Acid Concentration and Intrinsic Viscosity as a Function of Reaction Time at 180°C [62]

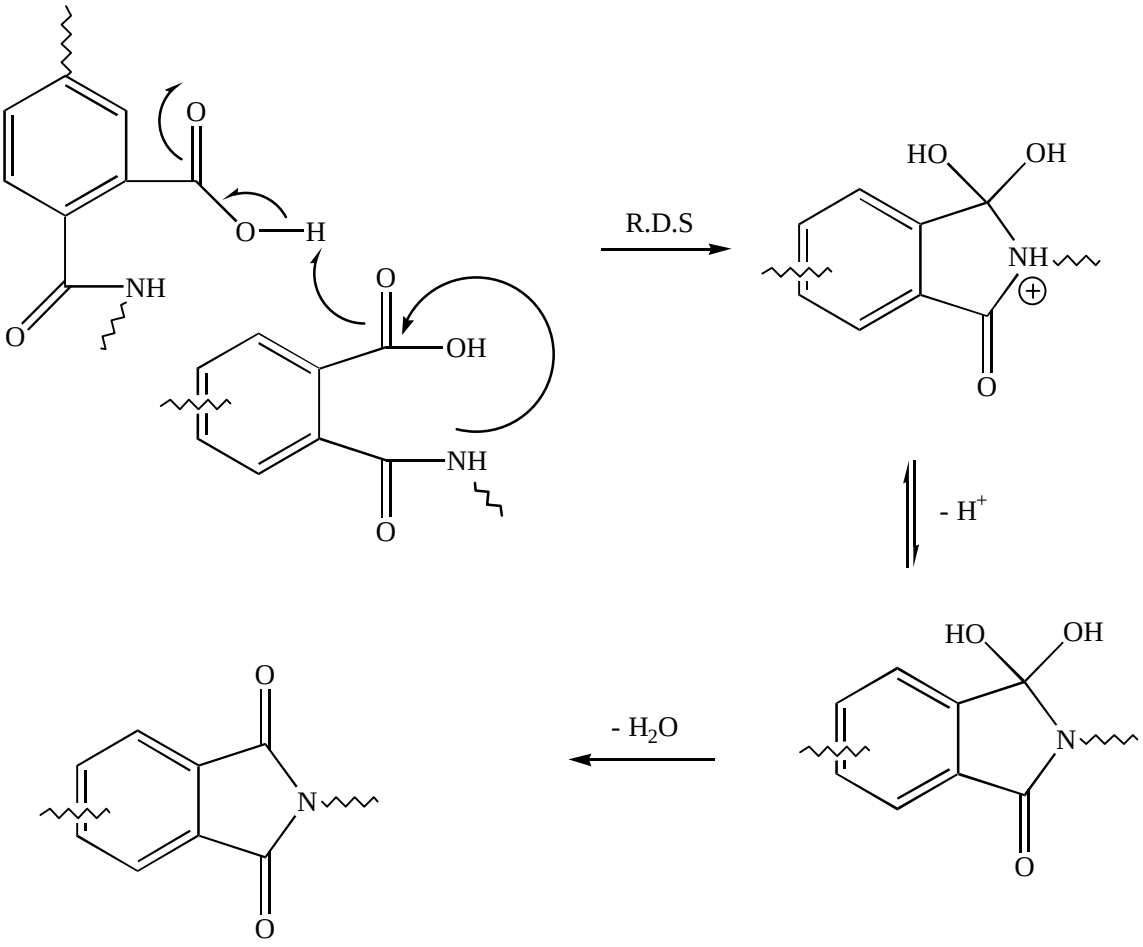

Figure 2.2.1.3.2: Proposed Mechanism for the Solution Imidization Process [62]

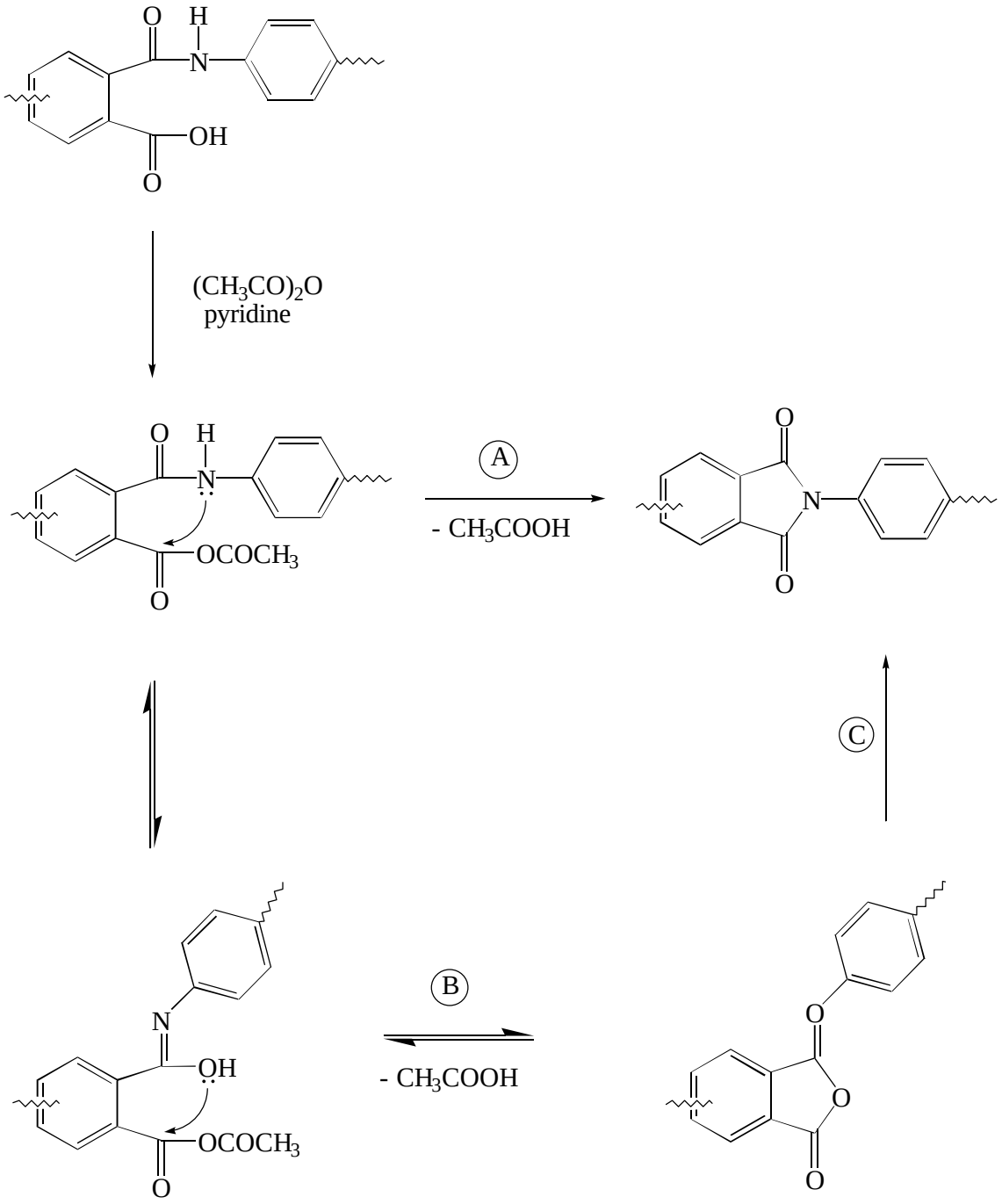

Figure 2.2.1.4.1: Proposed Mechanism for the Chemical Imidization Process[78-80]

be conducted at lower temperatures. In some cases, the amic anhydride species can tautomerize to yield an iminol which will cyclize to produce the kinetically-favored isoimide. Otherwise, the amic acid simply condenses acetic acid to produce the thermodynamically-favored imide. In addition, residual acetate can enforce attack on the isoimide to eventually lead to imide. Also, thermally treating the isoimide will cause conversion to the imide, but subsequent treatments near 300°C are necessary to ensure complete imidization.[80]

Chemical imidization has the advantage of decreased molecular weight reduction during the imidization, due to the lack of reverse propagation encountered with other methods of imidization. This may translate to enhanced mechanical properties, as have been reported for the PMDA-ODA based polyimides.[81] In addition, the use of isoimide precursors reportedly can provide improved processing.

2.2.2 Additional routes to polyimides

The methods of synthesizing polyimides that have been described thus far can be utilized for both soluble and insoluble systems. However, there are numerous other ways to produce polyimides, but many are limited to soluble polyimides or are restricted in some other manner.

2.2.2.1 One-step polyimide synthesis

Soluble polyimides can be prepared by a so-called one-step or single stage method.[82-84] Using this method, dianhydride and diamine are reacted in a high boiling solvent in excess of 180°C, wherein molecular weight buildup and imidization occur virtually simultaneously. The water of imidization is merely allowed to distill from the reaction mixture. Nitrobenzene, m-cresol, and α-chloronapthalene are used as solvents in these reactions.

Harris and coworkers have done extensive work using the one-step method,[85-93] which has primarily involved the development and use of phenylated monomers. The

reactivity of these monomers at lower temperature is insufficient for successful polymerization, but the one-step process allows high molecular weight polyimides to be synthesized.

2.2.2.2 Polyimides from ester-acid route

The development of the chemistry associated with the polymerization of monomeric reagents, more commonly referred to as PMR, was based upon the use of diester-diacid derivatives of tetracarboxylic dianhydrides.[94-96] The use of diester-diacid chemistry is advantageous because the monomers, unlike dianhydrides, are hydrolytically stable. Therefore, the rigorous reaction conditions utilized in the two-step polyimide synthesis are not necessary for successful polymerization. Furthermore, the diester-diacids usually possess a higher degree of solubility than the parent dianhydride or tetra-acid.

Moy and others have demonstrated the feasibility of the diester-diacid route in a "one-pot" synthesis using solution imidization conditions,[97,98] in which the dianhydride of interest is usually refluxed in methanol or ethanol to generate the corresponding diester-diacid. The alcohol is subsequently distilled off, and the diamine and solvent are added to accomplish the polymerization at elevated temperatures. The reaction is shown in Scheme 2.2.2.2.

2.2.2.3 Polyimides by nylon-salt method

As was mentioned earlier, initial efforts to make commercially-viable polyimides involved the use of nylon-salt type chemistry.[11-13] However, this method proved problematic for aromatic diamines due to problems with low molecular weights, intractability, and processing. More recently, Imai and others have resumed the utilization of aliphatic diamines in high pressure methods to produce high molecular weight crystalline polyimides by the salt method. [99-102]

2.2.2.4 Polyimides by nucleophilic substitution of imide precursors

Scientists at General Electric have been credited with creation of polyetherimides by nucleophilic substitution,[103-105] which is accomplished using the same techniques employed in the syntheses of polyarylene ether ketones and sulfones.[106-110] Specifically, dinitro-substituted bisimide monomers are reacted with bisphenolates to yield the polyimide (Scheme 2.2.2.4.1). More recently, Davies has reported a similar synthesis using bisphenols with potassium fluoride in place of preforming the bisphenolate through the use of alkaline bases.[111]

Nucleophilic substitution has also been utilized in the synthesis of polyesterimides using preformed imide precursors. In attempting to prepare new liquid crystalline polyimides, Kricheldorf and Pakull have reacted carboxyl-functionalized bis-trimellitimides (Figure 2.2.2.4) with bisphenols.[112] Similarly, Sato and coworkers have attempted to synthesize liquid crystalline poly(imide carbonates) by the melt esterification of N-bis(hydroxyalkyl)imides with bis(phenyl carbonates) (Scheme 2.2.2.4.2).[113-117]

Amide-imide exchange or transimidization chemistry has been utilized in synthesizing polyimides. Although early reports of this method[118] involved the high temperature formation of polyamic amide on route to the polyimide by use of a non-substituted bisimide, Imai[119] and Takekoshi[120,121] have conducted the polymerization under milder conditions. This reaction has been tailored so that the displacement of amine from the imide precursor takes place more easily as the basicity or nucleophilicity of the diamine increases. Rogers has employed the transimidization method in the synthesis of perfectly alternating imide siloxane copolymers,[122,123] which was accomplished through the use of weakly basic 2-aminopyrimidine. This amine is used to endcap imide oligomers, which were subsequently reacted with aminopropyl-terminated dimethyl siloxane oligomers under relatively mild conditions to produce high molecular weight copolymers. An example of the reaction is shown in Scheme 2.2.2.4.3.

2.2.2.5 Additional routes to polyimides

Several other methods have been used in the preparation of polyimides. Diisocyanates have been used in place of diamines to professedly yield seven member ring

structures which evolve carbon dioxide to give the polyimide, a process that can be used for production of polyimide foams.[124] The Diels-Alder reaction has been adapted for synthesizing polyimides by reaction of bisbenzocyclobutane derivatives with bismaleimides.[125] Furthermore, polyimides from the palladium-catalyzed coupling reaction of diaryl halide monomers have been reported.[126-128]

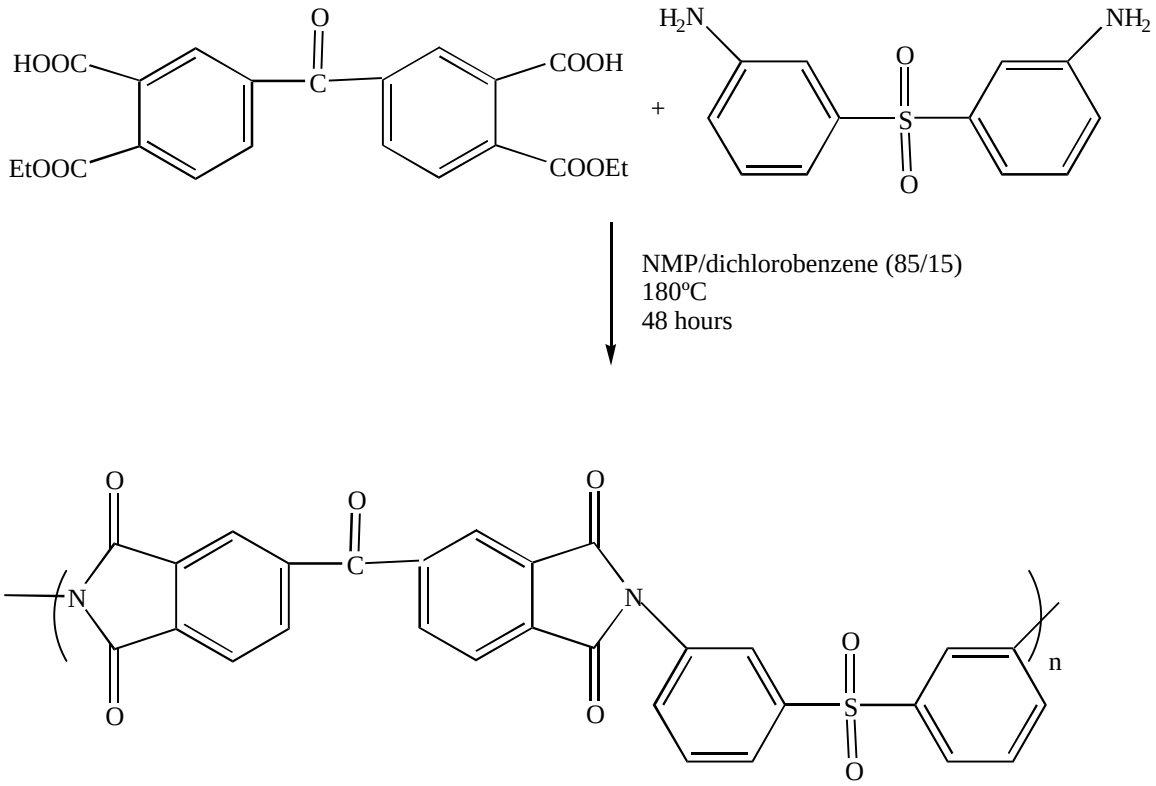

Scheme 2.2.2.2: Synthesis of BTDA-3,3'-DDS Using the Diester-Diacid of BTDA [97]

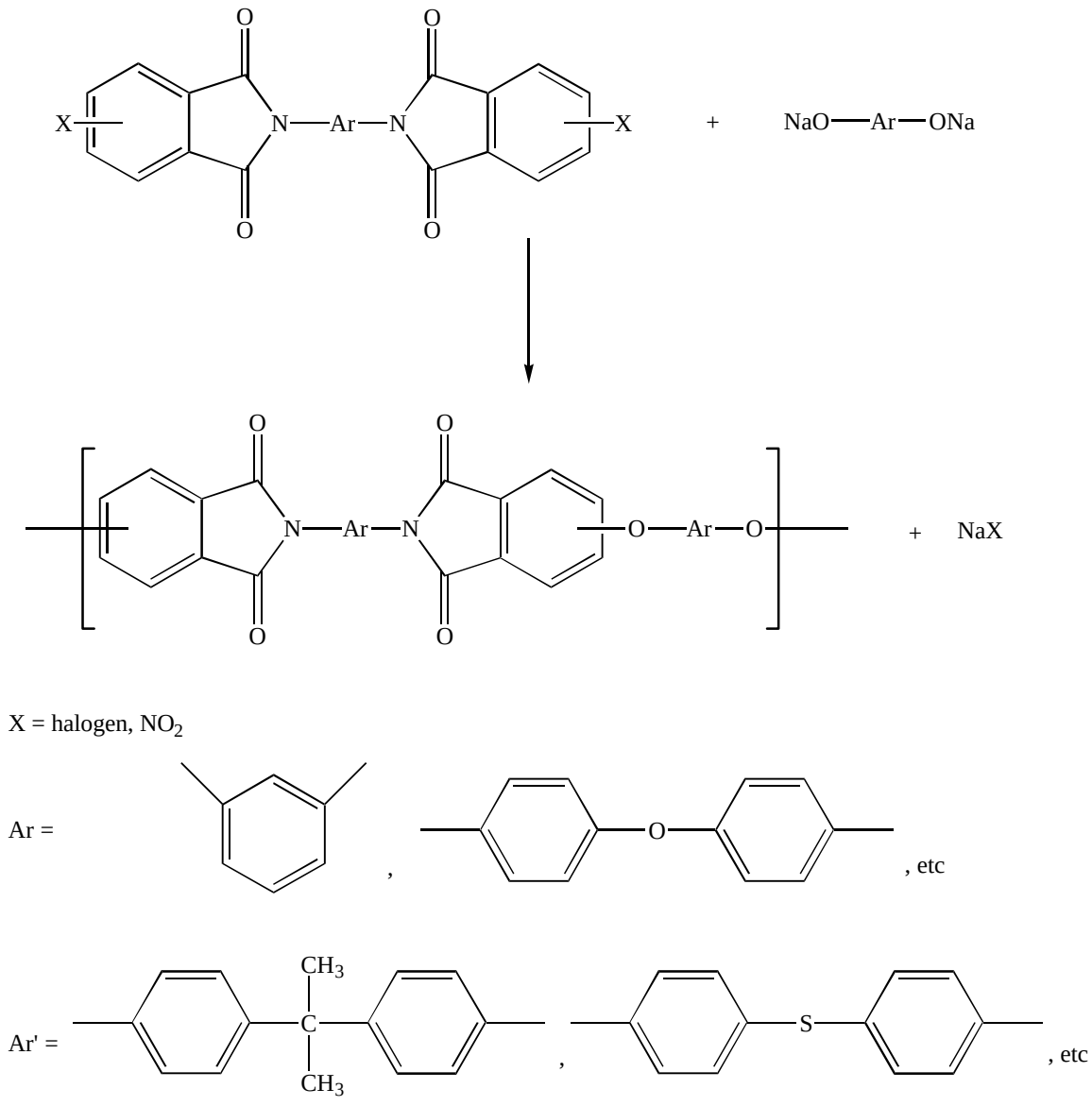

Scheme 2.2.2.4.1: Synthesis of Polyetherimides by Nucleophilic Substitution[4]

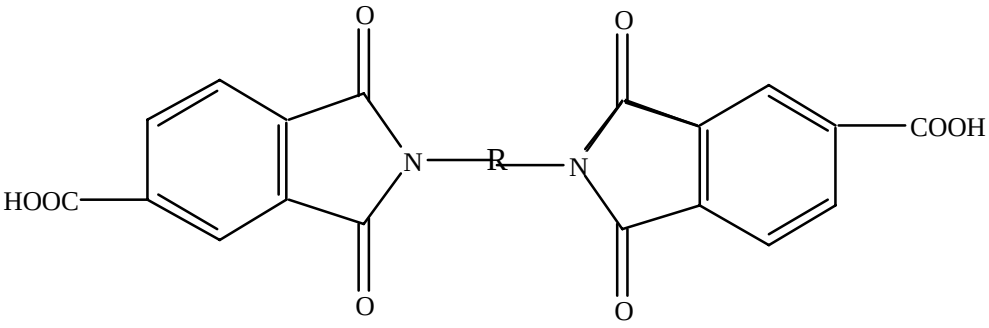

Figure 2.2.2.4: Bis(trimellitimides) for Polyesterimide Synthesis[2]

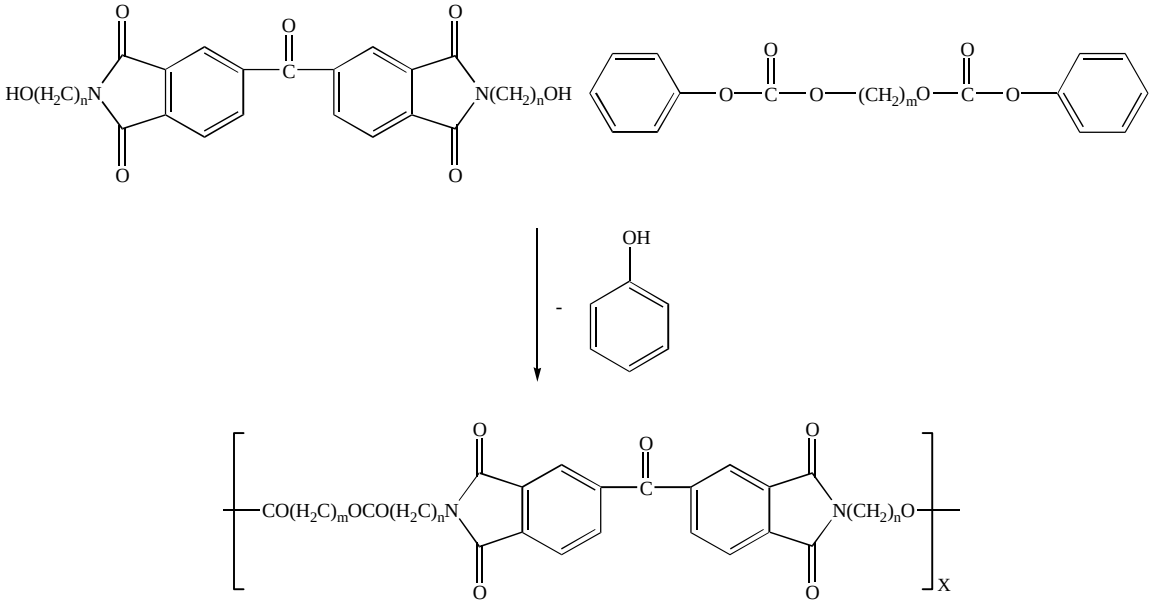

Scheme 2.2.2.4.2: Synthesis of Polyesterimides by Melt Transesterification[113]

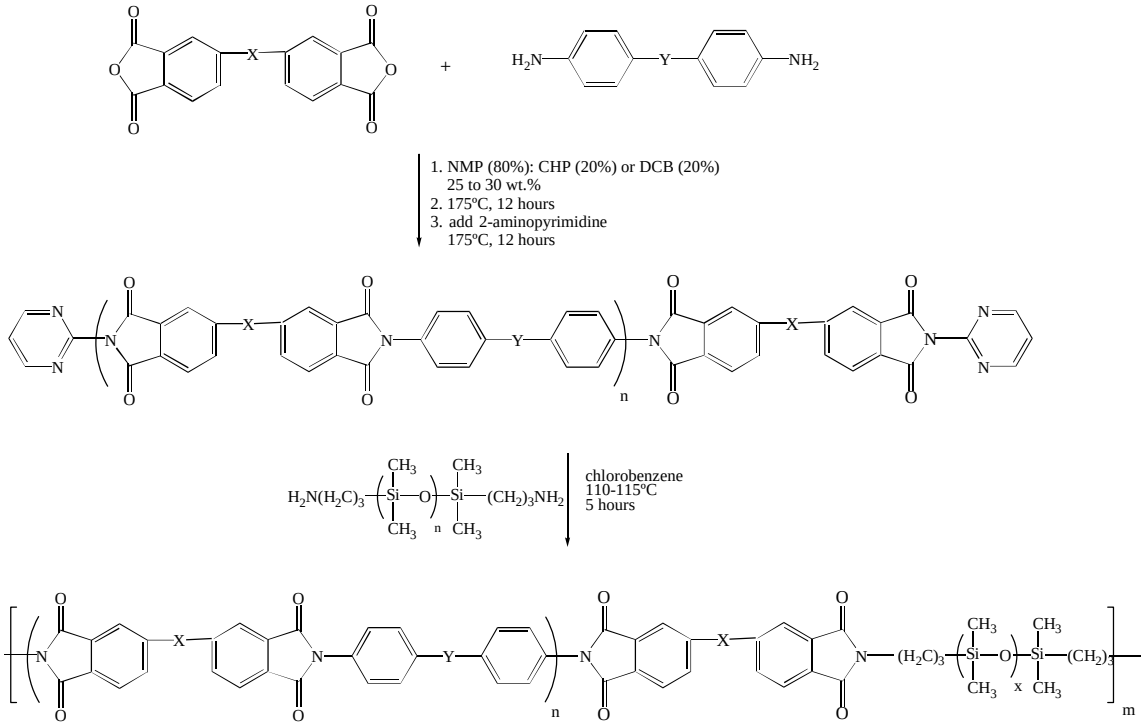

Scheme 2.2.2.4.3: Synthesis of Polyimide Siloxane Copolymers by Transimidization[123]

2.3 Structure-Property Relationships of Polyimides

Polyimides are generally regarded as materials possessing high levels of thermal stability as well as excellent mechanical and electrical properties.[4,6,8] If designed properly, this class of polymers can exhibit tremendous performance under a variety of environments such as short and long term exposures to extreme temperatures, stresses, chemicals, and atmospheres. Since the commercialization of Kapton polyimide by DuPont, tremendous effort has been spent in developing other processable polyimides with even greater performance capabilities.

The expansive body of literature devoted to polyimides has resulted in a number of generalities concerning the structure-property relationships of these particular polymers.[129] For example, thermal stability is greater in wholly aromatic polyimides that those containing aliphatic moieties. Within the polyimide chain, larger amounts of internal chain mobility will equate to decreased thermal transitions and increased solubility. More energy is required for more rigid systems to induce mobility, leading to higher transition temperatures. Flexible polyimides reportedly possess better hydrolytic stability than rigid polyimides.

Semi-crystalline order in polyimides is the result of close packing of the polymer chains, which is primarily achieved in fairly rigid structures with a high degree of regular ordering. However, many material applications necessitate the absence of crystallinity, and consequently, modifications are made in molecular design to accomplish this goal. Flexible linkages are often utilized to eliminate such ordering. Also, the presence of asymmetry along the polyimide backbone can in some cases hinder polyimide crystallization. In addition, pendant side moieties such as alkyl groups can be incorporated in polyimide chains to disrupt possible crystallinity.

As with all polymers, molecular weight plays an important role with polyimides. Higher molecular weights result in more polymer entanglement, which in turn leads to higher glass transition temperatures. Higher molecular weights can also diminish the level of crystallinity in a polyimide due to the lack of mobility associated with high polymer viscosity. This subject is covered in more detail in the following section.

With these factors in mind, research involving the modification of polyimide systems to increase processability has been generally focused in two areas: increased solubility and improved thermoplasticity or flow characteristics.[130] Numerous endeavors have been undertaken to accomplish these modifications, the majority of which have involved redesigning the polyimide molecular architecture. Those that have been mentioned so far include the incorporation of flexible spacers or bridging groups, bulky side groups, and asymmetry. In addition to impacting the physical properties of the polyimides, these molecular adaptations can also affect some of the chemical aspects.

2.4 Molecular Weight Control of Polyimides

The molecular weight of a polyimide is a critical factor, because this parameter often dictates the physical properties and processability of these materials. Therein, the polymer molecular weight impacts not only the end use of the material, but also the means by which processing is conducted. It is well documented that polymers, in general, exhibit an increase in properties such as tensile strength, modulus, density, and glass transition temperature with increasing molecular weight.[131,132] Specifically, these properties are optimized upon reaching the onset of the entanglement molecular weight of the polymer, which is usually in excess of 10,000 grams per mole. Therefore, it is not surprising that a majority of commercially available thermoplastic polymers report number average molecular weight values of 15,000 to 30,000 grams per mole. An example of this is shown in Figure 2.4.1, in which a rapid increase in strength is observed, indicative of polymer entanglement, followed by a plateau.

The rheological aspects of a polymeric material are also important since polymer viscosity is related to molecular weight. Consequently, melt processing of polymers requires control of molecular weight so that melt viscosity is not excessive and polymer flow is adequate. The generalized relationship of melt viscosity and molecular weight is given in Figure 2.4.2,. which shows two distinct regions. Initially, the melt viscosity increases approximately linearly with the weight average molecular weight (M_w) before entanglement. Upon entanglement the viscosity becomes proportional to $M_w^{3.4}$, and the

increase in melt viscosity is much more dramatic. Therefore, at very high molecular weight the melt viscosity becomes exceedingly high, resulting in drastically diminished processability.

Molecular weight control in polyimide synthesis is primarily achieved by the offset of monomer stoichiometry. However, this process results in the appearance of reactive endgroups at the end of the polymer chain, which can inadvertently increase molecular weight under different conditions or during processing. This undesirable outcome can be prevented by the use of a nonreactive monofunctional endcapper.[72,76,13]

3

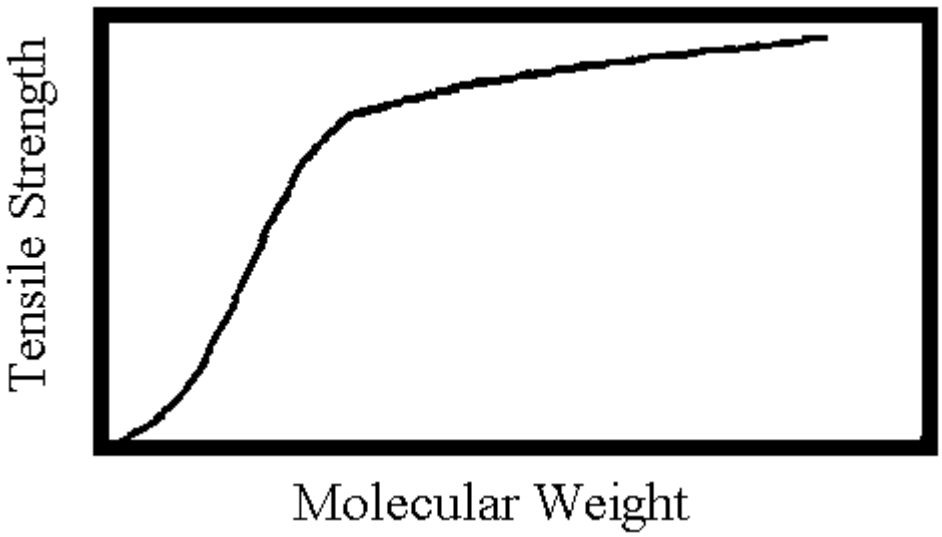

Figure 2.4.1: Effect of Polymer Number Average Molecular Weight (M_n) on Tensile Strength (σ_b) [131]

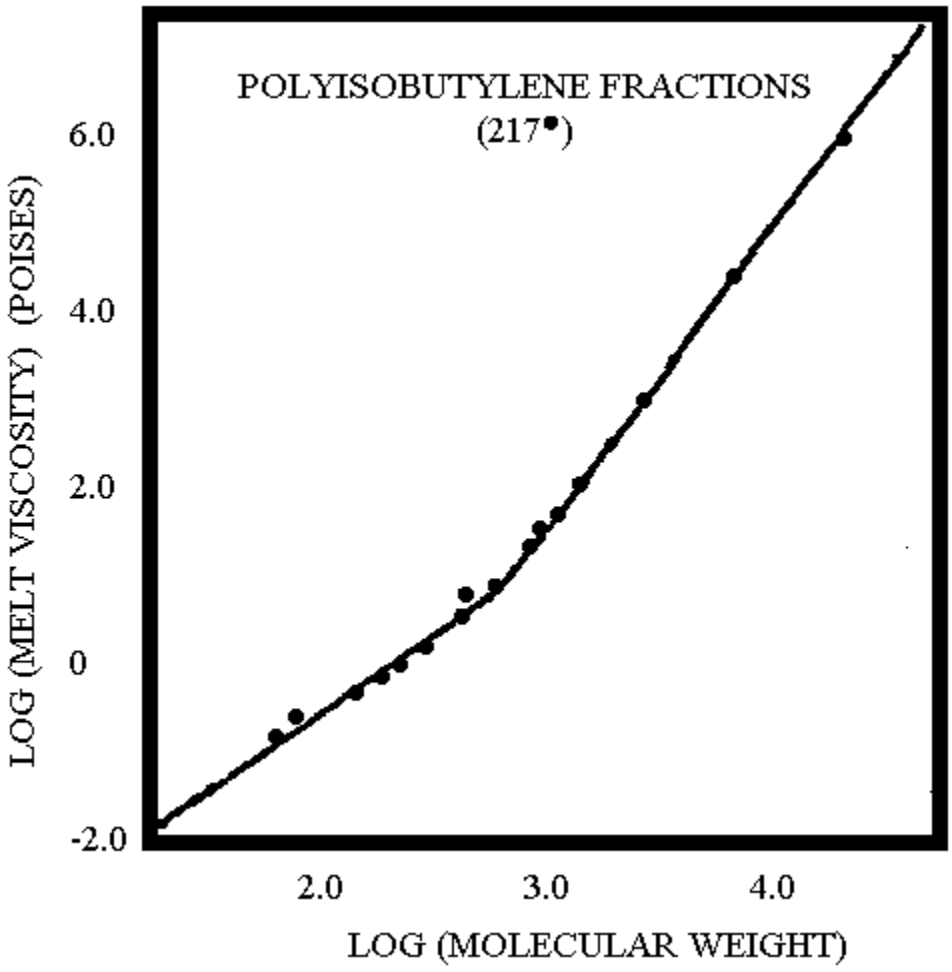

Figure 2.4.2: Effect of Polymer Weight Average Molecular Weight (M_w) on Melt Viscosity [132]

2.5 Semicrystalline Polyimides

Semicrystalline thermoplastic polymers are of great interest due to their ability to serve in applications in which processability, solvent and chemical resistance, and optimum mechanical properties are required. The use and potential of semicrystalline polyimides for such purposes has been realized. Regrettably, some of the factors which contribute to the outstanding performance of the aromatic polyimides are also somewhat problematic in terms of processability and practicality. The inherent stiffness of wholly aromatic polyimide backbones can lead to high transition temperatures and, thus, processing difficulties. In addition, this stiffness can hinder the mobility of the polymer chains and consequently the ability to crystallize.[134]

Efforts have therefore been made to improve the thermoplasticity of potentially useful semicrystalline polyimides. For example, ether linkages have been incorporated into the polyimide backbone, which provide a some degree of mobility and flexibility in the polymer chain and thus permit the needed chain alignment required for crystallization. The added flexibility can also serve to decrease transition temperatures. Some early research in this area involved the use of ODPA with various diamines to produce semicrystalline polyimides.[5]

NASA has conducted extensive research in the development of semicrystalline thermoplastic polyimides. Some early work by T. and A. St. Clair involved the use of 4,4'-bis(3,4-dicarboxyphenoxy)diphenylsulfide dianhydride (BDSDA) with a series of diamines.[135,136]

Another NASA invention was the advent of the Langley Research Center Thermoplastic Polyimide, commonly known as LARC-TPI (Figure 2.5.1).[40,137-140] While thermally imidized LARC-TPI has been acknowledged as being an amorphous material, chemically imidized samples have demonstrated crystallinity.[141] A melting point of around 272°C has been observed for this material. Furthermore, the crystallinity can be enhanced by annealing to produce a higher melting form of the polyimide, wherein a T_m of 288°C was seen.[142]

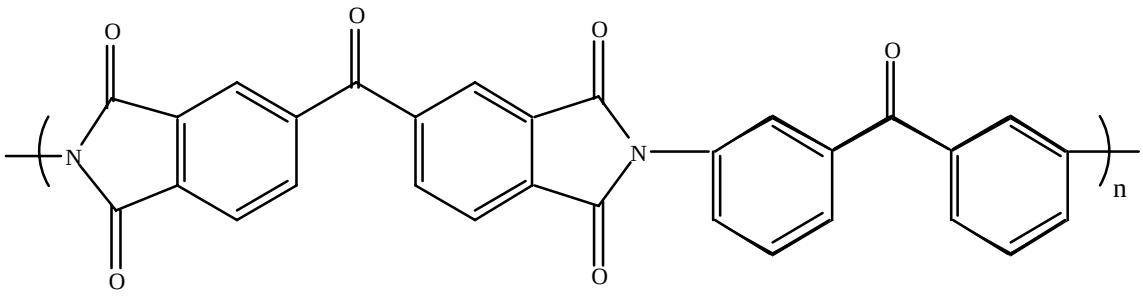

Figure 2.5.1: LARC-TPI

Studies on the solvent-induced crystallization of LARC-TPI in NMP have been performed.[143] One of the interesting findings was the appearance of dual melting phenomena by DSC of the polyimide samples after solvent treatments. It should be noted that the amount of higher melting material observed was directly proportional to the amount of solvent used. The use of larger quantities of NMP resulted in increasingly greater amounts of the higher melting polymer, with substantially large quantities of NMP producing a virtually unimodally-melting material (Figure 2.5.2). The duration of solvent exposure had the same effect as solvent quantity, as larger amounts of higher melting material were observed with prolonged exposure (Figure 2.5.3).

Hergenrother and coworkers synthesized a series of polyimides containing ether and carbonyl groups.[144-147] Diamines with multiple carbonyl and ether moieties were reacted with PMDA and BTDA to produce semicrystalline polyimides with superb chemical resistance and mechanical properties. Specifically, these systems were unaffected by 72 hour immersions in various deicing, jet, and hydraulic fluids, in addition to DMAC and chloroform. Of particular interest was the polyimide derived from BTDA and 1,3-bis(p-aminophenoxy-p-benzoyl)benzene (1,3-BABB), known as the Langley Research Center Crystalline Polyimide, or LARC-CPI (Figure 2.5.4). This material displayed a reasonable amount of crystallinity as evidenced by x-ray diffraction (Figure 2.5.5). The polyimide melted at 364°C[148] and demonstrated the ability to recrystallize from the glass at about 300°C after quench cooling (Figure 2.5.6).

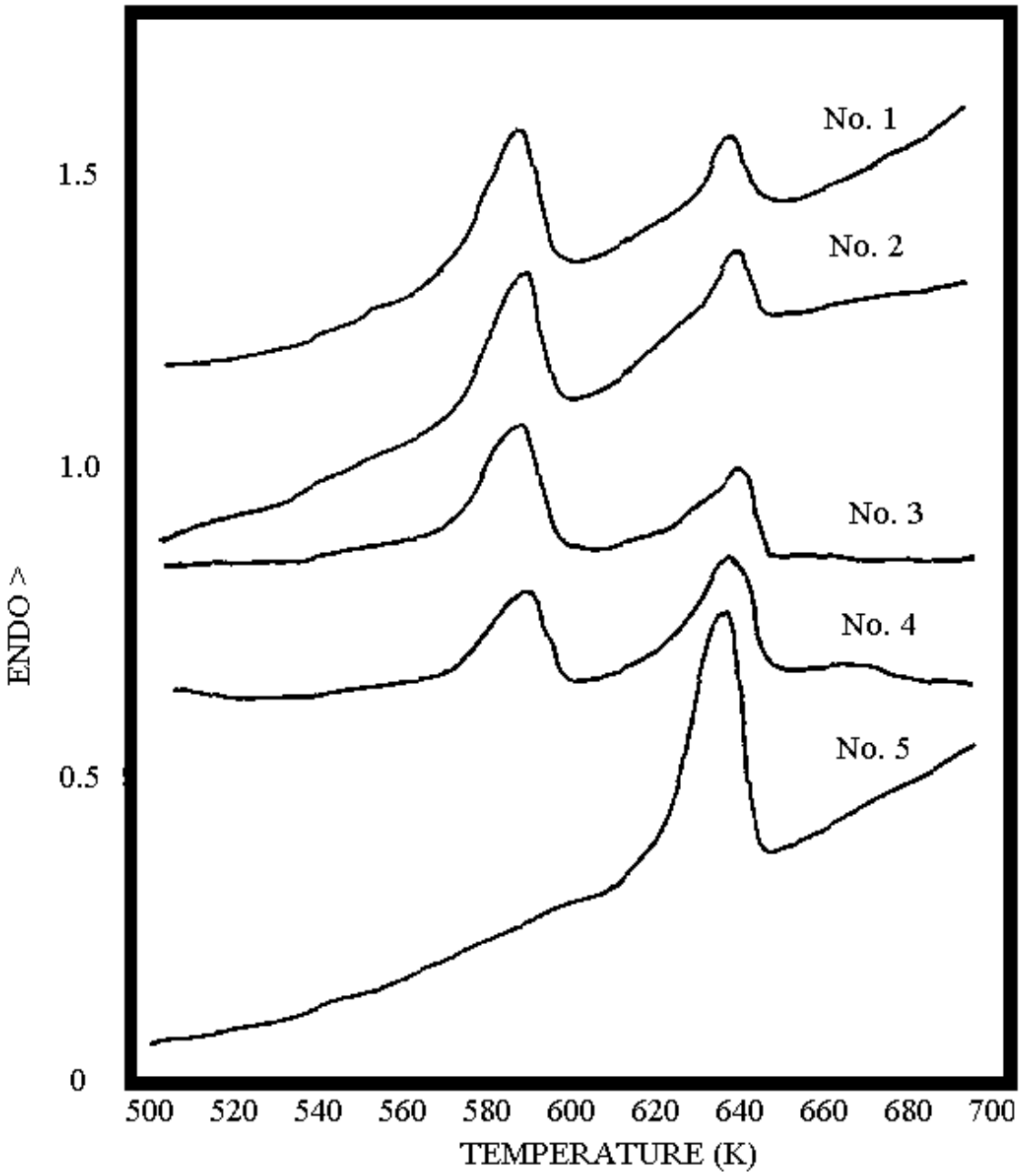

Figure 2.5.2: DSC Thermograms of LARC-TPI After Exposure to NMP at 200°C [143]

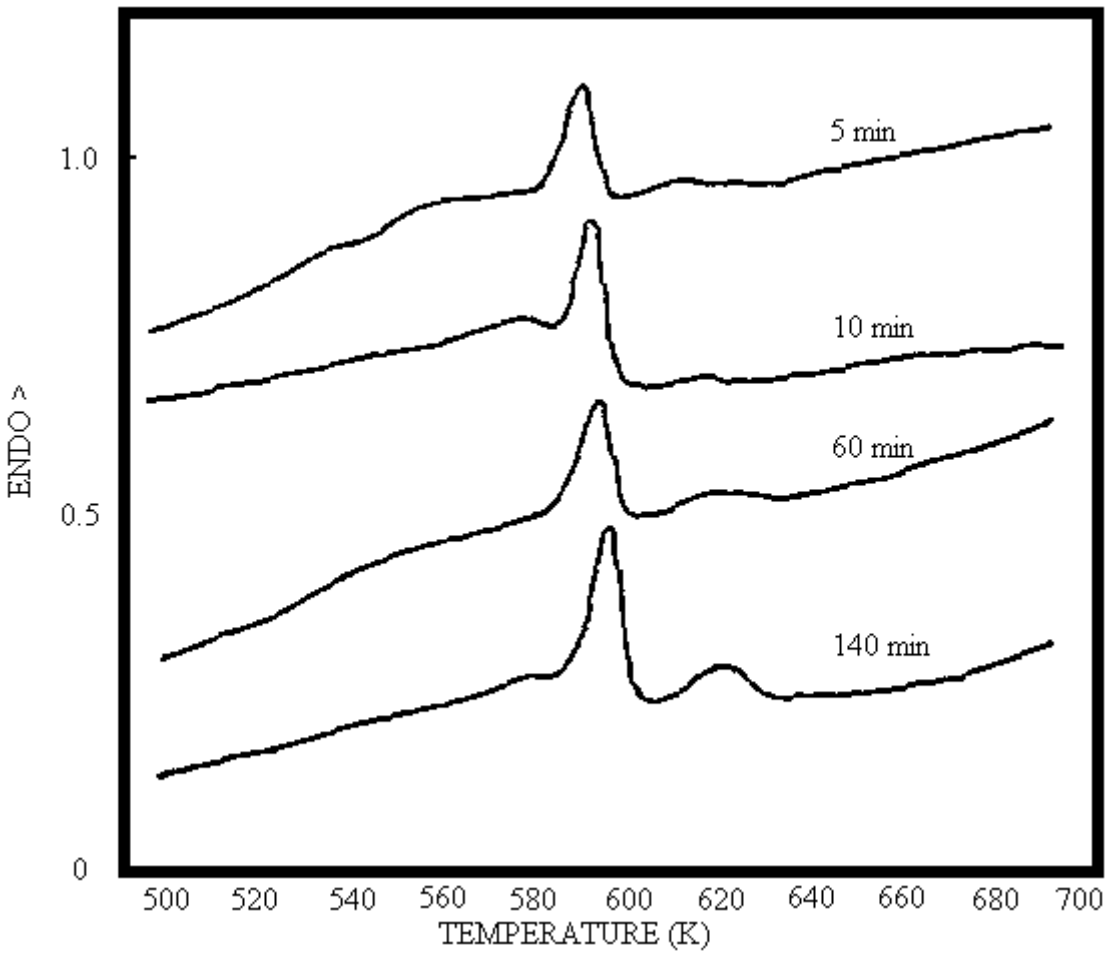

Figure 2.5.3: DSC Thermograms of LARC-TPI After Exposure to NMP at 160±10°C as a Function of Time [143]

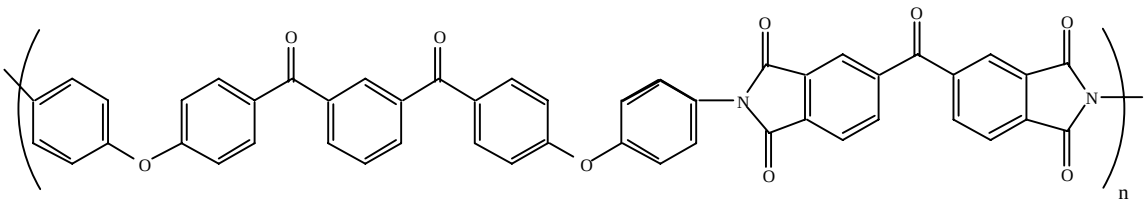

Figure 2.5.4: LARC-CPI

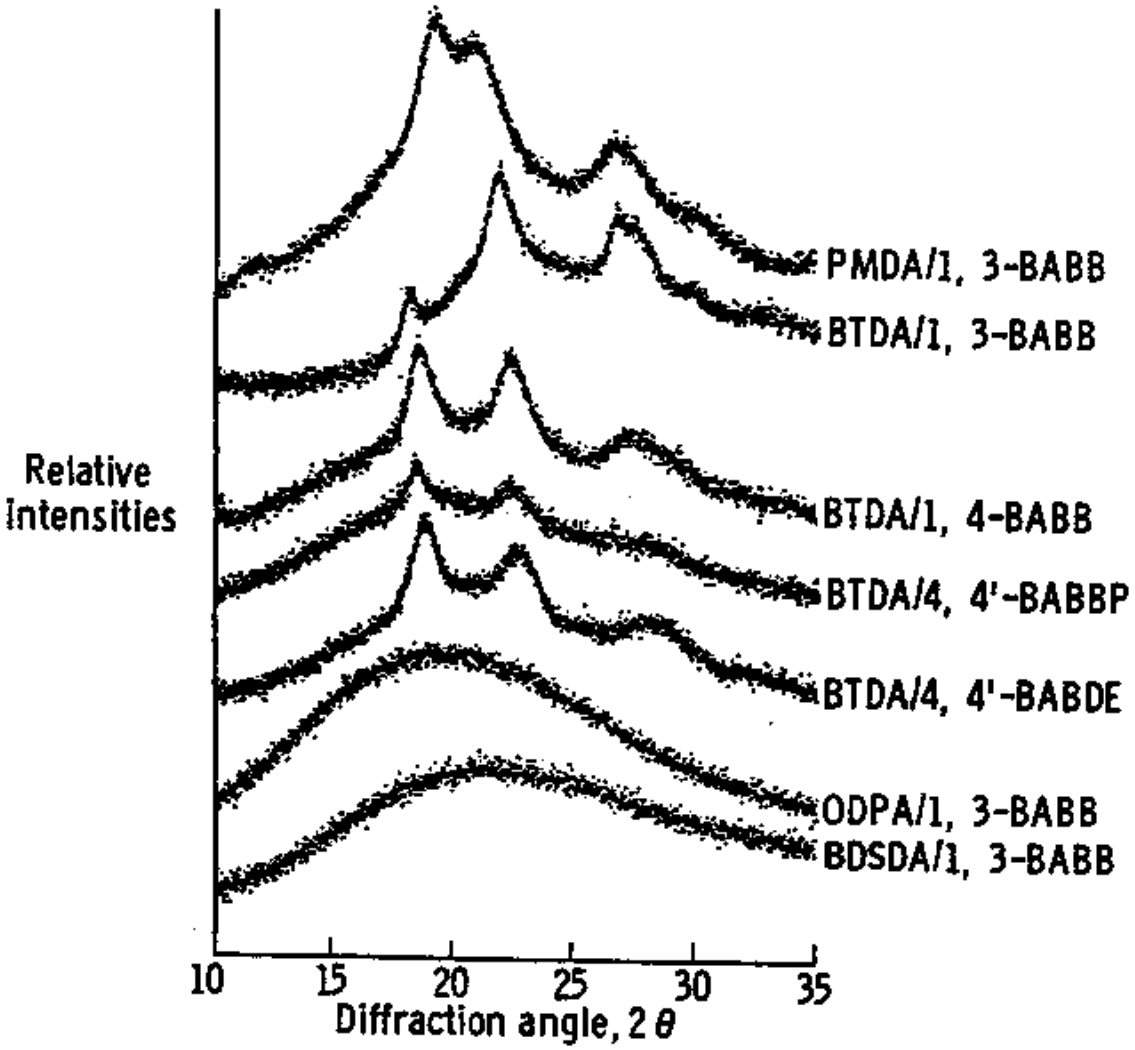

Figure 2.5.5: X-ray Diffractograms of Ether and Carbonyl-Containing Polyimide Films[144]

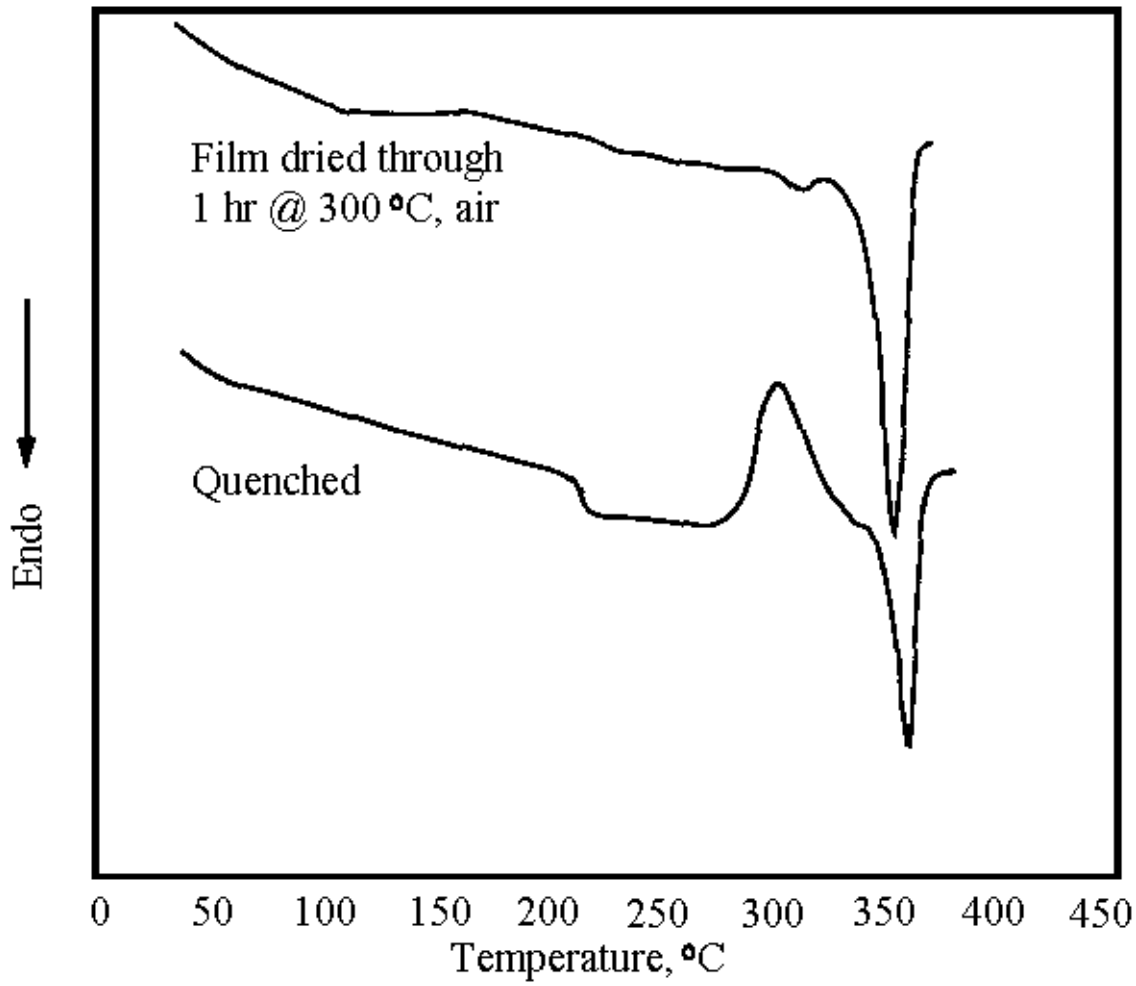

Figure 2.5.6: DSC Thermograms of LARC-CPI [148]

NASA developed a second generation of these semicrystalline polyimides, LARC-CPI-2 (Figure 2.5.7),[149,150] which is based upon ODPA and 1,4-BABB. Lower molecular weight samples of LARC-CPI-2 exhibit an interesting dual melting behavior (melting points of 334 and 364°C) upon multiple DSC scans (Figure 2.5.8). Between the two melting endotherms exists an exothermic process that is indicative of rapid melt recrystallization to the higher melting form of the polyimide. Annealing of LARC-CPI-2 in the exothermic region produces exclusively the higher melting form of the polyimide at an increased melting temperature of 371°C. It was discovered that the majority of the crystallinity associated with this polymer evolved between 125 to 150°C during the thermal imidization of the polyamic acid precursor. This has been attributed to a level of chain mobility that exists in that temperature range which allows for the crystallization to occur.

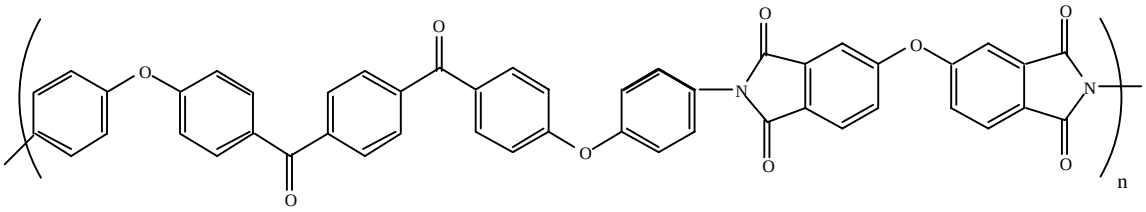

Figure 2.5.7: LARC-CPI-2

Pratt and coworkers at NASA prepared another semicrystalline polyimide based upon 4,4'-isophthaloyl-diphthalic anhydride (IPDA) and 1,3-BABB.[151,152] as shown in Figure 2.5.9. Imidization of this system produces a dual melting material with a stated thermodynamic melt occurring about 350°C. The authors claim that this particular system is one of the first examples of solvent induced crystallization in a polyimide.

Mitsui Toatsu has developed what is perhaps the most promising semicrystalline thermoplastic polyimide on the market in its NEW Thermoplastic Polyimide, or NEW TPI.[153,154] The structure of NEW-TPI, shown below, is based upon PMDA and 4,4'-bis(m-aminophenoxy)biphenyl (Figure 2.5.10). The polyimide has a T_g of 250°C and a T_m of 388°C.[155] Initial studies of this NEW-TPI powders indicated dual melting behavior as

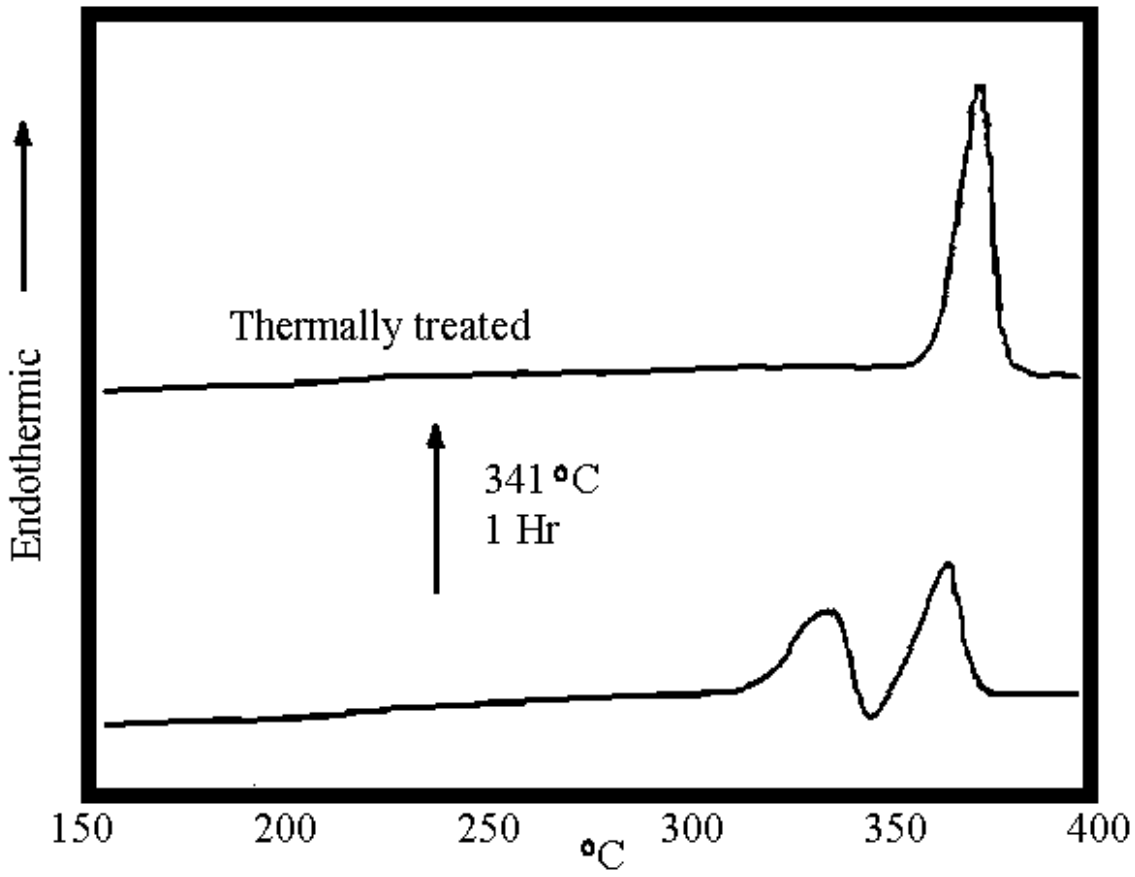

Figure 2.5.8: DSC Thermograms of As-received (Bottom) and Annealed (Top) Samples of LARC-CPI-2 [149]

well as a relatively high degree of crystallinity in as received samples.[156] However, even lower molecular weight samples of the polyimide could be rendered amorphous by quenching. Crystallization from the glass was detected at around 330°C. It was later established that NEW-TPI extruded films were amorphous.[157]

It has been well documented that this polyimide exhibits relatively slow crystallization kinetics as compared to other semicrystalline thermoplastics such as polyethylene terephthalate (PET), poly(ether ether ketone) (PEEK), and poly(phenylene sulfide) (PPS).[158,159] This behavior has been attributed to a number of reasons, including the presence of a rigid amorphous phase which decreases the chain mobility needed for crystallization. In addition, the "crank-shaft" conformation of polymer crystals may also hinder crystallizing (Figure 2.5.11).

Takekoshi has developed a number of semicrystalline polyimides in his work with polyetherimides.[160,161] Several of these polymers were based upon ether and thioether-containing dianhydrides. Sulfur-containing diamines have also been employed.

The AVAMIDS have also been considered for use as thermoplastic materials.[162-164] Among this class of polyimides are some semicrystalline systems, consisting primarily of combinations of PMDA with varying compositions of ether diamines.

Ether diamines containing hexafluoroisopropylidene and 1-phenyl-2,2,2-trifluoroethane linkages have been used to synthesize semicrystalline polyimides.[165,166] Specifically, polyimides prepared from either 2,2-bis[p-(p-aminophenoxy)phenyl]hexafluoropropane (4-BDAF) or 1,1-bis[p-(p-aminophenoxy)phenyl]-1-phenyl-2,2,2-trifluoroethane (3-FEDAM) and PMDA have demonstrated excellent solvent resistance and crystalline melting points (Figure 2.5.12). Furthermore, the solvent resistance was maintained even when 20 and 40% of 6FDA was used as a comonomer with PMDA in combination with 4-BDAF and 3-FEDAM, respectively.

Fay and coworkers have employed bisphenol-M based monomers in polyimide synthesis.[167] The structures of these monomers are given in Figure 2.5.13. While the authors claim that these monomers may yield liquid crystalline polyimides, the polyimides that were, in fact, synthesized and characterized do appear to be

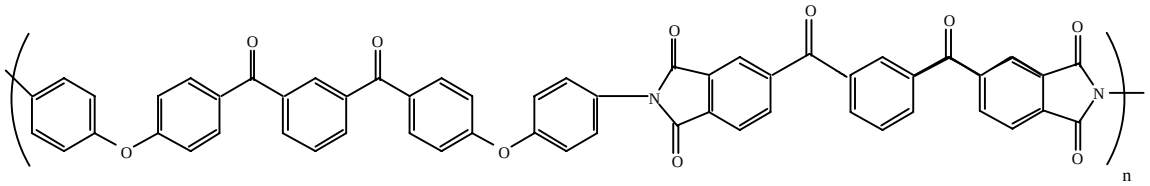

Figure 2.5.9: 1,3-BABB-IPDA

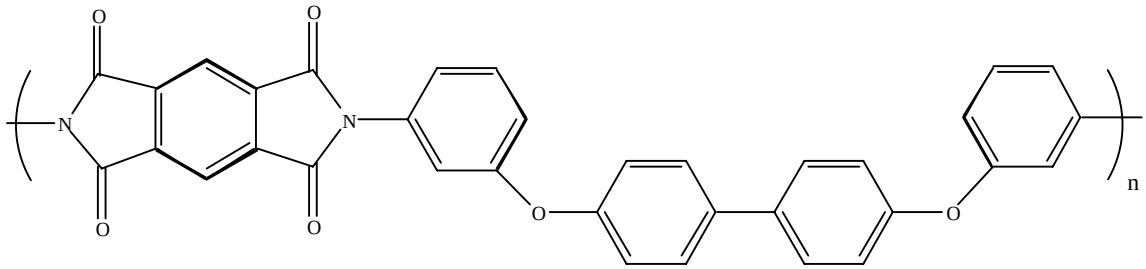

Figure 2.5.10: NEW-TPI

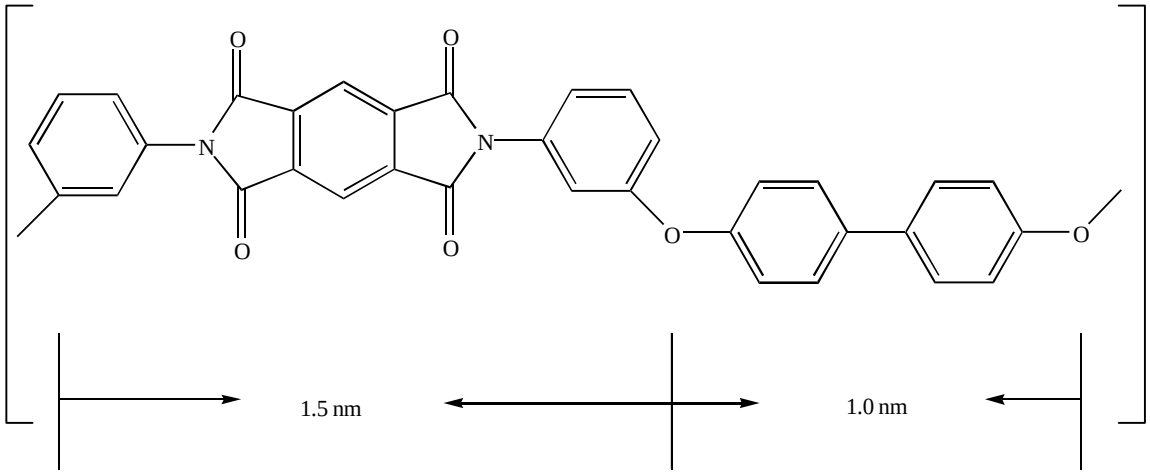

Figure 2.5.11: “Crank-shaft” Conformation of NEW-TPI [159]

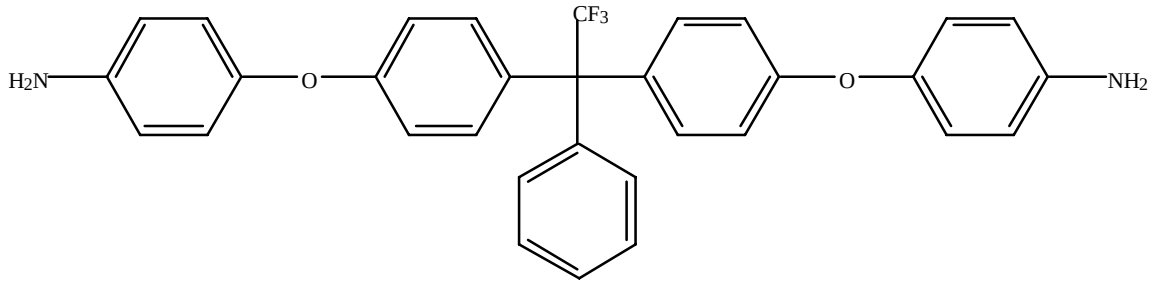

3-FEDAM

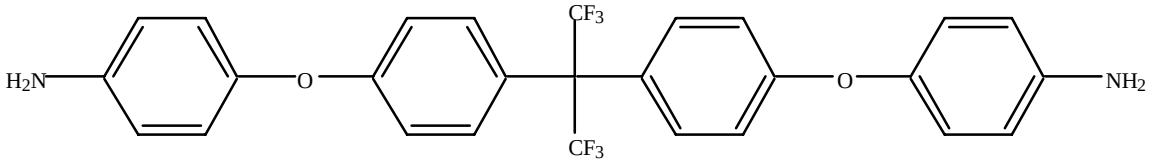

4-BDAF

Figure 2.5.12: 4-BDAF AND 3-FEDAM

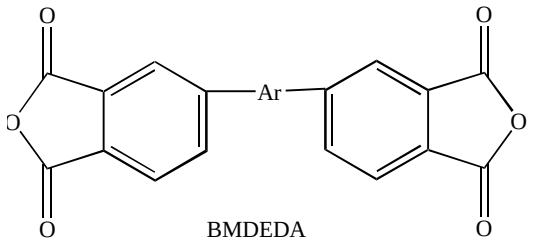

BMDEDA

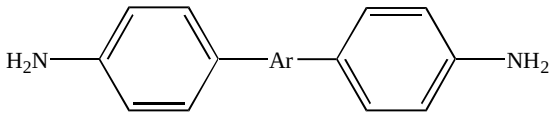

1,3-BAPDBB

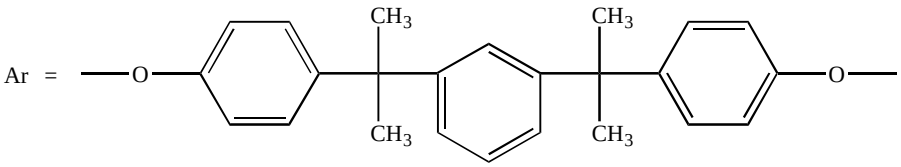

BISPHENOL M LINKAGE

Figure 2.5.13: Bisphenol M Containing Monomers[167]

semicrystalline in nature.

Recently, a series of new diamines was synthesized for the purpose of producing polyimides of improved melt processability.[130] Among these were various bis(m-aminophenoxy) based diamines. Quite a number of the polyimides from these diamines possessed semicrystalline character.

In addition to the incorporation of traditional short length bridging groups, alkylene and oxyalkylene bridging groups of varying lengths have been utilized in preparing semicrystalline polyimides. Harris et al. have been involved with the synthesis of semicrystalline polyimides based upon ODPA and oxyethylene-containing diamines.[168-172] The diamines differed in number of oxyethylene units present and also with regard to the isomerism associated with the aminophenoxy groups at the ends of the diamine (Figure 2.5.14). As received samples of the m,p-based polyimides are able to crystallize from the glass upon heating (Figure 2.5.15). The n=3 sample exhibits polymorphic behavior somewhat similar to that observed for LARC-CPI-2. Nonetheless, higher transition temperatures are observed for samples of p,p- orientation and at smaller values of n.

A direct descendant of the these polyimides is that derived from BTDA and 2,2-dimethyl-1,3-bis(p-aminophenoxy)propane (DMDA) (Figure 2.5.16).[173-175] Like the oxyethylene systems previously mentioned, BTDA-DMDA demonstrates cold crystallization capabilities (Figure 2.5.17). However, this polyimide has a relatively small crystallization window between T_g and T_m of 105°C, as compared to 180°C for PEEK. Furthermore, the T_g is much larger in BTDA-DMDA than in the oxyethylene polyimides, largely due to the rigidity imparted by the neopentyl-like moiety of the diamine. Annealing does raise the melting point of this material to about 360°C without affecting the glass transition temperature. Infrared measurements have shown that the crystallization of BTDA-DMDA involves a combination of intramolecular rotations as well as intermolecular chain packing.[176]

In an effort to develop new liquid crystalline polyimides from BPDA, Kricheldorf discovered that several alkylene diamines served to produce semicrystalline materials.[177] Bis(m-aminophenoxy)alkanes, bis(m-methyl-p-aminophenoxy)alkanes, diaminononane, and diaminodecane all produce crystalline polyimides in conjunction with BPDA. Long

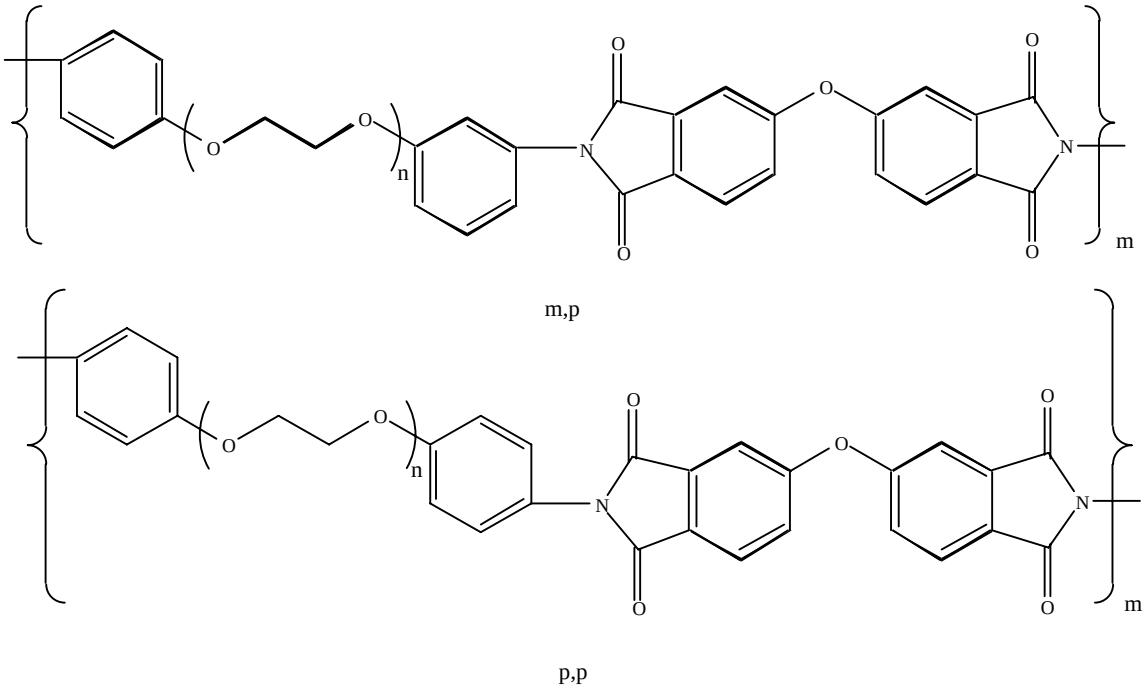

Figure 2.5.14: 1-(m-aminophenoxy)-2-(p-aminophenoxy)ethane (m,p) and 1,2-bis(p-aminophenoxy)ethane (p,p)[168-172]

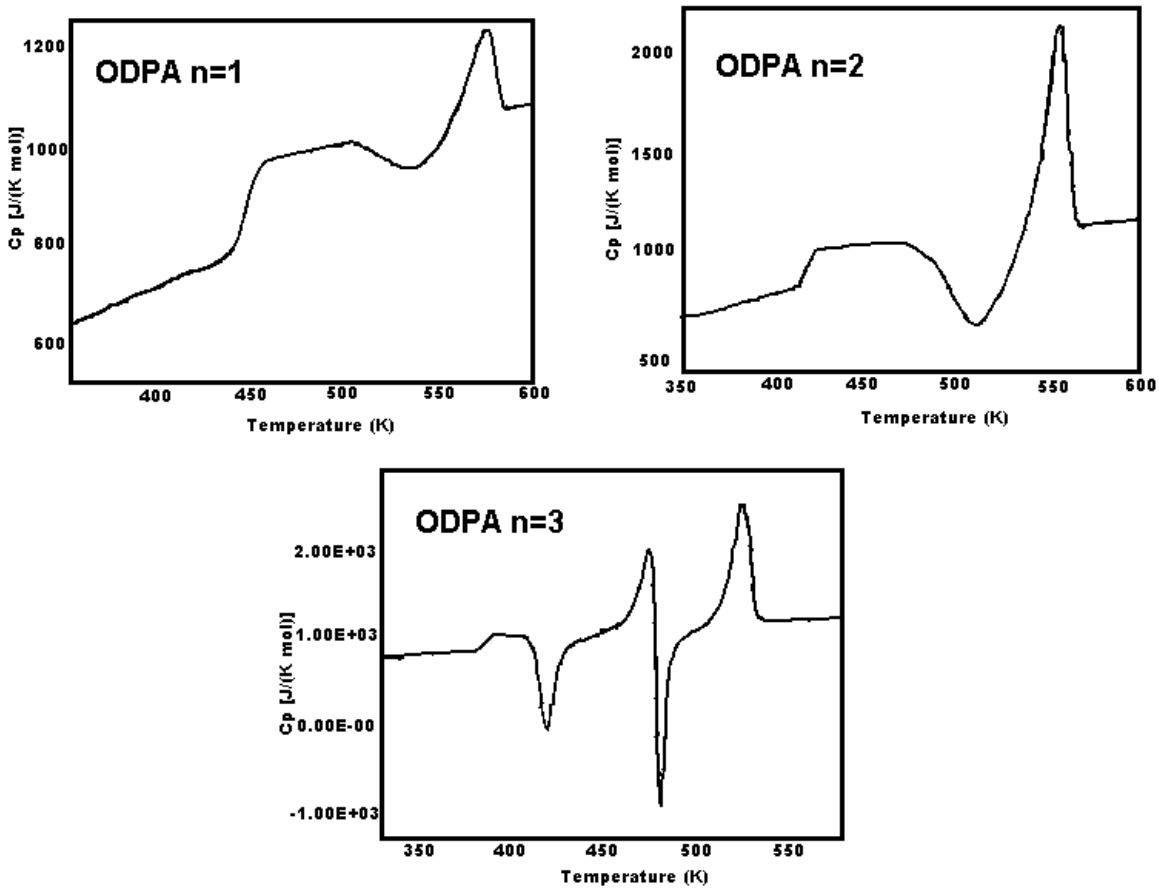

Figure 2.5.15: DSC Thermograms of 1-(m-aminophenoxy)-2-(p-aminophenoxy)ethane-ODPA Polyimides of Varying Oxyethylene Lengths [170]

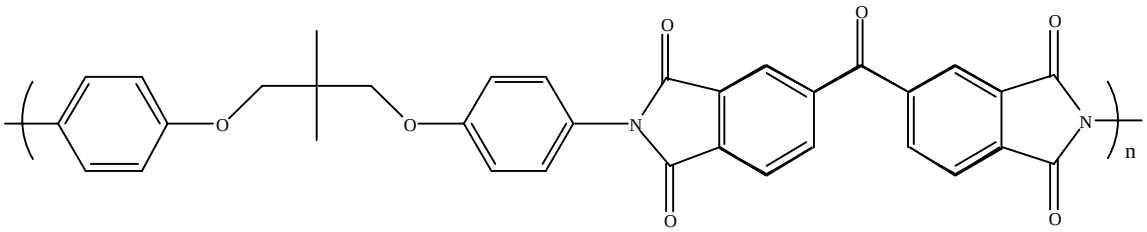

Figure 2.5.16: BTDA-DMDA

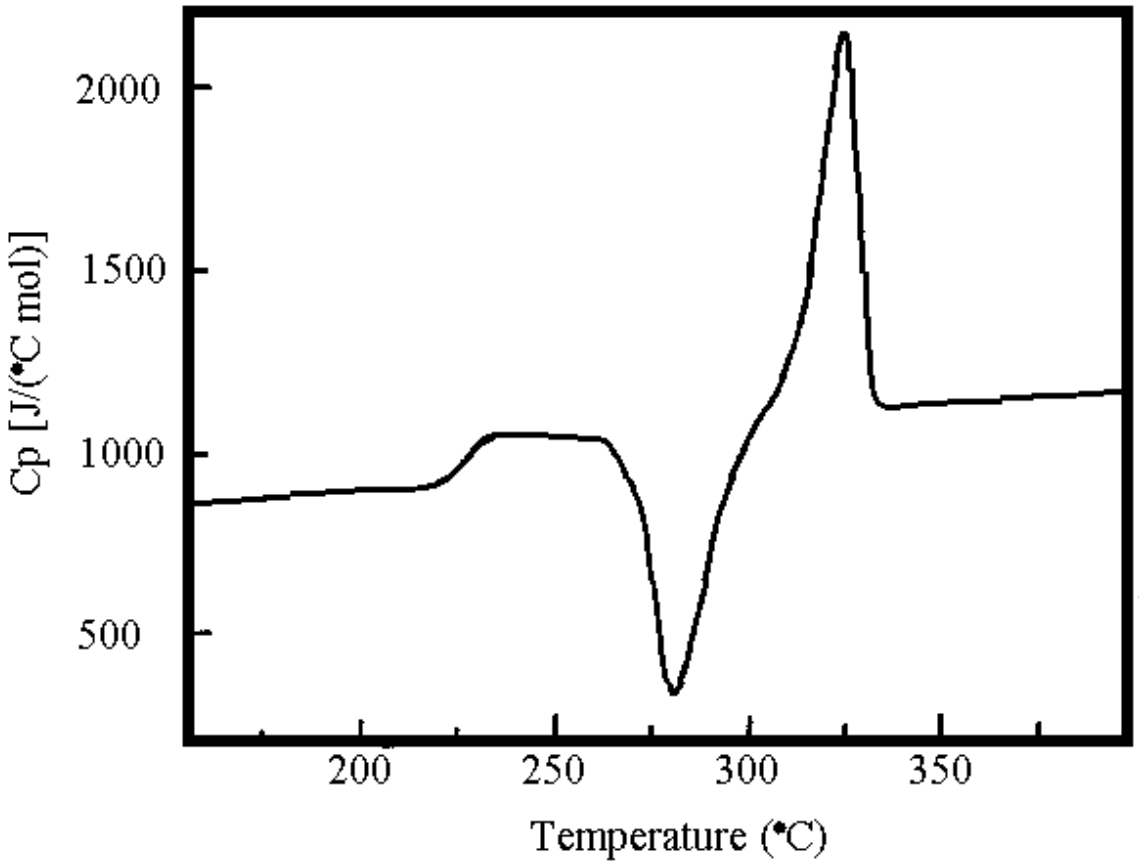

Figure 2.5.17: DSC Thermogram of BTDA-DMDA After Quenching from 400°C [173]

chain bis(p-aminophenoxy)alkanes reacted with BTDA, ODPA, and 4,4'-isopropylidene bis(phthalic anhydride) result in crystalline polymers.

Preston and Tropsha have been among those who have researched in the field of poly(alkylene imides).[33] Specifically, these polymers were synthesized by the classical two-step route in NMP. Polyimides with melting points in the range of 300-450°C were derived from PMDA and alkylene diamines of the formula NH_2-$(CH_2)_n$-NH_2, where n ranged from 5-10 and 12 units.

Polyimides have been prepared from the salt forms of 1,11-diaminoundecane and 4,4'-terphenyltetracarboxylic acid which possessed liquid crystalline character.[178] Polyimides from oxydiphthalic acid and aliphatic diamines were also prepared using high pressure techniques.[179] Analogous polyimides using biphenyltetracarboxylic acid were also made under similar conditions, in which high molecular weights were observed even after relatively short reaction times.[180] Melt reactions done at atmospheric pressure resulted in crosslinked products.

Koning et al. have synthesized semicrystalline polyimides from α,ω-diaminoalkanes by the classical route which demonstrated good thermooxidative stability by thermogravimetric analysis. In particular, the as-made polyimide from BTDA and diaminobutane possesses crystallinity that is easily eliminated upon melting, even utilizing very slow cooling rates. Nevertheless, crystallinity is able to be restored to this polyimide with annealing, and subsequent attempts have been made to further enhance the crystallinity of this polyimide.[181]

Imai and others have conducted high pressure syntheses of crystalline polyimides.[99-102] Specifically, aliphatic diamines were used in a preparation utilizing salts of the monomers (Scheme 2.5.1). By this method high molecular weight polymers were made at pressures ranging from 250 to 600 MPa and at temperatures from 140 to 330°C. Apparently, even the presence of water produced upon cyclization in the closed reaction vessels did not affect the molecular weight. In addition, it was noted that high molecular weights were observed even when the reaction was conducted below the melting point of the resulting polyimide. With these aliphatic diamines an odd-even effect is observed. Odd numbers of methylene units in the diamine produce amorphous polymers, while

crystallinity is seen in polyimides wherein the diamine moiety has an even number of methylene units. The use of aromatic diamines with the salt method results in low molecular weight, crystalline polyimides.

Nagata and coworkers have recently focused on preparing crystalline polyimide powders,[182] by a solution imidization method somewhat similar to what has been reported.[183] Unlike the polyimide powders synthesized by chemical imidization and subsequent milling in earlier investigations[184], the powders prepared by solution imidization had small particle sizes and where spherulitic in nature. Wide angle x-ray diffraction patterns of these polyimide powders and analogous films from thermal imidization suggests that powders are inherently more crystalline than the films (Figure 2.5.18).

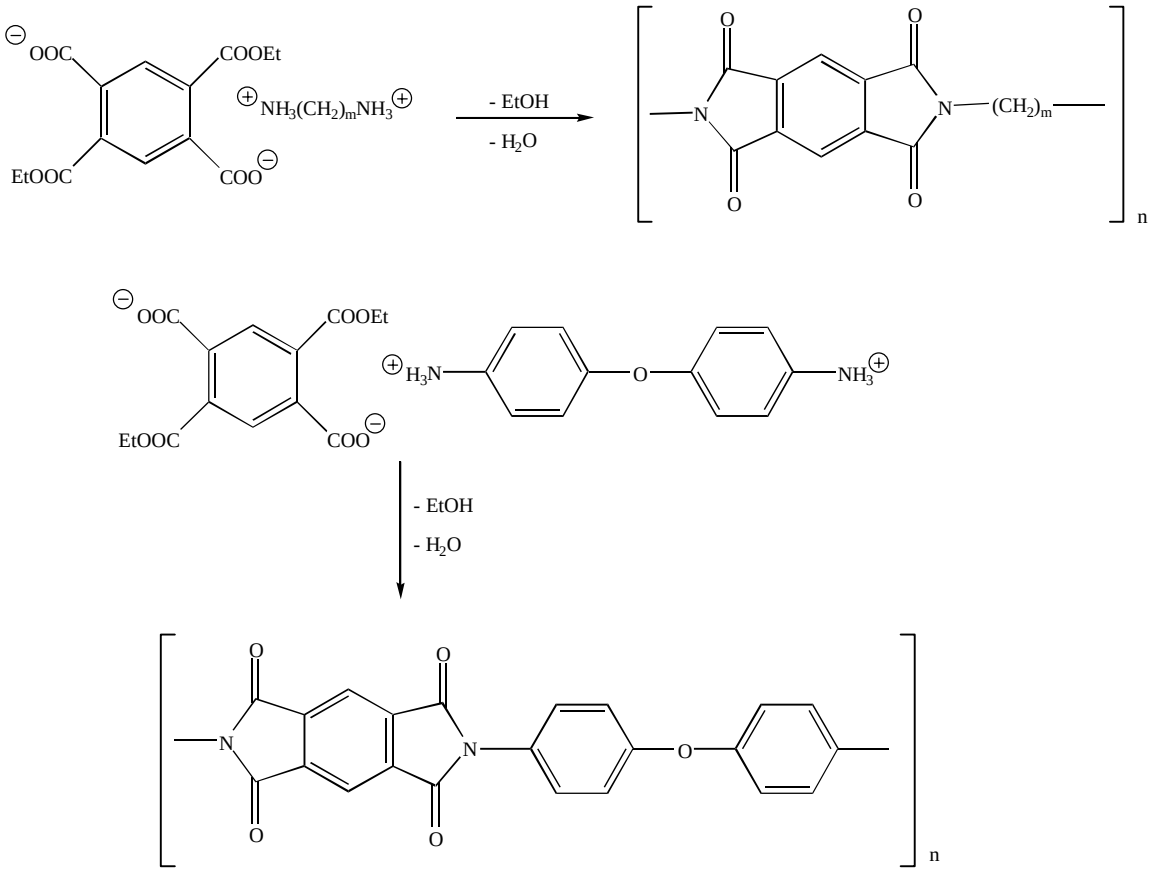

Scheme 2.5.1: Polyimides by High Pressure Salt Method[99]

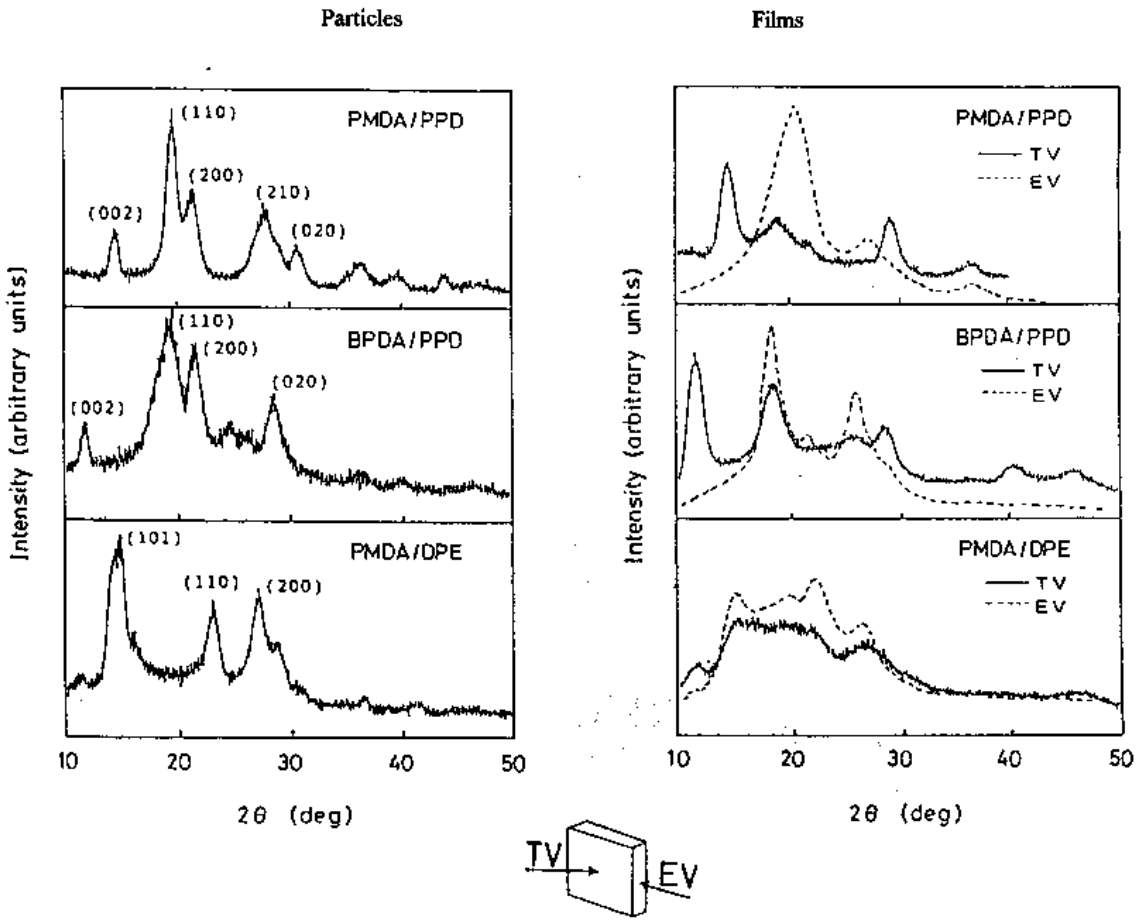

Figure 2.5.18: X-ray Diffractograms of Polyimide Particles and Films[182]

2.6 Polyimides with Pendant Alkyl Side Groups

As noted earlier, one of the main goals in polyimide research has been to improve processability by improving solubility and thermoplasticity. The incorporation of pendant side groups along the polymer chain is one means by which this may be accomplished. A model study was undertaken in which a series of aromatic disubstituted N,N'-diphenylpyromellitimides were synthesized and characterized to measure the effect of pendant groups on various parameters.[185] These side groups have been acknowledged to impart improved solubility. These groups may also disrupt the order in polyimide chains and thereby the ability to crystallize. This is of interest for applications requiring better flow characteristics. Furthermore, the presence of the pendant alkyl moieties can allow for further chemical and physical modifications such as those from crosslinking and photoimaging. What follows is a survey of various developments of polyimide materials possessing these alkyl side groups.

Jensen and Young carried out an extensive investigation involving the synthesis and characterization of polyimides based on p-alkyl-m,p'-diaminobenzophenone (Scheme 2.6.1).[186] The diamines in this work were prepared by Friedel-Crafts coupling of alkylbenzenes with p-nitrobenzoyl chloride (Scheme 2.6.2). The polyimides thermally imidized under vacuum tended to have glass transition temperatures that decreased as the length of the alkyl side group increased. The polyimide with the longest side chain had a T_g about 60°C lower than the polyimide made from m,p'-diaminobenzophenone. The authors also noted an increase in T_g with increasing alkyl length for the polymers prepared by thermal imidization in air, as opposed to under vacuum. This observation hinted at the possibility of crosslinking when the sample is imidized in air. This same pattern applied for results of thermogravimetric analysis, wherein earlier weight loss takes place with vacuum-cured polyimides having longer pendant alkyl chains and later weight loss occurs for these same polyimides which are instead imidized in air. These phenomena prompted the authors to propose processing the alkylated polyimides under vacuum and subsequently submitting the polymers to a post cure in air to induce crosslinking, ultimately producing polyimides with higher glass transitions. Tensile strength

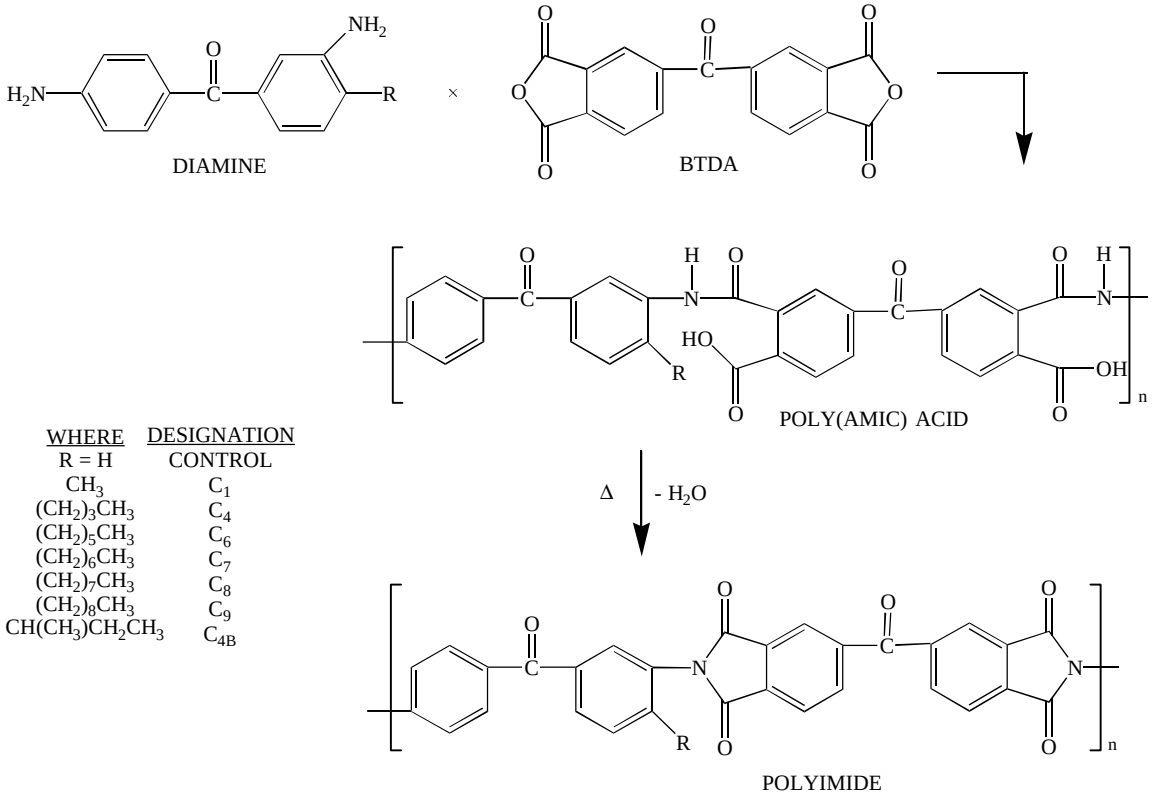

WHERE	DESIGNATION
R = H	CONTROL
CH_3	C_1
$(CH_2)_3CH_3$	C_4
$(CH_2)_5CH_3$	C_6
$(CH_2)_6CH_3$	C_7
$(CH_2)_7CH_3$	C_8
$(CH_2)_8CH_3$	C_9
$CH(CH_3)CH_2CH_3$	C_{4B}

Scheme 2.6.1: Polyimide Synthetic Scheme for Alkylated Benzophenone Diamines with BTDA[186]

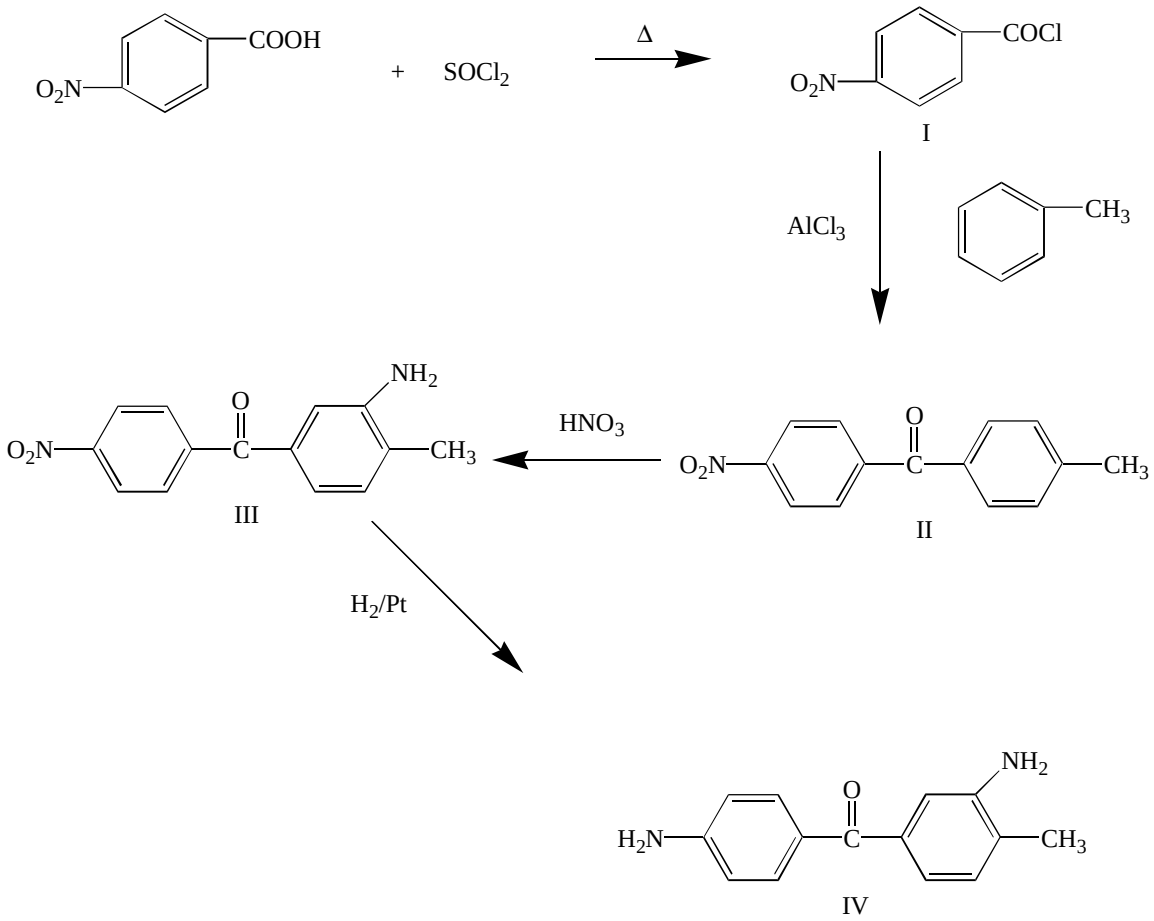

Scheme 2.6.2: Representative Synthetic Scheme for Alkylated Benzophenone Diamines[186]

measurements showed that the presence of pendant alkyl side chains did not have a significant effect on mechanical properties.

Helmer-Metzmann and coworkers have developed rigid rod polyimides with long pendant alkyl side chains (Scheme2.6.3).[187] Specifically, dodecyl groups were attached to totally aromatic pyromellitimides. This action resulted in a large increase in solubility as compared to the non-alkylated substrate.

Ayala et al. utilized a tert-butyl substituted dianhydride in synthesizing polyimides as candidates for gas separation membranes (Scheme2.6.4).[188] The use of such a dianhydride results in an increase in solubility. In comparison with analogous non- and phenyl-substituted dianhydrides, it was discovered that glass transition and decomposition temperatures of the tert-butyl containing polyimides are intermediate.

Moyer and associates have synthesized polyimides from tetramethylphenylene diamine (TMPDA) and BTDA (Figure 2.6.1).[189] These polymers exhibit good solubility in a variety of solvents. In addition, TMPDA-BTDA displays better thermooxidative stability than similar polyimides containing alkyl bridging groups.

Alkylated diamines have been examined for use in poly(etherimides). For example, tetramethylated Bisaniline P has been utilized to produce poly(etherimides) with higher glass transitions (Figure 2.6.2).[111] The use of methylated hydroquinone dianhydride has been reported in the patent literature.[190-192] The use of tetramethyl bisphenol dianhydride has also been reported[190,193,194], as have isopropyl bisphenol dianhydride[194,195], and mono-tert-butyl hydroquinone dianhydride.[196] Similar alkyl-substituted ether diamines have been used for polyimides.[197] The gas separation aspects of some related polyetherimides will be discussed later.

Fluorinated polyimides have become increasingly more important in recent times. The use of trifluoromethyl-containing monomers has extended to meet the needs of such materials. Polyimides evolving from fluorinated PMDA monomers have been fabricated which, by the presence of trifluoromethyl functionalities, have demonstrated relatively high thermal expansion coefficients yet lower dielectric constants, water absorption, and refractive indices.[198] Similarly, trifluoromethyl-containing benzidines also contribute to polyimides with higher thermal expansion coefficients. In a review of polyimides for gas

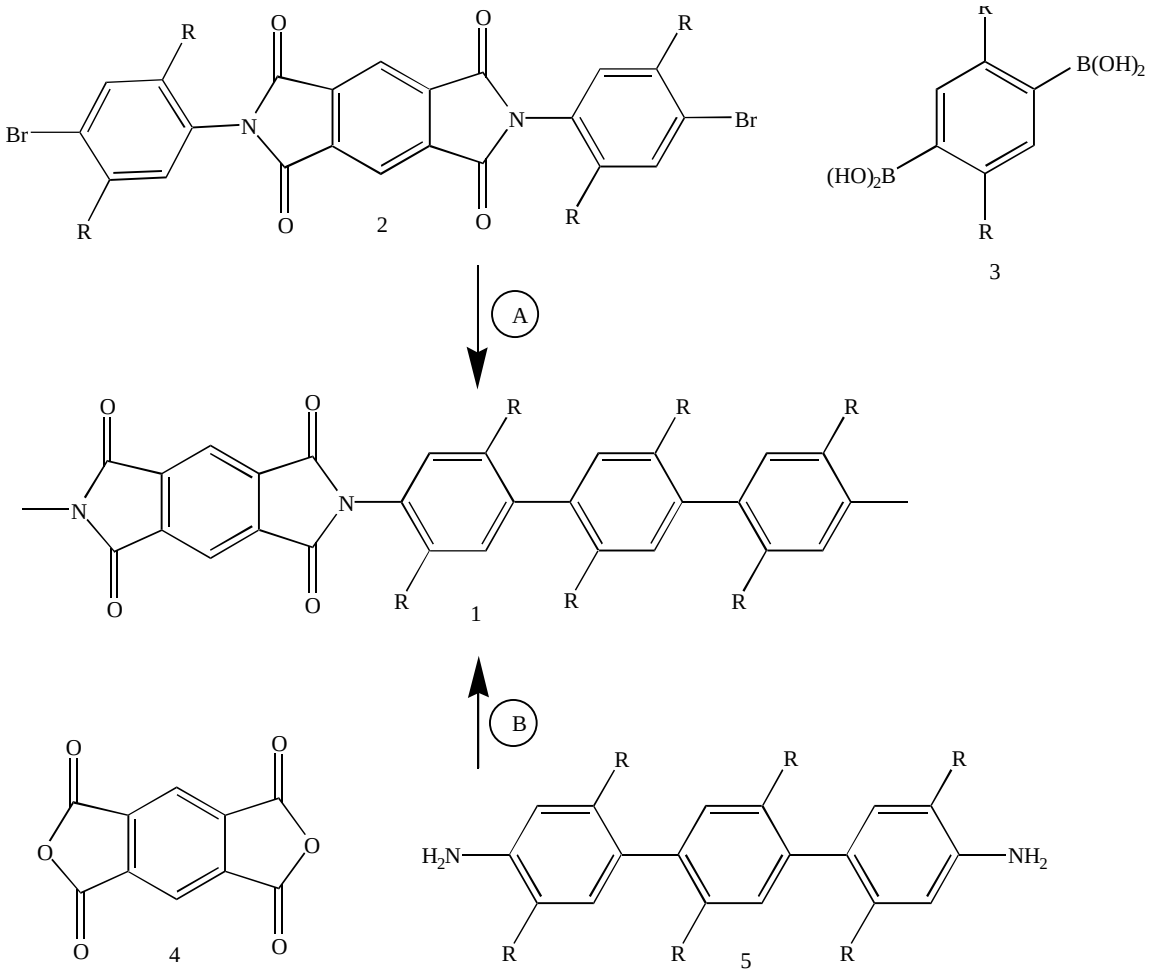

Scheme 2.6.3: Synthetic Schemes for Alkylated Rigid Rod Polyimides[187]

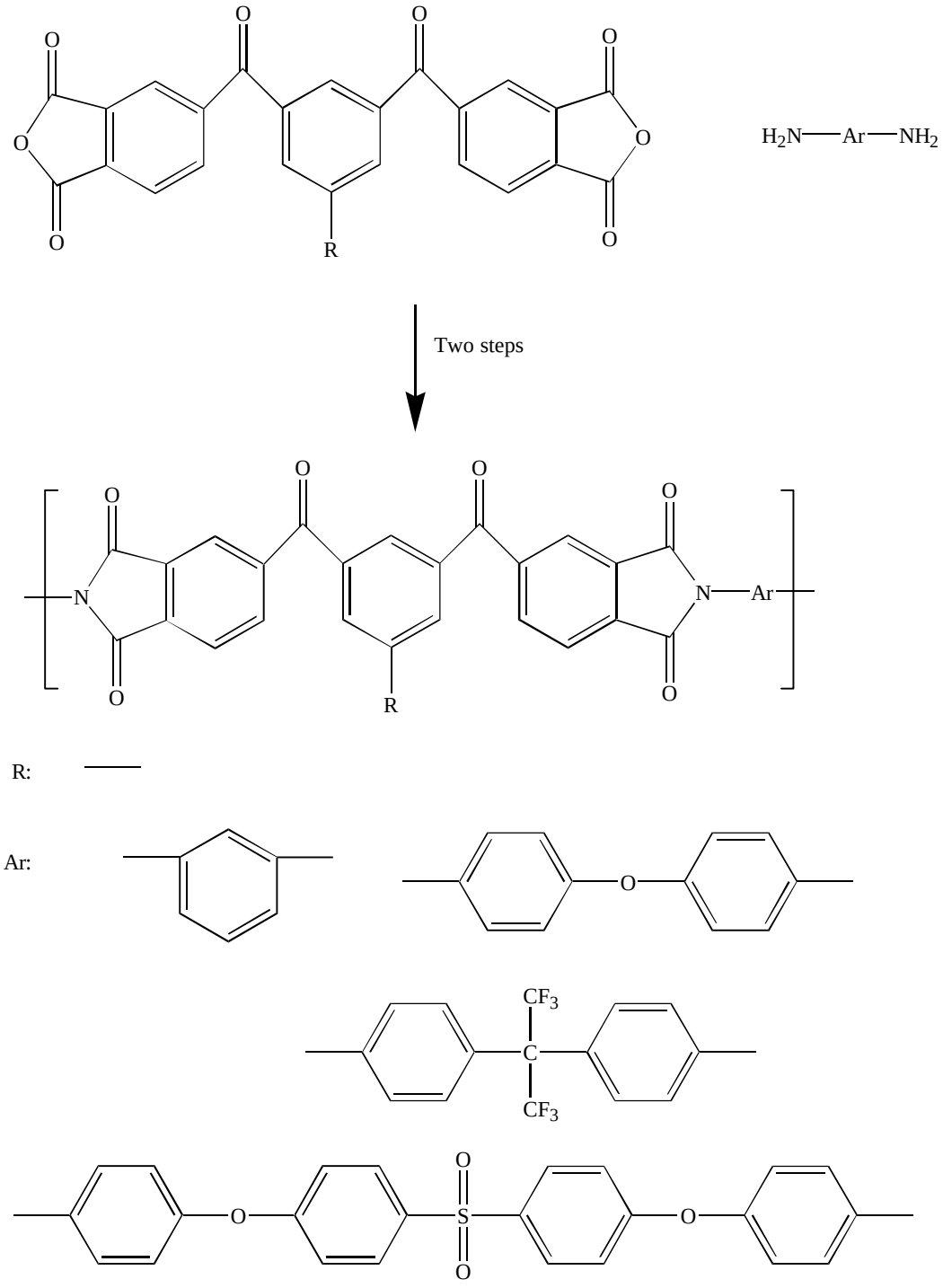

Scheme 2.6.4: Synthetic Scheme for tert-Butyl Substituted, Terphenyl-Containing Polyimides[188]

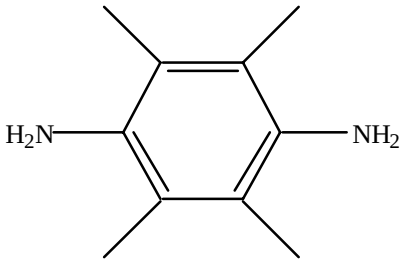

Figure 2.6.1: TMPDA

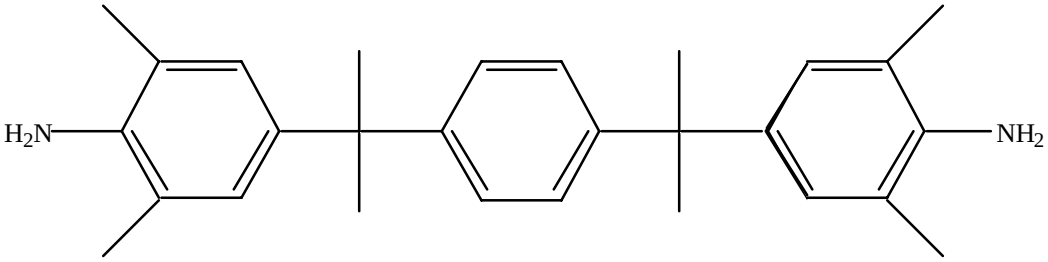

Figure 2.6.2: Tetramethyl Bisaniline P

separation membranes, Langsam has pointed out that trifluoromethyl groups can increase gas permeability.[199] Harris et al. has utilized alkylated benzidine monomers in synthesizing soluble polyimides,[200] using both dimethyl and bis(trifluoromethyl) benzidines for this purpose.

A novel fluoroalkyl diamine, 1-[2,2-bis(trifluoromethyl)-3,3,4,4,5,5,5-heptafluoropentyl]-3,5-diaminobenzene, has been synthesized and used in preparing polyimides (Figure 2.6.3).[201] The design of the monomer is particularly interesting and imparts noteworthy characteristics in the resulting polymers. The placement of the methylene functionality attached directly to the ring serves to maintain the reactivity of the amino groups despite the presence of several electron-withdrawing fluorine atoms. The thermal stabilities of the polyimides prepared from this diamine are aided by the lack of protons adjacent to the methylene moiety, thereby preventing the elimination of HF.

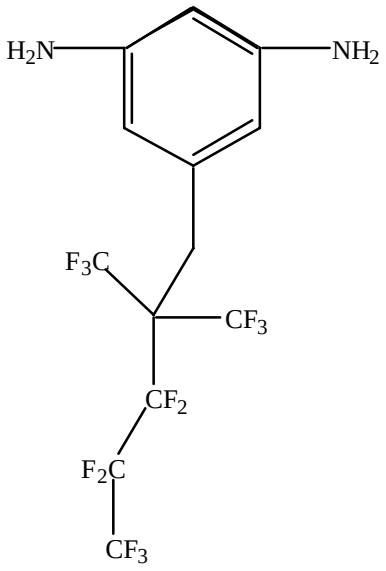

Figure 2.6.3: 1-[2,2-bis(trifluoromethyl)-3,3,4,4,5,5,5-heptafluoropentyl]-3,5-diaminobenzene[201]

In an attempt to study the affect of pendant alkyl side groups on solubility and crystallinity, Liaw and Liaw synthesized 1,4-bis(4-aminophenoxy)-2-tert-butylbenzene (BATB) for use in polyimides (Scheme 2.6.5).[202] Using this diamine, polyimides from BTDA, BPDA, and ODPA show some solubility in NMP and m-cresol upon heating. However, the polyimide made from BATB and DSDA is largely soluble while the polyimide from TPEQ (the non-alkylated analog of BATB) and DSDA is insoluble, demonstrating the impact of the tert-butyl group on solubility. All of the BATB polymers appeared amorphous from x-ray diffraction measurements. Mechanical properties of BATB-PMDA were similar to those of TPEQ-PMDA and better than those of a di-tert-butyl analog of BATB.

Subsequently, an alkyl-containing diamine, 1,4-bis(aminophenoxy)-2,5-di-tert-butylbenzene (BADTB), was synthesized and used in the preparation of polyimides (Scheme 2.6.6).[203] This diamine was made by the coupling of 2,5-di-tert-butylhydroquinone with p-chlorobenzene and subsequent reduction. From x-ray measurements performed on BADTB polyimides, the authors surmised that the di- tert-butyl substitution in the diamine actually leads to an increase in symmetry in the polyimides, which was not observed in the analogous non-alkyl and mono-tert-butyl containing polyimides. As a result, the BADTB-based polyimides are able to more efficiently pack and crystallize. Nevertheless, flexible, transparent polymer films could still be obtained. Yagci and Mathias have also recently prepared analogous BADTB-based polyimides.[204]

Liaw and coworkers have of late developed a new diamine monomer, 2,2'-dimethyl-4,4'-bis(aminophenoxy)biphenyl (DBAPB) (Figure 2.6.4).[205] The structure is shown below in Figure 2.6. The polyimide from DBAPB and DSDA exhibited solubility in aprotic solvents, unlike its unalkylated analog.

Becker and Schmidt have investigated the use of tert-butyl-p-phenylene diamine in synthesizing poly(amic esters) and polyimides.[206] This was one of the few examples of tert-butyl incorporation along the polyimide backbone.

Chiang and Mei have investigated the photocoupling of pendant alkyl-containing polyimides with aromatic ketones.[207] This research was based on the development of

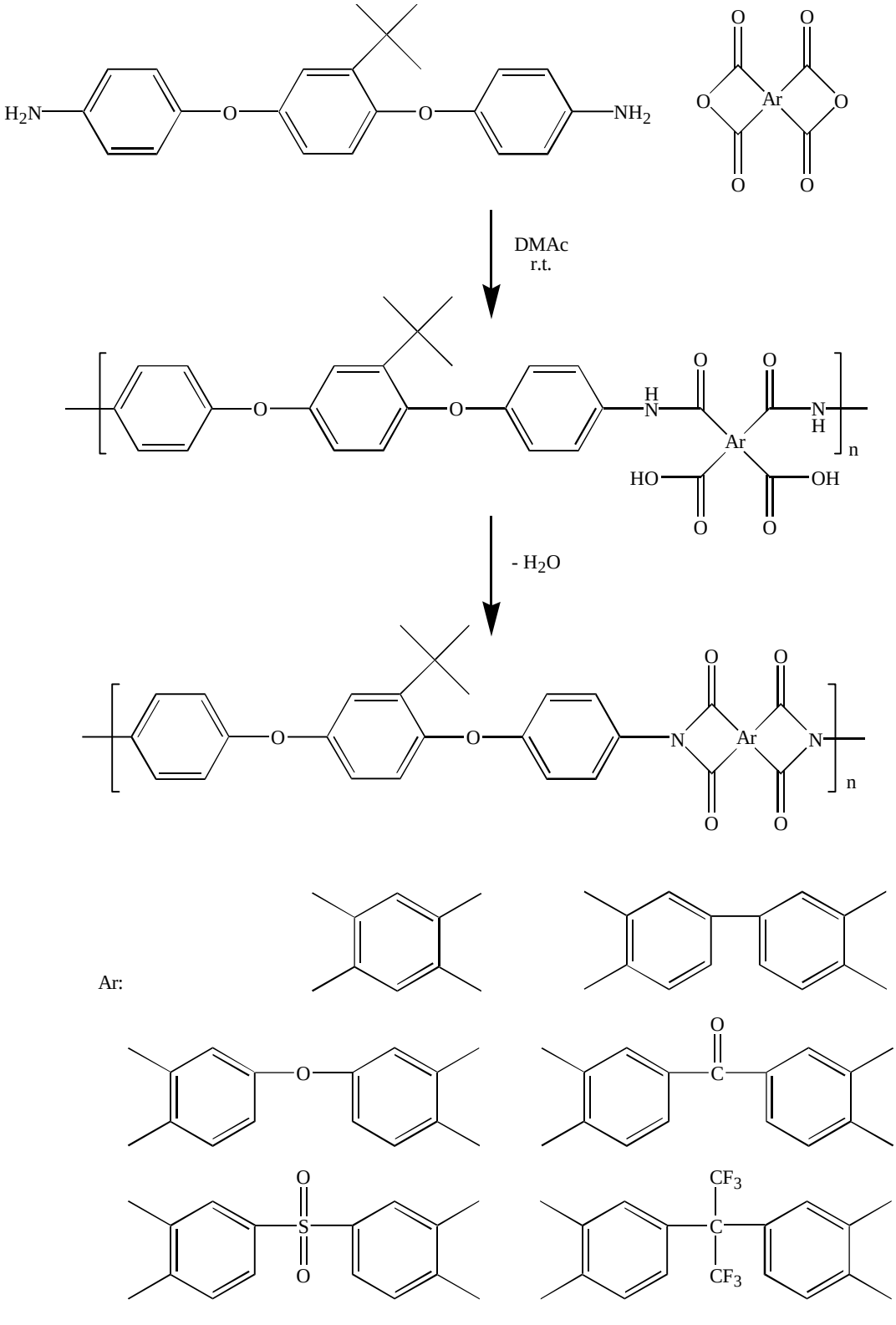

Scheme 2.6.5: Synthetic Scheme for BATB-Based Polyimides[202]

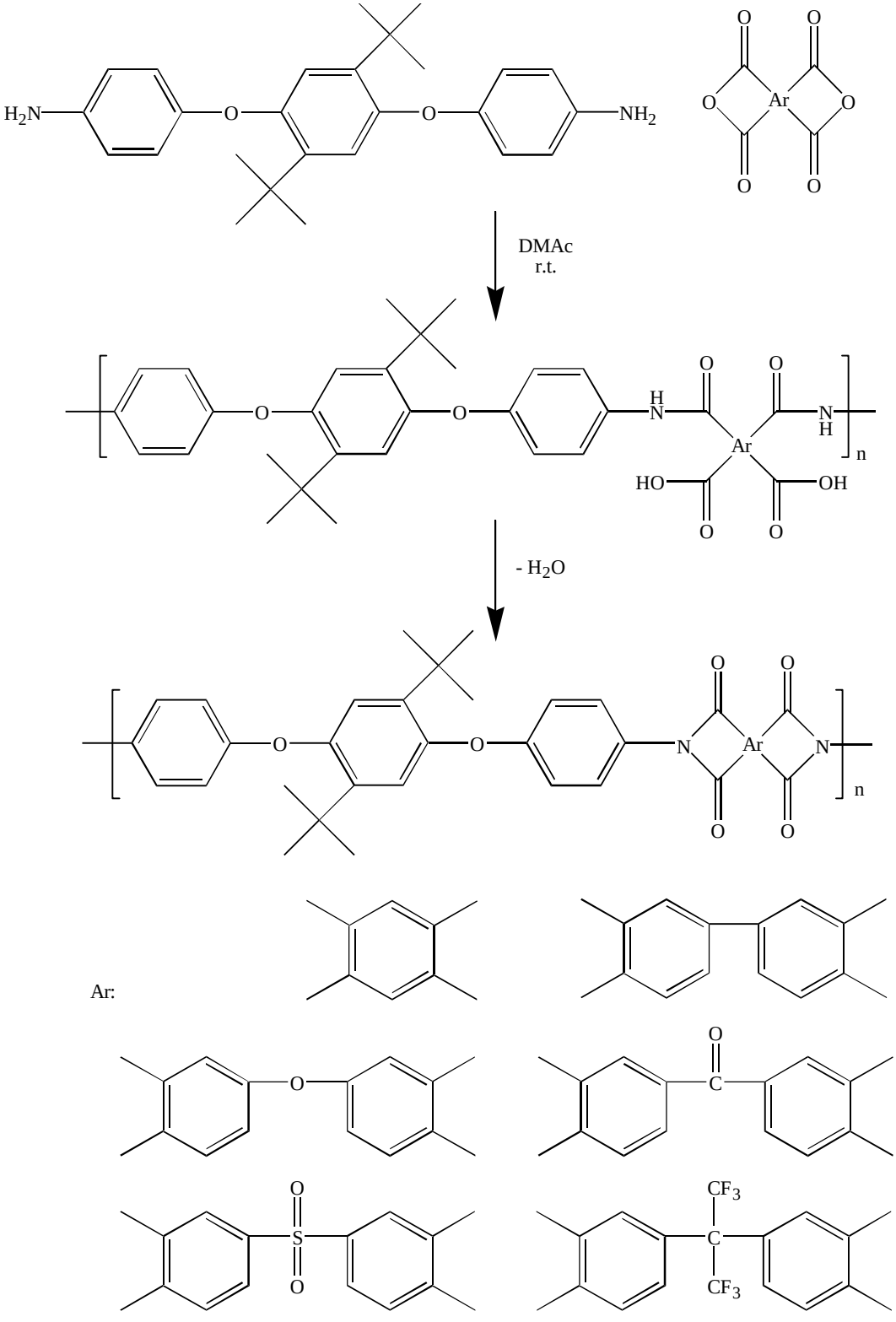

Scheme 2.6.6: Synthetic Scheme for BADTB-Based Polyimides[203]

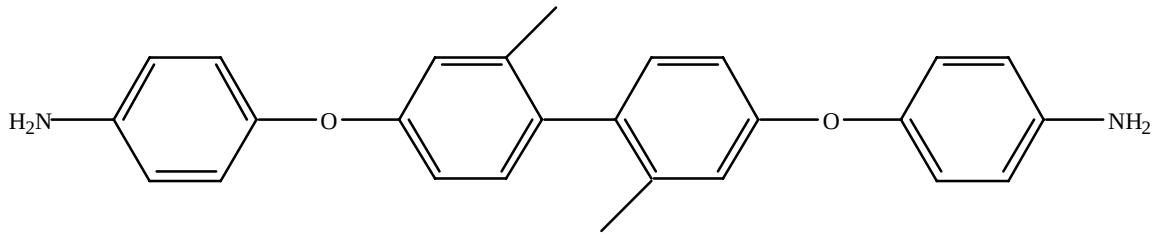

Figure 2.6.4: DBAPB[205]

photoimageable, fully imidized polyimides from BTDA and alkyl substituted diamines.[208] The work of Lin and coworkers demonstrated that photocoupling occurs by the hydrogen abstraction of a photoexcited ketone from an alkyl group, followed by the coupling of the radicals formed.[209] Chang and Mei envisioned the possibility of increasing the solubility of a specific polyimide by attaching free aromatic ketones to pendant alkyl groups along the polyimide backbone by UV-mediated coupling. However, the findings showed that hydrogen bonding resulted from the photocoupling, which actually caused a decrease in the polyimide solubility (Scheme 2.6.7). Chiang and Mei have also utilized methylthiomethyl diamines with BTDA to synthesize photosensitive polyimides with increased solubility.[210] Pfeifer has developed a series of several photosensitive and photocrosslinkable polyimides derived from diamines with alkyl groups ortho to the amine functionality.[211]

Extensive research has been conducted on pendant alkyl-containing polyimides for potential use as gas separation membrane materials. The presence of these functionalities have been tabbed as influencing gas permeability, selectivity, or both. For example, it has been discovered that the use of diamines with pendant alkyl groups in polyimides, polyamides, and poly(amide-imides) blended with polyimides can produce gas separation materials with both good selectivity and permeability.[212]

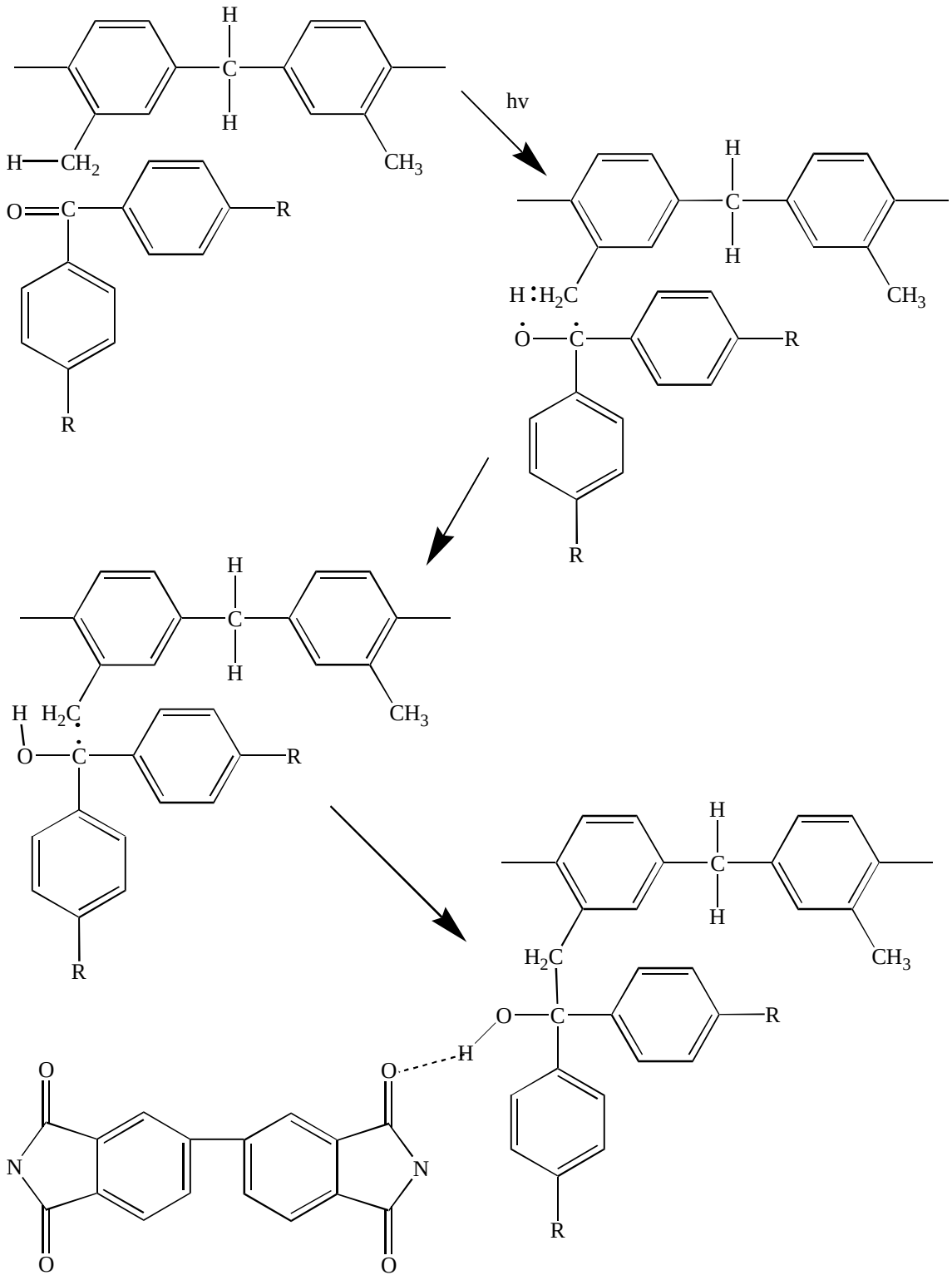

Scheme 2.6.7: Photocoupling and Hydrogen Bonding of Alkylated Polyimide with Benzophenone[210]

Polyimides derived from 5-(2,5-dioxo-tetrahydrofuryl)-3-methyl-3,3'-cyclohexane-1,2-dicarboxylic anhydride (DTMCDA) have been made.[213] The structure of DTMCDA is given below in Figure 2.6.5. Homo and copolymers derived from this monomer show exceptional permselectivity with nitrogen/oxygen gas mixtures.

It has been noted throughout the literature that employing aromatic diamines with alkyl groups ortho to the amine moiety can yield polyimides with improved environmental stability and permeability.[214-217] This comes as a result of the conformation of these alkyl groups relative to the imide linkage, causing hindered rotation about the C-N bond. Consequently, an increase in free volume is experienced which leads to an increase in permeability. Examples of this phenomena are polyimides produced from 2,4-diaminoxylene and TMPDA with BTDA. It has been noted that the solubilities and glass transition temperatures of these polyimides are enhanced by the presence of methyl groups.[218] Moreover, Hayes has pointed out that phenylene diamines with pendant alkyl groups ortho to the amine moiety can be employed to yield polyimides of greater hydrolytic stability.[197]

Li and associates have conducted research demonstrating that poly(ether imides) derived from methylated methylene dianilines have enhanced permeability with increasing methyl substitution on the dianilines.[219] This effect becomes more evident with diamines with ortho substituted methyl groups as opposed to their meta substituted isomers. In addition, selectivity is improved using ortho substituted dianilines.

Eastmond et al. have studied poly(ether imides) based on ether dianhydrides with pendant di-and tetra-tert-butyl and t-amyl groups for use as gas separation materials.[220] Their findings suggested that di-tert-butyl containing dianhydrides contributed to better permeability, although worse selectivity than similar dimethyl-containing dianhydrides. Also, the flexibility imparted by pendant di-t-amyl groups on hydroquinone ether dianhydride lowers permselectivity. The authors concluded that poly(ether imides) with bulky substituents have inherently better permeability.

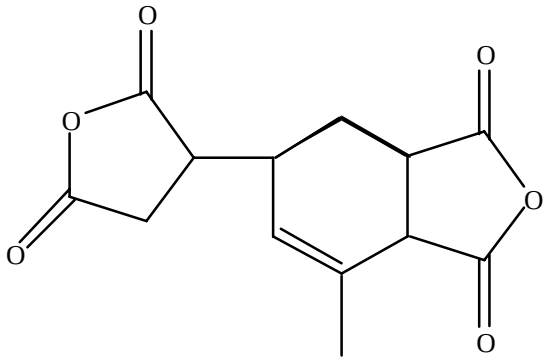

Figure 2.6.5: DTMCDA[213]

Chapter 3: Experimental

3.1 Solvents and Reagents

3.1.1 Solvents

3.1.1.1 1-Methyl-2-Pyrrolidone (NMP: Fisher) was dried over calcium hydride for at least 12 hours, distilled under reduced pressure, and stored over molecular sieves (b.p. 205°C/760 mm, 82°C/10 mm).

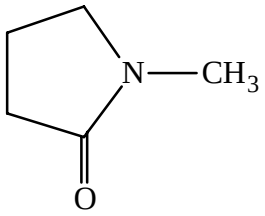

3.1.1.2 N,N-Dimethylacetamide (DMAc: Fisher) was dried over calcium hydride for at least 12 hours, distilled under reduced pressure, and stored over molecular sieves (b.p. 165°C/760 mm).

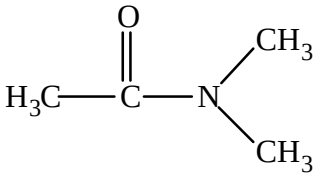

3.1.1.3 *o*-Dichlorobenzene (DCB: Fisher) was dried over phosphorus pentoxide for at least 12 hours and distilled under reduced pressure (b.p. 180°C/760 mm).

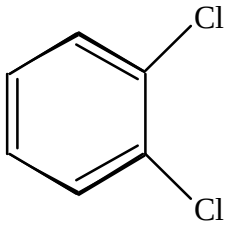

3.1.1.4 Acetic anhydride (Ac_2O: Fisher) was used as received (b.p. 138°C).

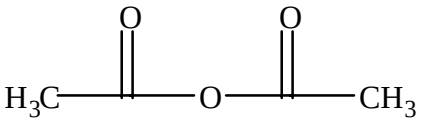

3.1.1.5 Acetic acid (AcOH: Fisher) was used as received (b.p. 116°C).

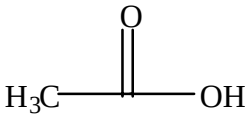

3.1.1.6 Triethylamine (NEt_3: Fisher) was used as received (b.p. 89°C).

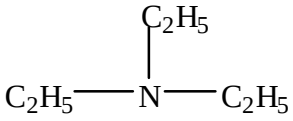

3.1.1.7 Sulfuric Acid (Mallinckrodt) was used as received.

3.1.1.8 Toluene (Fisher) was used as received (b.p. 110°C).

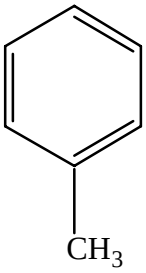

3.1.1.9 Ethanol (Absolute, AAPER Alcohol and Chemical) was used as received (b.p. 79°C).

3.1.1.10 Tetrahydrofuran (THF: Fisher) was used as received (b.p. 67°C).

3.1.1.11 Diethyl ether (Et_2O: Mallinckrodt) was used as received (b.p. 35°C).

3.1.1.12 Methylene chloride (Fisher) was used as received (b.p. 40°C).

3.1.1.13 Hexanes (EM Chemicals) were used as received (b.p. 68°C).

3.1.1.14 Isobutanol (Aldrich) was used as received (b.p. 108°C).

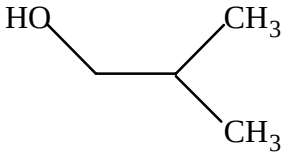

3.1.2 Monomers and Reagents

3.1.2.1 General reagents

3.1.2.1.1 Aluminum chloride

Supplier: Fisher

Molecular Formula: $AlCl_3$

Molecular Weight: 133.35

Purification: used as received

3.1.2.1.2 Phosphoric acid

Supplier: Aldrich

Molecular Formula: H_3PO_4

Molecular Weight: 98

Melting Point: 41-44°C

Purification: used as received

3.1.2.1.3 Potassium carbonate

Supplier: Fisher

Molecular Formula: K_2CO_3

Molecular Weight: 138.21

Melting Point: 891°C

Purification: used as received

3.1.2.1.4 Palladium on carbon

Supplier: Aldrich

Molecular Formula: 10% Pd/C

Purification: used as received

3.1.2.1.5 t-Butanol

Supplier: Aldrich

Molecular Formula: $C_4H_{10}O$

Molecular Weight: 74.12

Melting Point: 25-26°C

Purification: used as received

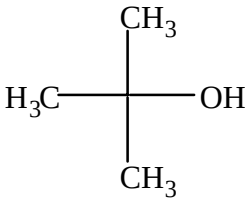

3.1.2.1.6 *p*-fluoronitrobenzene

Supplier: Aldrich

Molecular Formula: $C_6H_4NO_2F$

Molecular Weight: 141.1

Boiling Point: 205°C

Purification: used as received

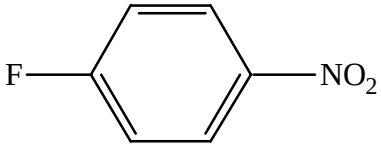

3.1.2.1.7 Hydrazine monohydrate

Supplier: Acros

Molecular Formula: $NH_2NH_2 \cdot H_2O$

Molecular Weight: 50.07

Boiling Point: 120°C

Purification: used as received

3.1.2.2 Bisphenols

3.1.2.2.1 Resorcinol

Supplier: Alfa Aesar

Molecular Formula: $C_6H_6O_2$

Molecular Weight: 110.11

Melting Point: 118°C

Purification: used as received

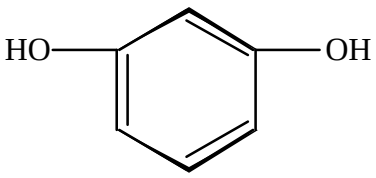

3.1.2.2.2 2-Methylresorcinol

Supplier: Aldrich

Molecular Formula: $C_7H_8O_2$

Molecular Weight: 124.14

Melting Point: 115°C

Purification: recrystallized from benzene prior to use

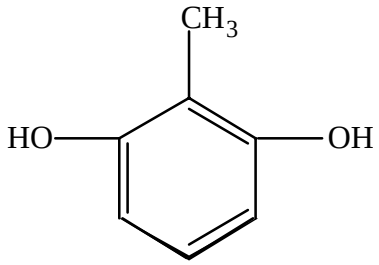

3.1.2.2.3 5-Methylresorcinol (Orcinol)

Supplier: Aldrich

Molecular Formula: $C_7H_8O_2$

Molecular Weight: 124.14

Melting Point: 107-108°C

Purification: Anhydrous 5-methylresorcinol was obtained from the recrystallization of 5-methylresorcinol monohydrate (orcinol monohydrate) from chloroform.

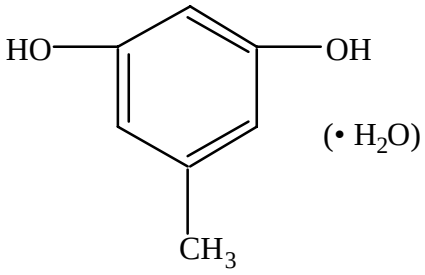

3.1.2.2.4 4-Hexylresorcinol

Supplier: Aldrich

Molecular Formula: $C_{12}H_{18}O_2$

Molecular Weight: 194.27

Melting Point: 65-67°C

Purification: used as received

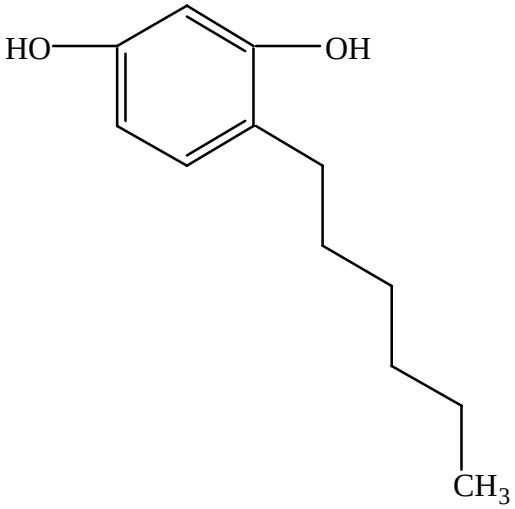

3.1.2.3 Dianhydrides and monofunctional anhydrides

3.1.2.3.1 3,3',4,4'-Biphenyltetracarboxylic dianhydride (BPDA)

Supplier: Chriskev

Molecular Formula: $C_{16}H_6O_6$

Molecular Weight: 294.22

Melting Point: 298-300°C

Purification: BPDA was obtained in monomer grade and was dried under reduced pressure for 12 hours at 150°C prior to use.

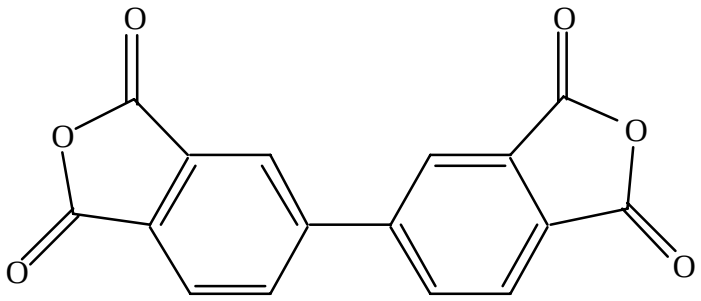

3.1.2.3.2 4,4'-Oxydiphthalic anhydride (ODPA)

Supplier: Occidental Chemical

Molecular Formula: $C_{16}H_6O_7$

Molecular Weight: 310.23

Melting Point: 225-227°C

Purification: ODPA was obtained in monomer grade and was dried under reduced pressure for 12 hours at 150°C prior to use.

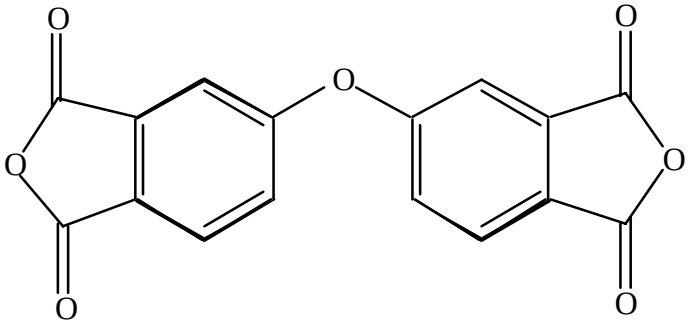

3.1.2.3.3 Pyromellitic dianhydride (PMDA)

Supplier: Allco Chemical

Molecular Formula: $C_{10}H_2O_6$

Molecular Weight: 218.12

Melting Point: 284-286°C

Purification: PMDA was obtained in monomer grade and was dried under reduced pressure for 12 hours at 150°C prior to use.

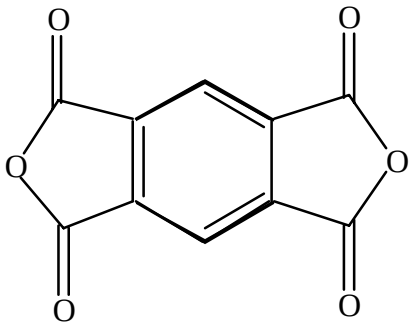

3.1.2.3.4 3,3',4,4'-Benzophenonetetracarboxylic dianhydride (BTDA)

Supplier: Allco

Molecular Formula: $C_{17}H_6O_7$

Molecular Weight: 322.23

Melting Point: 224-226°C

Purification: BTDA was obtained in monomer grade and was dried under reduced pressure for 12 hours at 150°C prior to use.

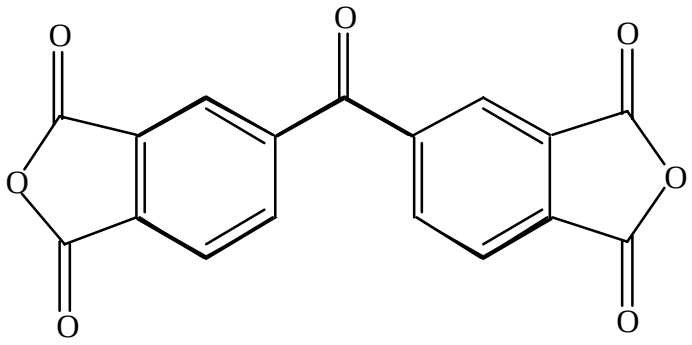

3.1.2.3.5 Hexafluoroisopropylidene-2,2'-bisphthalic acid anhydride (6FDA)

Supplier: Hoechst Celanese

Molecular Formula: $C_{19}H_6F_6O_6$

Molecular Weight: 444

Melting Point: 247°C

Purification: 6FDA was obtained in monomer grade and was dried under reduced pressure for 12 hours at 150°C prior to use.

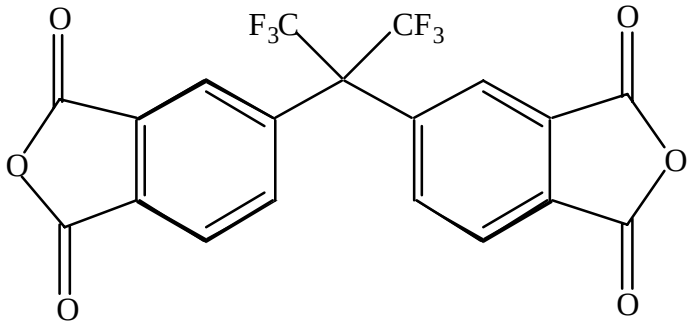

3.1.2.3.6 Phthalic anhydride (PA)

Supplier: Aldrich

Molecular Formula: $C_8H_4O_3$

Molecular Weight: 148.12

Melting Point: 130-131°C

Purification: PA was sublimed at 110°C under reduced pressure prior to use.

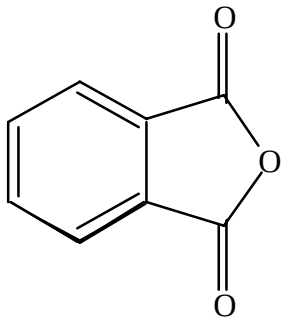

3.1.2.3.7 Succinic anhydride (SA)

Supplier: Aldrich

Molecular Formula: $C_4H_4O_3$

Molecular Weight: 100.07

Melting Point: 119-120°C

Purification: used as received

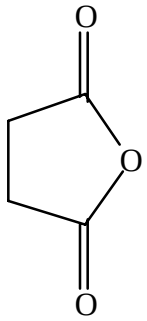

3.1.2.4 Diamines

3.1.2.4.1 1,4-bis(4-aminophenoxy)benzene (TPEQ)

Supplier: Ken Seika

Molecular Formula: $C_{18}H_{16}N_2O_2$

Molecular Weight: 292.34

Melting Point: 172-173°C

Purification: TPEQ was recrystallized from toluene and dried at 120°C prior to use.

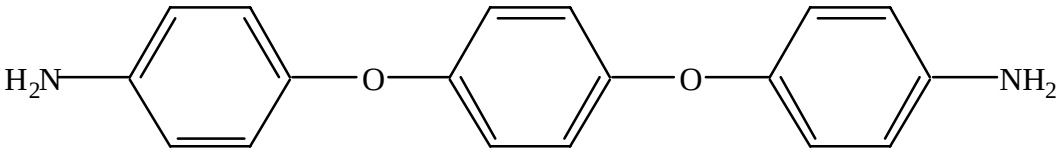

3.1.2.4.2 1,3-bis(4-aminophenoxy)benzene (TPER)

Supplier: Ken Seika

Molecular Formula: $C_{18}H_{16}N_2O_2$

Molecular Weight: 292.34

Melting Point: 116-118°C

Purification: TPER was recrystallized from ethanol and dried at 85-90°C prior to use.

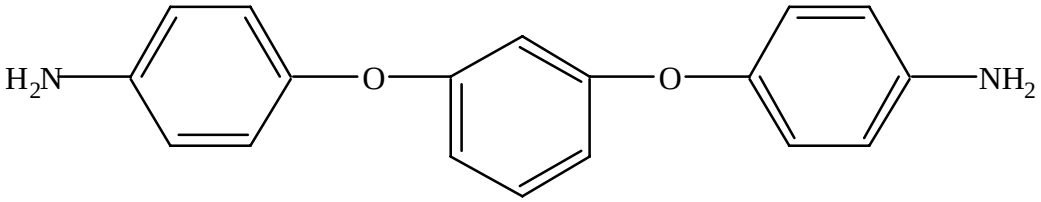

3.1.2.4.3 4,4'-bis(4-aminophenoxy)benzene (BAPB)

Supplier: Ken Seika

Molecular Formula: $C_{24}H_{20}N_2O_2$

Molecular Weight: 368.44

Melting Point: 170-172°C

Purification: used as received

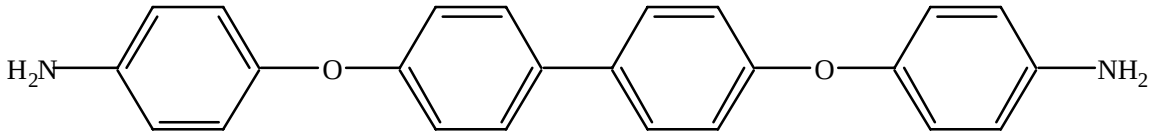

3.2 Monomer Synthesis

3.2.1 Synthesis of 2,6-bis(4-aminophenoxy)toluene (2,6-BAPT)

3.2.1.1 2,6-bis(4-nitrophenoxy)toluene (2,6-BNPT) was synthesized via the nucleophilic aromatic substitution reaction of *p*-fluoronitrobenzene with 2-methylresorcinol. To a 3-neck, 250 ml round bottom flask fitted with a nitrogen inlet, thermometer, overhead stirrer, Dean-Stark trap, and condenser were introduced 12.41g (0.1 mol) of 2-methylresorcinol, 29.02 g (0.21 mol) of potassium carbonate, 130 ml of DMAc, and 25 ml of toluene. The pink-red reaction mixture was heated to 145°C for at least 4 hours in order to dehydrate the system. After cooling, 21.7 ml (0.205 mol) of *p*-fluoronitrobenzene was added and the reaction mixture was again heated to 145°C for 5 hours to yield a spinach-green mixture. The excess toluene was distilled off, and the mixture was allowed to cool to room temperature and subsequently poured into water, resulting in a yellow solid. The solid was filtered and washed thoroughly with water and methanol. Afterwards, the product was recrystallized from acetic acid in 95% yield (m.p. 147-148°C). Elemental analysis calculated for $C_{19}H_{14}N_2O_6$ (366.33 g/mole): C, 62.30%; H, 3.85%; N, 7.65%. Found: C, 62.20%; H, 3.84%; N, 7.56%.

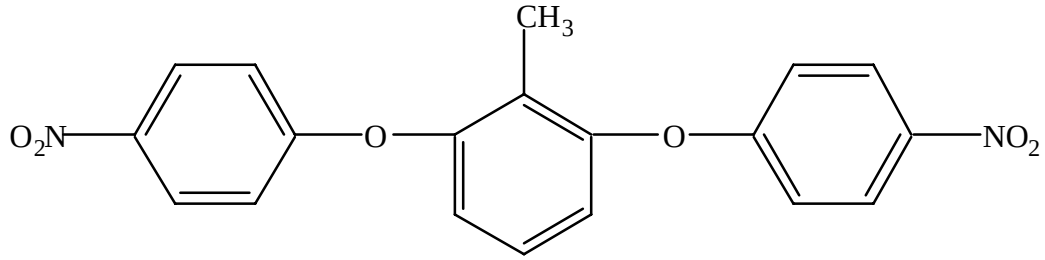

3.2.1.2 2,6-bis(4-aminophenoxy)toluene (2,6-BAPT) was synthesized via the reduction of

2,6-BNPT. To a 3-neck, 250 ml round bottom flask fitted with a magnetic stirrer, nitrogen inlet, addition funnel, and condenser was introduced 10.99 g (0.03 mol) of 2,6-BNPT with 100 ml THF. Upon dissolution of the 2,6-BNPT, 500 mg of 10% Pd/C catalyst was added along with 20 ml of ethanol. The reaction mixture was then heated to 50°C, at which point 10 ml (0.2 mol) of hydrazine monohydrate was added dropwise to the mixture. The mixture was allowed to stir at reflux for 12 hours. Afterwards, the catalyst was filtered off using Celite, leaving a yellow solution. Evaporation of the solvent yielded an off-white product which was subsequently recrystallized from ethanol to afford the title compound in 70% yield (m.p. 147-148°C). Mass spectrum (M^+ calculated for 306.36 g/mole) m/z (%): 307 (15), 306 (73), 212 (17), 197 (10), 183 (13), 170 (18), 152 (17), 108(100), 93 (46), 80 (83), 65 (42). Elemental analysis calculated for $C_{19}H_{18}N_2O_2$ (306.36 g/mole): C, 74.49%; H, 5.92%; N, 9.14%. Found: C, 74.29%; H, 6.13%; N, 8.95%.

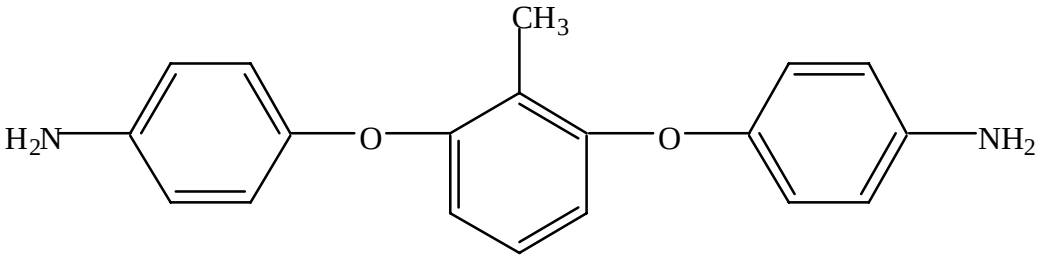

3.2.2 Synthesis of 3,5-bis(4-aminophenoxy)toluene (3,5-BAPT)

3.2.2.1 3,5-bis(4-nitrophenoxy)toluene (3,5-BNPT) was synthesized via the nucleophilic aromatic substitution reaction of *p*-fluoronitrobenzene with 5-methylresorcinol. Using identical reaction conditions and workup as described previously for 2,6-BNPT afforded the title compound in 95% yield (m.p. 155-156°C). Elemental analysis calculated for $C_{19}H_{14}N_2O_6$ (366.33 g/mole): C, 62.30%; H, 3.85%; N, 7.65%. Found: C, 62.00%; H, 3.87%; N, 7.59%.

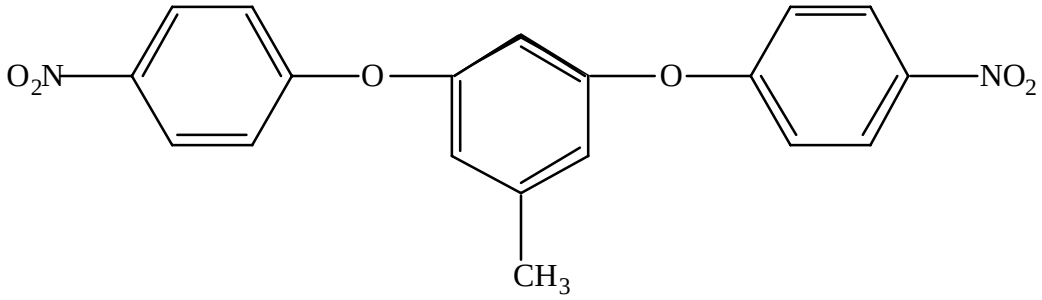

3.2.2.2 3,5-bis(4-aminophenoxy)toluene (3,5-BAPT) was synthesized via the reduction of 3,5-BNPT. Using identical reaction conditions and workup as described previously for 2,6-BAPT afforded the title compound in 87% yield (m.p. 139-140°C). Mass spectrum (M^+ calculated for 306.36 g/mole) m/z (%): 307 (11), 306 (57), 170 (24), 153 (11), 109 (13), 108(100), 89 (11), 80 (81), 65 (29). Elemental analysis calculated for $C_{19}H_{18}N_2O_2$ (306.36 g/mole): C, 74.49%; H, 5.92%; N, 9.14%. Found: C, 74.06%; H, 6.11%; N, 9.08%.

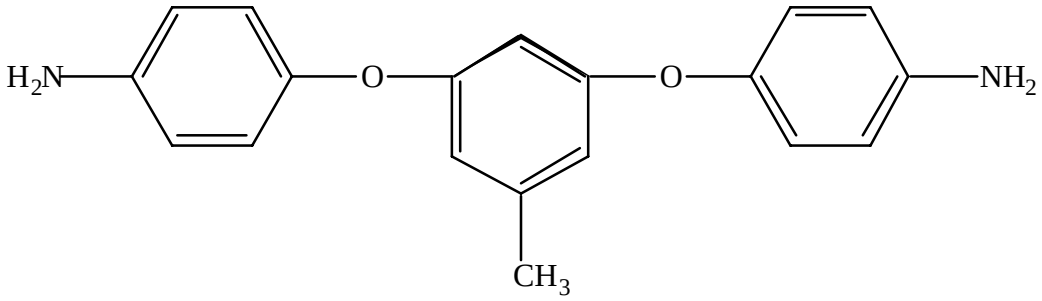

3.2.3 Synthesis of 1,3-bis(4-aminophenoxy)-4,6-di-t-butylbenzene (BAPDTB)

3.2.3.1 4,6-Di-t-butylresorcinol was prepared by the electrophilic alkylation of resorcinol. To a 50 ml round bottom flask were introduced 5 g (0.05 mol) of resorcinol and 13 ml (0.14 mol) of t-butanol. The flask was fitted with a condenser, and the reaction mixture was heated to 60°C. Once a homogeneous solution was obtained, 13 ml of 85% phosphoric acid was added. After 10-20 minutes the solution became murky, and the precipitation of the desired product occurred. The reaction mixture was allowed to cool to room temperature, yielding a white slurry. The slurry was added with stirring to water, and the di-t-butylresorcinol dihydrate was filtered and washed thoroughly with water.

The dihydrate was recrystallized from 50% MeOH and then dissolved in acetone, and subsequent evaporation of the acetone resulted in anhydrous di-t-butylresorcinol . The anhydrous product was recrystallized from hexanes to yield a white powder which was dried at 50°C under reduced pressure (m.p. 122-123°C; lit. m.p. 124-125°C)[221].

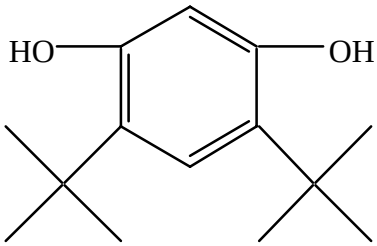

3.2.3.2 1,3-bis(4-nitrophenoxy)-4,6-di-t-butylbenzene (BNPDTB) was synthesized via the nucleophilic aromatic substitution reaction of *p*-fluoronitrobenzene with 4,6-di-t-butylresorcinol. To a 3-neck, 250 ml round bottom flask fitted with a nitrogen inlet, thermometer, overhead stirrer, Dean-Stark trap, and condenser were introduced 22.23g (0.1 mol) of 4,6-di-t-butylresorcinol, 29.02 g (0.21 mol) of potassium carbonate, 130 ml of DMAc, and 25 ml of toluene. The pink-red reaction mixture was heated to 145°C for at least 4 hours in order to dehydrate the system. After cooling, 21.7 ml (0.205 mol) of *p*-fluoronitrobenzene was added and the reaction mixture was again heated to 145°C for 16 hours to yield a spinach-green mixture. The excess toluene was distilled off, and the mixture was allowed to cool to room temperature and subsequently poured into water, resulting in a yellow-gold solid. The solid was filtered and washed thoroughly with water and methanol. Afterwards, the product was recrystallized from acetic acid in 87% yield (m.p. 182-183°C). Elemental analysis calculated for $C_{26}H_{28}N_2O_6$ (464.52 g/mole): C, 67.23%; H, 6.08%; N, 6.03%. Found: C, 67.26%; H, 6.19%; N, 6.00%.

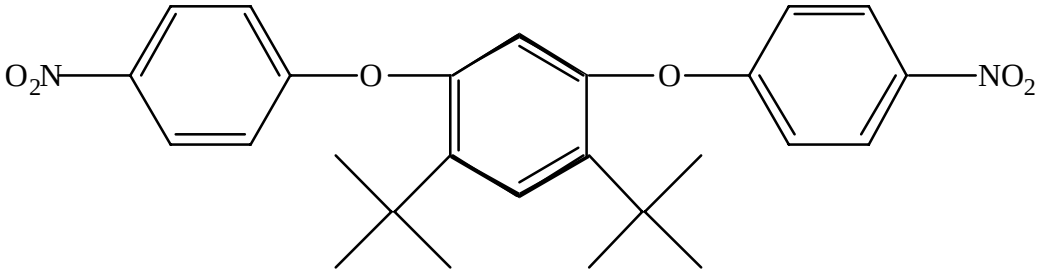

3.2.3.3 1,3-bis(4-aminophenoxy)-4,6-di-t-butylbenzene (BAPDTB) was synthesized via the reduction of BNPDTB. To a 3-neck, 250 ml round bottom flask fitted with a magnetic stirrer, nitrogen inlet, addition funnel, and condenser was introduced 13.94 g (0.03 mol) of 2,6-BNPT with 100 ml THF. Upon dissolution of the 2,6-BNPT, 500 mg of 10% Pd/C catalyst was added along with 30 ml of ethanol. The reaction mixture was then heated to 50°C, at which point 10 ml (0.2 mol) of hydrazine monohydrate was added dropwise to the mixture. The mixture was allowed to stir at reflux for 12 hours. Afterwards, the catalyst was filtered off using Celite, leaving a yellow solution. Evaporation of the solvent yielded an off-white product which was subsequently recrystallized from isobutanol to afford the title compound in 92% yield (m.p.207-208°C). Mass spectrum (M^+ calculated for 405.55 g/mole) m/z (%): 404 (18), 389 (13), 240 (10), 147 (12), 134 (20), 108(100), 93 (82), 80 (38), 65 (34). Elemental analysis calculated for $C_{26}H_{32}N_2O_2$ (405.55 g/mole): C, 77.19%; H, 7.97%; N, 6.92%. Found: C, 76.78%; H, 8.19%; N, 6.89%.

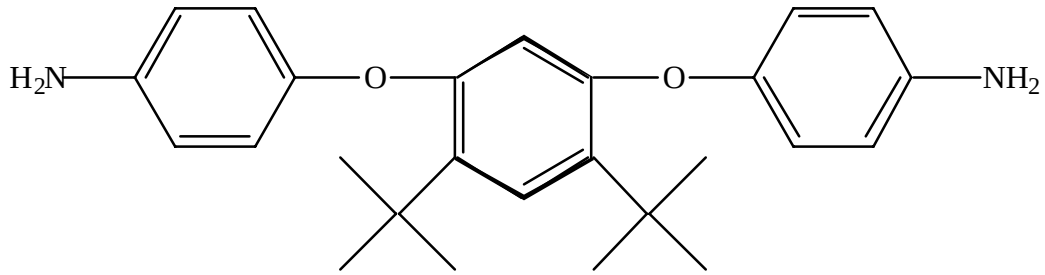

3.2.4 Synthesis of 1,3-bis(4-aminophenoxy)-4-hexylbenzene (BAPHB)

3.2.4.1 1,3-bis(4-nitrophenoxy)-4 -hexylbenzene (BNPHB) was synthesized via the nucleophilic aromatic substitution reaction of *p*-fluoronitrobenzene with 4-hexylresorcinol. To a 3-neck, 250 ml round bottom flask fitted with a nitrogen inlet, thermometer, overhead stirrer, Dean-Stark trap, and condenser were introduced 19.43g (0.1 mol) of 4-hexylresorcinol, 29.02 g (0.21 mol) of potassium carbonate, 130 ml of DMAc, and 25 ml of toluene. The pink-red reaction mixture was heated to 145°C for at least 4 hours in order to dehydrate the system. After cooling, 21.7 ml (0.205 mol) of *p*-fluoronitrobenzene was added and the reaction mixture was again heated to 145°C for 16 hours to yield a spinach-green mixture. The excess toluene was distilled off, and the

residual inorganic salts were filtered. After cooling, the filtered salts were washed with large amounts of methylene chloride, and the washings were added to the filtrate to yield an amber solution. The solution was then washed thoroughly with water and then dried over magnesium sulfate. Evaporation of the solvent resulted in an orange-amber oil. The oil was dissolved in a minimal amount of hot isopropanol, allowed to cool to room temperature, then placed in dry ice for several hours. A yellow product precipitated which was filtered, washed with cold isopropanol, and air dried (m.p. 59-60). Elemental analysis calculated for $C_{24}H_{24}N_2O_6$ (436.46 g/mole): C, 66.05%; H, 5.54%; N, 6.42%. Found: C, 63.38%; H, 5.47%; N, 6.43%.

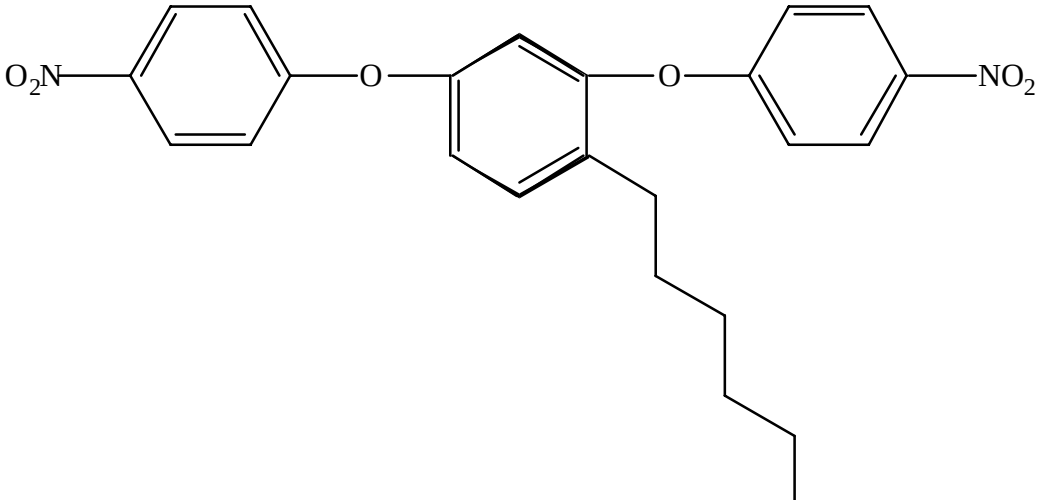

3.2.4.2 1,3-bis(4-aminophenoxy)-4-hexylbenzene (BAPHB) was synthesized via the reduction of BNPHB. To a 3-neck, 250 ml round bottom flask fitted with a magnetic stirrer, nitrogen inlet, addition funnel, and condenser was introduced 13.09 g (0.03 mol) of BNPHB with 60 ml THF. Upon dissolution of the 2,6-BNPT, 500 mg of 10% Pd/C catalyst was added along with 60 ml of ethanol. The reaction mixture was then heated to 50°C, at which point 10 ml (0.2 mol) of hydrazine monohydrate was added dropwise to the mixture. The mixture was allowed to stir at reflux for 12 hours. Afterwards, the catalyst was filtered off using celite, leaving a yellow solution. Evaporation of the solvent yielded a yellow-orange oil. The oil was dissolved in ether, washed thoroughly with salt water, and dried over magnesium sulfate. The ether was evaporated, and the oil that resulted was boiled in hexane for an hour. The mixture was allowed to cool before being

placed in dry ice. The off-white precipitated that formed was filtered, washed with hexane, air dried for several hours, and held under reduced pressure at room for 24 hours, affording the title compound in 85% yield (m.p. 48-49°C). Mass spectrum (M^+ calculated for 376.50 g/mole) m/z (%): 377 (10), 376 (46), 305 (33), 212 (14), 196 (17), 184 (12), 156 (12), 130 (12), 108(100), 93 (68), 80 (40), 65 (32). Elemental analysis calculated for $C_{24}H_{28}N_2O_2$ (376.50 g/mole): C, 76.56%; H, 7.50%; N, 7.44%. Found: C, 76.17%; H, 7.66%; N, 7.53%.

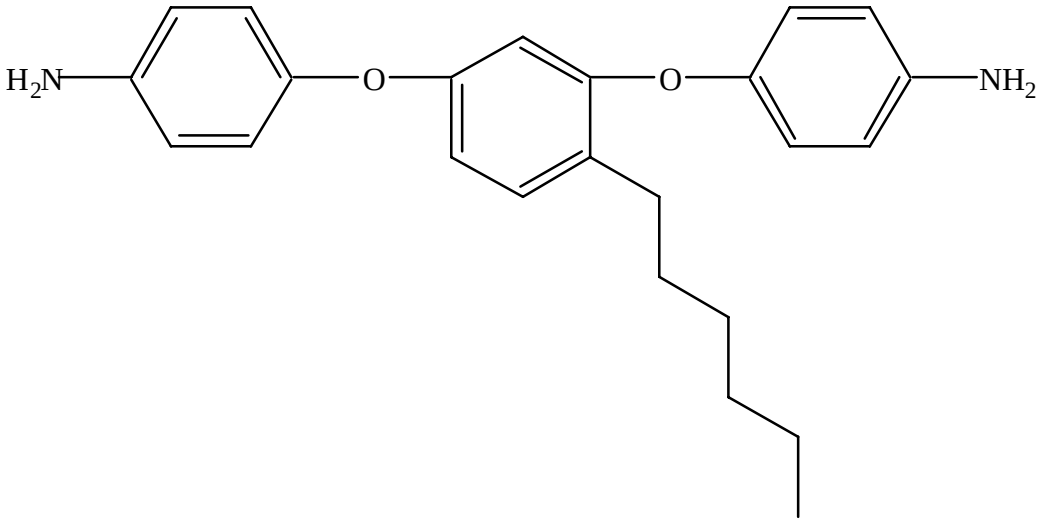

3.3 Polymer Synthesis

In synthesizing aromatic polyimide systems, the ability to successfully control molecular weight and endcap the desired polymer plays an important role. The step growth polymerization involved in preparing polyimides employs the use of the Carothers equation. By the stoichiometric adjustment of monomers to be polymerized, molecular weight control and functionalization with endgroups can be achieved.

3.3.1 Molecular Weight Control and Endgroup Functionalization

The Carothers equation used for controlling molecular weight in step growth

polymerizations is given as

$$X_n = \frac{2}{2 - pf_{av}} \qquad (3\text{-}1)$$

where X_n is the number average degree of polymerization, p is the extent of reaction and f_{av} is the average functionality of the polymer. X_n is more simply acknowledged for polymers by the relationship

$$X_n = 2\frac{M_n}{M_r} \qquad (3\text{-}2)$$

where M_n is the target molecular weight of the polymer and M_r is the molecular weight of the repeat unit of the polymer.

In attempting to achieve a controlled molecular weight polymer, a stoichiometric imbalance of the monomers is necessary. For a difunctional monomer AA reacting with a difunctional monomer BB where BB is in excess, the stoichiometric imbalance r is defined as

$$r = \frac{N_A}{N_B} \qquad (3\text{-}3)$$

where N_A and N_B are the number of molecules of AA and BB monomers, respectively. The quantity r is usually fixed to be less than unity and can be related to the degree of polymerization by the equation

$$X_n = \frac{1+r}{1-r} \qquad (3\text{-}4)$$

which rearranges to

$$r = \frac{X_n - 1}{X_n + 1} \qquad (3\text{-}5)$$

These relationships can be adapted so as to allow for the termination of polymer chains with monofunctional endgroups. Remembering that the stoichiometries of the monomeric species AA and BB were set so that BB exists in excess, the denominator of Equation 3-3 needs to be adjusted for the incorporation of monofunctional endgroup B. This is done to arrive at the equation

$$r = \frac{N_A}{N_B + 2N_B'} \qquad (3\text{-}6)$$

where N_B' is the number of monofunctional B molecules and is multiplied by 2 because of the monofunctionality. Equation 3-6 rearranges to

(3-7) $$N_B + 2N_B' = \frac{N_A}{r}$$

In the case of a polymer endcapped with monofunctional endgroups, the stoichiometric imbalance must not be present. In other words, r must be equal to 1 and

(3-8) $$N_B + N_B' = N_A$$

In essence, the number of moles of A functional groups must equal the total, monofunctional and difunctional, number of moles of B functional groups. If N_A is defined arbitrarily, N_B and N_B' can be determined by solving Equations 3-7 and 3-8 simultaneously.

3.3.2 Sample Calculation of Monomer Charges for the Synthesis of an Endcapped Polyimide

As an example of the synthesis of a step growth polyimide of controlled molecular weight and encapped with a monofunctional endgroup, the procedure for preparing the polyimide TPER-BPDA-PA of target number average 30,000 g/mole is used. TPER (amine) will be monomer A, BPDA (dianhydride) will be B, and PA (monofunctional anhydride) will be B' where B and B' are the same functional group.

molecular weight of TPER = M_A = 292.34 g/mole

molecular weight of BPDA = M_B = 294.22 g/mole

molecular weight of PA = M_B' = 148.12 g/mole

$M_r = M_A + M_B$ - (2)(molecular weight of water) = 292.34 +294.22 -(2)(18) = 550.56

Using Equation 3-2

$$X_n = 2\frac{M_n}{M_r} = \frac{(2)(30{,}000)}{550.56} = 108.97995$$

Then, using Equation 3-5

$$r = \frac{X_n - 1}{X_n + 1} = \frac{108.97995 - 1}{108.97995 + 1} = 0.981815$$

Reminded of Equations 3-7 and 3-8, N_A of TPER is set to 0.1. Thereby

$$N_B + 2N_B' = \frac{N_A}{r} = \frac{0.1}{0.981815} = 0.101852$$

$$N_B + N_B' = N_A = 0.1$$

Solving the above equations simultaneously for N_B' gives

N_B' = 0.101852 - 0.1 = 0.001852

Solving for N_B yields

N_B = (2)(0.1) - 0.101852 = 0.09815

Therefore, the monomer charges can be calculated as follows:

grams of TPER = $N_A M_A$ = (0.1)(292.34) = 29.234

grams of BPDA = $N_B M_B$ = (0.09815)(294.22) = 28.877

grams of PA = $2N_B'M_B'$ = (2)(0.001852)(148.12) = 0.547

3.3.3 Synthesis of Polyimides

For the synthesis of semicrystalline polyimides, a two step process was used. The initial step in this process was the preparation of a soluble polyamic acid of desired molecular weight. Imidization or cyclization of the polyamic acid was accomplished either by thermal cyclodehydration or in solution. In all of the polymerizations to be described, a standard reaction apparatus was utilized. This included a 3- or 4-neck round bottom flask equipped with an overhead mechanical stirrer, nitrogen inlet, and drying tube. For solution imidization reactions, the drying tube was replaced with an inverse Dean-Stark trap and condenser.

3.3.3.1 Synthesis of Polyamic Acid

To achieve a 30,000 molecular weight amic acid homopolymer of TPER-BPDA-PA, the Carothers equation was used to achieve an offset and obtain the charges mentioned below. A three-neck round bottom flask equipped with a mechanical stirrer, nitrogen inlet, and drying tube was utilized. To this apparatus was introduced 2.9234g (10.0 mmol) of TPER. A few ml of NMP was added to dissolve the diamine. To the solution was added 0.0547g (3.7 mmol) of PA followed by a few ml of NMP. Finally, 2.8877g (9.82 mmol) of BPDA was added to the solution. Enough NMP was added to achieve a 10% solids concentration (about 53 ml total). This solution was allowed to stir under nitrogen atmosphere for 24 hours. The resulting solution could then be imidized or submitted for analysis.

To achieve a 30,000 molecular weight amic acid of the same homopolymer mentioned above capped with a reactive amine end groups, the same procedure and charges were utilized. However, PA was not added. High molecular weight polyamic acid was synthesized simply by reacting equimolar amounts of diamine and dianhydride while maintaining a 5% solids concentration.

3.3.3.2 Thermal Imidization

To insure the complete imidization of a semicrystalline polyimide, thermal dehydration or imidization was used. Two general methods were employed. When thin polyimide films were required, polyamic acid solution was cast onto a glass plate. The plate was placed in a dry box in the presence of a nitrogen or dry air flow until smooth, non-tacky films were obtained. The plates were then placed in a vacuum oven, and the temperature was slowly raised to 100°C and subsequently held at this temperature for 1 hour. The temperature was then quickly raised to 200°C and held for an hour, and finally it was quickly raised to 300°C and held for an hour to achieve fully imidized films. The oven was allowed to cool to below 150°C before taking out the films.

In cases where thin films were not necessary, polyamic acid solution was poured into a petrie dish or aluminum pan. The solution was then held under vacuum overnight to facilitate the removal of some solvent. Afterwards, the heating cycle that was described previously was utilized to produce thermally imidized films or solids

3.3.3.3 Solution Imidization

For the synthesis of soluble polyimides or polyimide powders, solution imidization was employed. In the apparatus described above in preparing polyamic acid solution, the drying tube that was used was replaced with an inverse Dean Stark trap with condenser. o-Dichlorobenzene (DCB) was added to the trap and to the polyamic acid solution so as to achieve an 80/20 ratio of NMP to DCB. The solution was heated to about 180° and stirred. In the case of soluble polyimides, a homogeneous solution was maintained for 24 hours. Afterwards, the polyimide solution was allowed to cool to room temperature before being coagulated in a blender of methanol or water. The precipitated polyimide was filtered, washed with methanol or water, and dried in a vacuum oven for at least 12 hours at around 150°C before being heated to 300°C for an hour to ensure complete imidization.

The attempted syntheses of semicrystalline polyimides using solution imidization often resulted in premature precipitation of polymer from solution during the course of the cyclodehydration. The reaction mixture slurries that formed in such cases were allowed to cool before being poured into a beaker of water or methanol with stirring, followed by filtration and washing with water or methanol. The polyimide powders were dried in a vacuum oven for at least 12 hours at about 235-250°C before being heated to 300°C for an hour to ensure complete imidization.

3.4 Characterization

3.4.1 Intrinsic Viscosity

Measurements were made on samples dissolved in NMP using a Canon-Ubbelohde

viscometer at 25°C in a water bath. The values for intrinsic viscosity were obtained at four different concentrations wherein the results were linearly extrapolated to zero concentration.

3.4.2 Gel-Permeation Chromatography (GPC)

GPC was performed using a Waters GPC/ALC 150-C chromatograph equipped with a differential refractometer and on-line differential viscometric detector. Molecular weight determinations were made through the use of universal calibration methods.[222]

3.4.3 Fourier Transform Infrared Spectroscopy (FTIR)

FTIR spectra were collected using a Nicolet Impact 400 FTIR spectrometer. Samples were analyzed as either bulk imidized films or as potassium bromide pellets.

3.4.4 Nuclear Magnetic Resonance Spectroscopy (NMR)

Proton and carbon NMR spectra were obtained using a Varian Unity 400 MHz instrument. Samples were analyzed in the form of solutions in either deuterated dimethyl sulfoxide (DMSO-d6) or chloroform ($CDCl_3$).

3.4.5 Mass Spectroscopy (MS)

Mass spectra were obtained using a Fisions VG Quattro instrument.

3.4.6 Thermogravimetric analysis (TGA).

TGA was performed using either a Perkin Elmer TGA 7 instrument or a Seiko TG/DTA instrument. Measurements were made in both air and nitrogen environments under dynamic and isothermal scans.

3.4.7 Differential Scanning Calorimetry (DSC)

DSC was performed using either a Perkin Elmer DSC 7 or a Seiko DSC 220C instrument. Measurement s were made in nitrogen environments at various heating and cooling rates.

3.4.8 Particle Size Analysis

A Shimadzu SA-CP3 particle size analyzer was used to measure the mean particle sizes of the semicrystalline polyimide powders. Suspensions of the powders in water and in the presence of a stabilizer were utilized for the measurements.

3.4.9 Rheological analysis

Parallel plate melt viscosity data was collected from a Bohlin VOR Rheometer.[223] Both thermally and solution imidized polyimides were used to make samples which had a diameter of 25 mm and were about 1 mm thick. Measurements were made in nitrogen environments at a frequency of 0.1 Hz. .

3.4.10 Wide Angle X-ray Scattering (WAXS)

WAXS measurements were conducted using a Nicolet diffractometer using CuK_a radiation with a wavelength of 1.54 Å.[224] Scans were obtained in 0.05° increments at angles between 5-50°.

Chapter 4: Results and Discussion

4.1 Molecular weight analysis

The insolubility of semicrystalline polyimides generally limits the degree of characterization that can be performed in the solution phase. However, an alternative that can be used to characterize the molecular weight of semicrystalline polyimides is to measure polyamic acid properties in solution. Even though polyamic acid is quite soluble in polar aprotic solvents, the use of polyamic acids in molecular weight characterization presents some challenges. The subject of isolating polyamic acids by precipitation in water has been discussed in the literature, but it is also well known that these amic acids are extremely hydrolytically unstable.[2,38] Thus, hydrolysis of the amic acid can result in a back reaction to carboxylic acids and consequently decrease molecular weight. Another problem in using polyamic acids is their strong affinity for polar aprotic solvents. As a result, it is very hard to completely eliminate the solvent from the amic acid, despite attempts to precipitate the amic acid in water or other nonsolvents. A proton NMR spectrum of a polyamic acid precipitated from NMP is shown in Figure 4.1.1. It is clear to see that in the range of 1.5 to 3.5 ppm, there is a large amount of NMP present, despite painstaking efforts to remove it. As with other analyses involving precipitated amic acids, the presence of a residual solvent can greatly impact the results unless it can be accounted for.

Because of this, molecular weight measurements were conducted on fresh polyamic acid solutions that were either analyzed directly from the reaction flask, or after having been stored at below freezing temperatures. These measurements were related to the known polymer concentrations in NMP upon preparing the polyamic acid. The method of choice for analyzing the molecular weights of the amic acids was universal calibration gel permeation chromatography (GPC). These measurements were done according to a published procedure developed at this university using NMP solutions containing a slight amount of phosphorous pentoxide (P_2O_5).[222] A representative chromatogram is shown in Figure 4.1.2, in which a unimodal molecular weight distribution

was observed. A summary of the GPC results for some TPER-BPDA amic acids is shown in Table 4.1, demonstrating good molecular weight correlation to target values. The slightly lower observed values are likely within experimental error, but could also represent a small amount of hydrolysis, prior to measurements

4.2 1,4-Bis(4-aminophenoxy)benzene (TPEQ)Based Polyimides

The molecular design of a polymer is very important in synthesizing semicrystalline polyimides. While excess flexibility in the polyimide backbone will prevent the regular ordering necessary for crystallization, a sufficient degree of flexibility must be present in order to avoid the high degree of chain stiffness associated with largely aromatic polyimides. This can contribute to elevated transition temperatures and result in materials that will degrade before they melt.[134]

This research focused on efforts to molecularly design and synthesize semicrystalline polyimides that demonstrate sufficient melt stability to be fabricated thermoplastically above the polymer's melting point. Central to this objective has been the controlled incorporation of isomeric ether linkages into the polyimide backbone, whose presence is known to impart certain desirable mechanical properties, e.g., toughness, to aromatic polymers.

The monomer 1,4-bis(4-aminophenoxy)benzene, referred to as TPEQ (triphenyl ether diamine-hydroquinone), has been investigated. This particular diamine demonstrates flexibility as a result of its ether bridges, but also shows symmetry and some rigidity, permitting semicrystallinity in specific systems. The polyimides prepared from this diamine will be described.

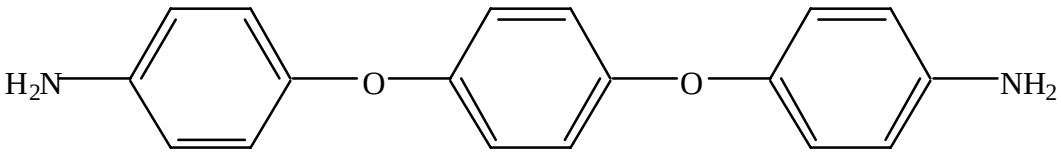

TPEQ

[1,4-bis(4-aminophenoxy)benzene]

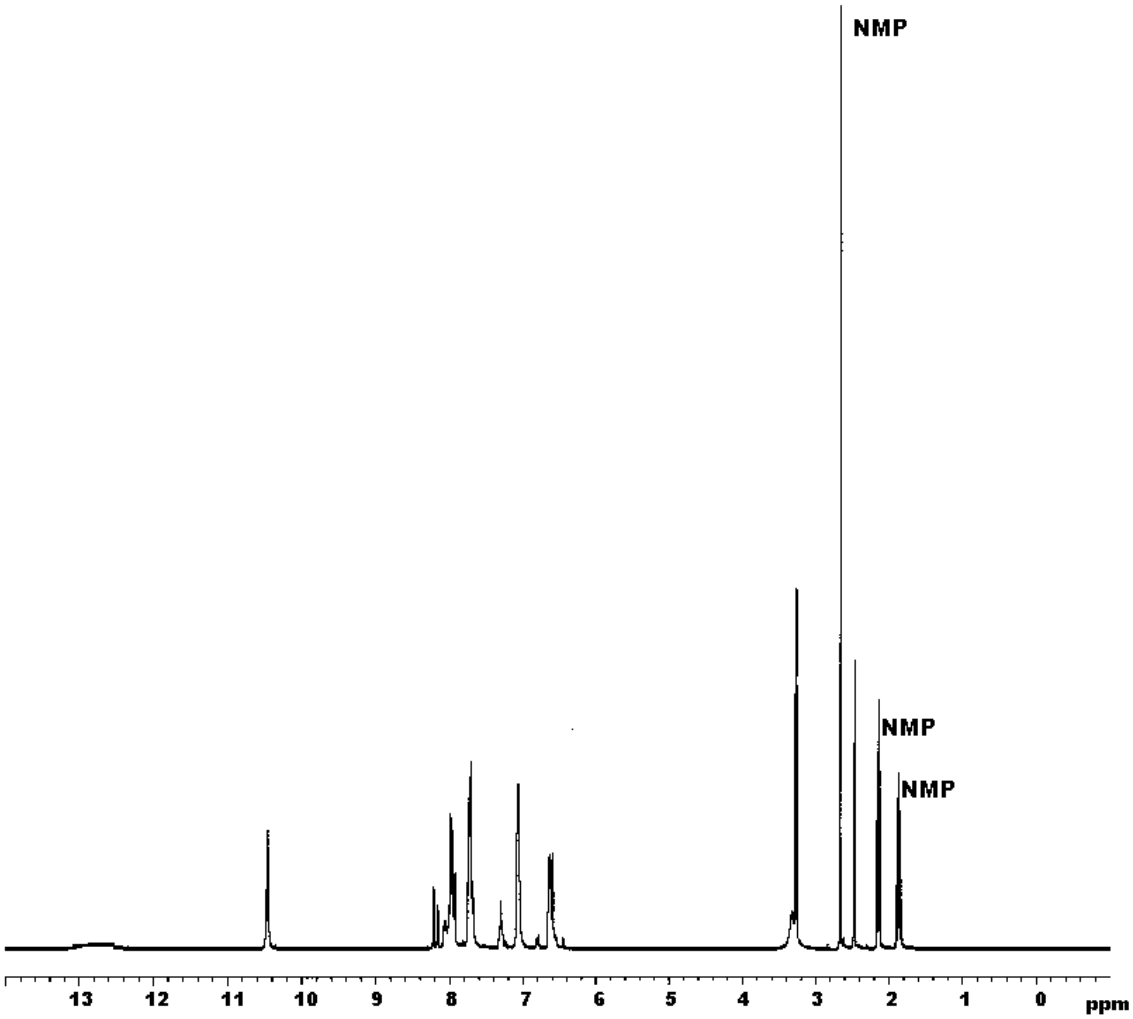

Figure 4.1.1: Proton NMR Spectrum of a Precipitated Polyamic Acid (in DMSO-d6)

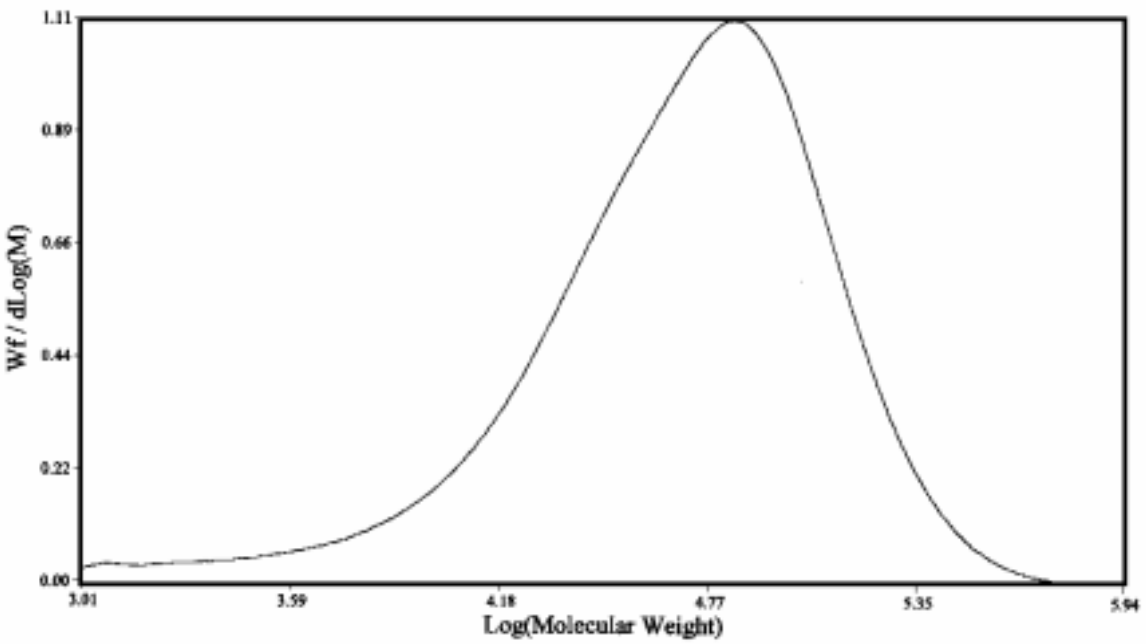

Figure 4.1.2: GPC Chromatogram of a TPER-BPDA-PA Polyamic Acid

Table 4.1: GPC Molecular Weights of Various TPER-BPDA Polyamic Acids*

sample	Target M_n (g/mole)	Experimental M_n (kg/mole)	M_w/M_n
PA endcapped	10,000	9.5	1.8
PA endcapped	20,000	18.6	2.7
PA endcapped	30,000	27.9	2.4
"1/2" PA endcapped	30,000	30.9	2.5
amine terminated	30,000	27.1	2.5

*in NMP containing 0.2% P_2O_5 at 60°C[222]

4.2.1 Polyimide semicrystalline powders derived from TPEQ

Semicrystalline polyimides offer advantages such as excellent solvent resistance and good thermooxidative stability. However, a prerequisite for the commercial use of these particular materials is that they must be able to be easily and efficiently processed above the melting point to avoid polymer degradation. This is particularly challenging for systems with melting points in excess of 400°C, since it is difficult to modify common processes to withstand such harsh conditions.

Newer composite technologies, such as polymer matrix powder processing of composite materials, do overcome some of these drawbacks. This method also avoids the use of traditional solvents, which are considered to be environmentally unfriendly. Molding powders are often produced via milling or grinding, but these procedures are labor intensive and can yield inadequately sized particles for powder processing. However, it was recently discovered that several semicrystalline polymers, such as PEEK, can be synthesized directly in the form of small polymeric particles, which are essential in both powder prepregging or in blending the polymer matrix resin with the reinforcing fiber in a composite.[75]

Semicrystalline polyimides have demonstrated these desirable capabilities as well.[182,183] These polyimides were synthesized by solution methods and exhibited small particle sizes, which facilitated their use as composite matrix materials where small-sized polymer particles are essential. Another aspect of this research focused on the synthesis and characterization of semicrystalline polyimide powders derived from TPEQ and a related isomeric diamine, described in a later section. The TPEQ polyimide repeat units are shown in Figure 4.2.1.1.

The polyimide powders were prepared by the classical two step route of first synthesizing the polyamic acid precursor and then cyclizing it via solution imidization. The synthesis is shown in Scheme 4.2.1; normally 10% solids concentrations were used. It is important to note that each of these polyimide powders was endcapped with phthalic anhydride (PA) to provide nonreactive phthalimide endgroups. The number average molecular weights of the polymers were targeted to 30,000 g/mole using the

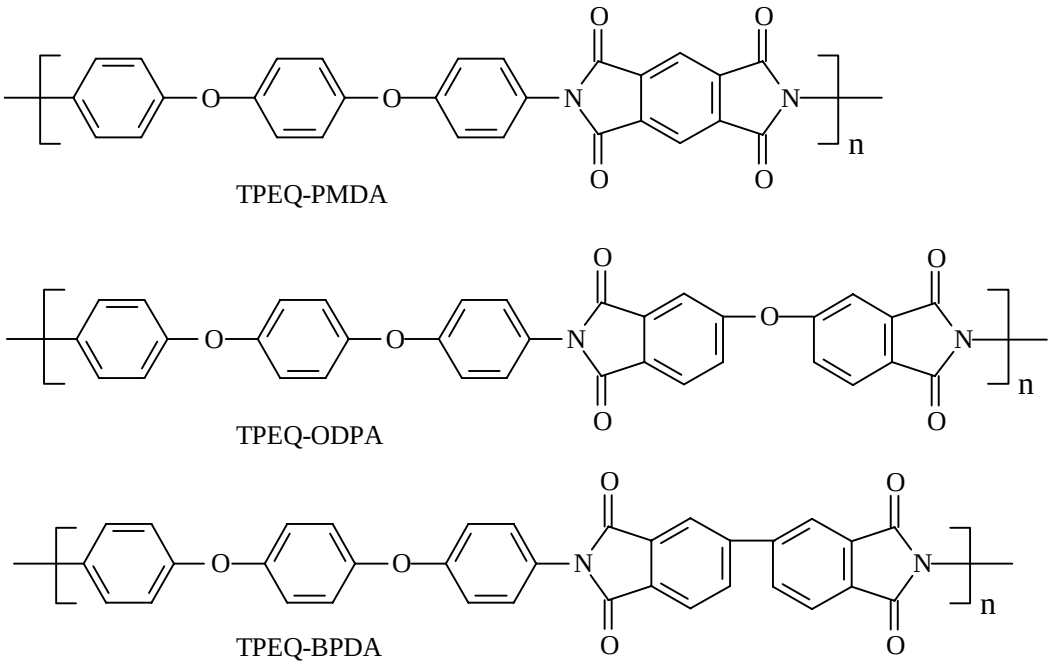

Figure 4.2.1.1: TPEQ-Based Polyimides

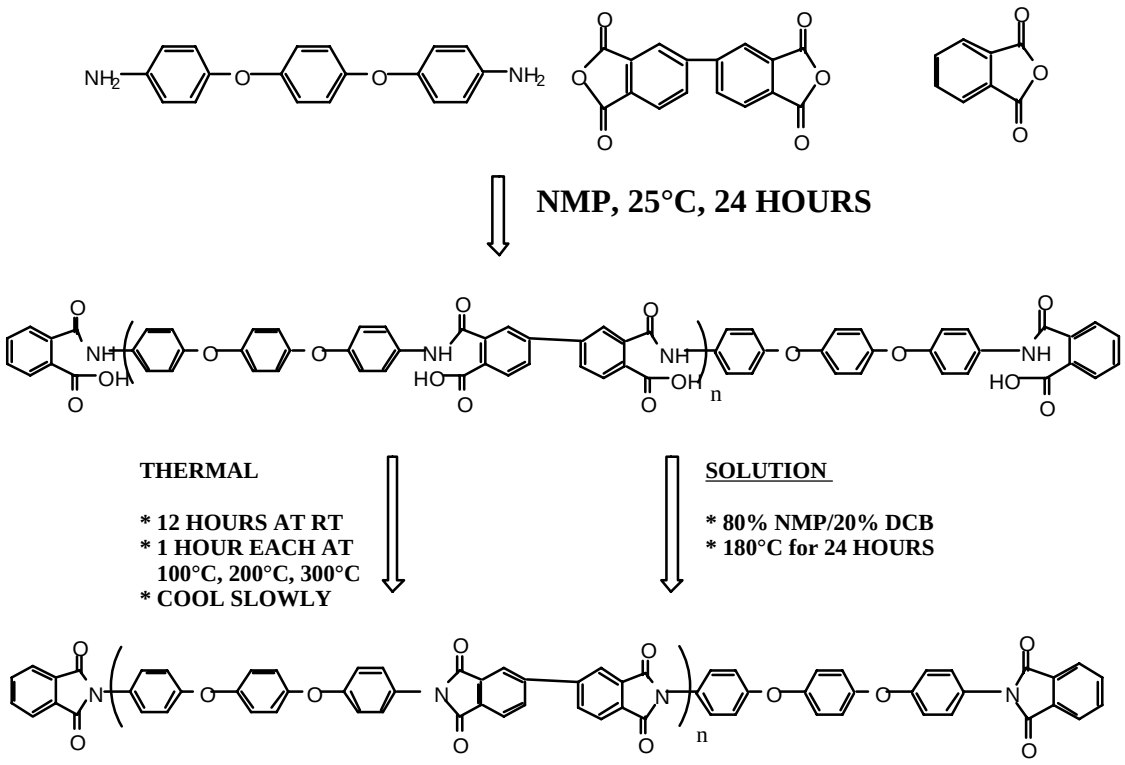

Scheme 4.2.1: Synthesis of TPEQ Polyimide Powders

Carothers relationship.[225]

Solution imidization was accomplished by adding o-dichlorobenzene (ODB), an azeotroping agent, to an existing polyamic acid solution in NMP, and then heating the solution to 180°C. The solution was normally observed to become turbid during the course of the imidization, indicating that semicrystalline material had precipitated from the solution. Most of the polymer precipitated from solution to give a slurry. This is dependent on time and the crystallinity and/or solubility of the resulting polyimide. The slurry was then poured into water or methanol to wash the particles. At this point the resulting polymer was not fully imidized, but rather consisted of a combination of cyclized imide moieties and a minor fraction of uncyclized amic acid units. Complete cyclization was achieved by drying the polymer at 150-225°C for several hours and then subsequently treating the polymer above the glass transition temperature at 300°C for an hour. The FTIR spectrum of an imidized polyimide powder is shown in Figure 4.2.1.2 and is characterized by the appearance of imide bands at 1770 cm^{-1}, 1716 cm^{-1}, 1369 cm^{-1}, and 741 cm^{-1}, a phenomenon that is well established in the literature.[4]

Duplicate samples of each polyimide were synthesized for analysis. In order to measure particle size, one sample polyimide was used that had been precipitated during imidization, but had been thoroughly washed with water. The second sample, which was used for thermal analysis, was the completely cyclized polyimide mentioned previously.

Particle size analysis was performed using undried samples of polyimide powders because it was thought that the polymer might aggregate upon heating, which would result in distorted particle sizes. A particle size analyzer was employed to measure the size as a function of the sedimentation rate of the particles in a suspension of water containing a stabilizer. The results of these measurements for selected polyimides are summarized in Table 4.2.1, and ranged from 2 to 15 µm average diameter. It should be noted that the general particle size requirements for powder prepregging fabricated composites are within this size range. Dry (electrostatic) and wet (suspension) powder prepregging are the predominant methods utilized for this purpose.[226-231] Dry powder prepregging ordinarily requires polymer particles on the order of about 50 µm, while wet powder prepregging requires particles of no more than 20 µm in size. It should be noted that the

ability to imidize the powders under the conditions mentioned above may be beneficial, whereby fully imidized powders may demonstrate a resistance against particle aggregation. This would make fully imidized powders very desirable for powder processing of composite materials.

A representative TGA thermogram for one of the TPEQ-based powders in air is shown in Figure 4.2.1.3. No significant weight loss was observed prior to 500°C, indicating that the fully imidized powders display good thermooxidative stability. The 5% weight loss values for the TPEQ polyimides are summarized in Table 4.2.1, which shows that each of these polyimides experienced a 5% weight loss at temperatures greater than 500°C.

DSC analysis was performed for the TPEQ-based powders using a 10°C/min first heat ramp at 200-450°C, followed by quench cooling and a second heat ramp in the same range. The polymers based upon PMDA and BPDA did not exhibit any transitions in this range, which is not uncommon, given the rigidity inherent in such systems.[232,233] DSC performed at higher temperatures indicates that TPEQ-BPDA-PA has a melting point of 471°C, which overlaps with the decomposition of the polyimide.[234] TPEQ-ODPA-PA, on the other hand, shows a melting point of 409°C and a T_g of 232°C. This latter system also displayed interesting thermal behavior which has been extensively investigated.[235] This will be reviewed in more detail in the next section.

These polyimides are similar, however, in that they are insoluble in virtually all common organic solvents, which is one of the more desirable features of these polymers. Some of the materials have also demonstrated resistance to strong organic acids such as trifluoroacetic acid and methanesulfonic acid. Sufficient amounts of triflic acid and sulfuric acid can solubilize these polyimides to some extent, but degradation under these conditions remains a possibility as well.

4.2.2 TPEQ-ODPA-PA Polyimide

The first and second heat DSC thermograms of 30 kg/mol TPEQ-ODPA-PA are shown in Figure 4.2.2.1. As was noted above and seen in the first heat thermogram, as-

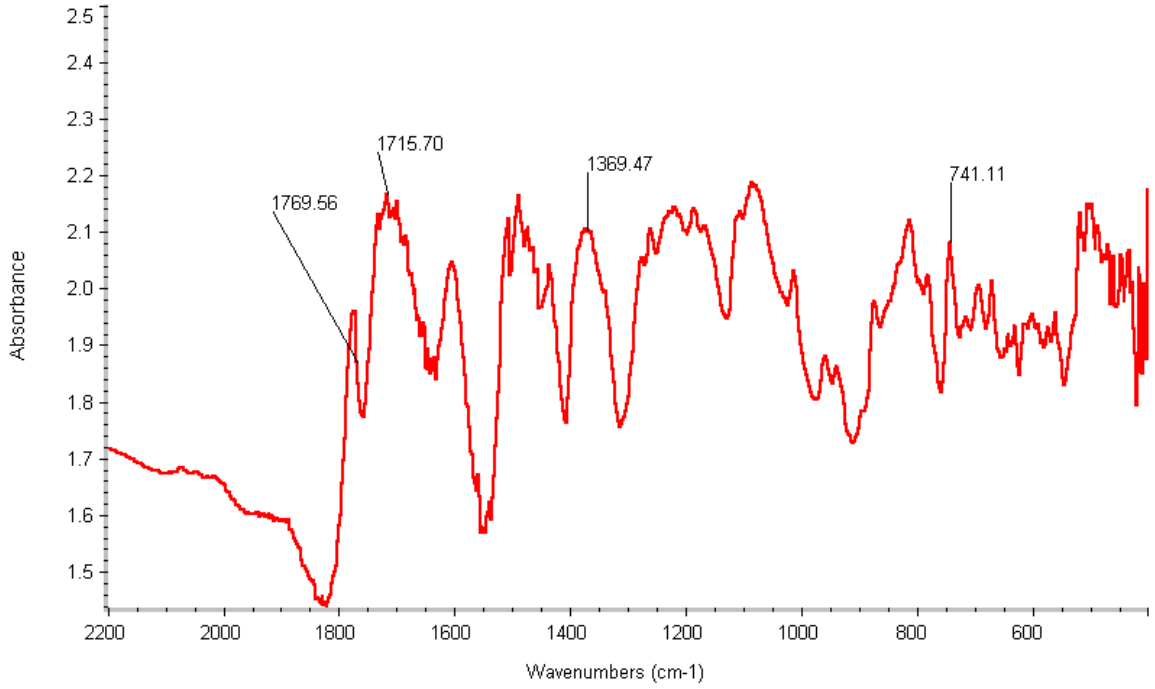

Figure 4.2.1.2: FTIR Spectrum of a Fully Imidized Polyimide Powder

Table 4.2.1: Summary of Thermal and Particle Size Analyses

Polyimide	Particle Size (µm)	5% wt. loss (°C)*	T_g (°C)**	T_m (°C)***
TPEQ-PMDA-PA	2	521	-	-
TPEQ-BPDA-PA	-	522	-	-
TPEQ-ODPA-PA	16	518	232	409

*in air, 10°C/min
**from second heat
***from first heat

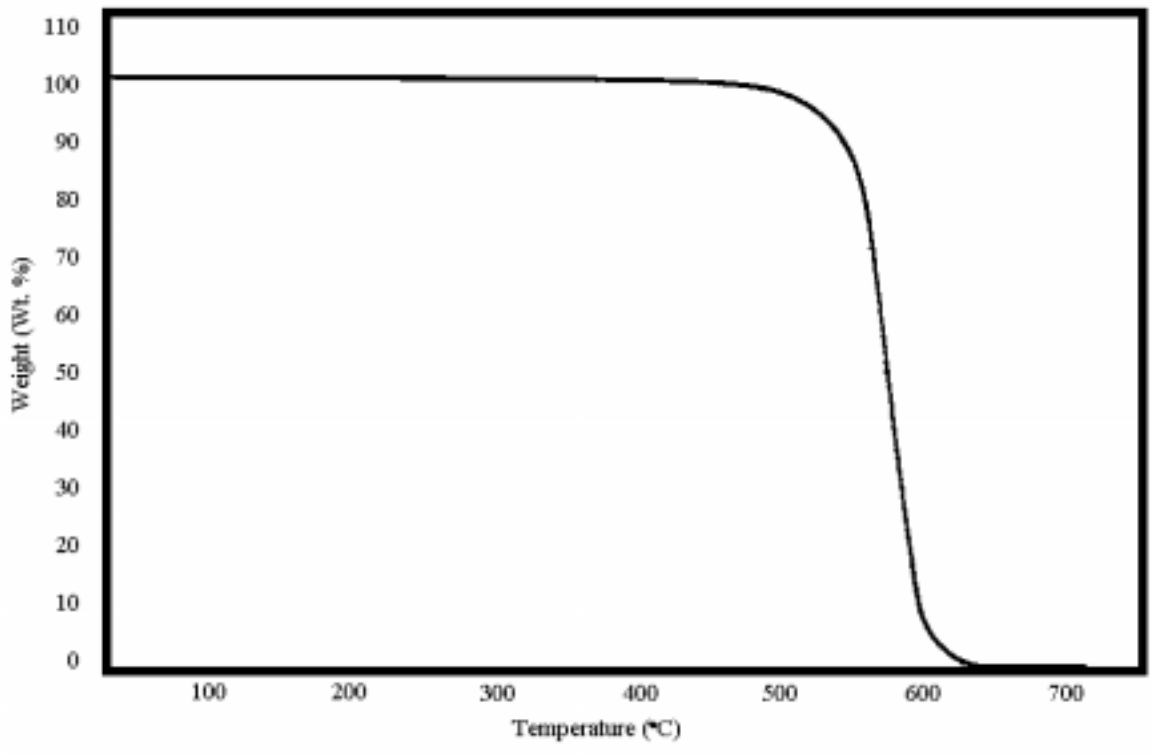

Figure 4.2.1.3: TGA Thermogram of TPEQ-BPDA-PA Polyimide Powder in Air at 10°C/min

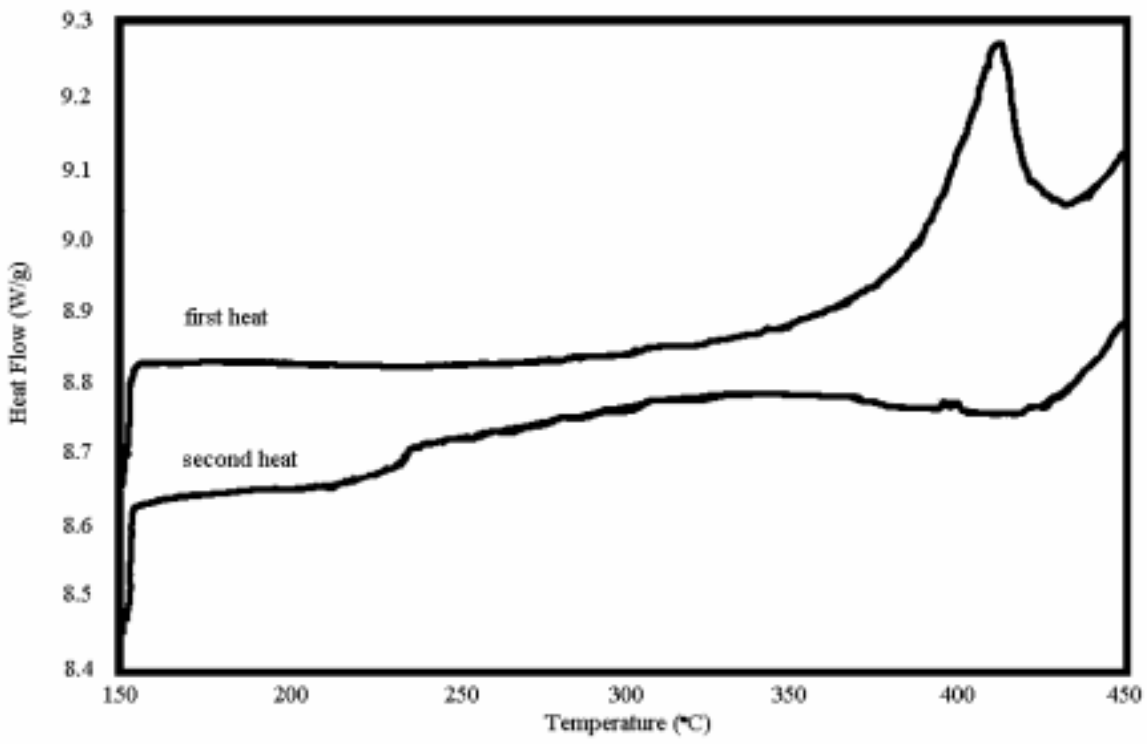

Figure 4.2.2.1: DSC Thermograms of 30 kg/mole TPEQ-ODPA-PA at 10°C/min

made (post-drying) samples of this polyimide exhibited a melting point slightly above 400°C. However, quenching this system from the melt resulted in an amorphous polymer, as demonstrated from the second heat. This phenomenon can be attributed to a number of factors, including insufficient chain mobility for crystallization as a result of the material's high molecular weight, or the possibility that the polymer had decomposed in some way. In order to study this tendency more thoroughly, bulk imidized samples of TPEQ-ODPA-PA of varying molecular weights were prepared and submitted for thermal analysis (TGA and DSC), as well as for analysis by x-ray scattering and melt rheology.

A series of TPEQ-ODPA-PA films consisting of number average molecular weights of 10K (10,000), 12.5K, 15K, 20K, and 30K were synthesized by the classical two step route. The polyamic acids were imidized using the bulk imidization technique described earlier. In addition, three 10K films of differing degrees of imidization were prepared. One of these 10K samples underwent bulk imidization for only an hour at 100°C and is herein designated as 10K (100°C). Another sample was imidized for an hour at 100°C and an hour at 200°C and is designated as 10K (200°C). The third and remaining 10K sample was imidized for a total of three hours (one hour each at 100, 200, and 300°C), and is referred to as 10K (300°C). All of the samples were considered to be "as-made" if no additional thermal treatment was carried out prior to characterization.

TGA analyses of the polyimides were conducted in both air and nitrogen environments. Figure 4.2.2.2 shows the TGA thermograms in nitrogen of the 10K samples, which clearly indicates that the onset of weight loss occurs at higher temperatures as the level of imidization increases. This results from the loss of water and solvent as the imidization proceeds. The 10K (100°C) sample, however, had a lower level of imidization than the 10K (200°C) sample and thus gave off more water. A similar trend was observed for the 10K (200°C) samples when compared to the 10K (300°C) sample. Significant weight loss was not observed for the 10K (300°C) sample until exceeding 500°C, which was similar to what was observed for the fully imidized powders. The use of an air environment for this experiment yielded similar results, indicating that imidization was not noticeably affected by atmosphere.

TGA analyses at 10°C/min was then performed on all the film samples to

determine the onset of decomposition. In this instance, onset is defined as the point at which 5% weight loss occurs, and this value was determined in both air and nitrogen atmospheres. The 5% weight loss values for each sample are given in Figure 4.2.2.3. The values given for the 10K (100°C) and 10K samples were obtained after the initial weight losses indicated in Figure 4.2.2.2 were recorded. Even though the samples analyzed in nitrogen displayed significantly higher weight loss temperatures than their in-air counterparts, the weight losses for all of the samples occurred in excess of 500°C, once again demonstrating the excellent high temperature resistance to decomposition. These results also indicate that there did not appear to be any obvious correlation between weight loss and the molecular weight of the sample.

A number of DSC studies were performed on the TPEQ-ODPA-PA films. The first heat DSC thermograms of the samples at 10°C/min are shown in Figure 4.2.2.4. The 10K (100°C) sample exhibited endothermic and exothermic transitions in a range corresponding to the weight loss observed in Figure 4.2.2.2. This behavior is attributed to solvent loss, cyclization and the water evolved therein, and crystallization.[150] While the melting endotherm occurred at 428°C, there was also an exotherm around 275°C, which is indicative of additional crystallization. The 10K (200°C) sample exhibited a broad endotherm corresponding to weight loss, as evidenced by TGA – once again a result of the solvent loss that occurred upon imidization. As was the case with the 10K (100°C) sample, a crystallization exotherm appeared at approximately 275°C, followed by melting at 428°C. The 10K (300°C) sample showed an endotherm around 280°C, which may be characteristic of premelting of polymer crystals, and subsequently complete melting occurs at 428°C. The melting enthalpies for all the 10K samples were comparable, indicative of rapid crystallization upon imidization of the 10K (100°C) and 10K (200°C) materials.

The 12.5K and 15K samples show weak endotherms occurring around 315°C. These likely are caused by the thermal history arising from the 300°C imidization step, from which premelting may transpire. This behavior, however, was not observed for the 20K and 30K samples. Nonetheless, all of the samples displayed very similar enthalpies of melting. With the inclusion of the 10K samples, no molecular weight–melting enthalpy correlation was observed, implying that the mechanism of crystallization upon imidization

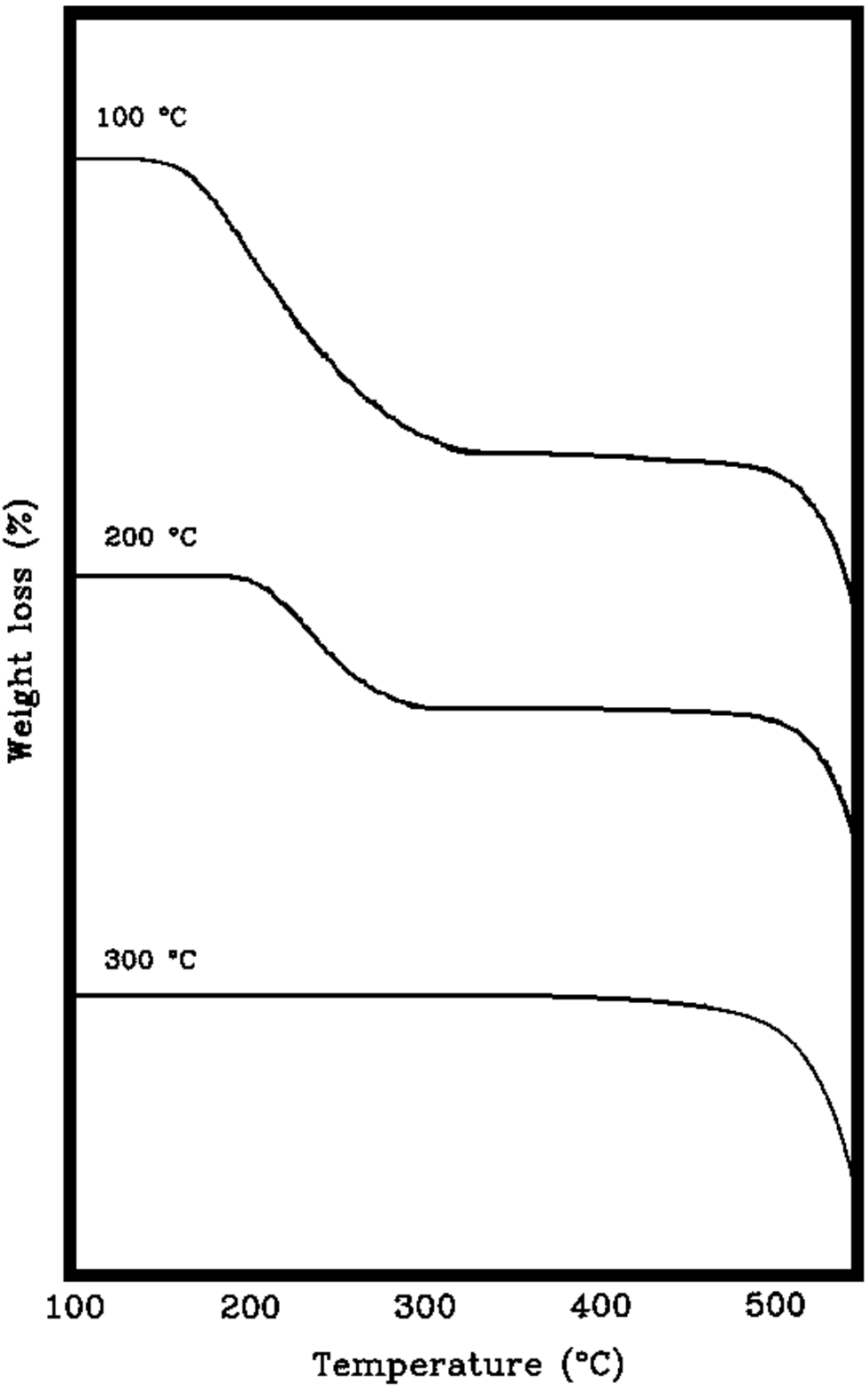

Figure 4.2.2.2: Influence of Imidization Temperature on TGA Weight Loss Behavior of 10K TPEQ-ODPA-PA Samples (10°C/min)

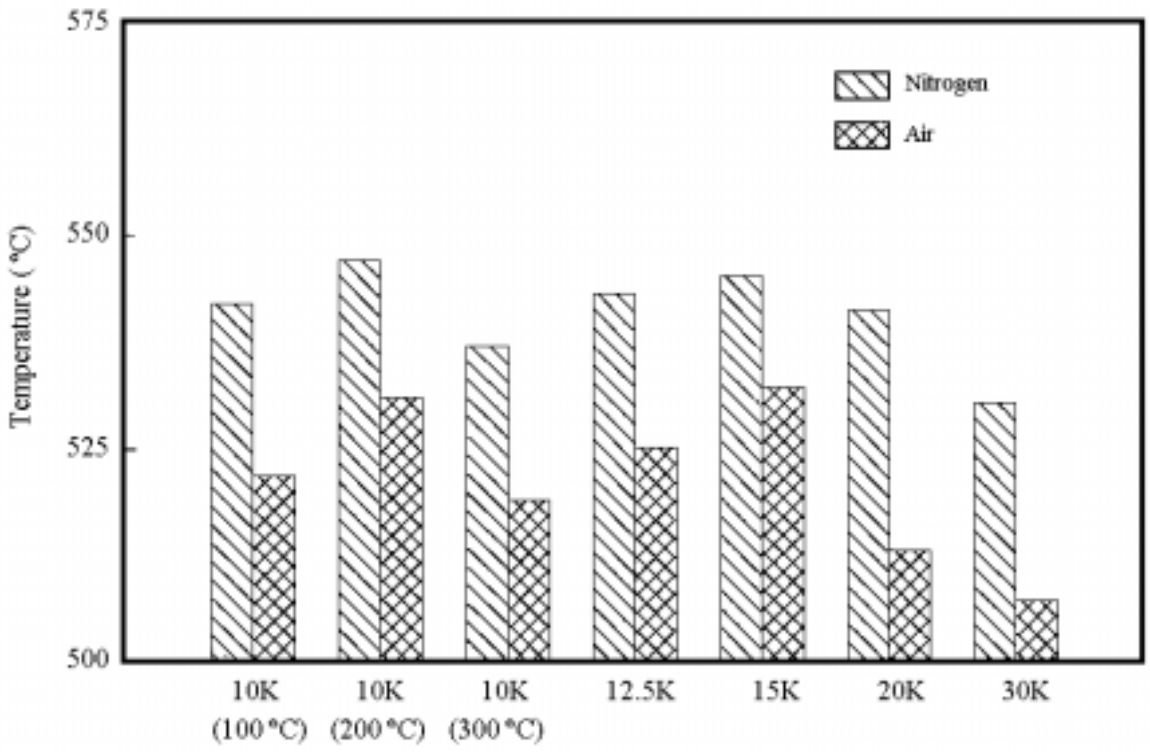

Figure 4.2.2.3: 5% Weight Loss Temperature of Fully Cyclized TPEQ-ODPA-PA Samples

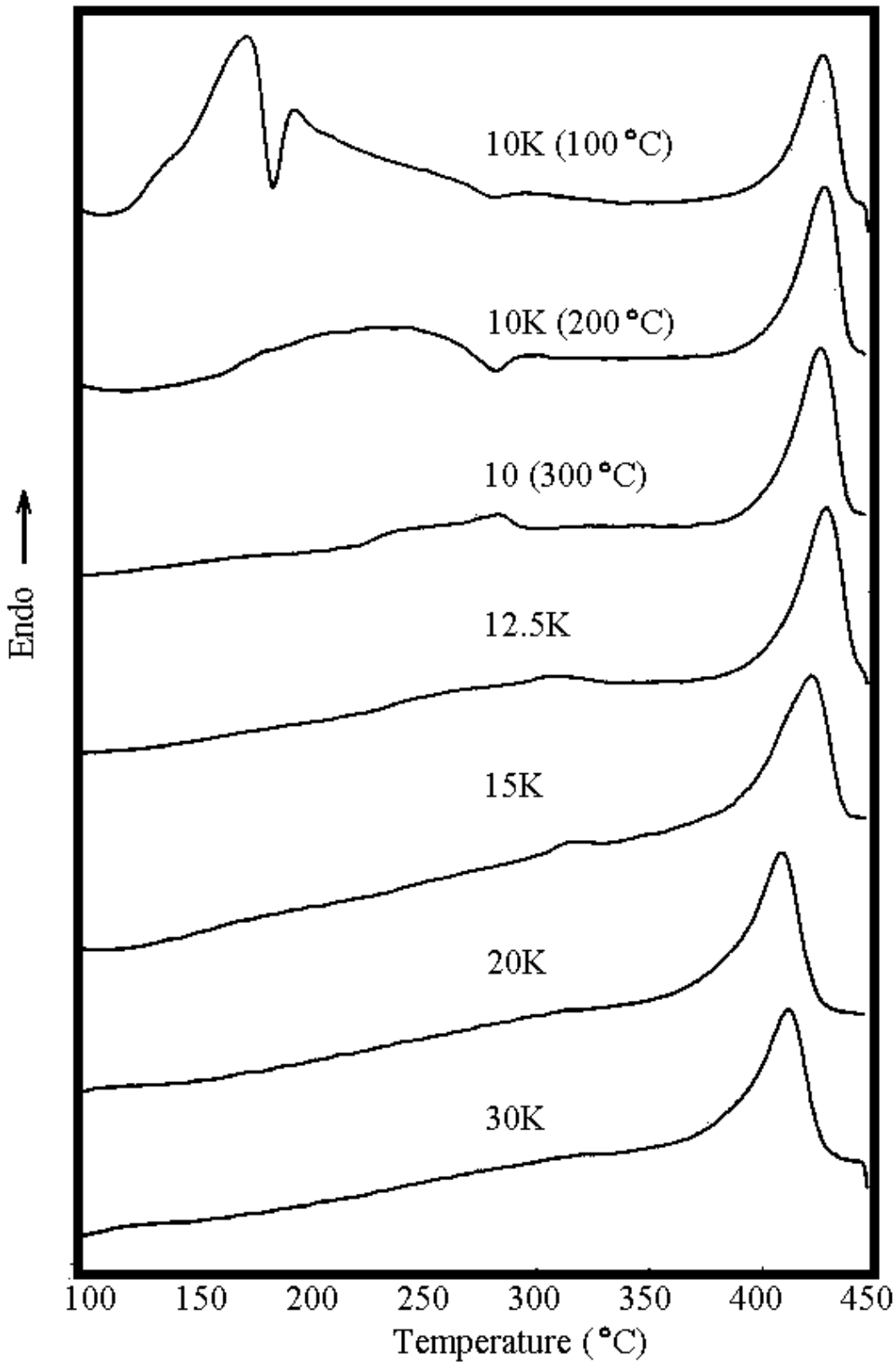

Figure 4.2.2.4: First Heat DSC Thermograms of TPEQ-ODPA-PA Samples at 10°C/min

was independent of molecular weight. Furthermore, the lack of an obvious glass transition in these samples was apparent. This resulted from the crystallinity of these samples and, as a consequence, restricted mobility of the amorphous phase. The presence of a rigid amorphous phase above the glass transition may also have served to decrease the magnitude of transitions of any mobile amorphous fractions.

The quenching and reheating of these samples generated the second heat thermograms shown in Figure 4.2.2.5. Each of the 10K samples exhibited a prominent glass transition around 225°C, followed by a crystallization exotherm peaking at 312°C, and then a melting endotherm at 420°C. Similar behavior was observed in the 12.5K sample, which showed a glass transition around 226°C, a crystallization exotherm at 313°C, and a melting endotherm at 422°C. However, the 15K sample showed a glass transition at 231°C, and then a very broad, yet obscure, crystallization exotherm, followed by a small melting endotherm at 415°C. While the 20K and 30K polyimides displayed glass transitions at approximately 237°C, no additional transitions were noted.

In general, a molecular weight/thermal transition correlation is much more apparent in the second heats. For example, the glass transition increased from about 225°C for the 10K samples to roughly 238°C for the 30K sample, a tendency common among polymers. The 10K and 12.5K samples, in fact, demonstrated a strong inclination to crystallize from the glass, certainly as a result of the mobility of these particular samples. The 15K, 20K, and 30K samples, however, were viscous to the point where the mobility of these systems was sufficiently hindered to prevent crystallization during the 10°C/min heating rate utilized for the second heats. To summarize, all the samples generally demonstrated slow crystallization rates, as evidenced by the fact that even the second heat thermograms of the 10K and 12.5K samples were approximately 30% lower than those experienced on the first heat.

The “as-is” 15K polyimide samples were also tested to determine whether crystallinity could be chemically induced, or whether melt treatment resulted in irreversible chemical changes that would totally eliminate the ability to recrystallize. This procedure involved using slower heating rates on the second heat to determine if that would enable a larger crystallization window, thereby overcoming the slow crystallization kinetics. The

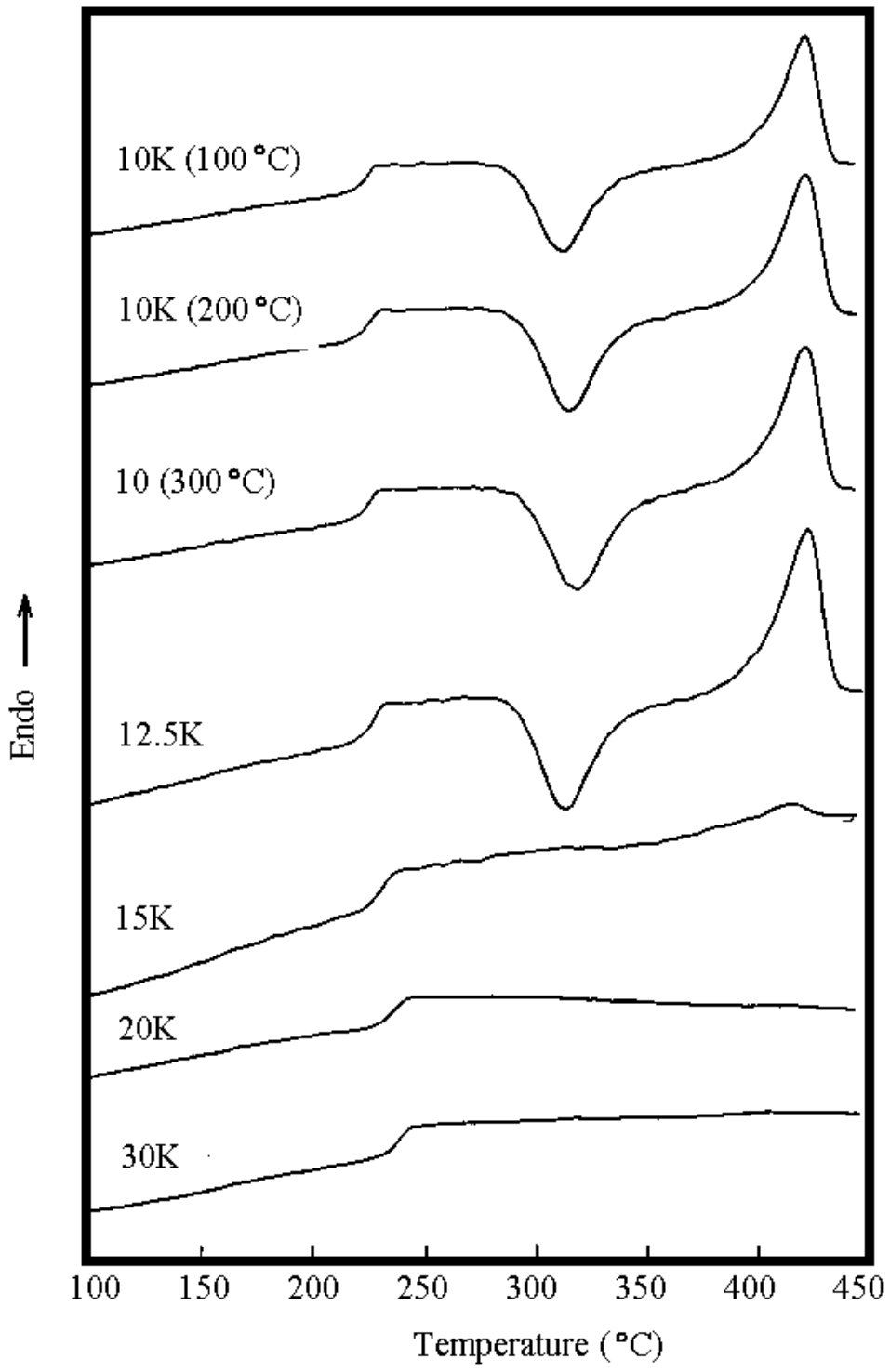

Figure 4.2.2.5: Second Heat DSC Thermograms of TPEQ-ODPA-PA Samples at 10°C/min

DSC traces resulting from this experiment are given in Figure 4.2.2.6 and clearly indicate that areas of the crystallization exotherm and the melting endotherm increase as the heating rates are decreased. This implies that slower heating rates do contribute to higher levels of crystallinity as a result of the wider crystallization window (T_m-T_g). In addition, isothermal crystallization at 320°C results in an even higher enthalpy of melting. These findings confirm that low polymer mobility was the primary factor in hindering crystallization in these samples.

Similar experiments were performed on the 20K and 30K polyimides, and the resulting DSC thermograms of the 30K material are shown in Figure 4.2.2.7. In examining both samples, it was determined that crystallinity could not be regenerated using either slower heating rates or isothermal crystallization. However, solvent induced crystallization was attempted on the 30K sample, which involved boiling a quenched sample of the polyimide in NMP for 3 hours under nitrogen. Although the polyimide did not dissolve, the NMP did adequately plasticize it to enhance its mobility and, consequently, its ability to recrystallize, as was seen in other polyimide systems mentioned earlier.[143] The samples were then washed with water and held at room temperature overnight under vacuum. The resulting DSC of the solvent-treated polyimide showed a large endotherm early, denoting the loss of residual NMP absorbed by the polymer, followed by an exotherm wherein crystallization could occur, and ultimately a large melting endotherm. Based on these results, it can again be concluded that loss of crystallinity is not irreversible, but rather a result of sluggish crystallization kinetics.

Wide-angle x-ray scattering patterns of the as-made and quenched 15K polyimide samples are shown in Figure 4.2.2.8. While the as-is 15K sample displayed a level of crystalline defraction in the range of approximately 40%, only a broad amorphous halo was seen for the quenched sample.

To understand the effects of melt treatments, especially the influence of melt time and temperature on crystallinity, DSC studies were conducted on the 10K (300°C) and 12.5K samples to measure the heats of crystallization (ΔH_c) after various melt treatments. For this particular experiment, the polyimide samples were heated at 20°C/min to various temperatures in the melt and held there for varying lengths of time. The samples were

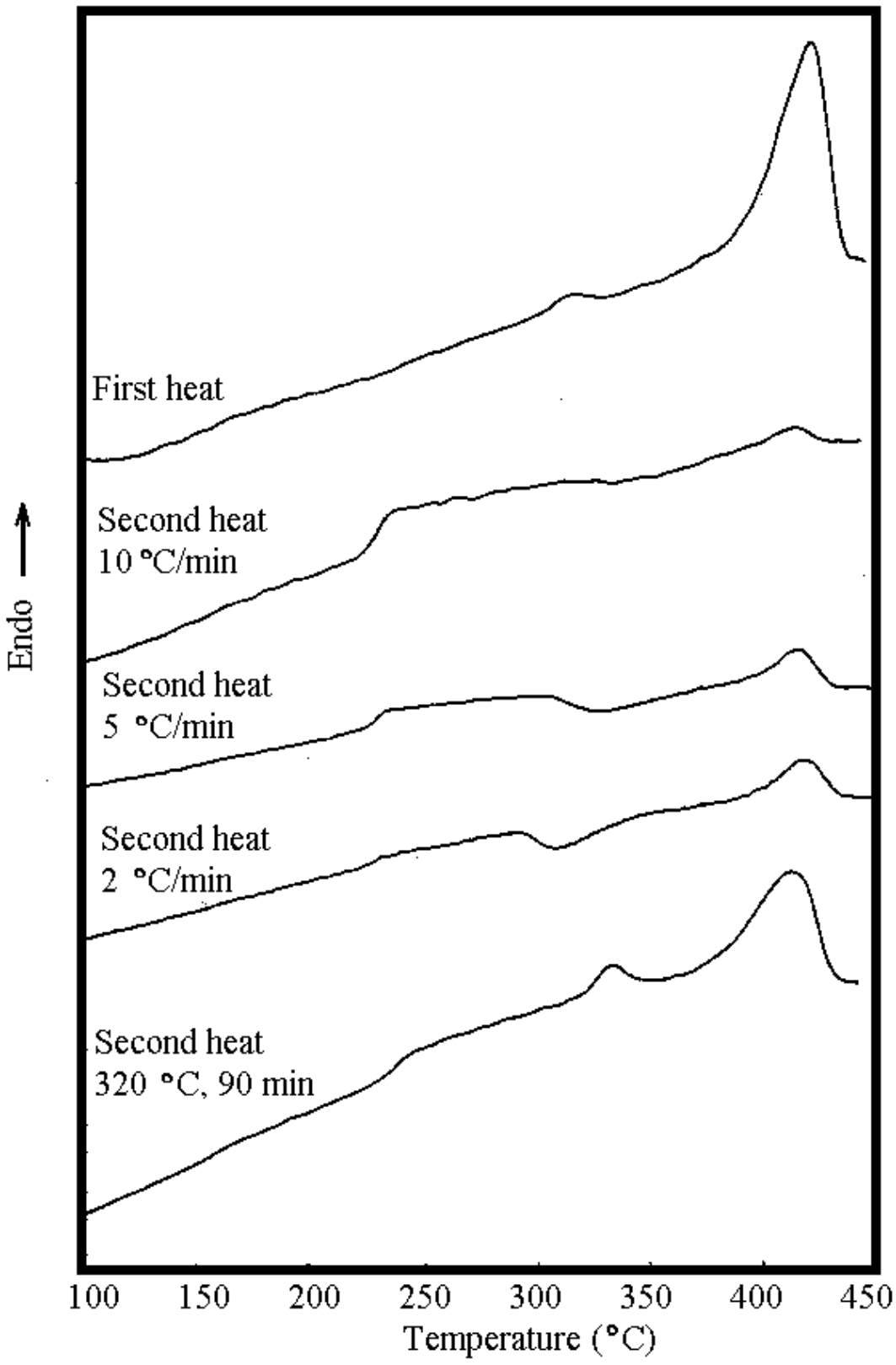

Figure 4.2.2.6: DSC Thermograms of 15K TPEQ-ODPA-PA at 10°C/min

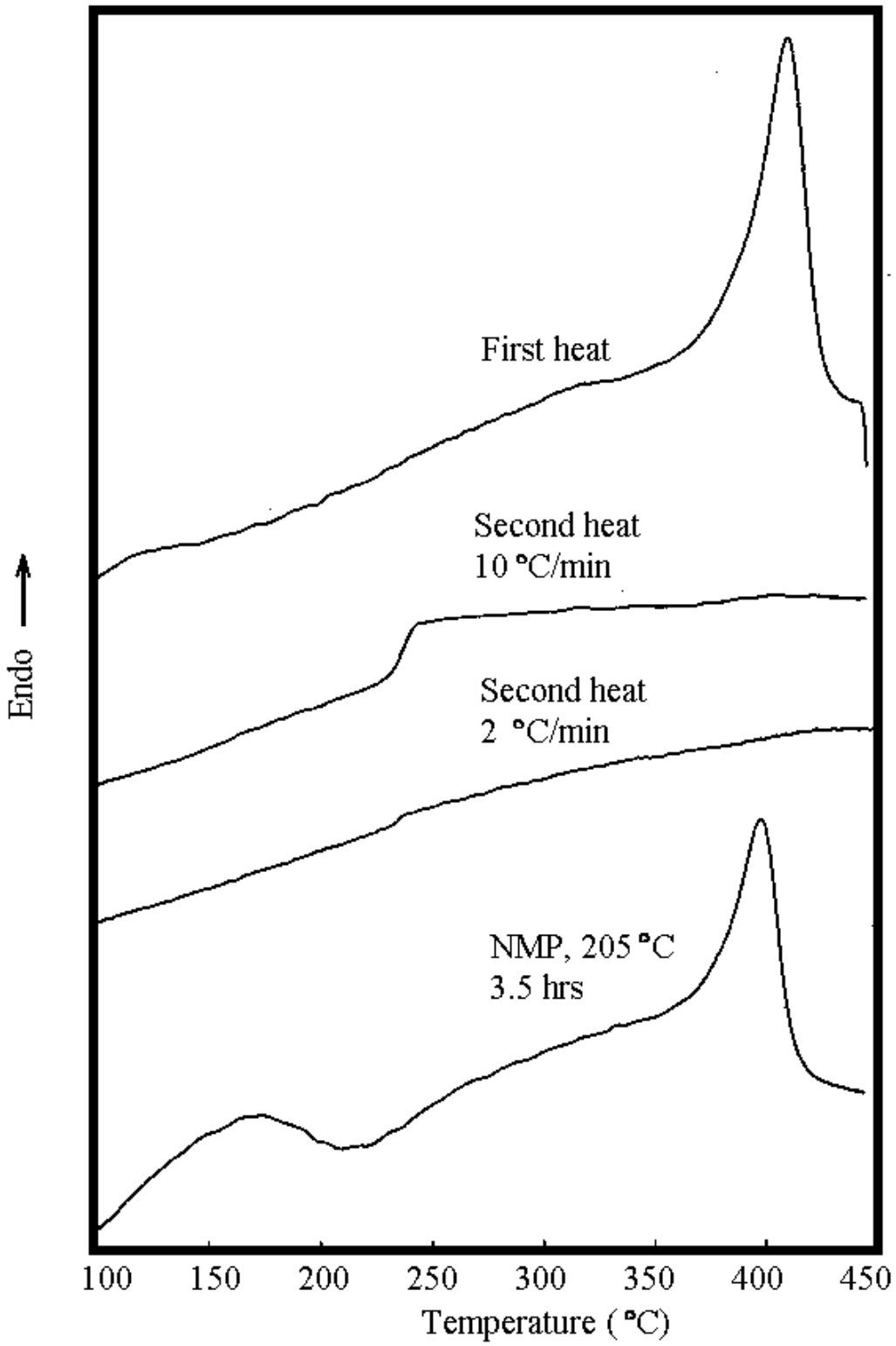

Figure 4.2.2.7: DSC Thermograms of 30K TPEQ-ODPA-PA at 10°C/min

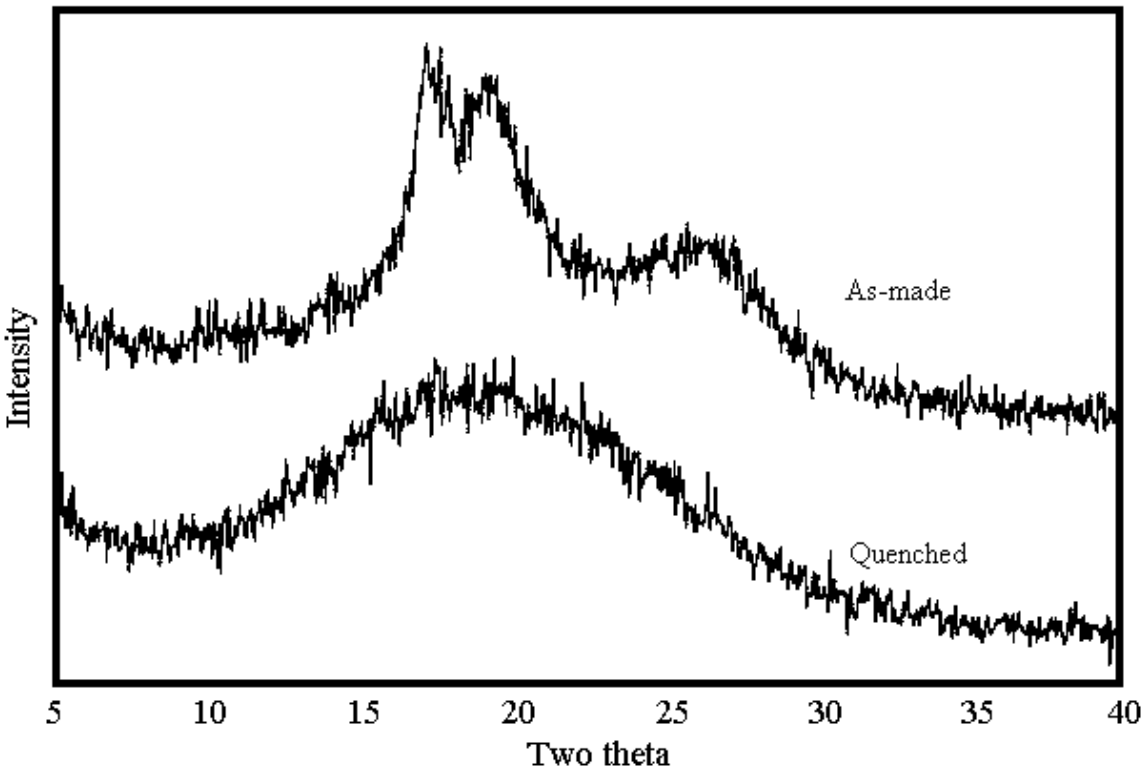

Figure 4.2.2.8: Wide Angle X-ray Scattering (WAXS) Patterns for 15K TPEQ-ODPA-PA

then quenched at 200°C/min to 100°C, and reheated at 10°C/min. The heats of crystallization were measured upon reheating.

The results obtained for the 10K (300°C) sample are summarized in the 3-D graph in Figure 4.2.2.9, which shows that the melt temperature had a relatively minor effect on ΔH_c – providing that the melt time was brief. However, when the melt time was increased to 5 minutes, the decrease in ΔH_c became much more pronounced at increased melt temperatures. It was also observed that the sample held at a lower melt temperature retained some crystallinity even after 12 minutes in the melt, despite the fact that the ΔH_c was significantly diminished. These decreases in ΔH_c are likely due to chemical changes such as cross-linking, branching, or chain extension occurring in the melt.

The results obtained for the 12.5K sample are summarized in the 3-D graph in Figure 4.2.2.10. Unlike the 10K sample, the 12.5K polyimide demonstrated that ΔH_c was highly melt temperature dependent, even after very short melt times. Furthermore, virtually no crystallization was observed after prolonged melt times, even at the lowest melt temperature treatment. Therefore, the results from the melt time/temperature study for the 10K and 12.5K samples indicate that the melt stability of the TPEQ-ODPA-PA system is highly dependent on the molecular weight of the sample.

As a consequence of these findings, further work was conducted to investigate the likelihood of molecular weight changes in the melt. To do so, an isothermal melt viscosity measurement of the 12.5K sample was performed 450°C. The resulting complex viscosity measurement, as a function of time, is shown in Figure 4.2.2.11 and reveals that the viscosity changed by an order of magnitude during the interval of the experiment. This increase in viscosity, likely due to chain extension or crosslinking (as noted earlier), would therefore severely hinder the mobility of the polyimide and eliminate its ability to recrystallize.

The 12.5K sample was then subjected to treatment at 445°C for 1 and 7 minutes, respectively. The DSC traces of these materials upon reheating are shown in Figure 4.2.2.12. It should be noted that the sample treated for 7 minutes did display an increased T_g, indicative of a molecular weight increase, which is similar to the findings for the higher molecular weight samples described earlier.

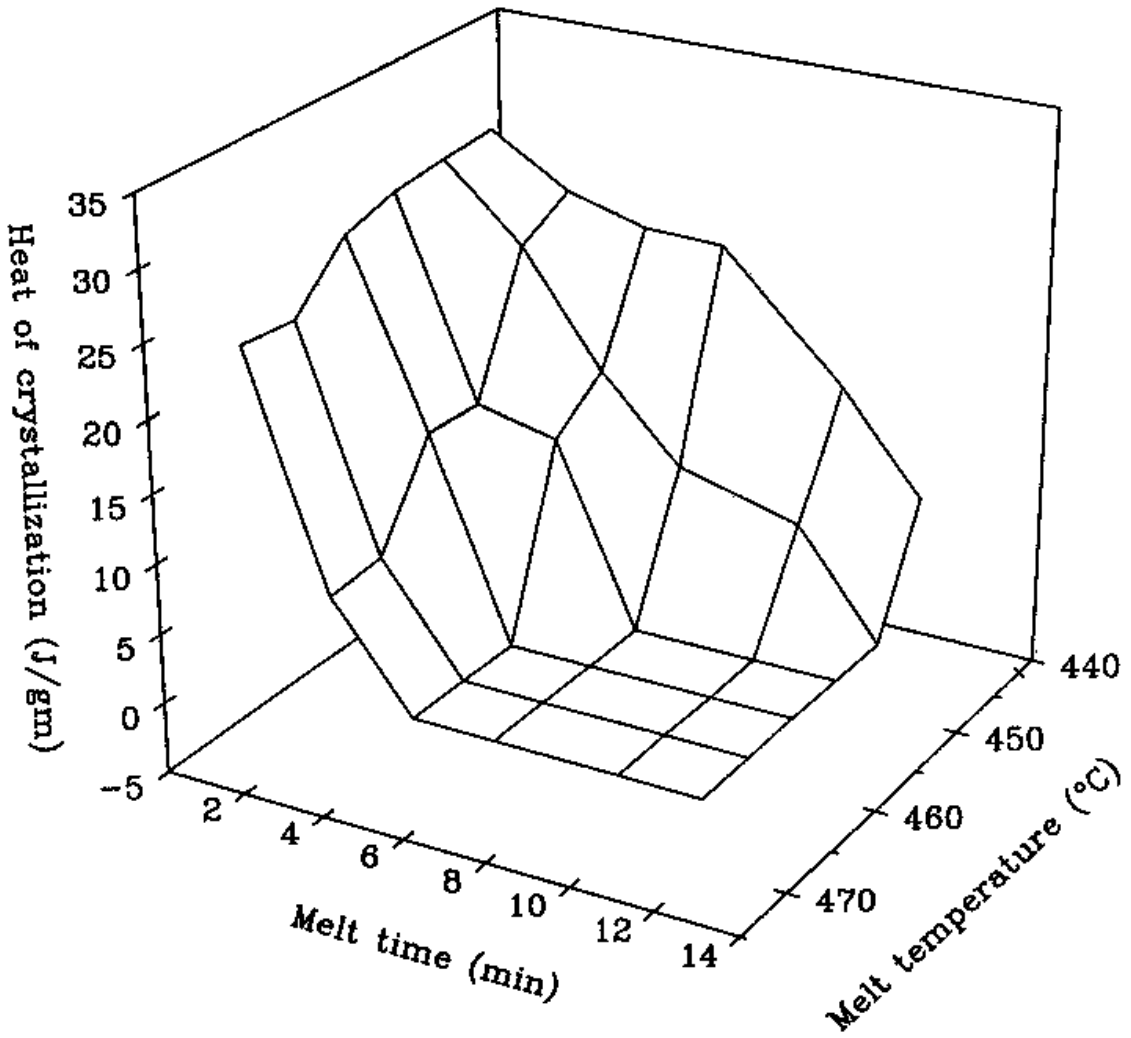

Figure 4.2.2.9: Effect of Temperature and Time in the Melt under Nitrogen on the Heat of Crystallization of 10K (300°C) TPEQ-ODPA-PA[224,235]

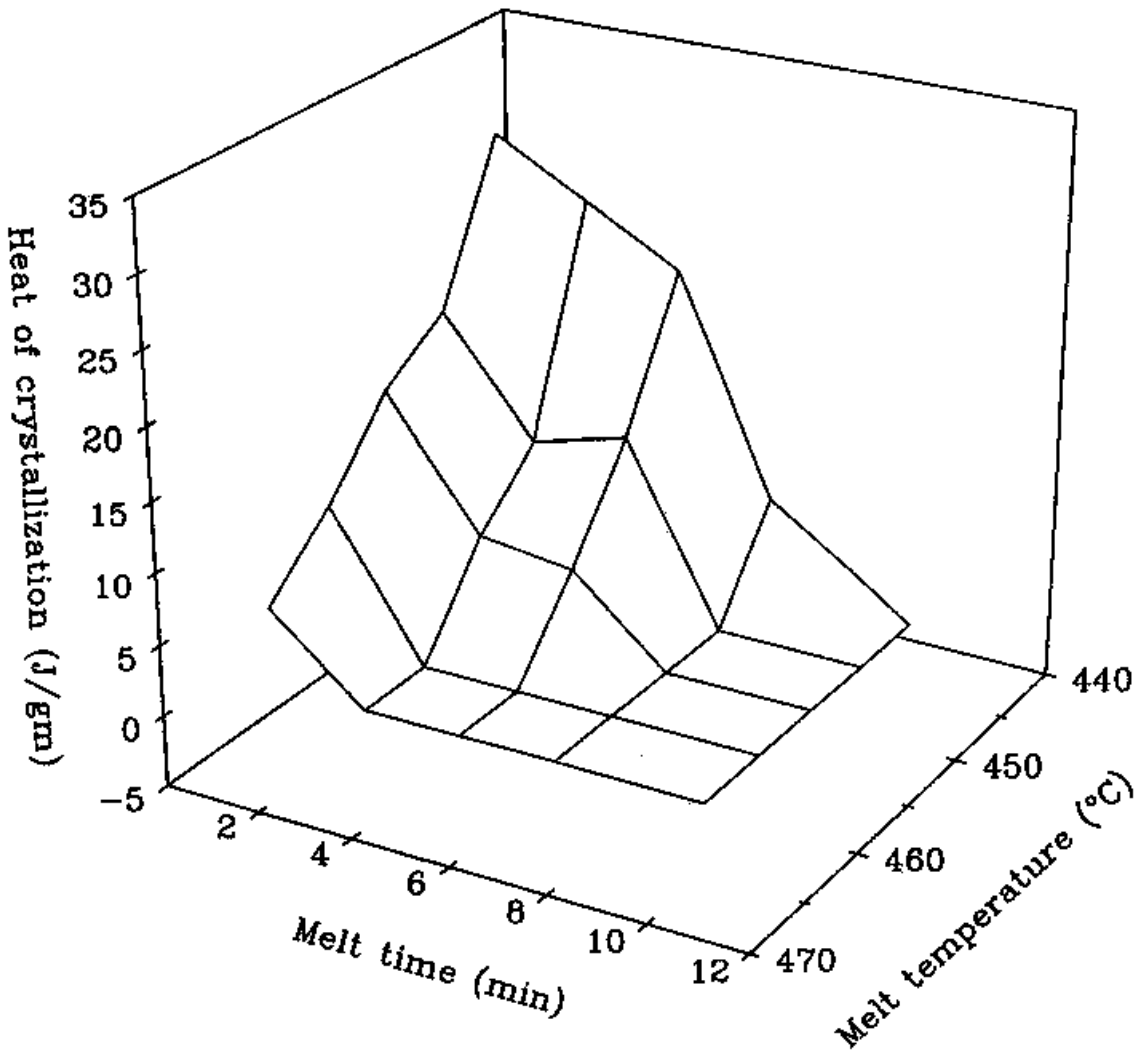

Figure 4.2.2.10: Effect of Temperature and Time in the Melt under Nitrogen on the Heat of Crystallization of 12.5K TPEQ-ODPA-PA[224,235]

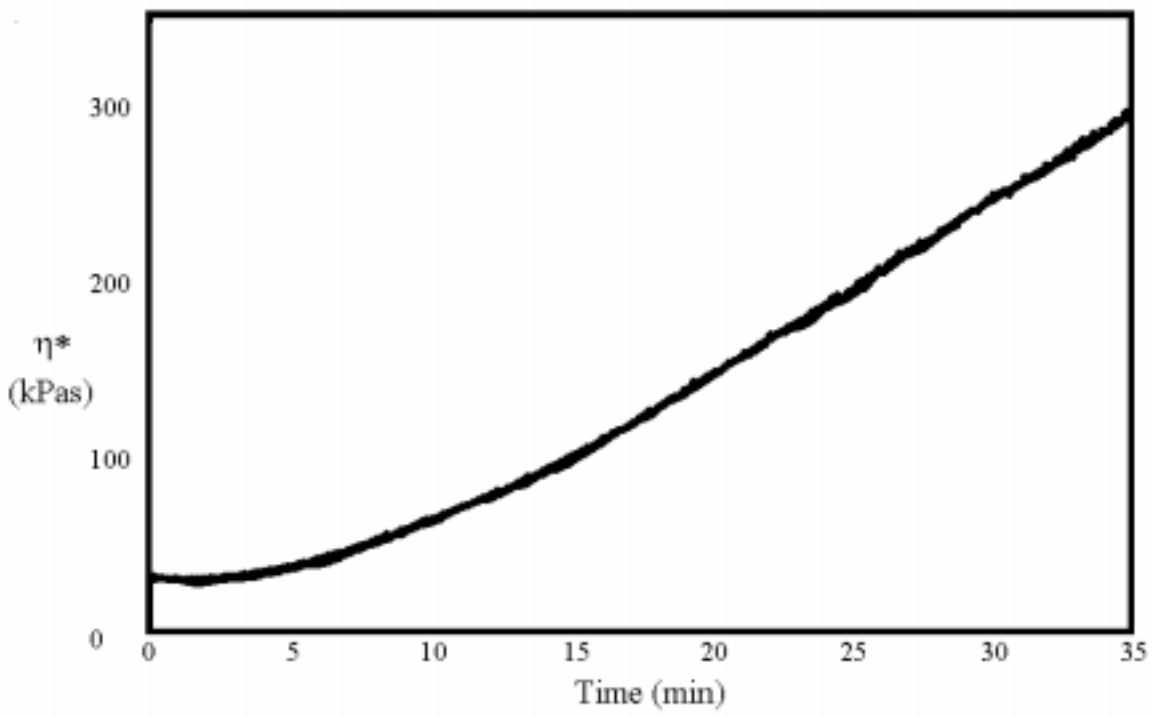

Figure 4.2.2.11: Complex Viscosity at 450°C Under Nitrogen as a Function of Time for 12.5K TPEQ-ODPA-PA

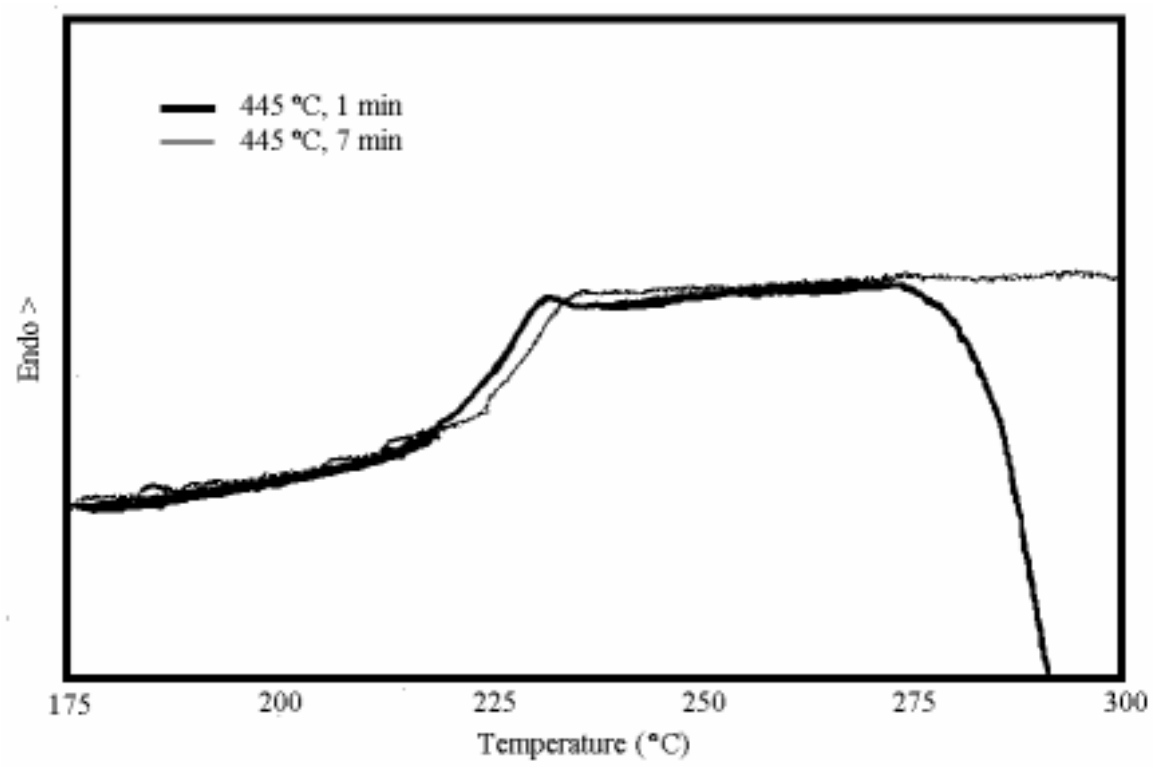

Figure 4.2.2.12: DSC Scans for Melt-Treated 12.5K TPEQ-ODPA-PA at 10°C/min

4.3 1,3-Bis(4-aminophenoxy)benzene (TPER) Based Polyimides

To reiterate, a major goal of this research was to synthesize and develop processable semicrystalline polyimides via the incorporation of ether linkages into the polyimide backbone because their inclusion is known to impart desirable mechanical properties, such as toughness, to aromatic polymers. To achieve this goal, an additional diamine was utilized.

The monomer 1,3-bis(4-aminophenoxy)benzene, referred to herein as TPER (triphenyl ether diamine-resorcinol), is a meta-catenated isomer of TPEQ. The meta-orientation of the aminophenoxy groups would be expected to result in polyimides with lower transition temperatures and, thus, improved processability. In this section, the polyimides prepared from this diamine will be described.

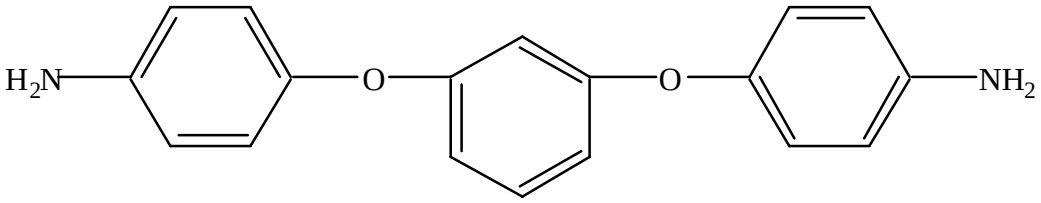

TPER

[1,3-bis(4-aminophenoxy)benzene]

4.3.1 Polyimide semicrystalline powders derived from TPER

30 kg/mol TPER polyimide powders were synthesized using the same procedure as was described for the TPEQ polyimide powders. The repeat units of these polyimides are shown in Figure 4.3.1.1. While the polyimides from PMDA and BPDA precipitated from solution when imidized, the ODPA polyimide remained in solution for the duration of the imidization process. Once cooled, the solution formed a gel and was then precipitated. It was noted that this polyimide was no longer soluble in organic solvents, indicating its semicrystalline nature. Samples of each polyimide were synthesized and analyzed in a similar fashion to the TPEQ powders.

The particle size and thermal analyses for these powders are summarized in Table 4.3.1. As can be seen, the particle sizes ranged from 12 to 25 μm, and the 5% weight loss values, again, were in excess of 500°C. While the polyimide powder based on PMDA did not exhibit any transitions up to 450°C, the polyimides derived from BPDA and ODPA did. The DSC thermograms of TPER-ODPA-PA are shown in Figures 4.3.1.2. The lowered transitions seen for the ODPA polyimide, as well as the appearance of thermal transitions of the BPDA polyimide (unlike what was observed for the TPEQ powders) exemplify the effect of the meta orientation in TPER. It should be noted that the TPER-BPDA-PA polyimide has been shown to demonstrate particularly interesting behavior[236] and, thus, will be examined in greater detail. Like the TPEQ polyimide powders, the TPER-based powders demonstrated excellent chemical resistance in the presence of both organic solvents and strong organic acids.

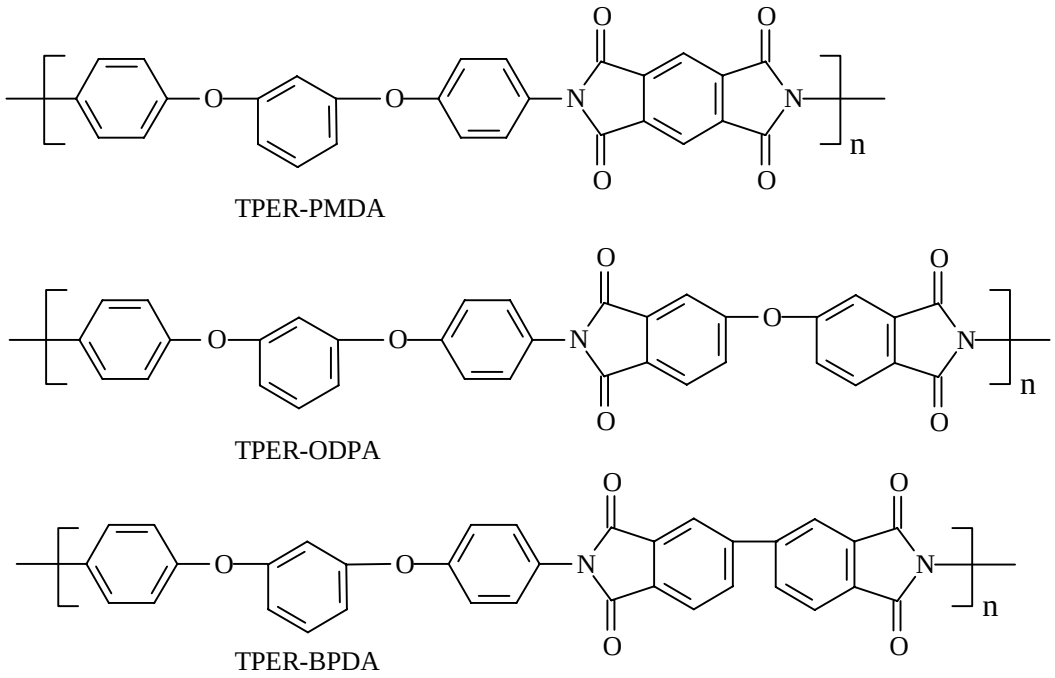

Figure 4.3.1.1: TPER-Based Polyimides

Table 4.3.1: Summary of Thermal and Particle Size Analyses

polyimide	particle size (µm)	5% wt. Loss (°C)*	T_g (°C)**	T_m (°C)***
TPER-PMDA-PA	13	526	-	-
TPER-BPDA-PA	25	520	233	402
TPER-ODPA-PA	25	519	215	335

*in air, 10°C/min

**from second heat

***from first heat

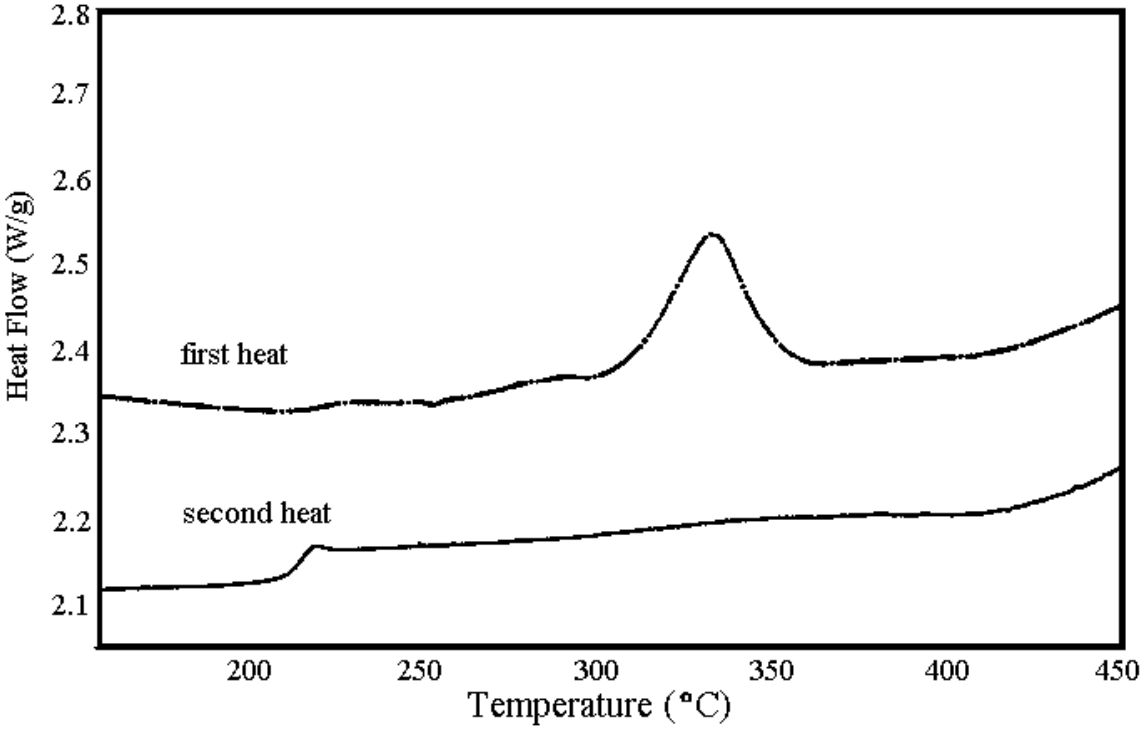

Figures 4.3.1.2: DSC Thermograms of TPER-ODPA-PA at 10°C/min

4.3.2 TPER-BPDA-PA Polyimide

4.3.2.1 Degree of imidization of TPER-BPDA-PA powder

As was mentioned earlier, solution imidization was used to synthesize the TPEQ and TPER-based polyimide powders. In the case of crystalline polyimides, such as the ones targeted in this research, the polyimide begins to precipitate from solution during imidization. However, premature precipitation results in an incomplete level of cyclization. Therefore, without subsequent heat treatments, unspecified amounts of uncyclized amic acid moieties remain in the polymer. Depending on the method of processing, this can be result in either major or minor problems. For example, when a polyimide is synthesized using dry powder processing, the evolution of water from imidization can be problematic. Thus, it is important to gauge the water that is evolved during synthesis.

As a model study, the degree of imidization of TPER-BPDA-PA polyimide powders formed during solution imidization was investigated. More specifically, research was conducted to study the effect of extending the reaction time of the solution imidization on the degree of imidization. During the synthesis of the TPER-BPDA-PA system at a 10% solids concentration, precipitation of the polyimide particles begins to take place within 90 to 100 minutes after the start of the imidization reaction. After 2 hours, the reaction mixture was added with stirring to a beaker of acetone, and the polyimide particles were subsequently filtered and washed. The polymerization was repeated utilizing solution imidization periods of 4, 6, 8, 10, 12, and 14 hours.

A known procedure was used to completely dry the polyimide without inducing further imidization.[43] The polyimide powders were immersed in acetone and sonicated. Afterwards, the particles were filtered and washed, placed under vacuum at room temperature for over two days, and dried at 50-60°C for four hours. At this point, the polymer powders were analyzed.

Initially, FTIR was used to determine the level of imidization in the powders, as this has been widely used for similar studies involving polyimide films by referencing polyamic acid absorbances to polyimide absorbances. Unfortunately, this technique was ineffective when used with the powders, as it was difficult to distinguish partly imidized powders from the fully imidized ones.

Since the amount of water loss occurring during solution imidization is equal to the amount of imide formation, the degree of imidization can be determined by tracking the weight loss that occurs due to cyclodehydration of the polyamic acid. This can be accomplished utilizing isothermal TGA, according to the relationship denoted in the equation

$$\text{degree of imidization} = \left(1 - \frac{\text{percent weight loss of polymer after 1 hr at 300°C}}{\text{theoretical percent weight loss of amic acid}}\right) \times 100$$

where

$$\text{theoretical percent weight loss} = \left(\frac{36\ \text{g/mol}}{\text{molecular weight of repeat unit}}\right) \times 100$$

As a result of repeated trials, 300°C was found to be the primary reaction temperature at which complete imidization could take place. The results of the study as determined by TGA measurements are shown in Table 4.3.2.1. It is clear to see from these results that the percent of imidization for the TPER-BPDA-PA powders generally ranged from about 65 to 70%. The fact that there was no significant increase or change over time in these percentages implies that extending the imidization reaction did not increase the degree of imidization of the polyimide particles.[237] The relatively high level of imidization in the precipitated powders shows promise with regard to commercial processing. Furthermore, the presence of a few amic acid groups in these powders might possibly be used in some advantageous manner.

4.3.2.2 Thermal analysis

First and second heat DSC thermograms of 30 kg/mol TPER-BPDA-PA are shown in Figure 4.3.2.2.1. As was noted above and seen in the first heat thermogram, as-

Table 4.3.2.1: Influence of Imidization Reaction Time on the Percent Imidization by TGA

imidization time (hrs)	weight loss (%)	% imidization
2	2.0	69
4	2.3	65
6	2.2	67
8	2.6	65
10	1.9	71
12	-	-
14	2.3	64

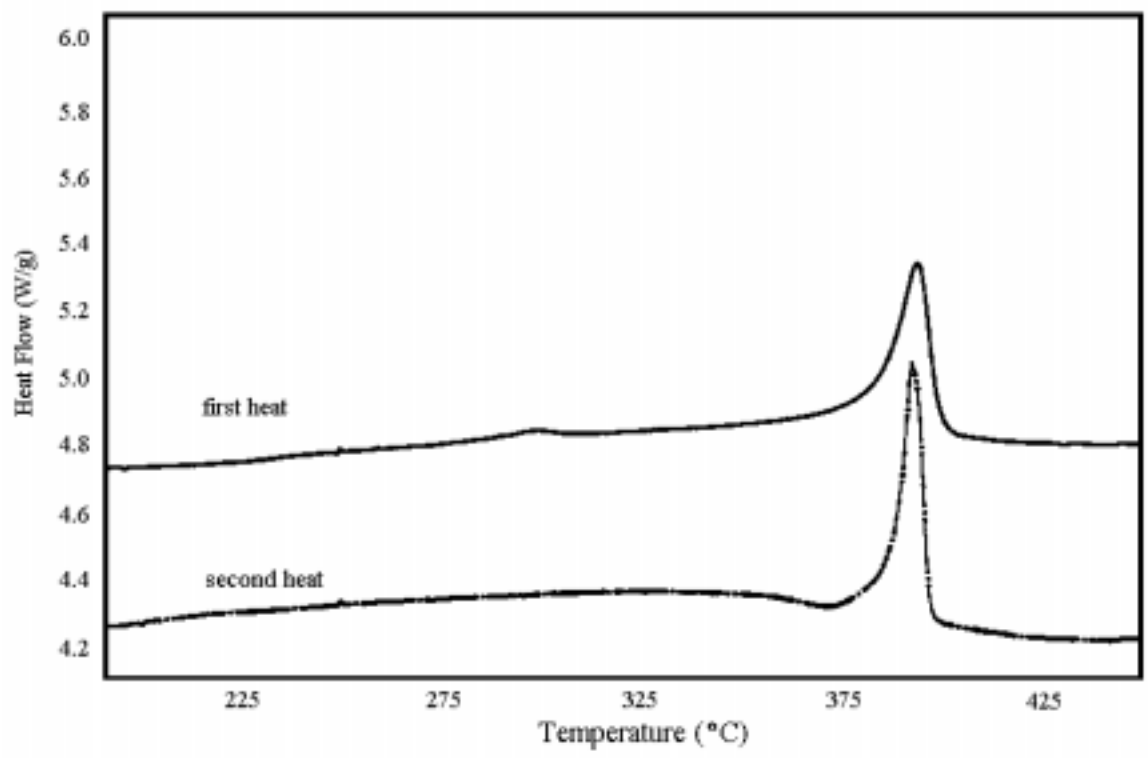

Figure 4.3.2.2.1: DSC Thermograms of 30,000 g/mole TPER-BPDA-PA at 10°C/min

made (after drying) samples of this polyimide exhibited a melting point approaching 400°C. Unlike the TPEQ-ODPA-PA, quenching this particular system from the melt did not result in an amorphous polymer. Instead, the strong melting endotherm observed in the first heat was seen in the second heat. In general, the polyimide's molecular order and mobility was sufficient for rapid crystallization to occur upon cooling from the melt, which is extraordinary given the material's high molecular weight. This unique behavior had not been noted in the polyimide literature until fairly recently.[238] In order to study this matter more thoroughly, bulk imidized samples of TPER-BPDA-PA of varying molecular weights were prepared and submitted for thermal analysis (TGA and DSC), dynamic mechanical analysis, and melt rheology.

A series of TPER-BPDA films consisting of number average molecular weights of 20K and 30K were synthesized by the classical two step route. The polyamic acids were imidized using the bulk imidization technique described earlier, and the resulting FTIR spectrum is shown in Figure 4.3.2.2.2. Subsequently, 30K films consisting of varying compositions of phthalimide endcapping were prepared. One sample that was fully endcapped with phthalic anhydride is thus designated as PA endcapped. Another sample was only partially endcapped by using only half of the molar amount of phthalic anhydride necessary to fully endcap the polyimide and as such is designated as half endcapped. The remaining sample was an amine terminated TPER-BPDA and is designated as amine terminated. A commercial material, Aurum New TPI, was also included in the analysis. All of the samples were considered as as-made if no additional thermal treatments were carried out prior to characterization.

TGA of the polyimides was conducted in both air and nitrogen environments, and the results are shown in Table 4.3.2.2. All of the samples demonstrated excellent weight loss profiles, as judged by the fact that 2% weight loss was not observed below 500°C. Furthermore, it appears that the nature of the endgroup did not adversely affect the weight loss characteristics of the polymers. Nevertheless, it should be noted that the TGA results do not account for any chemical changes that might have occurred under these experimental conditions.

A number of DSC studies were performed on the TPER-BPDA and New TPI

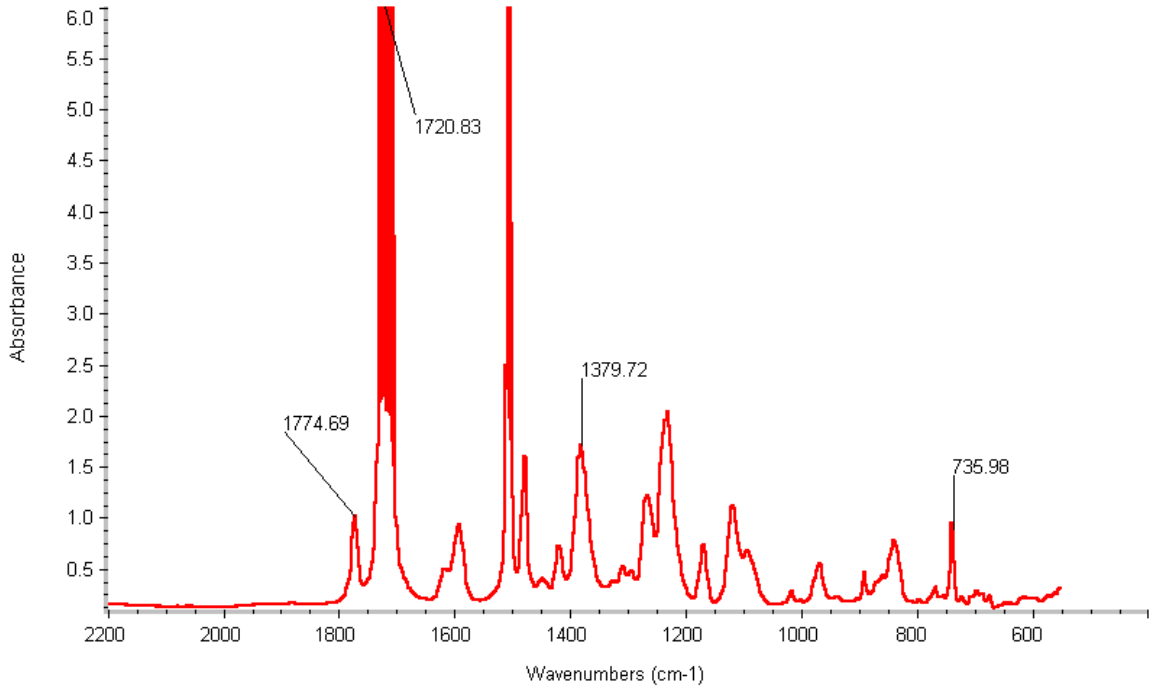

Figure 4.3.2.2.2: FTIR Spectrum of TPER-BPDA-PA

Table 4.3.2.2: Results of TGA of the TPER-BPDA Polyimides

polymer	M_n (kg/mole)	2% wt. loss T in air (°C)	2% wt. loss T in N_2 (°C)
PA endcapped	20	502	539
PA endcapped	30	526	545
amine terminated	30	527	549
half endcapped	30	527	549

films. The first heat DSC thermograms of the samples are shown in Figure 4.3.2.2.3, which shows that the TPER polyimides displayed weak glass transitions around 230°C. In addition, the weak endotherms detected at approximately 300°C were probably caused by the thermal history arising from the 300°C imidization step, from which premelting of less perfect crystals may have occurred. These were followed by somewhat broad, weak exotherms wherein additional crystallization of these imperfect crystals may have taken place. Afterwards, strong melting endotherms were seen at 390°C. There were no distinct differences noted between the 20K and 30K samples. The amorphous New TPI sample displayed a glass transition at 250°C, followed by a crystallization exotherm at around 327°C, and then a melting endotherm at 385°C. All of these samples were heated to 425°C and held there for a minute.

The quenching of these samples and subsequent reheating generated the second heat thermograms shown in Figure 4.3.2.2.4. All of the TPER samples displayed weak transitions around 210°C, which is likely indicative of the glass transition of the polyimide, followed by very weak crystallization exotherms. Very sharp melting endotherms are seen at 395°C. Based on these results, one can observe several interesting features of the TPER-BPDA polyimides. For example, none of these samples could be quenched into a pure amorphous state after the first heat, a phenomenon which implies that there were extremely fast crystallization kinetics at work on these particular materials, despite the high molecular weight of the samples. Thus, these TPER-BPDA samples compare much more favorably than the lower molecular weight samples of TPEQ-ODPA-PA which, as mentioned earlier, could be easily rendered amorphous by melt treatments. Also the increase in melting temperatures and the sharpness of the melting endotherms noted between the first heat (390°C) and the second heat (395°C) is a strong indicator of the regularity of the crystals after quenching and reheating. Finally, no correlation was developed between molecular weight and thermal behavior over the range 20K to 30K, although this is not particularly relevant given the outstanding performance of the 30K material. New TPI was observed to be quenched to the amorphous state, in accordance with the literature.[157-159,239-241]

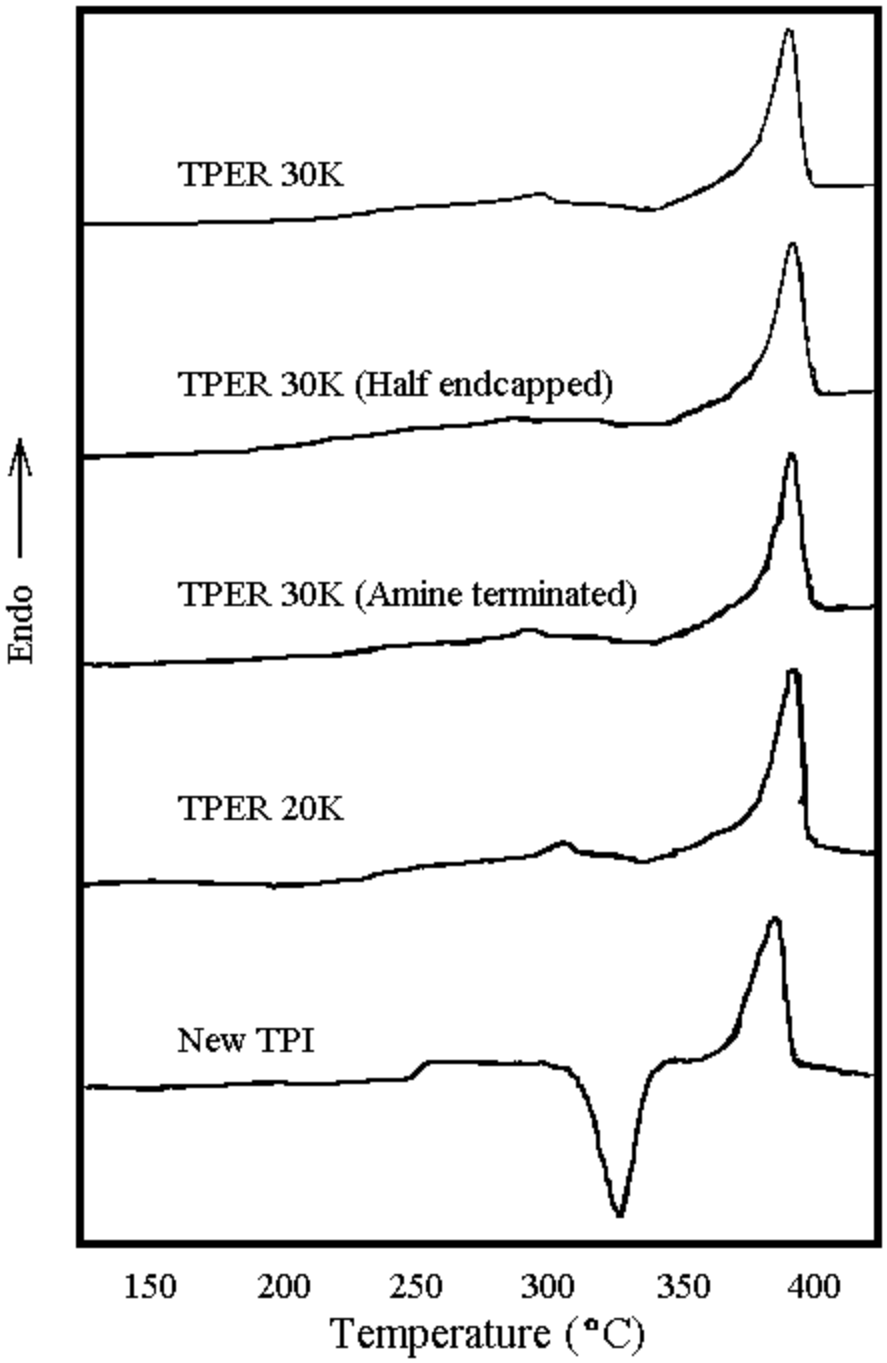

Figure 4.3.2.2.3: First Heat DSC Thermograms of TPER-BPDA Samples at 10°C/min

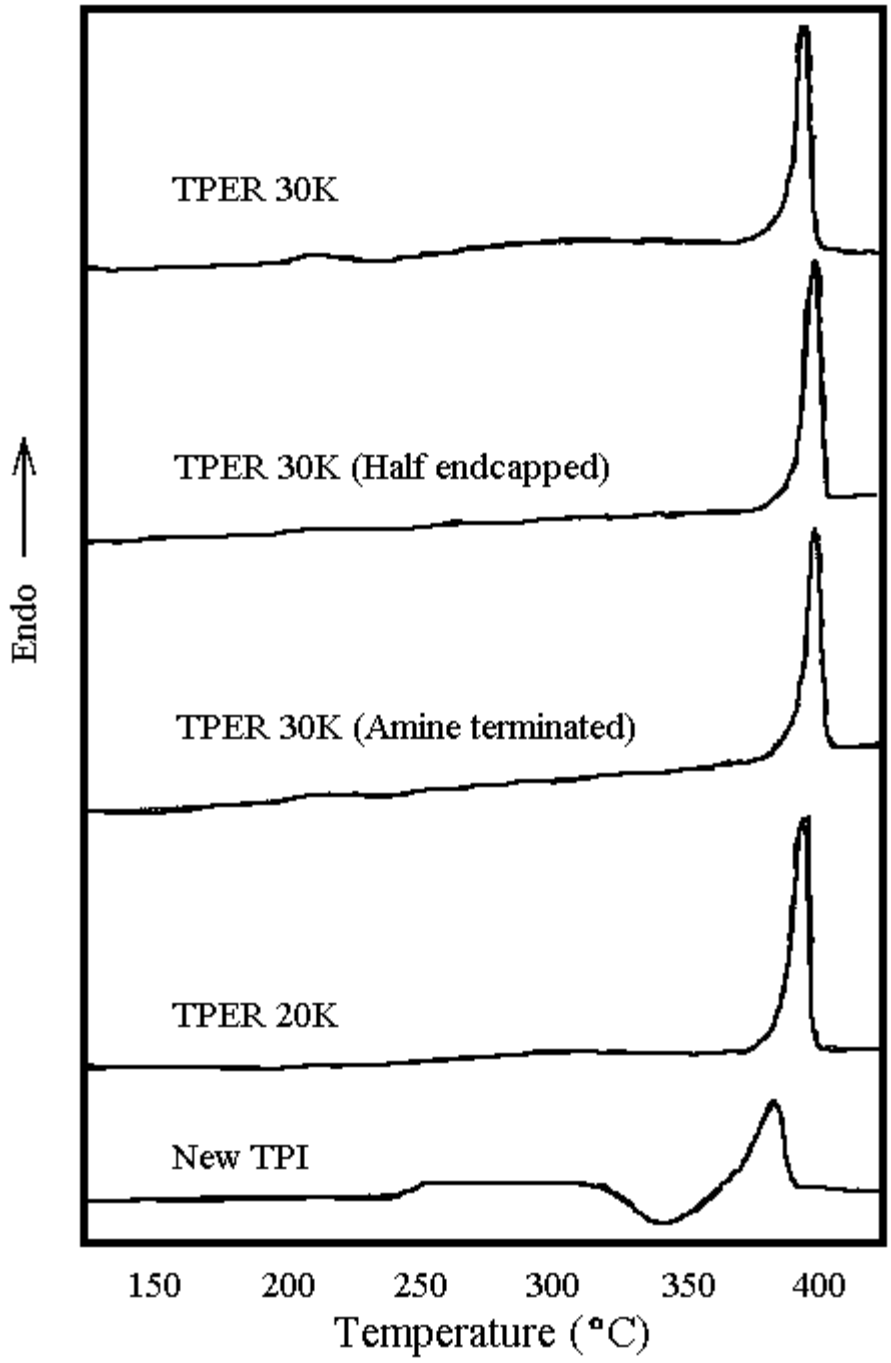

Figure 4.3.2.2.4: Second Heat DSC Thermograms of TPER-BPDA Samples at 10°C/min

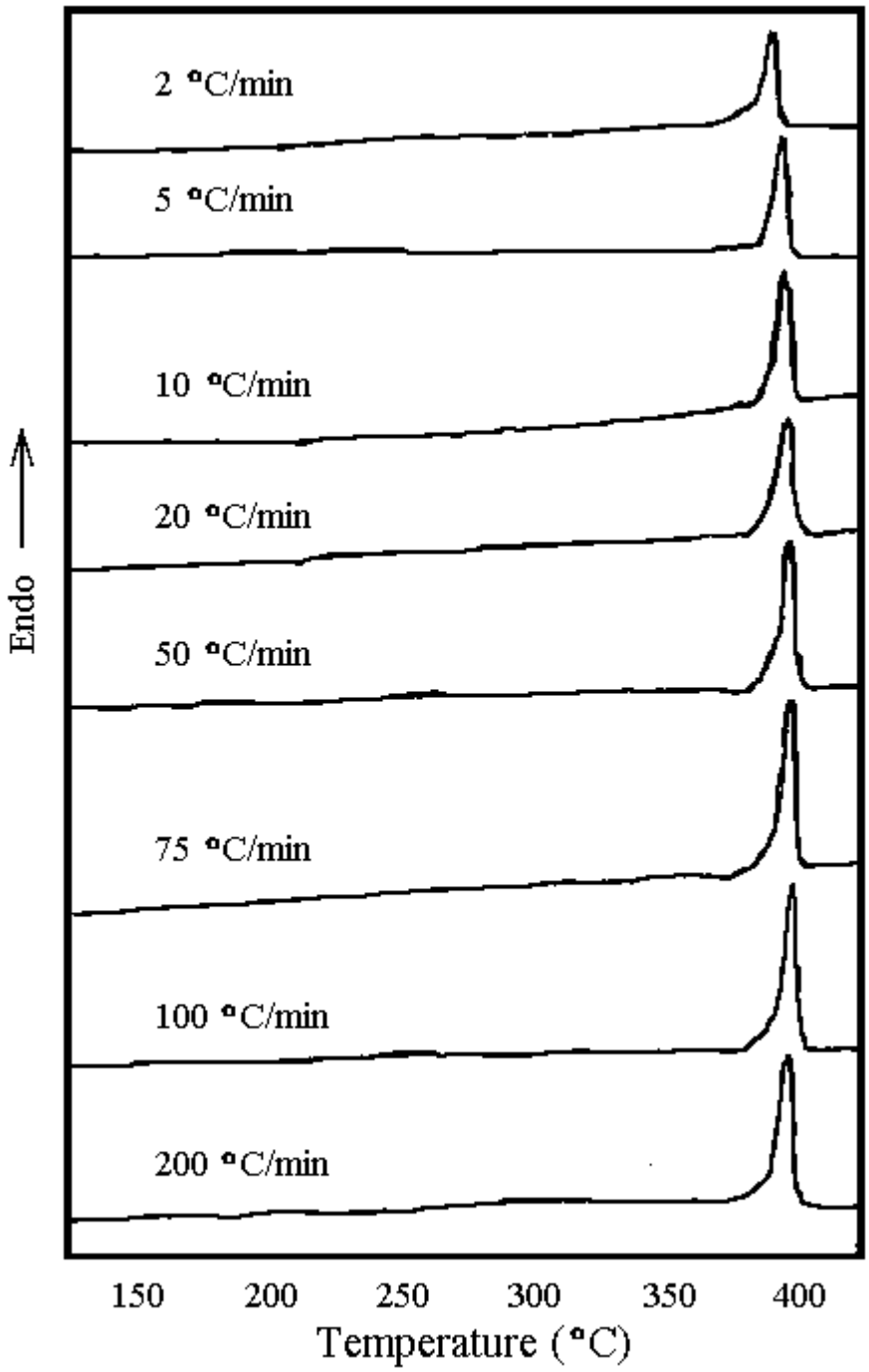

Figure 4.3.2.2.5: Influence of Cooling Rate on the DSC Thermograms of TPER-BPDA-PA Polyimide

In order to study to see the effects of cooling rates on the melting of TPER-BPDA, PA endcapped samples were held at 425°C for a minute, then cooled at different rates, and subsequently reheated. The thermograms generated from this experiment are shown in Figure 4.3.2.2.5. No clear glass transition was apparent in the samples, which were cooled at rates up to 100°C/min and provided evidence that crystallization during cooling could not be prevented. Only in the case of the sample cooled at 200°C/min does the appearance of a glass transition become clear.

Dynamic mechanical analysis (DMA) was utilized to define some of the temperature transitions in TPER-BPDA-PA. DMA spectra of an as-made sample and a slowly-cooled sample from the melt are shown in Figure 4.3.2.2.6. Most prominent is a tan delta transition around 240°C for the as-made sample, corresponding to the T_g of the polyimide. This transition occurs at a higher temperature for the slowly cooled sample, reflecting the influence of crystallinity. In other words, the perfection of the crystals upon cooling will result in reduced mobility in the amorphous phase, and thus the increased restriction would result in an elevated T_g. The magnitude of the transition in the as-made sample was larger than that of the slow cooled sample for much the same reason. Furthermore, the storage modulus decreased more slowly in the slow cooled sample. Similarly, the sub-glass β relaxation around 100°C in the as-made sample was more prominent than the analogous relaxation at a higher temperature seen in the slow cooled sample. A low temperature γ relaxation that appears to be independent of the crystal morphology of the polymer occurred in both samples around -90°C, which has been observed before in arylene ether-containing polymers.[242]

As was described for the lower molecular weight TPEQ-ODPA-PA films, DSC studies were conducted on the PA endcapped TPER-BPDA samples to measure the heats of crystallization (ΔH_c) and melting (ΔH_m) of the polyimides after various melt treatments. The polyimide samples were heated at 20°C/ min to various temperatures in the melt and held there for varying lengths of time. The samples were then cooled at 10°C/min to room temperature, where they were then reheated at 10°C/min. The heats of crystallization were measured upon cooling, as were the heats of melting from the subsequent melting endotherms.

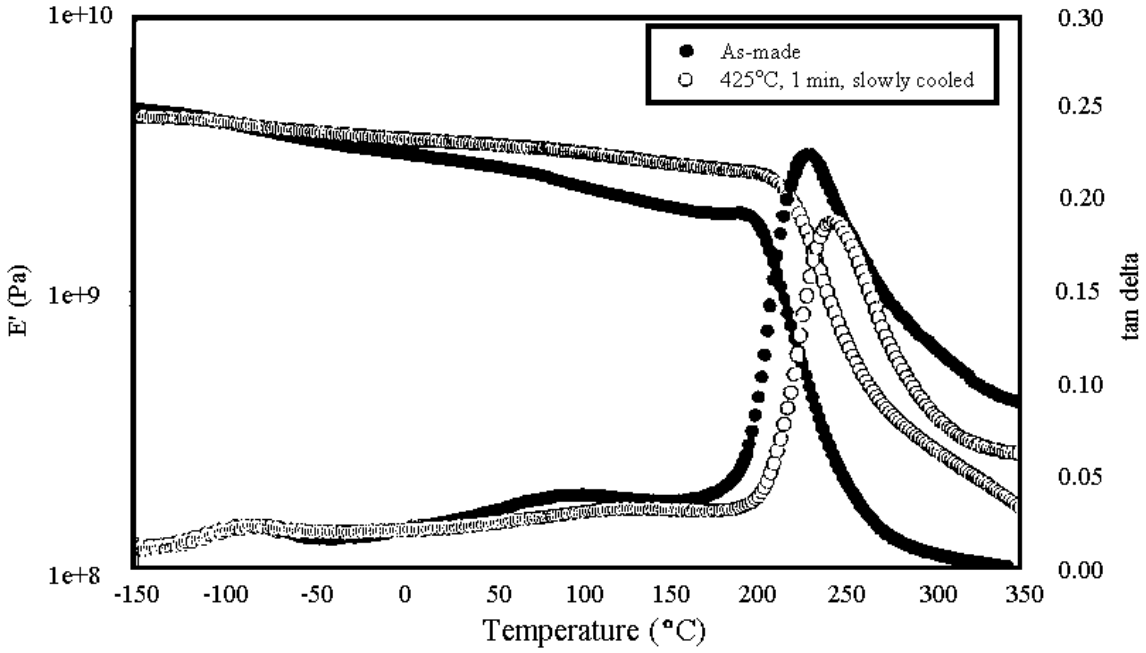

Figure 4.3.2.2.6: DMA Spectra of As-made and Slow Cooled (1°C/min) Samples of TPER-BPDA-PA

The ΔH_m measurements as a function of melt time and temperature are summarized in the 3-D graph in Figure 4.3.2.2.7. From this plot one notes that TPER-BPDA-PA has exceptional melt stability at 420°C for up to 45 minutes without diminishing the ΔH_m. This signifies a treatment roughly 25° higher than the melting point of the polymer. At 430°C, the polyimide showed no decrease in ΔH_m up to 30 minutes, and even at 450°C the polyimide continued to demonstrate melt stability for 20 minutes. However, using experimental conditions exceeding those just described, ΔH_m did decrease, implying a loss of crystallinity as a consequence of the chemical changes mentioned for the TPEQ-ODPA-PA system. Nonetheless, these results point to the likelihood of successfully melt processing this polyimide system with minimal loss in crystallinity and the desirable properties resulting thereof. The stress-strain behavior of this polyimide is shown in Figure 4.3.2.2.8, wherein the polyimide exhibits the characteristics of a tough high performance material. Recent studies have shown that TPER-BPDA-PA demonstrates good adhesive properties as well.[243]

The ΔH_c measurements as a function of melt time and temperature are summarized in the 3-D graph in Figure 4.3.2.2.9. The heats of crystallization measured after melt treatments up to 410°C showed little, if any, melt time dependence, similar to what was seen in Figure 4.3.2.2.7 for the measured heats of melting. However, above 410°C the decrease in ΔH_c becomes much more pronounced with longer melt times. For example, after melt treatment of 45 minutes at 450°C, no crystallization was observed upon cooling. After heating, however, there was roughly a 50% retention in the measured ΔH_m, implying that a great deal of crystallization had occurred upon reheating this particular sample. This was evidenced by an exotherm following the glass transition and illustrates the ability of this particular system to crystallize from the glass after even excessively harsh melt treatments. To conclude, at temperatures of up to 410°C, the polyimide demonstrated heats of crystallization upon cooling from the melt that were virtually equal to the heats of melting. This suggests that melt processing a polyimide such as TPER-BPDA-PA would not require subsequent treatments, e.g., annealing, because of the sufficient crystallinity inherent in the system. Thus again points to the highly desirable, unique crystallization

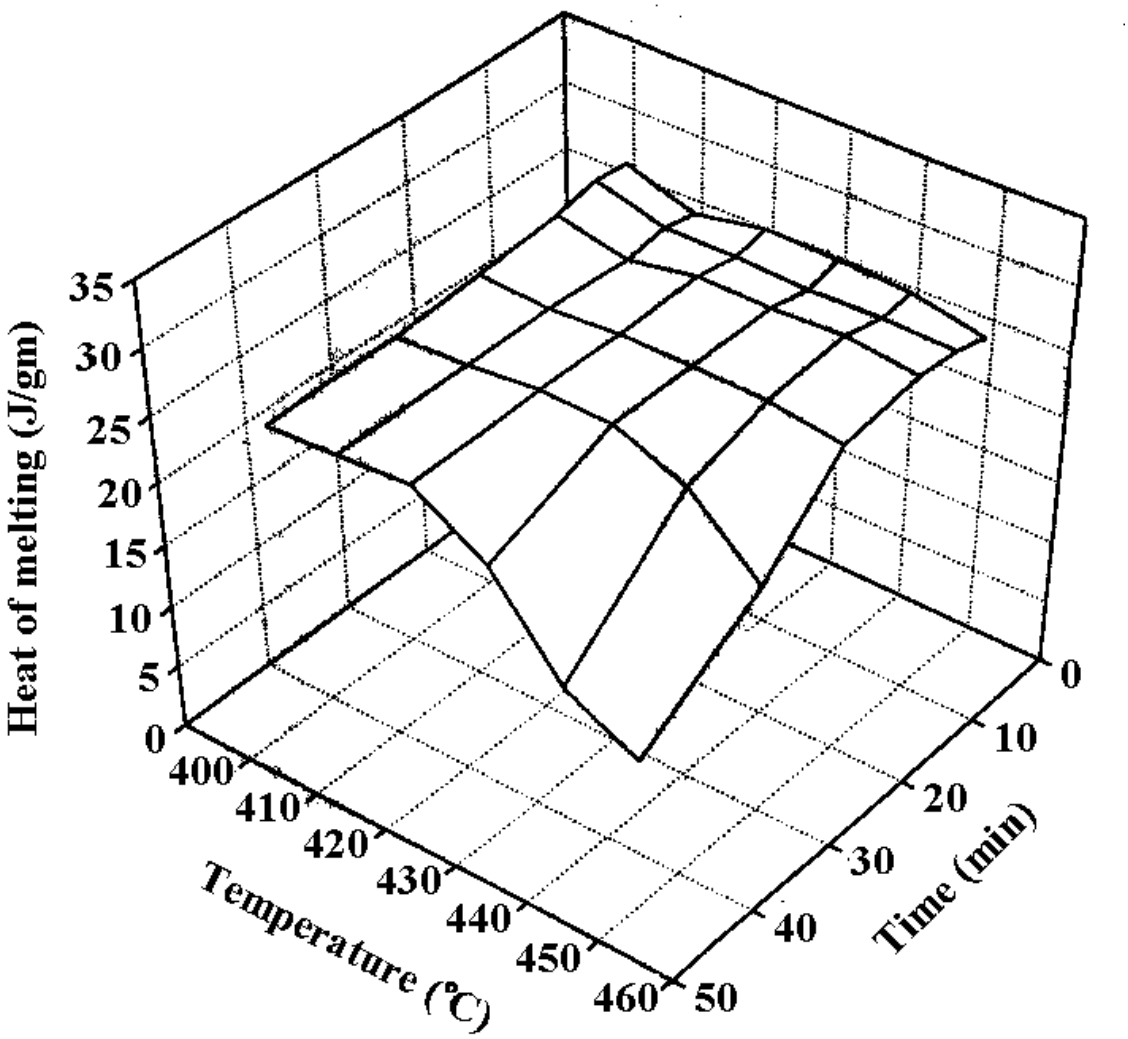

Figure 4.3.2.2.7: Effect of Temperature and Time in the Melt on the Heat of Melting of 30K TPER-BPDA-PA[224,236]

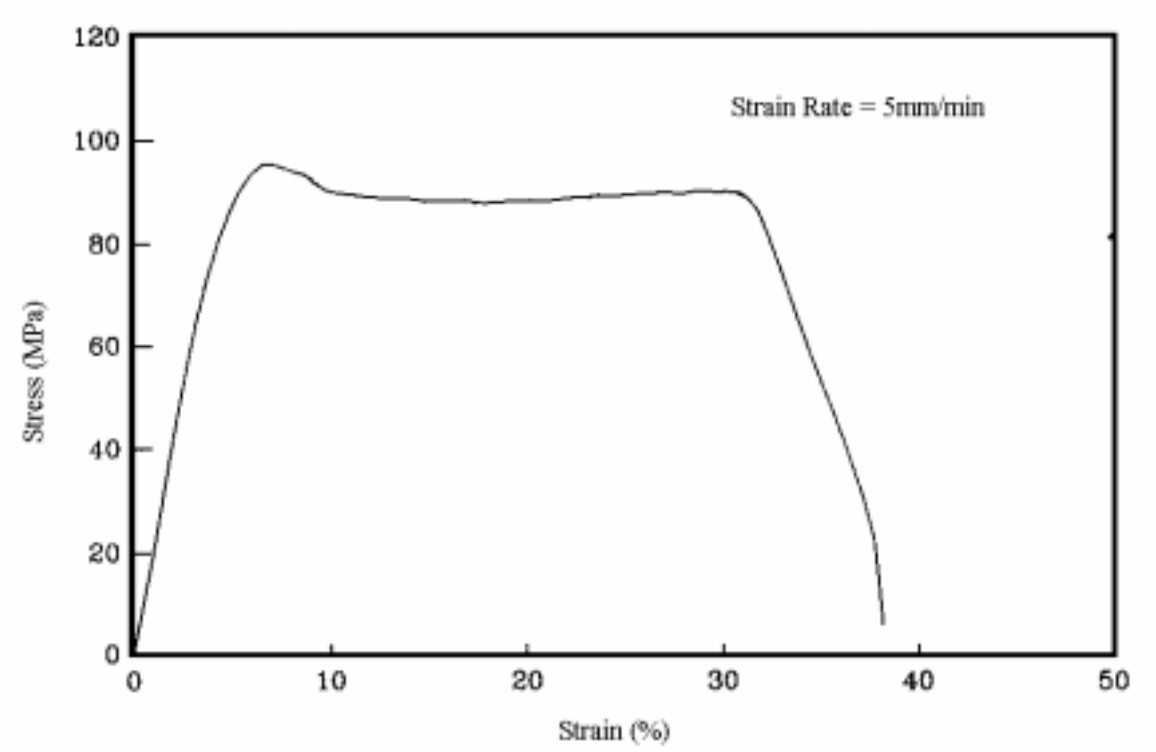

Figure 4.3.2.2.8: Room Temperature Stress-Strain Behavior of TPER-BPDA-PA

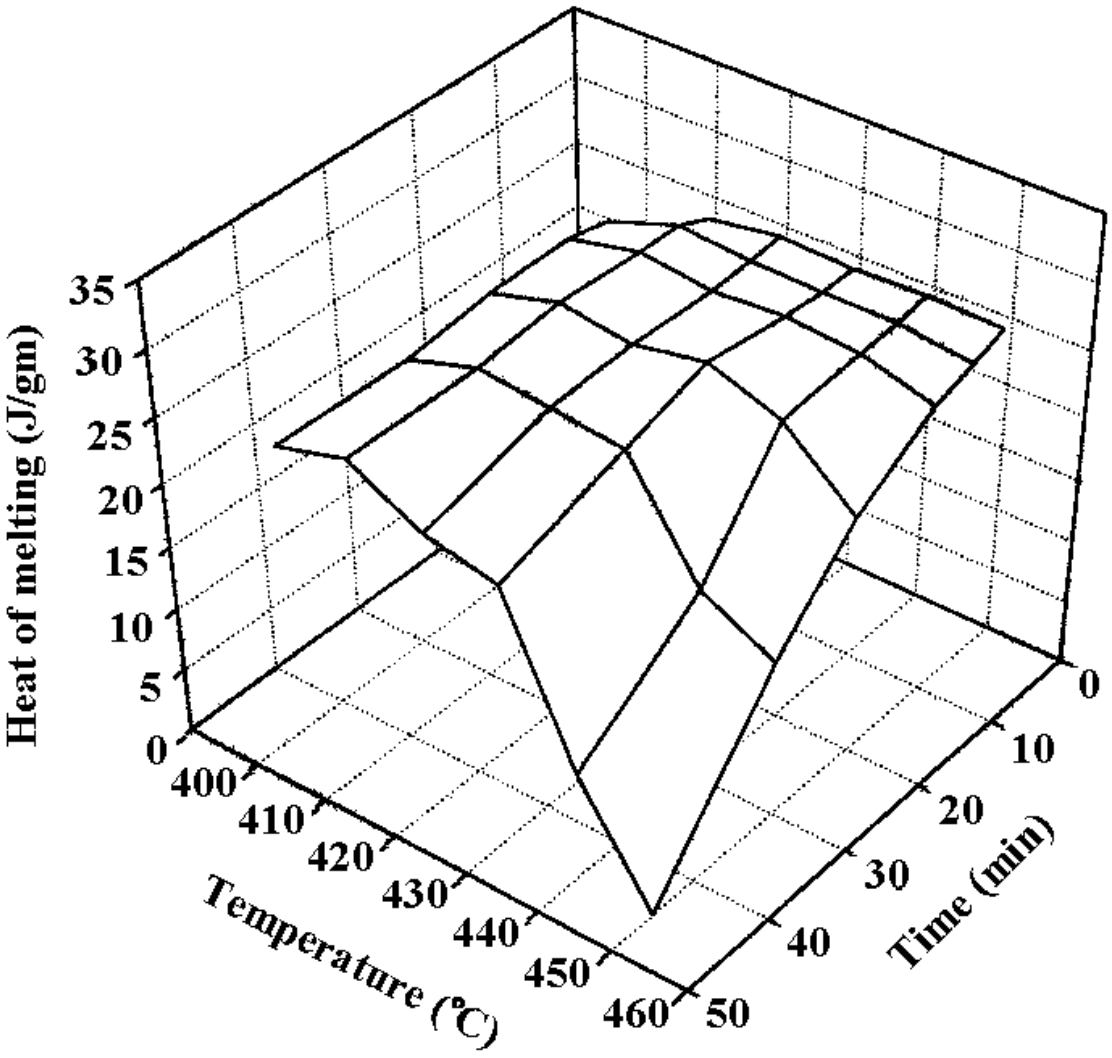

Figure 4.3.2.2.9: Effect of Temperature and Time in the Melt on the Heat of Crystallization of 30K TPER-BPDA-PA[224,236]

kinetics of this polyimide.

It is clear that the differences in the melt stability of TPEQ-ODPA versus TPER-BPDA systems must be related to the differences in the chemical structures of the polyimides. The biphenyl linkage in the BPDA can be considered more thermally stable than the ether linkage in ODPA. Furthermore, the electron rich ether linkage is probably more susceptible to the electronic effects that may be magnified at higher temperatures, as just described.

Additional DSC studies were conducted to gauge the effect of endgroup chemistry on thermal stability. Recall that the TGA of PA endcapped, "half endcapped," and amine terminated samples of TPER-BPDA yielded similar results, despite the nature of the endgroups. DSC of these same samples was performed wherein the samples were subjected to 430°C for 30 minutes, cooled to room temperature at 10°C/min, and reheated to 425°C at 10°C/min. The cooling and reheating scans from this experiment are given in Figure 4.3.2.2.10. As evident in the cooling scan, the PA endcapped sample exhibited a high level of crystallization upon cooling, consistent with what was presented in the melt time/temperature findings. The half endcapped sample only displayed two very small exotherms, signifying that the ability to recrystallize has been acutely suppressed. Furthermore, the amine terminated sample showed only a very broad, indistinguishable exotherm showing crystallization has been even more greatly reduced. The heating scans corresponded to these cooling curves. In fact, the heating scan of the PA endcapped sample showed only a weak glass transition and later a large melting endotherm. In contrast, the half endcapped sample showed a stronger glass transition, followed by a somewhat broad crystallization exotherm. Subsequently, the polyimide melting endotherm that was observed is lesser in magnitude than that of the PA endcapped sample. Finally, the amine terminated sample showed a prominent glass transition, but had no crystallization exotherm and an almost indistinguishable melting endotherm. Therefore, it is clear that some modification happened in the melt that was highly dependent on the nature of the endgroup. This change was hypothesized to be more likely a consequence of similar molecular weight increases described for the TPEQ-ODPA-PA system, which would have increased the melt viscosity, and thus limit mobility and crystallization.

Isothermal melt rheology at 430°C was utilized to verify this hypothesis. The isothermal melt viscosities of the PA endcapped, half endcapped, and amine terminated samples are given in Figure 4.3.2.2.11. The influence of time on the melt viscosities of these samples is apparent. The PA endcapped sample shows only a very slight increase in viscosity over time as a result of the stability imparted by the use of phthalimide endcapping, which helps to serve as a protective group against high temperature degradation. The half endcapped sample exhibited a steep increase in the first 1000 seconds of the experiment before somewhat leveling off. This behavior was much more pronounced in the amine terminated sample. These viscosity increases suggest increases in molecular weight. It can be assumed that as the quantity of reactive amine groups is increased, the tendency toward increased molecular weight is also magnified, possibly by a complex process. And, in fact, the nature of the viscosity increases does help to determine somewhat the means by which the molecular weight had increased. Crosslinked systems generally exhibit viscosity increases that occur in an exponential fashion. This is in contrast to the leveling off observed in this experiment with the half endcapped and amine terminated samples. The molecular weight increase under melt conditions may be attributable to some sort of chain extension mechanism. One possibility is transimidization, given the inclination of other condensation polymers, like polyesters, to undergo similar processes.[224] An example of a possible mechanism is shown in Scheme 4.3.2.2. Polyimides with reactive endgroups have been shown to have a tendency to increase in molecular weight at elevated temperatures.[244]

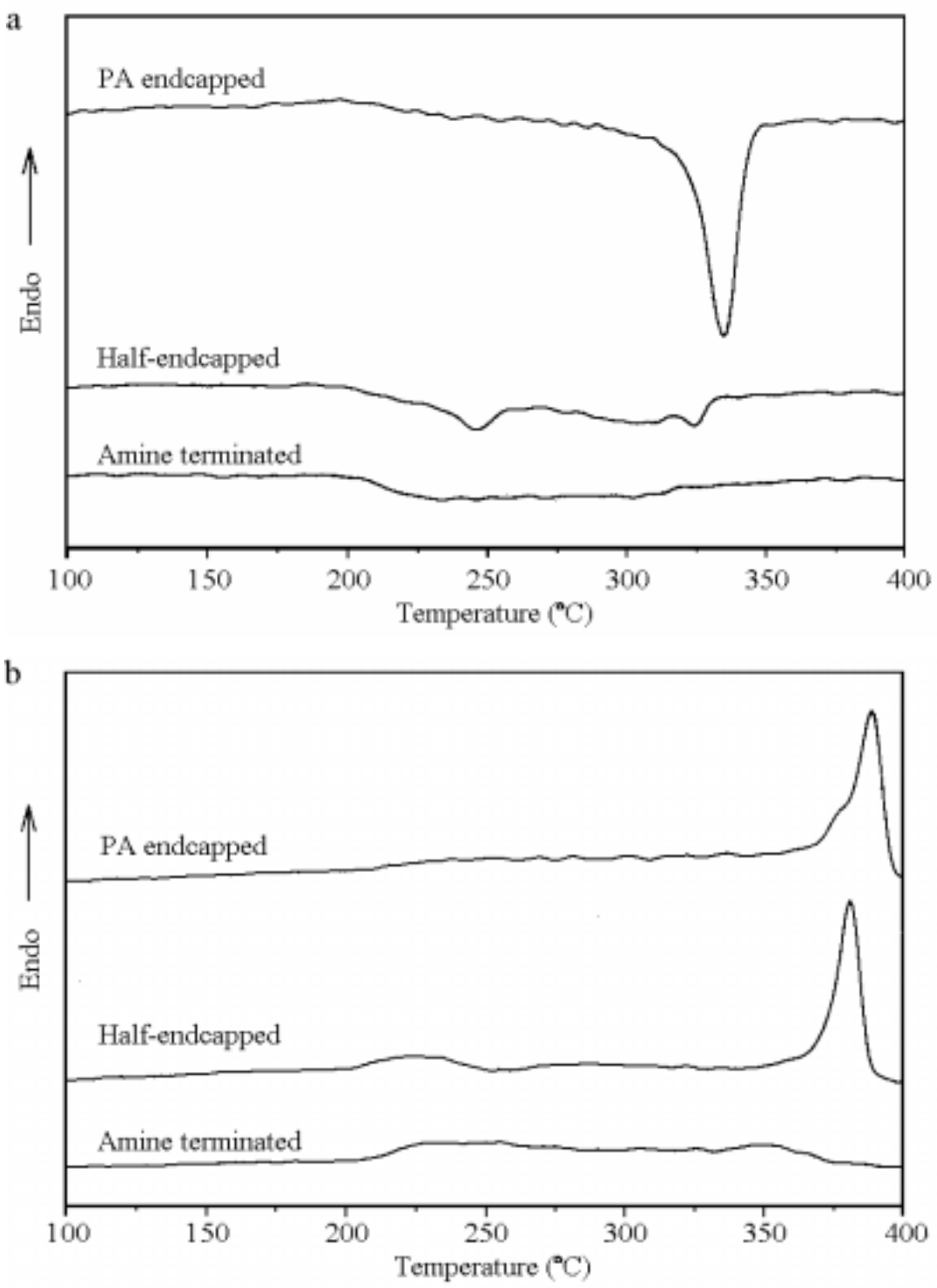

Figure 4.3.2.2.10: DSC Cooling (a) and Heating (b) Scans of TPER-BPDA Samples of Different Degree of Endcapping (10°C/min)

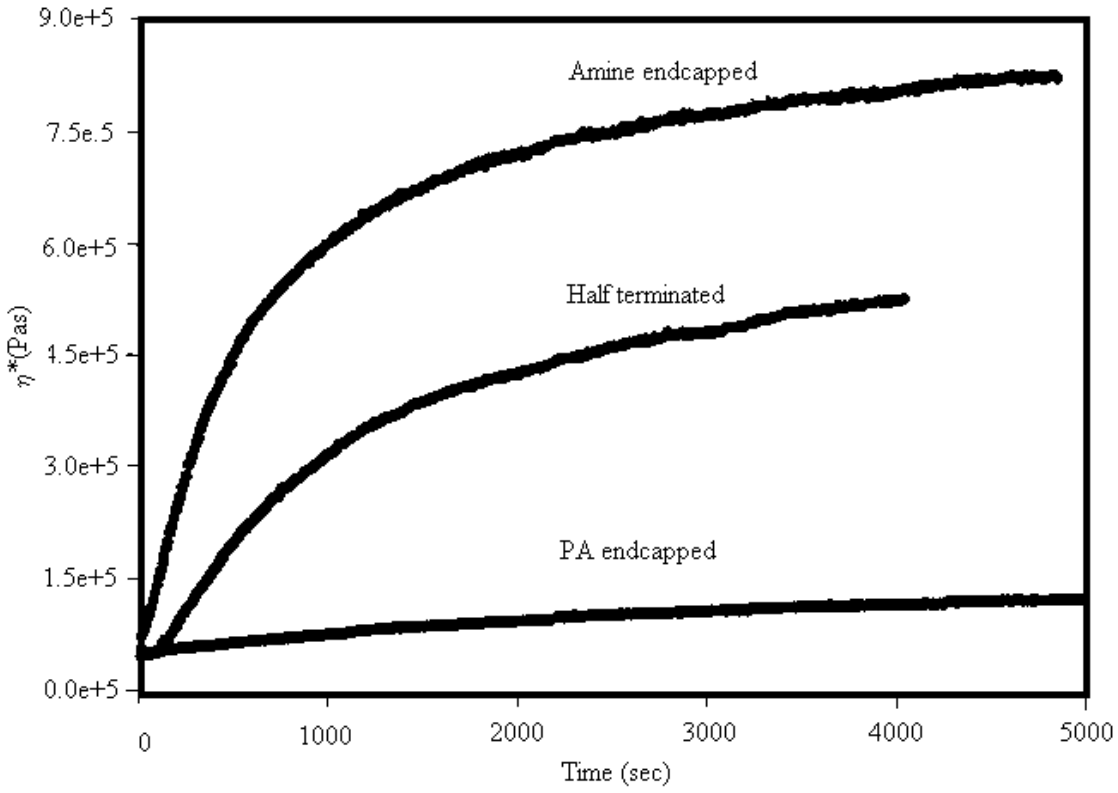

Figure 4.3.2.2.11: Isothermal Melt Rheology at 430°C of the TPER-BPDA Samples of Different Degree of Endcapping

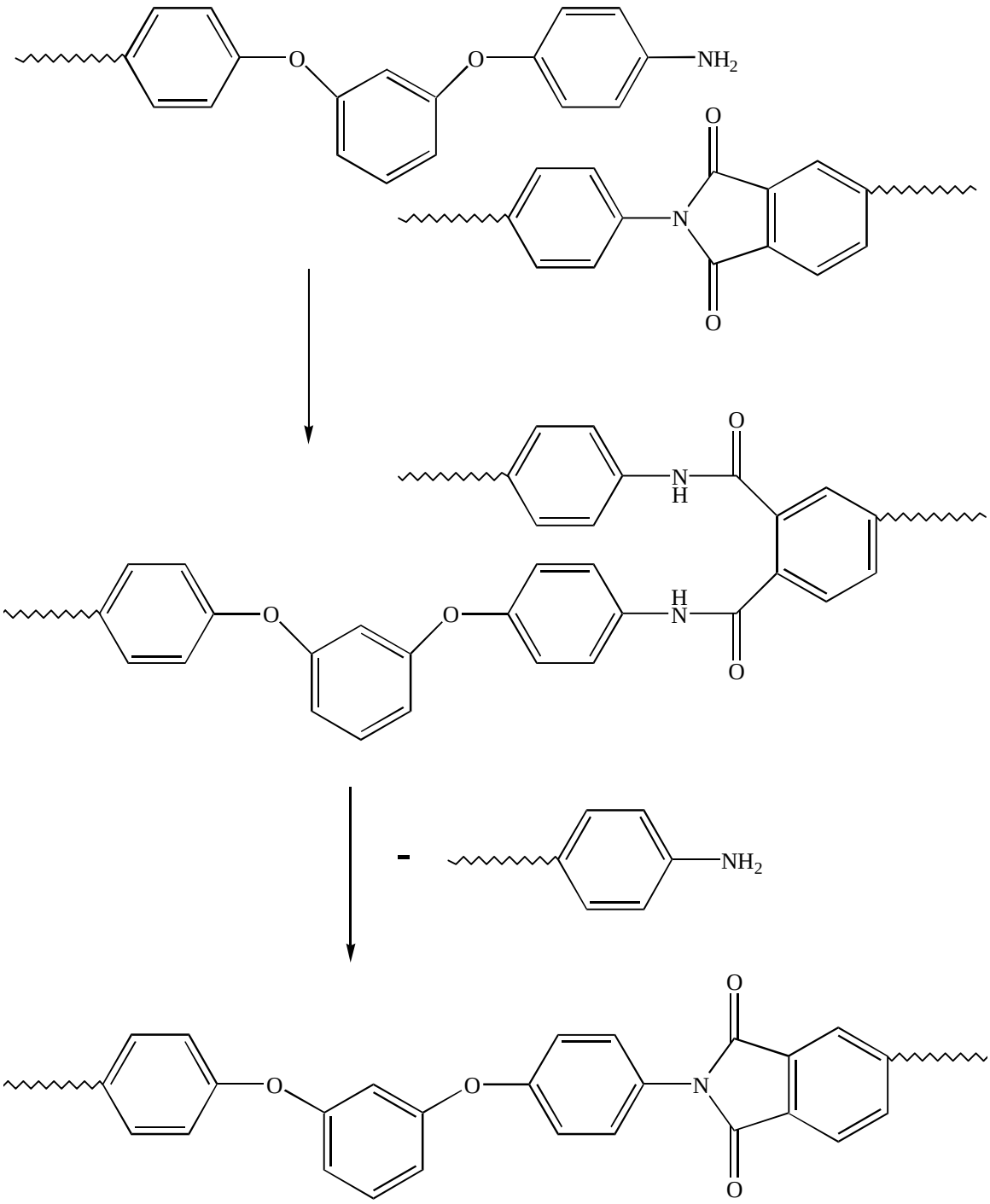

Scheme 4.3.2.2: Proposed High Temperature Transimidization

4.4 Polyimides from Pendant Alkyl-Containing Analogues of TPER

Given the superb performance and thermal stability of the TPER-BPDA-PA system, it is interesting to note that it is able to retain, or even regain, significant amounts of crystallinity despite harsh melt treatments. Unfortunately, the inherent solvent resistance of this polyimide does not allow for extensive characterization in the solution state. As a consequence, research has been conducted to modify the backbone of this polyimide – specifically to chemically incorporate pendant alkyl groups. These alkyl groups were expected to disrupt the regular order necessary for crystallization, possibly yielding an amorphous, soluble polyimide. As was discussed in the literature review, several alkyl-containing monomers have been used to synthesize polyimides with potential as materials for gas separation membranes. Thus, the focus of this section is on the synthesis and characterization of novel alkyl-containing diamines analogous to TPER, the preparation of polyimides from these diamines, and the characterization of these new polyimides.

4.4.1 Synthesis of Pendant Alkyl-Containing Analogues of TPER by Alkylresorcinol Precursors

A means of incorporating alkyl groups is the nucleophilic aromatic substitution reaction of alkylresorcinols with p-halonitrobenzene to yield dinitro compounds. These could be subsequently reduced to yield diamines analogous to TPER, which possess pendant alkyl groups on the center ring of the resulting triphenyl ether diamine. The commercial availability of alkylated resorcinol products would aid in the syntheses of these alkyl-containing diamines. Some of the resorcinols used are shown in Figure 4.4.1. These diamines, once made, could be used in the preparation of polyimides similar to those described in the previous section, the only differences being the presence of the alkyl groups.

4.4.1.1 Synthesis of 4,6-Di-t-butylresorcinol

The title compound was not commercially available, and thus was prepared by the electrophilic aromatic alkylation of resorcinol with tert-butanol, according to published literature procedures.[221,245] The synthetic route is shown in Scheme 4.4.1.1. Originally sulfuric acid was utilized as a catalyst, but the product was somewhat difficult to purify as indicated by the presence of a reddish tint. Consequently, phosphoric acid was substituted as the catalyst. Even though the catalyst amount needed in this case was much larger, the resulting product was significantly cleaner and was essentially obtained in the same yield (ca. 90%) as with the sulfuric acid catalyst. The proton NMR spectrum of this product is given in Figure 4.4.1.1. Most notable in this spectrum are the aromatic proton resonances at 6.05 and 7.25 ppm, phenolic proton resonances at 4.9 ppm, and t-butyl proton resonances at 1.45 ppm.

4.4.1.2 Syntheses of 1,3-bis(4-nitrophenoxy)alkylbenzenes

The title compounds were prepared by the aromatic nucleophilic coupling of p-fluoronitrobenzene with the alkyresorcinols shown in Figure 4.4.1. These reactions were performed at 135-145°C in DMAC in the presence of potassium carbonate and toluene. The synthetic route is shown in Scheme 4.4.1.2. The potassium carbonate deprotonates resorcinol to produce the reactive bisphenolate, while the toluene dehydrates the reaction media by azeotroping the water that is produced during the reaction. The reaction times needed for the methylresorcinols were much less than those for hexylresorcinol and di-t-butylresorcinol, due to the steric hindrance associated with the latter two resorcinols. Nevertheless, high yields (80-95%) were obtained after purification of the dinitro compounds. The new compounds prepared by this method and their corresponding proton NMR spectra are listed below.

2,6-bis(4-nitrophenoxy)toluene: Figure 4.4.1.2.1

3,5-bis(4-nitrophenoxy)toluene: Figure 4.4.1.2.2

1,3-bis(4-nitrophenoxy)-4-hexylbenzene: Figure 4.4.1.2.3

1,3-bis(4-nitrophenoxy)-4,6-di-t-butylbenzene: Figure 4.4.1.2.4

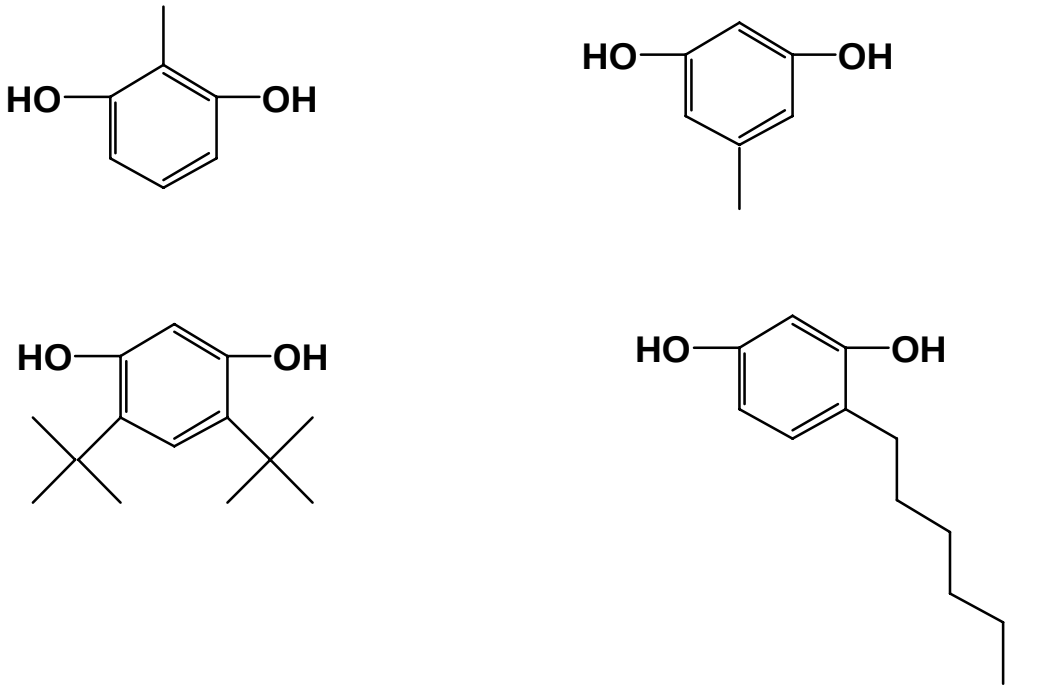

Figure 4.4.1: Alkylresorcinols Used in the Syntheses of Pendant Alkyl-Containing Diamines

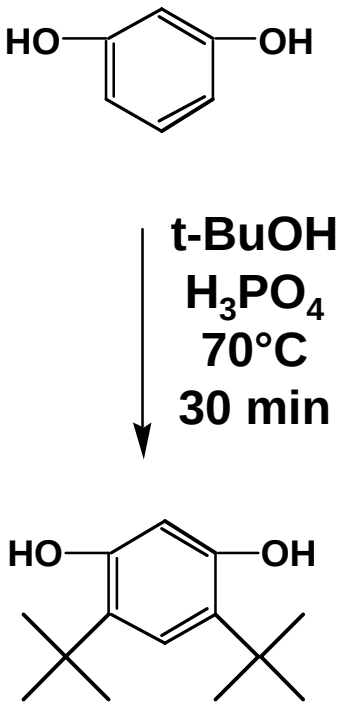

Scheme 4.4.1.1: Synthesis of Di-t-butylresorcinol by Electrophilic Aromatic Substitution

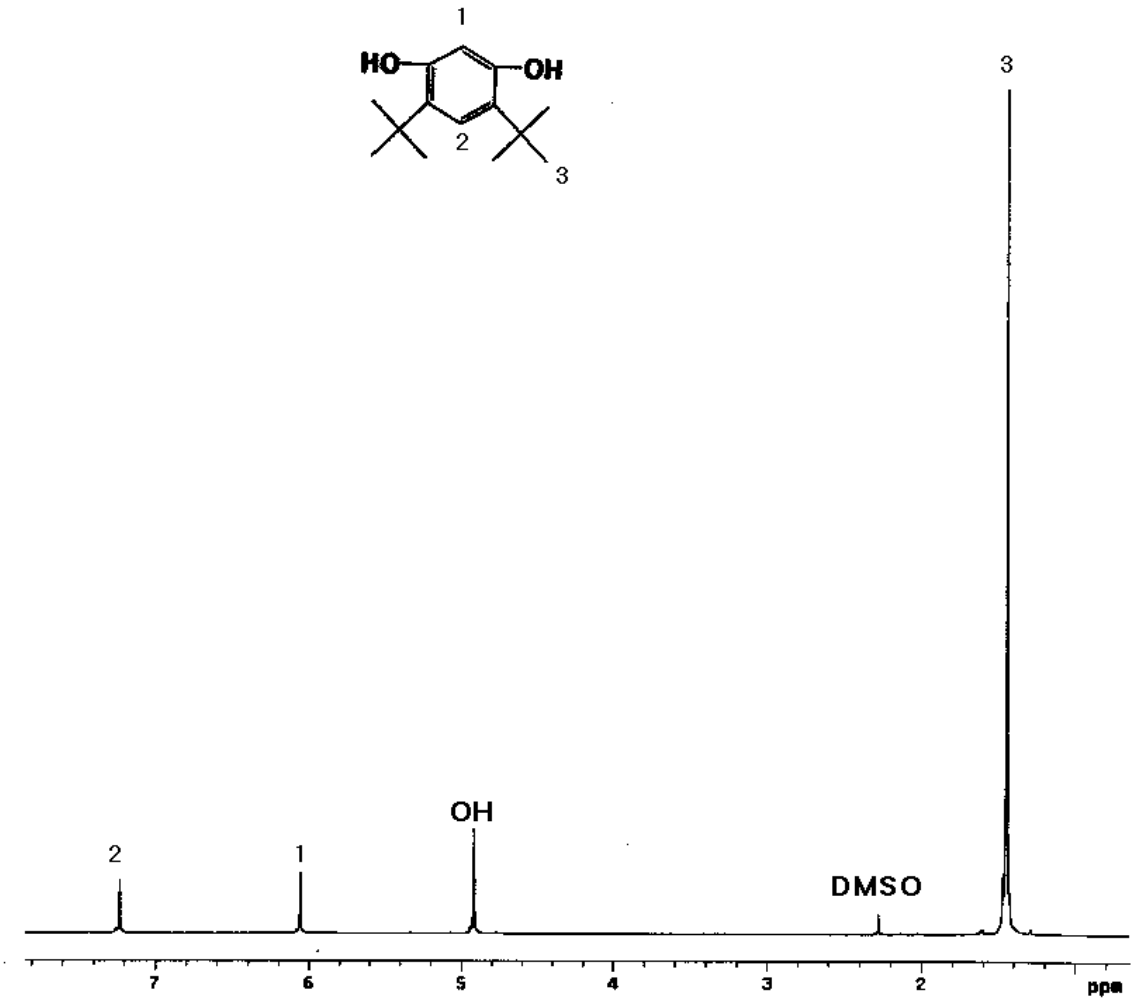

Figure 4.4.1.1: Proton NMR Spectrum of Di-t-butylresorcinol (in DMSO-d6)

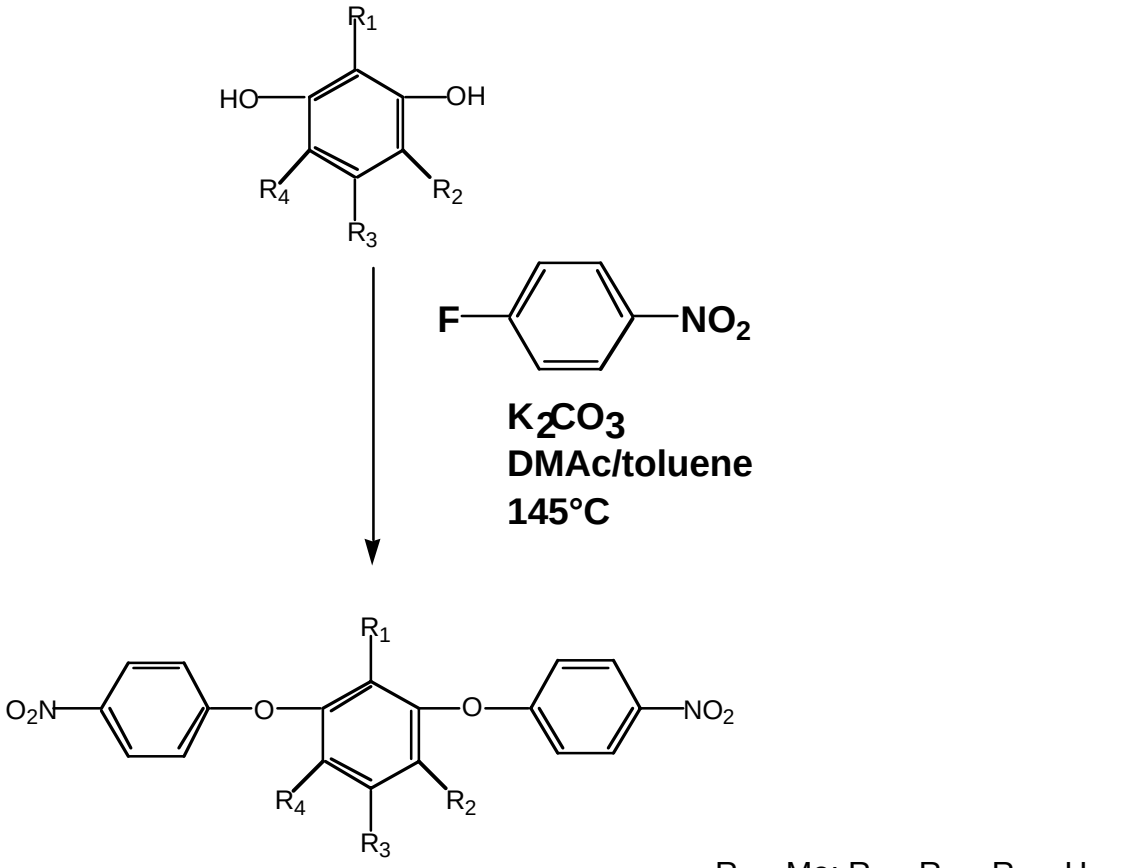

R_1 = Me; R_2 = R_3 = R_4 = H
R_1 = R_2 = R_4 = H; R_3 = Me
R_1 = R_2 = R_3 = H; R_4 = n-He
R_1 = R_3 = H; R_2 = R_4 = t-Bu

Scheme 4.4.1.2: Synthesis of 1,4-bis(4-nitrophenoxy)alkylbenzenes by Nucleophilic Aromatic Substitution

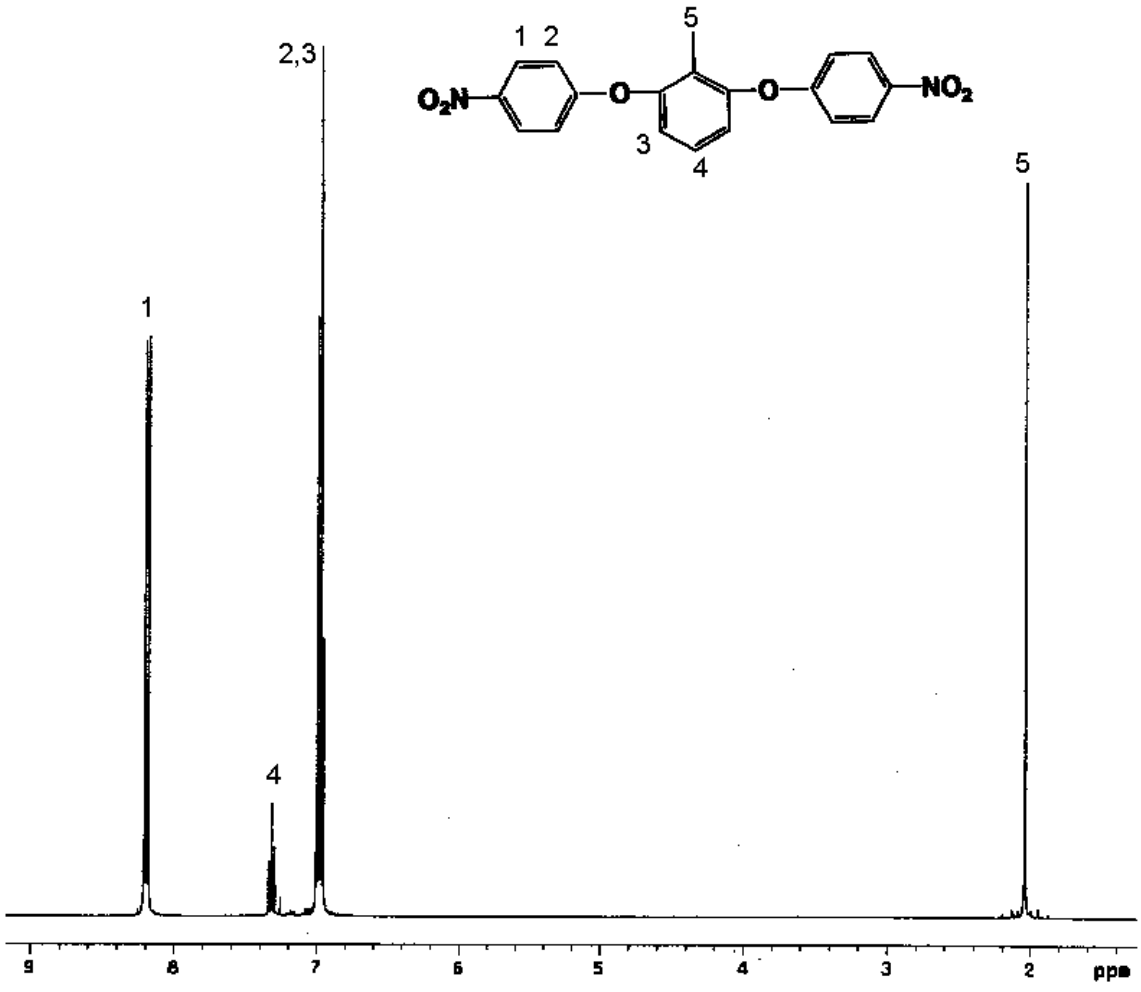

Figure 4.4.1.2.1: Proton NMR Spectrum of 2,6-bis(4-nitrophenoxy)toluene (in $CDCl_3$)

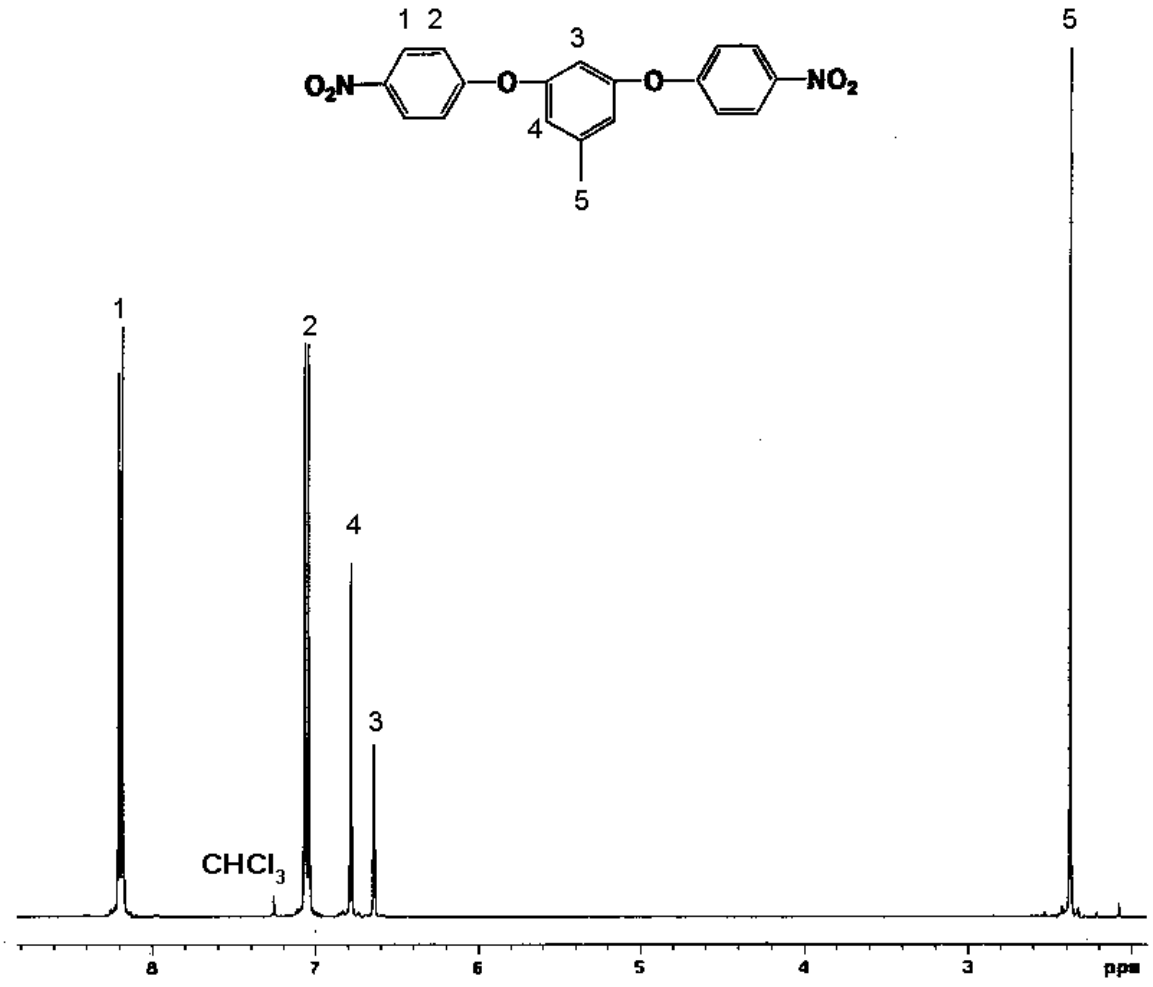

Figure 4.4.1.2.2: Proton NMR Spectrum of 3,5-bis(4-nitrophenoxy)toluene (in $CDCl_3$)

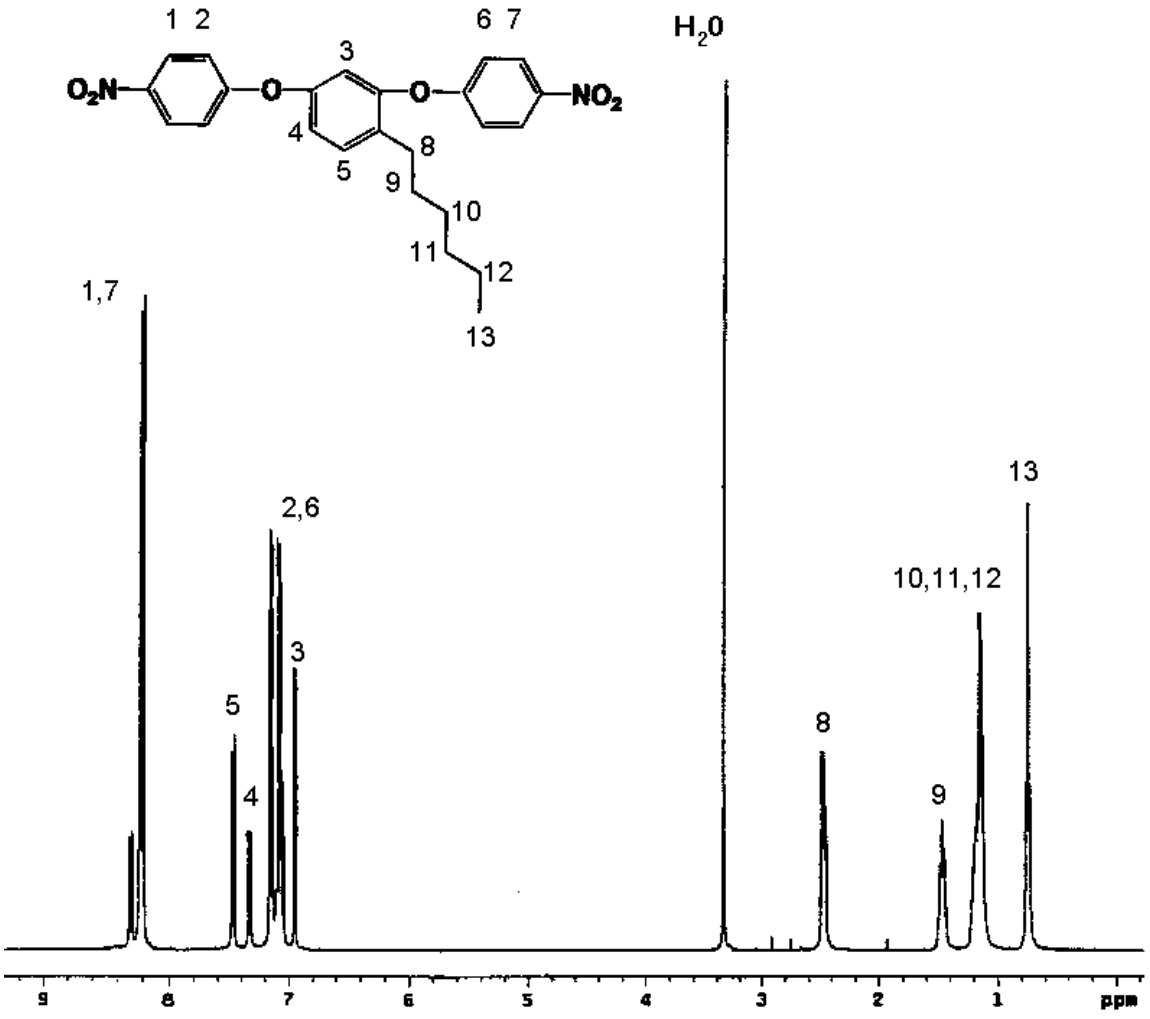

Figure 4.4.1.2.3: Proton NMR Spectrum of 1,3-bis(4-nitrophenoxy)-4-hexylbenzene (in DMSO-d6)

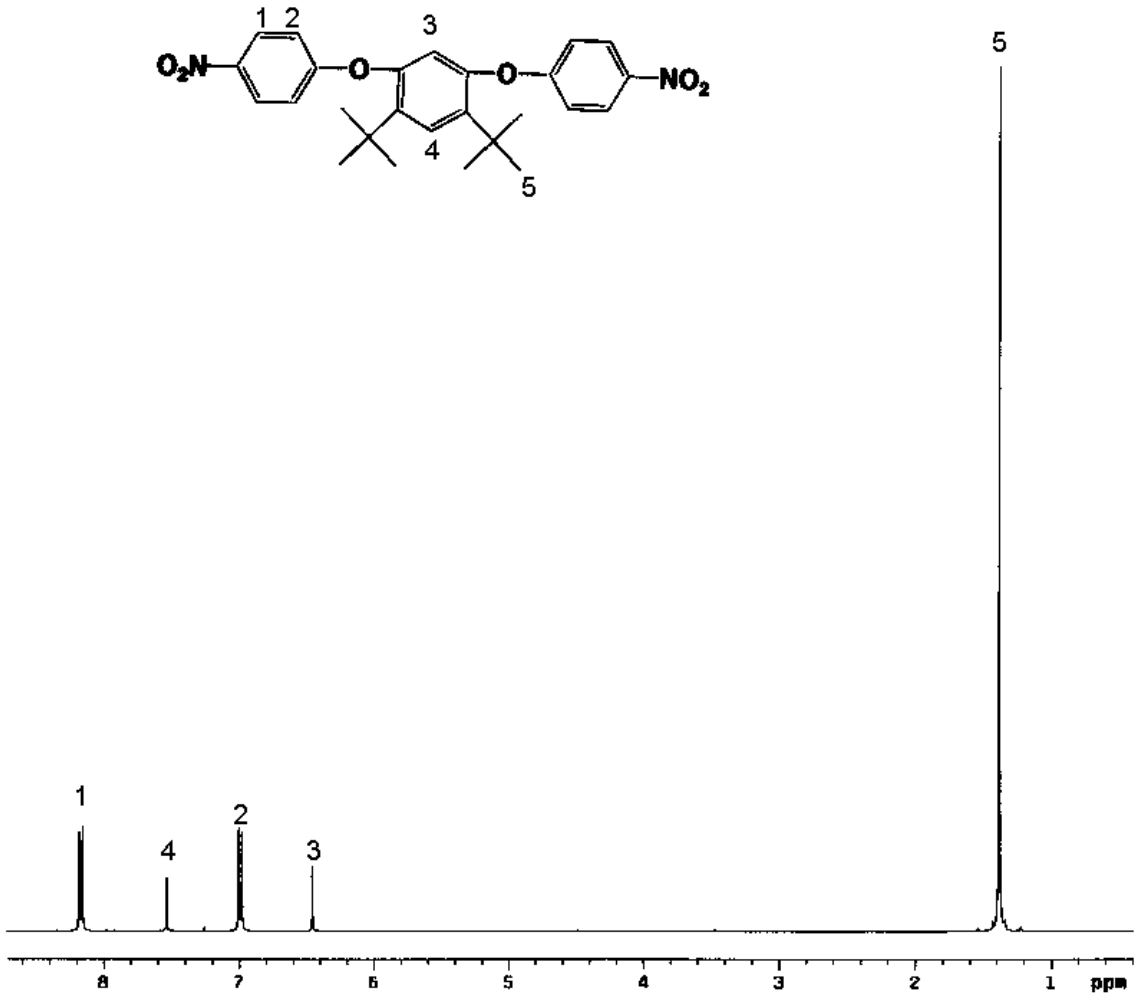

Figure 4.4.1.2.3: Proton NMR Spectrum of 1,3-bis(4-nitrophenoxy)-4,6-di-t-butylbenzene (in $CDCl_3$)

4.4.1.3 1,3-bis(4-aminophenoxy)alkylbenzenes

The title compounds were prepared by the hydrogenation of the dinitro compounds previously described. Hydrazine monohydrate was used as a reducing agent in conjunction with 10% palladium on carbon as a catalyst. The reactions were performed using the co-solvent combination of ethanol and THF at reflux as shown in Scheme 4.4.1.3. These reactions were usually allowed to proceed overnight before isolating the diamine products. Yields of the various products ranged from 70-92%. The diamines were characterized by proton NMR, elemental analysis and MS. The new diamines made, their
acronyms, and their corresponding spectra are listed below.

2,6-bis(4-aminophenoxy)toluene (2,6-BAPT): Figure 4.4.1.3.1

3,5-bis(4-aminophenoxy)toluene (3,5-BAPT): Figure 4.4.1.3.2

1,3-bis(4-aminophenoxy)-4-hexylbenzene (BAPHB): Figure 4.4.1.3.3

1,3-bis(4-aminophenoxy)-4,6-di-t-butylbenzene (BAPDTB): Figure 4.4.1.3.4

4.4.1.4 Polyimides from 1,3-bis(4-aminophenoxy)alkylbenzenes

Polyimides were synthesized from these new diamines via the classical two step route at 10% solids concentrations. BPDA, PMDA, and ODPA dianhydrides were used in the preparations. The resulting polyamic acid solutions were both thermally imidized as cast films and solution imidized.

Of most interest amongst the polyimides made were the BPDA-based polyimides, on the basis of the discussion presented of the TPER-BPDA-PA system. Like TPER-BPDA-PA, the 30,000 g/mole target molecular weight polyimides derived from 2,6- and 3,5-BAPT precipitated from solution during solution imidization, indicating that these polymers possessed some degree of crystallinity. In contrast, the polyimide from BAPHB remained in solution for the duration of the solution imidization, pointing to the likelihood that BAPHB-BPDA-PA is amorphous. In this case, it was thought that the hexyl side chain probably disrupted the crystalline order of the polymer. High molecular weight

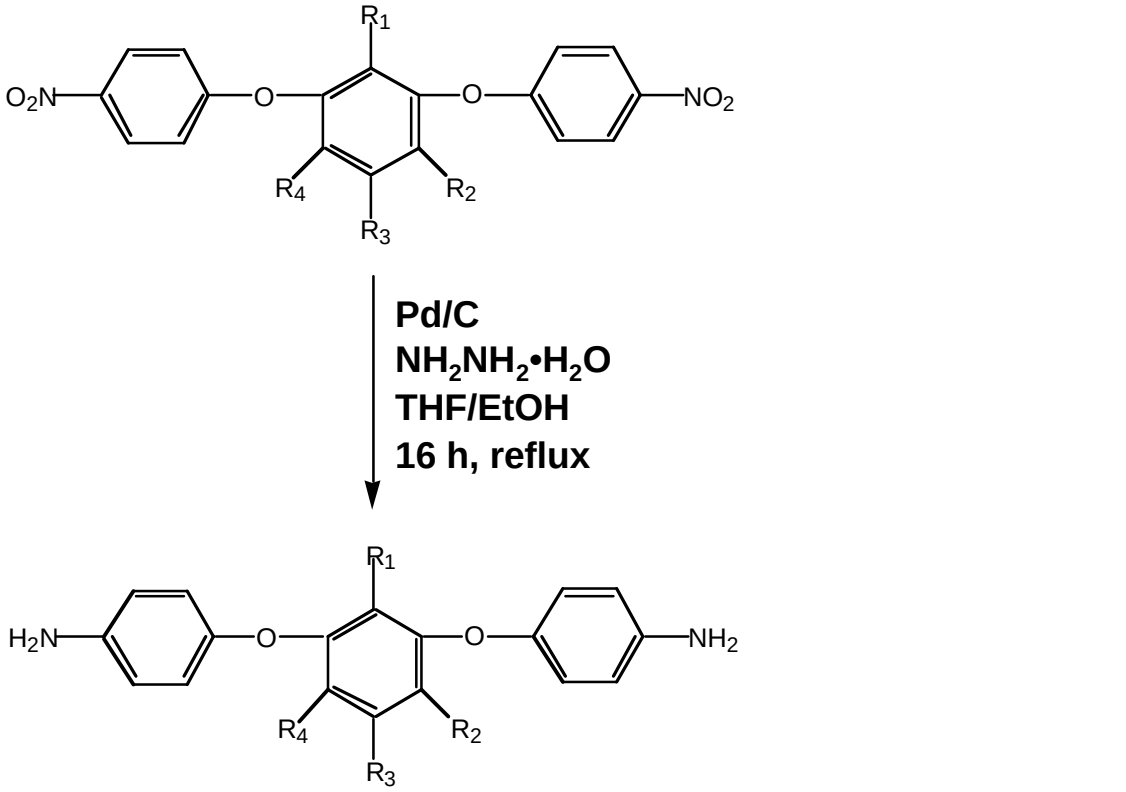

R_1 = Me; R_2 = R_3 = R_4 = H
R_1 = R_2 = R_4 = H; R_3 = Me
R_1 = R_2 = R_3 = H; R_4 = n-He
R_1 = R_3 = H; R_2 = R_4 = t-Bu

Scheme 4.4.1.3: Synthesis of 1,3-bis(4-aminophenoxy)alkylbenzenes by the Reduction of 1,3-bis(4-nitrophenoxy)alkylbenzenes

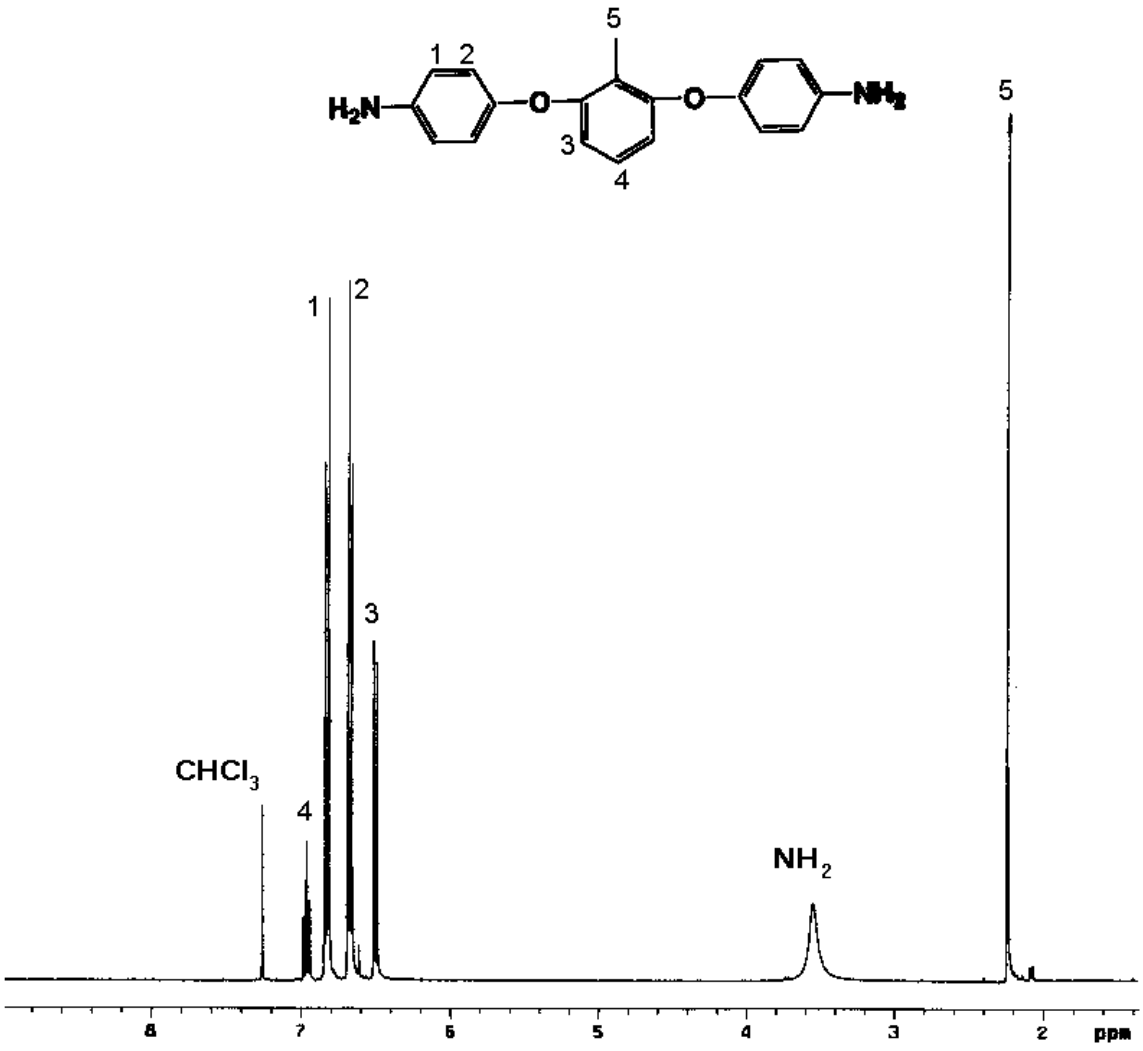

Figure 4.4.1.3.1: Proton NMR Spectrum of 2,6-bis(4-aminophenoxy)toluene (2,6-BAPT) in $CDCl_3$

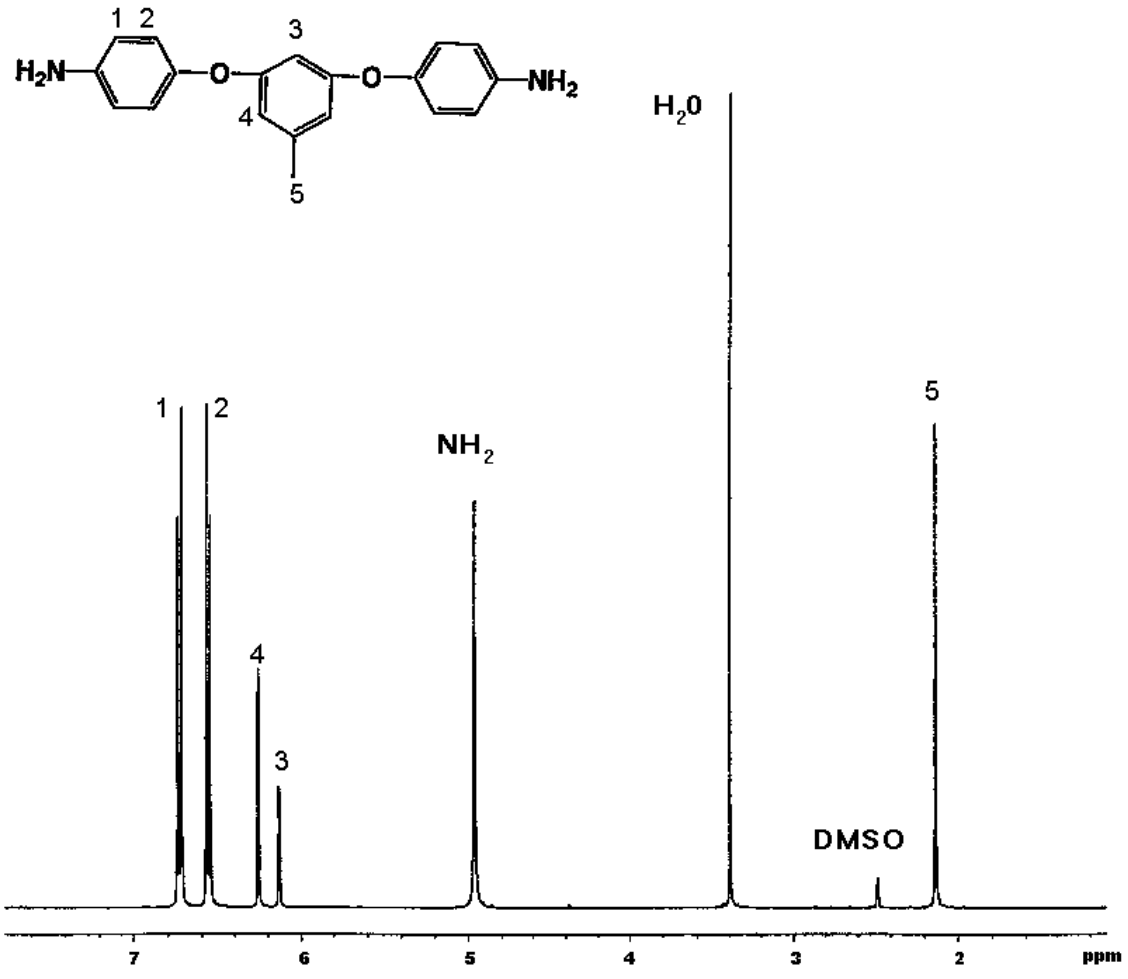

Figure 4.4.1.3.2: Proton NMR Spectrum of 3,5-bis(4-aminophenoxy)toluene (3,5-BAPT) in DMSO-d6

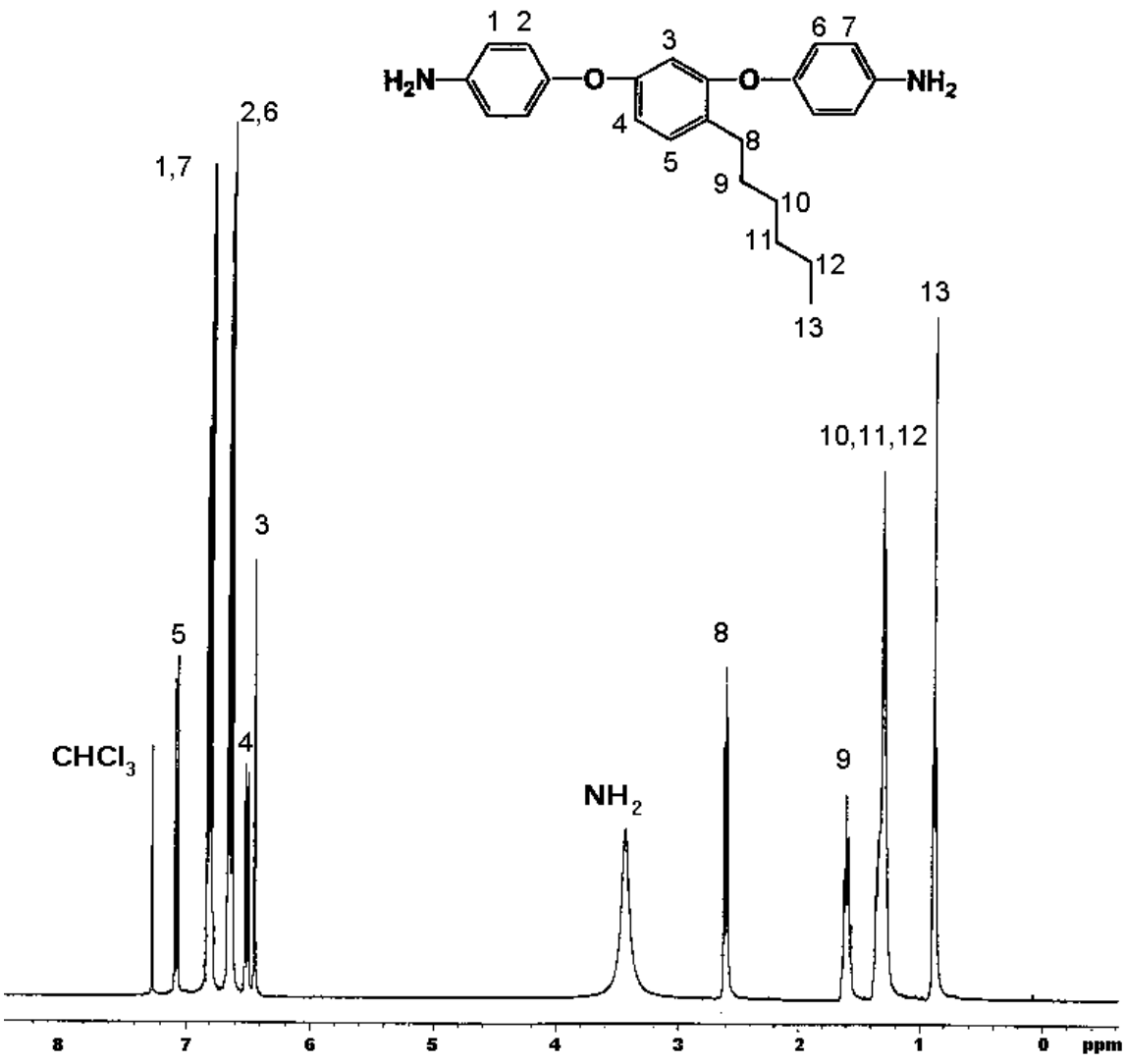

Figure 4.4.1.3.3: Proton NMR Spectrum of 1,3-bis(4-aminophenoxy)-4-hexylbenzene (BAPHB) in $CDCl_3$

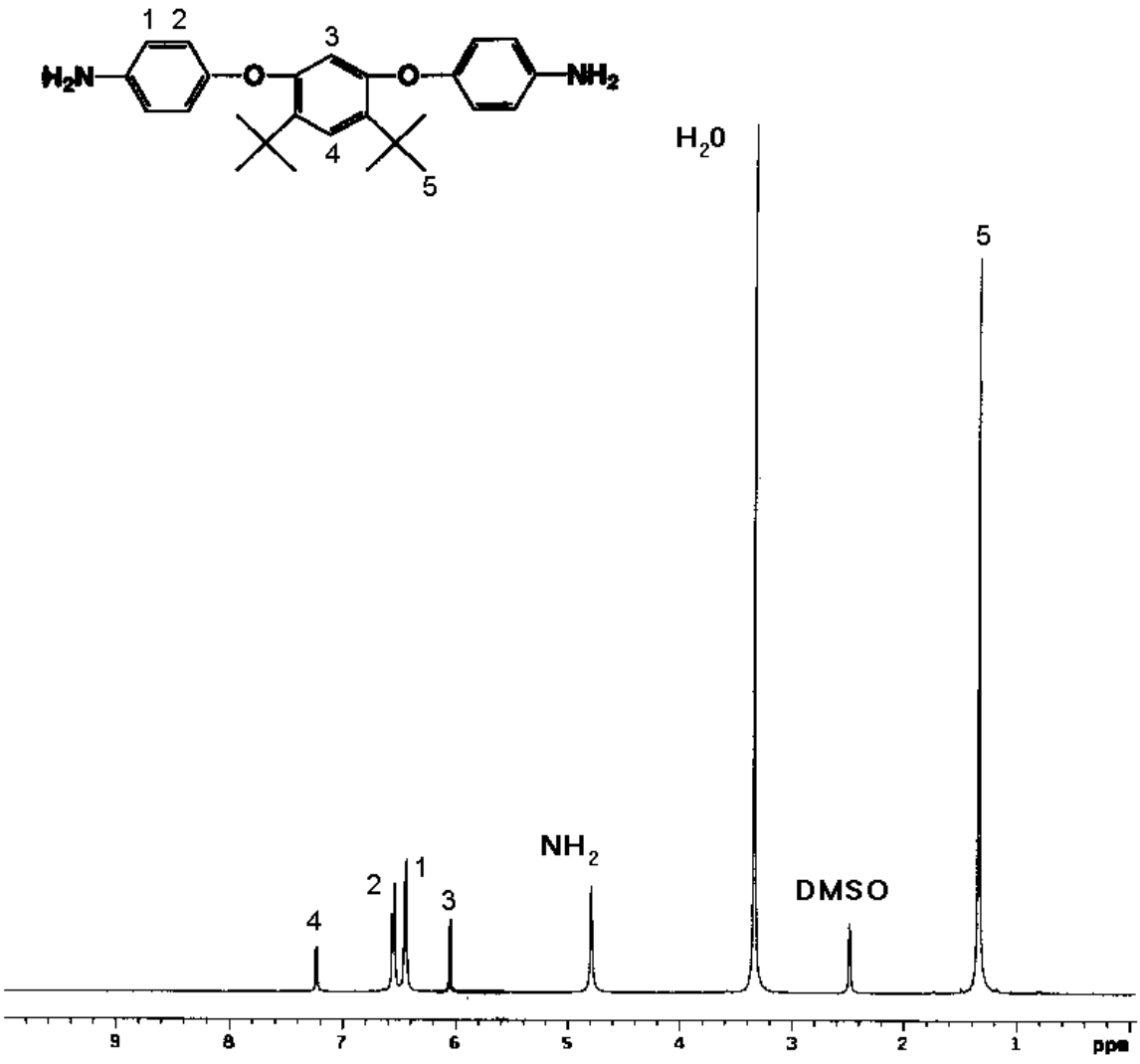

Figure 4.4.1.3.4: Proton NMR Spectrum of 1,3-bis(4-aminophenoxy)-4,6-di-t-butylbenzene (BAPDTB) in DMSO-d6

polyimides could not be synthesized from BAPDTB.

Of the polyimides prepared from PMDA, none were soluble as noted by precipitation from solution during the solution imidization. However, all of the polyimides prepared from ODPA remained in solution during the solution imidization. The polyimides from 2,6- and 3,5-BAPT behaved similarly to TPER-ODPA-PA. Upon cooling in solution, these systems had a tendency to form insoluble gels. However, BAPHB-ODPA-PA was completely soluble, once again signifying that this particular system is probably amorphous.

Solubility tests were performed on 5% (by weight) solutions of the BAPHB-BPDA-PA and BAPHB-ODPA-PA polyimides, and the results are summarized in Table 4.4.1.4.1. One should note that the BPDA-based polyimide appears to be the more soluble of the two.

The thermal analyses of the 2,6-BAPT polyimides are summarized in Table 4.4.1.4.2. As compared to the TPEQ and TPER polyimides, TGA analysis reveals that, overall, the pendant alkyl containing polymers demonstrate lower 5% weight loss temperatures. This is not surprising, considering the decreased thermooxidative stability imparted by the presence of the alkyl moieties of these polyimides. 2,6-BAPT-BPDA-PA shows no thermal transitions up to 420°C, indicating that the methyl group present in the polyimide is sufficient to inhibit crystallization. Inspection of the polymer sample after DSC analysis revealed that no polyimide flow occurred, possibly the result of crosslinking that may have taken place as a result of the formation of benzylic radicals during thermal imidization. While the polyimide based upon PMDA also displayed no transitions, the ODPA polyimide demonstrated interesting thermal behavior, as seen by DSC (Figure 4.4.1.4.1). Upon the first heat, dual melting behavior was observed as seen in the melting endotherms at 323°C and 381°C. The appearance of the larger, higher melting endotherm was surpising, considering that TPER-ODPA-PA melts at only 335°C. The second heat shows a T_g of about 221°C, comparable to that of TPER-ODPA-PA.

The thermal analyses of the 3,5-BAPT polyimides are summarized in Table 4.4.1.4.3. These polyimides demonstrated the highest 5% weight loss temperatures of the alkylated polyimides discussed here and would thus be considered as the most analogous

to the TPER-based polyimides. However, 3,5-BAPT-BPDA-PA also demonstrated no thermal transitions up to 420°C. Like its isomer, this polyimide also did not appear to flow – again, a possible result of crosslinking. DSC thermograms of the ODPA-based polyimide are shown in Figure 4.4.1.4.2. This polyimide exhibited a melting endotherm around 319°C. It should be pointed out that the depression in the melting point, as compared to TPER-ODPA-PA, was attributed to the methyl group in 3,5-BAPT. A glass transition was observed at around 210°C, similar, but slightly lower, than what was observed with the TPER-ODPA-PA system.

The thermal analyses of the BAPHB-based polyimides are summarized in Table 4.4.1.4.4. These polyimides demonstrated the lowest 5% weight loss temperatures of the alkylated polyimides discussed here. This was expected as a result of the presence of the hexyl group. A TGA thermogram of BAPHB-ODPA-PA is shown in Figure 4.4.1.4.3, in which a two-step decomposition is observed. The first step is representative of the loss of the hexyl group, followed by the decomposition of the residual polyimide backbone. This type of behavior might be exploited as a means of processing crystalline polyimides, initially applying the amorphous alkylated polyimide and then pyrolysing the alkyl group, in this case a hexyl side chain, to yield the crystalline polymer in processed form. DSC of BAPHB-BPDA-PA displayed discernible glass transitions around 185°C in both heats, which is shown in Figure 4.4.1.4.4. Given the solubility characteristics of this material, it is obvious that this polyimide is highly amorphous. The hexyl group is sufficiently large and flexible to cause ample disruption in the ordering, and thus reduce the polyimide's ability to crystallize. The PMDA polymer, however, displayed no transitions and was insoluble. DSC thermograms of the ODPA-based polyimide are shown in Figure 4.4.1.4.5. The polyimide also yielded visible glass transitions in both heats occurring around 160°C. The large depression in T_g, as compared to the TPER-ODPA-PA and BAPT-ODPA-PA polyimides, was again attributed to the hexyl group.

Table 4.4.1.4.1: Solubilities of BAPHB-Based Polyimides

polyimide	NMP	DMAC	THF	$CHCl_3$
BAPHB-BPDA-PA	S (hot)	S (hot)	I	S
BAPHB-ODPA-PA	S (hot)	I	I	I

S-soluble

I-insoluble

Table 4.4.1.4.2: Thermal Analyses of the 2,6-BAPT Polyimides

polyimide	5% wt. loss T (°C)*	T_g (°C)**	T_m (°C)***
BAPT-PMDA-PA	490	-	-
BAPT-BPDA-PA	481	-	-
BAPT-ODPA-PA	482	221	323, 381

*in air, 10°C/min

**from second heat

***from first heat

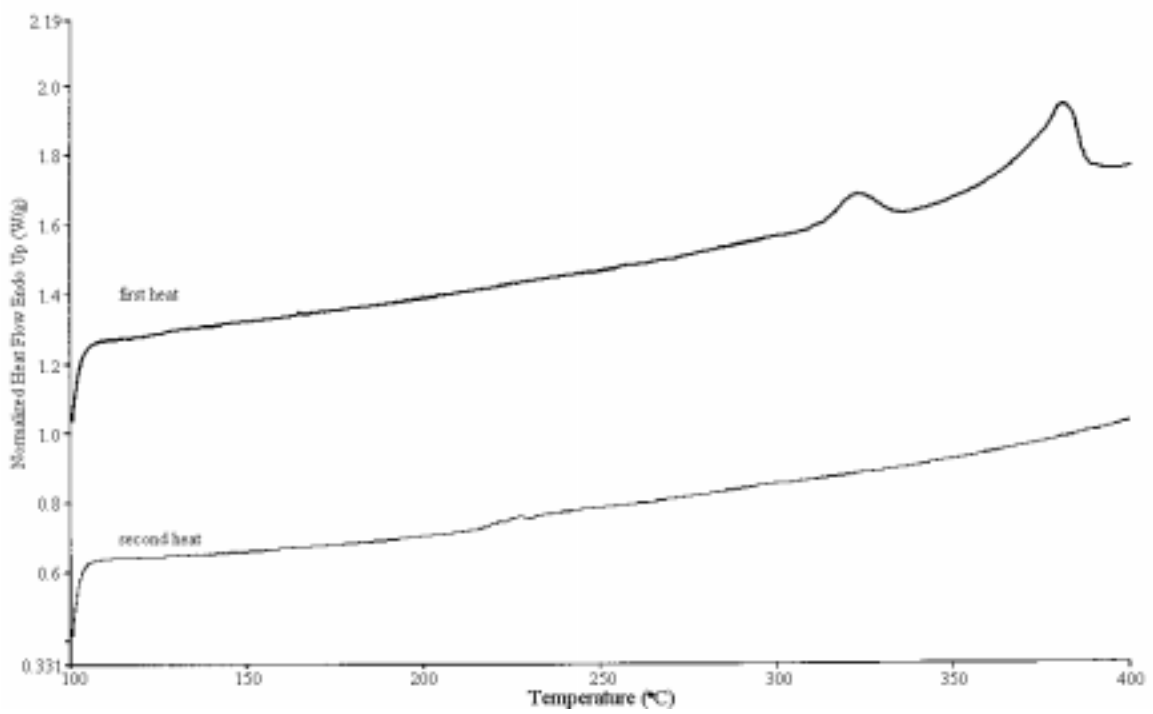

Figure 4.4.1.4.1: DSC Thermograms of 2,6-BAPT-ODPA-PA at 10°C/min

Table 4.4.1.4.3: Thermal Analyses of the 3,5-BAPT Polyimides

polyimide	5% wt. loss T (°C)*	T_g (°C)**	T_m (°C)***
BAPT-PMDA-PA	528	-	-
BAPT-BPDA-PA	521	-	-
BAPT-ODPA-PA	534	210	319

*in air, 10°C/min

**from second heat

***from first heat

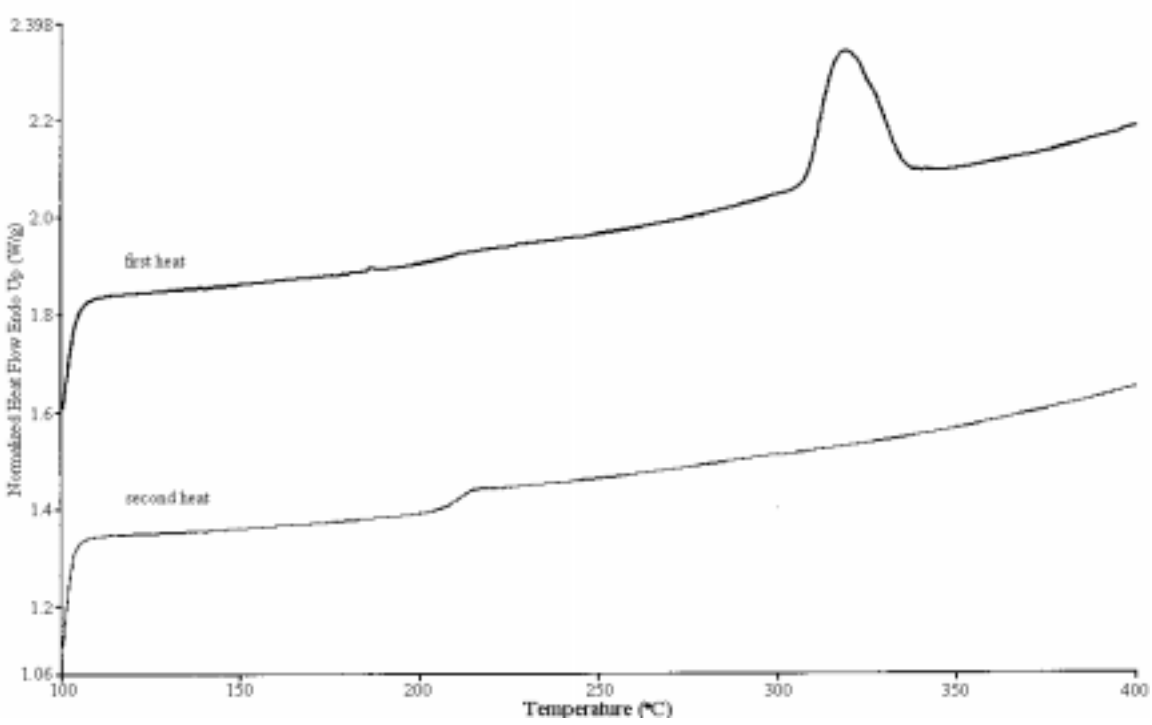

Figure 4.4.1.4.2: DSC Thermograms of 3,5-BAPT-ODPA-PA at 10°C/min

Table 4.4.1.4.4: Thermal Analyses of the BAPHB-Based Polyimides

polyimide	5% wt. loss T (°C)*	T_g (°C)**	T_m (°C)***
BAPHB-PMDA-PA	454	-	-
BAPHB-BPDA-PA	473	185	-
BAPHB-ODPA-PA	480	160	-

*in air, 10°C/min

**from second heat

***from first heat

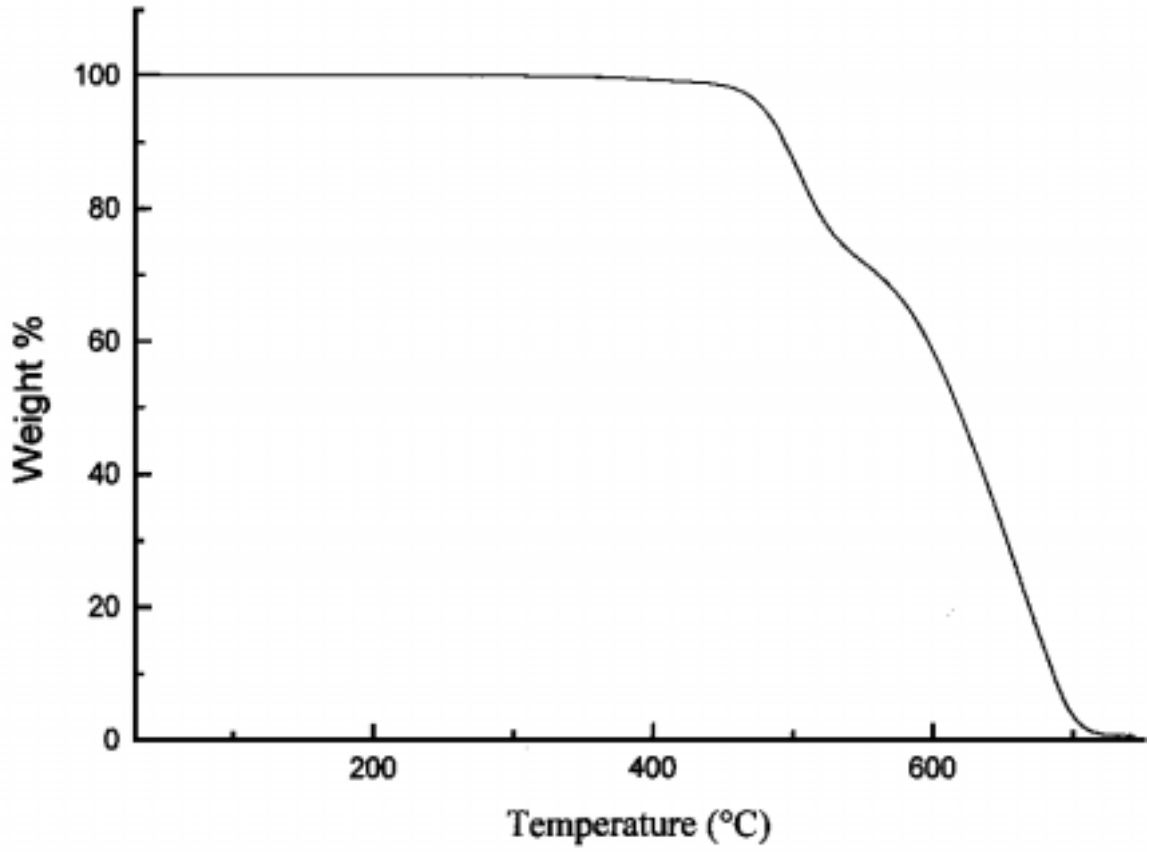

Figure 4.4.1.4.3: TGA Thermogram of BAPHB-ODPA-PA at 10°C/min

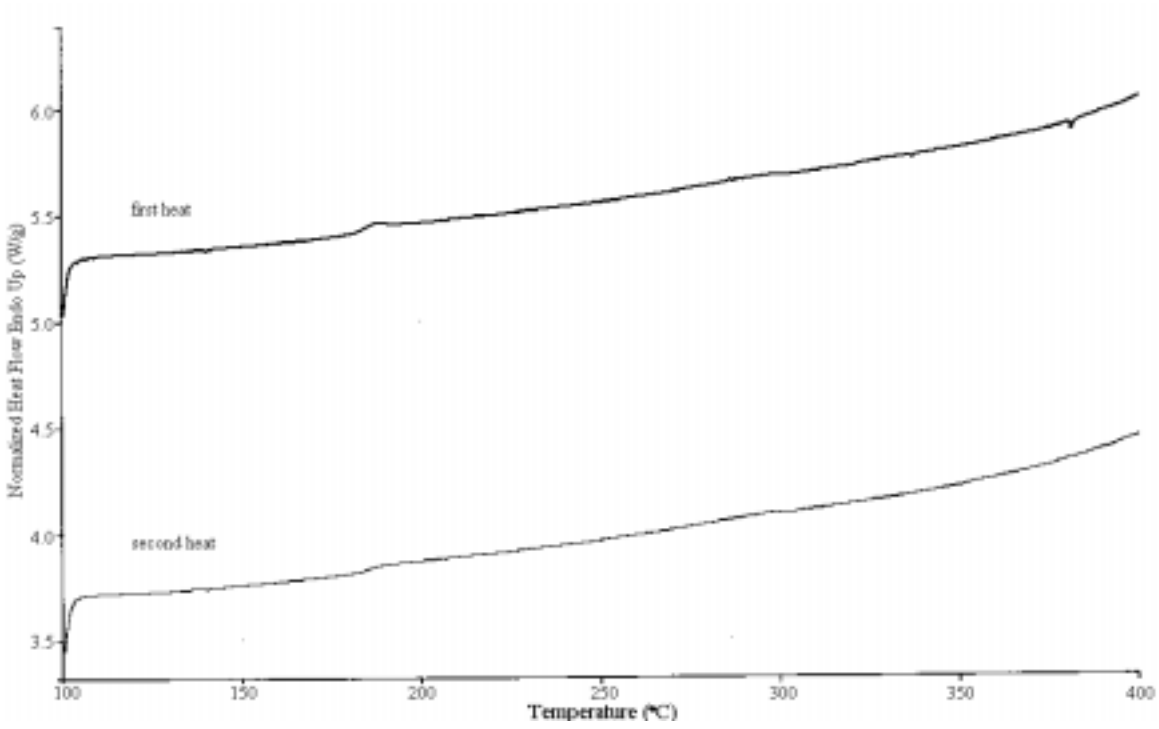

Figure 4.4.1.4.4: DSC Thermograms of BAPHB-BPDA-PA at 10°C/min

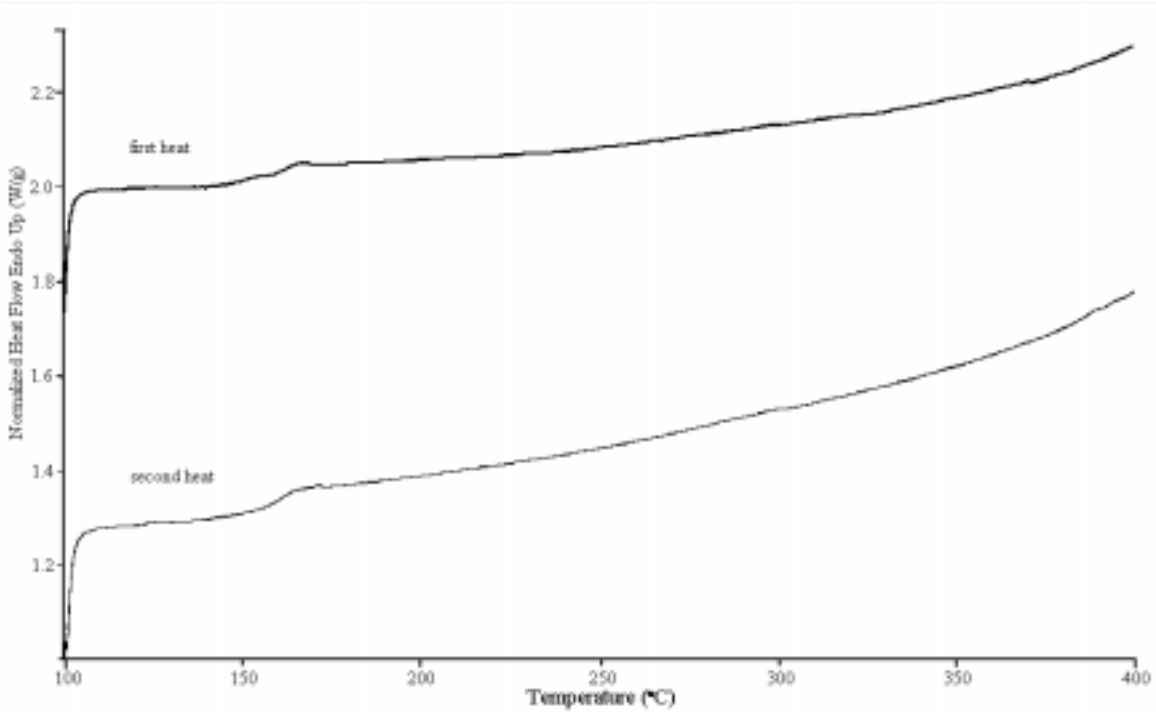

Figure 4.4.1.4.5: DSC Thermograms of BAPHB-ODPA-PA at 10°C/min

Chapter 5: Conclusions

The major thrust of this research was the design, synthesis, and characterization of potentially processable semicrystalline polyimides. This research primarily involved the usage of ether containing diamines. Novel ether diamines with pendant alkyl groups were also prepared and utilized for polyimide synthesis and characterization.

Polyimides derived from 1,4-bis(p-aminophenoxy)benzene, or TPEQ, were synthesized via the classical two step method. Solution imidization of polyamic acid precursors derived from TPEQ and specific rigid dianhydrides produced semicrystalline partially (e.g. 70%) cyclized polyimide powders with mean particle sizes ranging from 2 to 16 μm. These polymers demonstrated good thermooxidative stability as evidenced by 5% weight loss temperatures in excess of 500°C. Up to 450°C, only the polyimide prepared from TPEQ and oxydiphthalic anhydride (ODPA) exhibited thermal transitions. A T_g of 232°C and a T_m of 409°C were observed for this particular system.

Further studies on bulk imidized samples of TPEQ-ODPA indicated that lower molecular weight (e.g., 10K Mn) samples of the polymer possessed the ability to recrystallize from the glass after undergoing rapid quench cooling from the melt. This tendency was observed for samples of molecular weights of less than 15 kg/mole. However, a 15 kg/mole sample of TPEQ-ODPA was annealed to successfully regenerate a significant amount of crystallinity in the polyimide. A 30 kg/mole sample was solvent treated with NMP to also regenerate a relatively large amount of crystallinity. These two latter observations suggested that higher molecular weight samples lack sufficient mobility to recrystallize from the glass after rapid cooling. The effect of melt time and temperature on crystallization and melting was studied on 10 and 12.5 kg/mole samples, and it was discovered that the recrystallizability of the samples decreased with increased time and temperature. The increase in melt viscosity under analogous melt conditions points to a mechanism involving increasing molecular weight during the time in the melt.

Polyimides from 1,3-bis(p-aminophenoxy)benzene, or TPER, were synthesized via the classical two step method. Solution imidization of polyamic acid precursors derived from TPER and specific rigid dianhydrides produces semicrystalline polyimide powders

with mean particle sizes ranging from 13 to 25 μm. These polymers demonstrated good thermooxidative stability as evidenced by 5% weight loss temperatures in excess of 500°C. The polyimides prepared from biphenyl dianhydride (BPDA) and ODPA exhibited thermal transitions up to 450°C. TPER-BPDA displayed a T_g at 233°C and a T_m at 402°C, while TPER-ODPA had a T_g and T_m at 215°C and 335°C, respectively.

Molecular weight measurements were successfully performed on TPER-BPDA amic acids by the direct analysis of the solution from the reaction flask. Good molecular weight agreement with theory was observed for these polymers by quantitative GPC measurements employing a viscosity detector.

The degree of imidization of TPER-BPDA powders prepared by solution imidization was monitored. This entailed measuring the weight loss associated with the cyclodehydration of the polyamic acid to the polyimide. The effect of time of subjection to solution imidization conditions on the degree of imidization was also studied. The polyimide powders in this experiment were estimated to be approximately 65 to70% imidized as justified by isothermal TGA weight losses.

The thermal behavior of bulk imidized samples of TPER-BPDA was investigated in further detail. This particular system demonstrates an extraordinary ability to recrystallize from the melt, even when rapidly cooled from the melt. Furthermore, this is achieved at high molecular weights of 30 kg/mole. The effect of melt time and temperature on crystallization and melting was studied on this polyimide. It was demonstrated that the stability of the polyimide to maintain crystallizability was excellent, as compared to other polyimides investigated, such as lower molecular weight samples of TPEQ-ODPA. The superior stability of TPER-BPDA as opposed to TPEQ-ODPA may be attributable to the presence of the more stable biphenyl linkage in the dianhydride reactant.

The effect of endgroups on the thermal stability of TPER-BPDA was studied utilizing phthalimide endcapped samples, amine terminated samples, and “half” phthalimide endcapped samples. While these samples showed virtually similar TGA weight loss profiles, DSC analysis proved that the crystallizability of the samples from the melt decreased with increasing amounts of amine termination. Corresponding to this, the

melt viscosities associated with these samples increased with increasing amine termination. This implies that the amine terminated samples are susceptible to molecular weight increases in the melt which hinder the polyimide mobility and subsequently the ability to recrystallize.

New pendant alkyl-containing diamines analogous to TPER were synthesized from alkylated resorcinols. The resorcinols were coupled with p-fluoronitrobenzene by aromatic nucleophilic substitution to form dinitro compounds. These compounds were reduced with hydrazine to yield the corresponding diamines.

Polyimides based on these new diamines were prepared by reaction with pyromellitic dianhydride (PMDA), BPDA, and ODPA. The polyimides based upon 1,3-bis(p-aminophenoxy)-4-hexylbenzene (BAPHB) in general demonstrated lower thermooxidative stabilities, lower glass transition temperatures, and improved solubility. BAPHB-BPDA was amorphous, in stark contrast to TPER-BPDA. BAPHB-ODPA was also amorphous. The polyimides based on 2,6- and 3,5-bis(p-aminophenoxy)toluene (2,6-BAPT and 3,5-BAPT) appeared to be semicrystalline.

REFERENCES

1. C. E. Sroog, *J. Polym. Sci.: Macromol. Rev., 11*, 161 (1976)
2. C. E. Sroog, *Prog. Polym. Sci., 16*, 561 (1991)
3. M. I. Bessonov, M. M. Koton, V. V. Kudryavtsev, and L. A. Laius, *Polyimides: Thermally Stable Polymers*, Plenum, New York (1987)
4. *Polyimides*, D. Wilson, H. D. Stenzenberger, and P. M. Hergenrother (eds), Blackie, New York (1990)
5. N. A. Adrova, M. I. Bessonov, L. A. Laius, and A. P. Rudakov, *Polyimides*, Technomic, Stamford, CT (1970)
6. *Polyimides: Synthesis, Characterization, and Applications*, K. L. Mittal (ed.), Plenum, New York (1984)
7. *Polyimides: Materials, Chemistry, and Characterization*, C. Feger, M. M. Khojasteh, and J. E. McGrath (eds.), Elsevier, New York (1989)
8. *Polyimides*, M. K. Ghosh and K. L. Mittal (eds.), Marcel Dekkar, New York (1996)
9. T. M. Bogert and R. R. Renshaw, *J. Am. Chem. Soc., 30*, 1135 (1908)
10. S. Brandt, *J. Prakt. Chem., 4*, 163 (1958)
11. W. M. Edwards and I. M. Robinson, US Patent 2710853 (1955)
12. W. M. Edwards and I. M. Robinson, US Patent 2867609 (1959)
13. W. M. Edwards and I. M. Robinson, US Patent 2880230 (1959)
14. W. M. Edwards, US Patent 3179614 (1965)
15. A. L. Endrey, Can. Patent 659328 (1962)
16. A. L. Endrey, US Patent 3179631 (1965)
17. A. L. Endrey, US Patent 3179633 (1965)
18. C. E. Sroog, A. L. Endrey, S. V. Abramo, C. E. Berr, W. M. Edwards, and K. L. Oliver, *J. Polym. Sci., A3*, 1373 (1965)
19. L. W. Frost and J. Kesse, *J. Appl. Polym. Sci., 8*, 1039 (1964)
20. V. M. Svetlichnyi, K. K. Kalnin'sh, V. V. Kudryavtsev, and M. M. Koton, *Dokl. Akad. Nauk. SSSR (Engl. Trans.), 237*, 693 (1977)
21. K. K. Kalnin'sh, G. I. Solov'eva, B. G. Belen'kii, V. V. Kudryavtsev, and M. M. Koton, *Dokl. Akad. Nauk. SSSR (Engl. Trans.), 204*, 473 (1972)

22. M. J. Breckner and C. Feger, *J. Polym. Sci., Part A: Polym. Chem.*, *25*, 2005 (1987)
23. M. J. Breckner and C. Feger, *J. Polym. Sci., Part A: Polym. Chem.*, *25*, 2479 (1987)
24. M. M. Koton, V. V. Kudriavtsev, and V. M. Svetlichnyi in *Polyimides: Synthesis, Characterization, and Applications*, K. L. Mittal (ed.), Plenum, New York, 1, 171 (1984)
25. V. M. Svetlichnyi, V.V. Kudriavtsev, N. A. Adrova, and M. M. Koton, *Zh. Org. Khim. (Eng. Trans.), 10(9)*, 1907 (1974)
26. M. M. Koton, V.V. Kudriavtsev, N. A. Adrova, K. K. Kalnin'sh, A. M. Dubnova, and V. M. Svetlichnyi, *Polym Sci. USSR., 16(9),* 2411 (1974)
27. S. Ando, T. Matsuura, and S. Nishi, *Polymer, 33(14)*, 2934, (1992)
28. C. E. Sroog, *J. Polym. Sci.*: *Part C, 16*, 1191 (1967)
29. G. M. Bower and L. W. Frost, *J. Polym. Sci.*: *Part A*, *1*, 3135 (1963)
30. W. Volksen and P. M. Cotts in *Polyimides: Synthesis, Characterization, and Applications*, K. L. Mittal (ed.), Plenum, New York, 1, 163 (1984)
31. P. M. Cotts and W. Volksen in *Polymer*s *in Electronics: ACS Symposium Series 242*, T. Davidson (ed.), Washington, DC, 227 (1984)
32. C. C. Walker, *J. Polym. Sci., A26*, 1649 (1988)
33. J. Preston and Y. Tropsha, *Polym. Eng. Sci., 34(4)*, 305 (1994)
34. C. Koning, L. Teuwen, E. W. Meijer, and J. Moonen, *Polymer*, *35(22)*, 4889 (1994)
35. J. J Jones, F. W. Ochynski, and F. A. Rackley, *Chem. Ind.*, 1686 (1962)
36. J. A. Kreuz, , A. L. Endrey, F. P. Gay, and C. E. Sroog, *J. Polym. Sci., A4*, 2607 (1966)
37. C. Sroog, Macromolec. *Syntheses, 3*, 83 (1969)
38. F. W. Harris in *Polyimides*, D. Wilson, H. D. Stenzenberger, and P. M. Hergenrother (eds), Blackie, New York, 1 (1990)
39. W. Volksen, *Adv. Polym. Sci., 117*, 111(1994)
40. V. L. Bell, B. L. Stump, and H. Gager, *J. Polym. Sci., 14*, 2275 (1976)
41. M. Navarre in *Polyimides: Synthesis, Characterization, and Applications*, K. L. Mittal (ed.), Plenum, New York, 1, 429 (1984)

42. D. E. Kranbuehl, S. E. Delos, P. K. Jue, and R. K. Schenllenberg in *Polyimides: Synthesis, Characterization, and Applications*, K. L. Mittal (ed.), Plenum, New York, 1, 207 (1984)
43. S. Numata, K. Fujisaki, and N. Kinjo in *Polyimides: Synthesis, Characterization, and Applications*, K. L. Mittal (ed.), Plenum, New York, 1, 259 (1984)
44. E. Pyun, R. J. Mathisen, and C. S. P. Sung, *Macromolecules*, *22*, 1174 (1989)
45. D. R. Ray and S. D. Senturia in *Polyimides: Synthesis, Characterization, and Applications*, K. L. Mittal (ed.), Plenum, New York, 1, 249 (1984)
46. M. F. Grenier-Loustalot, F. Joubert, and P. Grenier, *J. Polym. Sci., Part A: Polym. Chem.*, *29*, 1649 (1991)
47. C. Johnson and S. L. Wunder, *J. Polym. Sci., Part B: Polym. Phys.*, *31*, 677 (1993)
48. W. Volksen in *Recent Advances in Polyimide Science and Technology*, W. D. Weber and M. R. Gupta (eds.), Society of Plastic Engineers, Poughkepsie, NY, 102 (1987)
49. L. A. Laius, M. I. Bessonov, Y. V. Kallistova, N. A. Adrova, and F. S. Florinskii, *Polym. Sci. USSR, A9(10)*, 2470 (1967)
50. L. A. Laius and M. I. Tsapovetskii in *Polyimides: Synthesis, Characterization, and Applications*, K. L. Mittal (ed.), Plenum, New York, 1, 295 (1984)
51. R. Ginsburg and J. R. Susko in *Polyimides: Synthesis, Characterization, and Applications*, K. L. Mittal (ed.), Plenum, New York, 1, 237 (1984)
52. L. A. Laius, M. I. Bessonov, and F. S. Florinski, *Vysokomol. Soyed, A13(9)*, 2006 (1971)
53. R. W. Snyder, B. Thompson, B. Bartges, D. Czerniawski, and P. C. Painter, *Macromolecules*, *22*, 4166 (1989)
54. P. M. Cotts, N. Nishioka, and S. A. Swanson in Proceedings from the Workshop on Recent Advances in *Polyimides* and Other High Performance *Polymer*s, ACS, Reno, NV (1987)
55. P. M. Cotts, *Org. Coatings Appl. Polym. Sci. Proc.*, *48*, 278 (1983)
56. M. I. Tsapovetskii, L. A. Laius, M. I. Bessonov , and M. M. Koton, *Dokl. Akad. Nauk. SSSR (Engl. Trans.)*, *240*, 732 (1978)
57. P. R. Young and A. C. Chang, *SAMPE Prepr.*, *30*, 889 (1985)

58. P. R. Young, J. R. J. Davis, A. C. Chang, and J. N. Richardson, *J. Polym. Sci., Part A: Polym. Chem., 28*, 3107 (1990)
59. P. R. Young and A. C. Chang, *SAMPE J., 22*, 70 (1986)
60. E. Sacher, *J. Macromo. Sci., Phys., 25(4)*, 405 (1986)
61. P. Hermans and J. Streef, *Makromol. Chem., B3*, 74 (1964)
62. Y. J. Kim, T. E. Glass, G. D. Lyle, and J. E. McGrath, *Macromolecules*, *26*, 1344 (1993)
63. C. A. Pryde, J. Polym. Sci, *Part A: Polym. Chem.*, *27*, 711 (1989)
64. R. A. Dine-Hart and W. W. Wright, *J. Appl. Polym. Sci.*, *11*, 609 (1967)
65. S. V. Vinogradova, V. V. Korshak, and Y. Vygodskii, *Polym. Sci. USSR*, *8*, 888 (1966)
66. S. V. Vinogradova, Y. Vygodskii, V. V. Korshak, N. A. Churochkina, D. R. Tur, and V. G. Danilov , *Polym. Sci. USSR*, *13*, 1695 (1971)
67. W. J. Farrisey and P. S. Andrews, US Patent 3787367 (1964)
68. W. J. Farrisey and P. S. Andrews, US Patent 3870677 (1975)
69. F. W. Harris and L. H. Lanier in *Structure-Solubility Relationships in Polymer*s, F. W. Harris and R. B. Seymour (eds.), Academic Press, New York, 183 (1977)
70. J. Bateman and D. A. Gordon, US Patent 3856752 (1974)
71. S. V. Vinogradova, Y. S. Vygodskii, and V. V. Korshak, *Polym. Sci. USSR, 12*, 2254 (1970)
72. J. E. McGrath, M.E. Rogers, C. A. Arnold, Y. J. Kim, and J. C. Hedrick, *Makromol. Chem., Macromol. Symp., 51*, 103 (1991)
73. J. D. Summers, PhD Dissertation, Virginia Tech (1988)
74. B. C. Johnson, PhD Dissertation, Virginia Tech (1984)
75. T. Lin, K. W. Stickney, M. Rogers, J. S. Riffle, J. E. McGrath, H. Marand, T. H. Yu, and R. M. Davis, *Polymer*, *34*, 722 (1993)
76. C. A. Arnold, J. D. Summers, Y. P. Chen, R . H. Bott, D. Chen, and J. E. McGrath, *J. Thermoplas. Compos. Mater., 3(1)*, 4 (1990)
77. M. M. Koton, T. K. Meleshko, V. V. Duryavtsev, P. P. Nechayev, Y. V. Kamzolkina, and N. N. Bogorad, *Polym. Sci. USSR, 24*, 791 (1982)

78. R. J. Angelo, R. C. Golike, W. E. Tatum, and J. A. Kreuz in *Recent Advances in Polyimide Science and Technology*, W. D. Weber and M. R. Gupta (eds.), Society of Plastic Engineers, Poughkeepsie, New York, 67 (1987)
79. W. R. Roderich, *J. Org. Chem.*, 29, 745 (1964)
80. P. M. Cotts in *Polyimides: Synthesis, Characterization, and Applications*, K. L. Mittal (ed.), Plenum, New York, 1, 223 (1984)
81. M. L. Wallach, *J. Polym. Sci., A-2*, 953 (1968)
82. Beck & Co., French Pat. 1373383 (1964)
83. S. V. Vinogradova, G. L. Slonimskii, Y. S. Vygodskii, A. A. Askadskii, A. I. Mzhel'skii, N. A. Churochkina, and V. V. Korshak, *Polym. Sci. USSR, 11(12)*, 3098 (1969)
84. S. V. Vinogradova, Y. S. Vygodskii, and V. V. Korshak, *Polym. Sci. USSR, 12(9)*, 2254 (1970)
85. F. W. Harris and S. L. C. Hsu, *High Perform. Polym.*, *1*, 3 (1989)
86. F. W. Harris, W. A. Feld, and L. H. Lanier in *Applied Polymer Symposium No. 26*, N. Platzer (ed.), Wiley, New York, 421 (1975)
87. F. W. Harris, S. O. Norris, L. H. Lanier, B. A. Reinhardt, R. D. Case, S. Varaprath, S. M. Padaki, M. Torres, and W. A. Feld in *Polyimides: Synthesis, Characterization, and Applications*, K. L. Mittal (ed.), Plenum, New York, 1, 3 (1984)
88. S. Z. D. Cheng, F. E. Arnold, A. Zhang, D. Shen, J. Y. Park, C. J. Lee, and F. W. Harris, *Polym. Prep.*, *33*, 313 (1992)
89. S. Z. D. Cheng, Z. Wu, M. Eashoo, S. L. Hsu, and F. W. Harris, *Polymer*, *32*, 1803 (1991)
90. M. Tomikawa, S. Z. D. Cheng, and F. W. Harris, *Polym. Prep.*, *36(1)*, 707 (1995)
91. F. W. Harris, Y. Sakaguchi, M. Shibata, and S. Z. D. Cheng, *High Perform. Polym.*, *9(3)*, 251 (1997)
92. F. W. Harris, F. Li, S. H. Lin, J. Chen, and S. Z. D. Cheng, *Macromol. Symp.*, *122*, 33 (1997)
93. S. H. Lin, F. Li, S. Z. D. Cheng, and F. W. Harris, *Macromolecules*, *31(7)*, 2080 (1998)

94. H. R. Lubowitz, US Patent 3528950 (1970)
95. H. R. Lubowitz, *Polym. Prep., 12*, 329 (1971)
96. M. Fryd and B. T. Merriman, US Patent 4533574 (1985)
97. T. M. Moy, PhD Dissertation, Virginia Tech (1993)
98. T. M. Moy, C. D. DePorter, and J. E. McGrath, *Polymer*, *34(4)*, 819 (1993)
99. Y. Imai, *Polym. Prep., 35(1)*, 399 (1994)
100. K. Itoya, Y. Kumagai, M. Kakimoto, and Y. Imai, *Polym. Prep. Jpn., 41*, 355 (1992)
101. K. Itoya, Y. Kumagai, M. Kakimoto, and Y. Imai, *Polym. Prep. Jpn., 41*, 2131 (1992)
102. K. Itoya, Y. Kumagai, M. Kakimoto, and Y. Imai, *Polym. Prep. Jpn., 42*, 2109 (1993)
103. T. Takekoshi, J. G. Wirth, D. R. Heath, J. E. Kodhznowski, J. S. Manello, and M. J. Webber, *J. Polym. Sci., Polym. Chem. Ed., 18*, 3069 (1980)
104. T. Takekoshi in *Polyimides*, D. Wilson, H. D. Stenzenberger, and P. M. Hergenrother (eds), Blackie, New York, 38 (1990)
105. T. Takekoshi in *Polyimides*, M. K. Ghosh and K. L. Mittal (eds.), Marcel Dekker, 7 (1996)
106. R. N. Johnson, A. G. Farnham, R. A. Clendinning, W. F. Hale, and C. Merriam, *J. Polym. Sci.,* A-*1(5),* 2375 (1967)
107. T. E. Attwood, P. C. Dawson, J. L. Freeman, L. R. J. Hoy, J. B. Rose, and P. A. Staniland, *Polymer*, *22*, 1096 (1981)
108. H. M. Colqhoun and D. F. Lewis, *Polymer*, *29*, 1902 (1988)
109. M. J. Mullins and E. P. Woo, *Rev. Macromol. Chem. Phys., C-27*, 313 (1987)
110. R. May in *Encyclopedia of Polymer Science and Engineering*, 2nd ed., J. L. Kroschwitz (ed.), Wiley, New York, 12, 313 (1988)
111. M. Davies, J. N. Hay, and B. Woodfine, *High Perform. Polym., 5*, 37 (1993)
112. H. R. Kricheldorf and R. Pakull, *Polymer*, *28*, 1772 (1987)
113. M. Sato, T. Hirata, T. Kamita, and K. Makaida, *Eur. Polym. J., 32(5),* 639 (1996)
114. M. Sato, T. Hirata, and K. Makaida, *Makromol. Chem. Phys., 193*, 1729 (1992)
115. T. Hirata, M. Sato, and K. Makaida, *Makromol. Chem. Phys., 194*, 2861 (1993)

116. T. Hirata, M. Sato, and K. Makaida, *Makromol. Chem. Phys.*, *195*, 1611 (1994)
117. T. Hirata, M. Sato, and K. Makaida, *Makromol. Chem. Phys.*, *195*, 2267 (1994)
118. Neth. Pat. Appl. 6413552 (1965)
119. Y. Imai, *J. Polym. Sci., Polym. Let., 8*, 555 (1970)
120. T. Takekoshi, US Patent 384870 (1974)
121. T. Takekoshi and E. J. Kochanowski, US Patent 3850885 (1974)
122. M. E. Rogers, PhD Thesis, Virginia Tech (1993)
123. M. E. Rogers, T. E. Glass, S. J. Mecham, D. Rodrigues, G. L. Wilkes, and J. E. McGrath, *J. Polym. Sci., Part A: Polym. Chem.*, *32*, 2663 (1994)
124. P. S. Carleton, W. J. Farrisey, and J. S. Rose, *J. Appl. Polym. Sci.*, *16*, 2893 (1972)
125. L. S. Tan and F. E. Arnold, *J. Polym. Sci., Part A: Polym. Chem.*, *26*, 1819 (1988)
126. R. J. Perry, S. R. Turner, and R. W. Blevins, *Macromolecules*, *27*, 4058 (1994)
127. R. J. Perry, S. R. Turner, and R. W. Blevins, *Macromolecules*, *26*, 1509 (1993)
128. R. J. Perry, and S. R. Turner, J. Macromol. Sci., *A-28*, 1213 (1991)
129. C. E. Sroog in *Applications of High Temperature Polymer*s, R. R. Luise (ed.), CRC Press, Boca Raton, 99 (1997)
130. S. Tamai, A. Yamaguchi, and M. Ohta, *Polymer*, *37(16)*, 3683 (1996)
131. A. Rudin in *The Elements of Polymer Science and Engineering*, Academic Press, Orlando (1982)
132. F. W. Billmeyer, Jr. in *Textbook of Polymer Science*, 3rd ed., Wiley, New York (1984)
133. D. A. Scola, R. A. Pike, J. H. Vontelli, and C. M. Brunette, *High Perform. Polym.*, *1(1)*, 17 (1989)
134. T. Takekoshi, *Adv. Polym. Sci.*, *94*, 1 (1990)
135. T. L. St. Clair and A. K. St. Clair, *J. Polym. Sci., Polym. Chem. Ed.*, *15*, 1529 (1977)
136. T. L. St. Clair and A. K. St. Clair, US Patent 4180648 (1979)
137. D. J. Progar, V. L. Bell, and T. L. St. Clair, US Patent 4065345 (1977)
138. V. L. Bell, US Patent 4094862 (1978)
139. A. K. St. Clair, L. T. Taylor, and T. L. St. Clair, US Patent 4284461 (1981)

140. A. K. St. Clair and T. L. St. Clair, US Patent 4543295 (1985)

141. T. H. Hou, N. T. Wakelyn, and T. L. St. Clair, *J. Appl. Polym. Sci.*, *36*, 1731 (1988)

142. T. L. St. Clair, H. D. Burks, N. T. Wakelyn, and T. H. Hou, *Polym. Prep., 28(1)*, 90 (1987)

143. J. Wang, A. T. DiBenedetto, J. F. Johnson, S. J. Huang, and J. L. Cercena, *Polymer*, *30*, 719 (1985)

144. P. M. Hergenrother, N. T. Wakelyn, and S. J. Havens, *J. Polym. Sci., Part A: Polym. Chem., 25*, 1093 (1987)

145. P. M. Hergenrother and S. J. Havens, *J. Polym. Sci., Part A: Polym. Chem., 27*, 1161 (1989)

146. P. M. Hergenrother, M. W. Beltz, and S. J. Havens, *J. Polym. Sci., Part A: Polym. Chem., 29*, 1483 (1991)

147. S. J. Havens and P. M. Hergenrother, *J. Polym. Sci., Part A: Polym. Chem., 30*, 1209 (1992)

148. P. M. Hergenrother in *Polyimides*, D. Wilson, H. D. Stenzenberger, and P. M. Hergenrother (eds), Blackie, New York, 158 (1990)

149. D. K. Brandom and G. L. Wilkes, *Polymer, 35(26)*, 5672 (1994)

150. D. K. Brandom and G. L. Wilkes, *Polymer, 36(21)*, 4083 (1995)

151. J. R. Pratt, T. L. St. Clair, M. K. Gerber, and C. R. Gautreaux in *Polyimides: Materials, Chemistry, and Characterization*, C. Feger, M. M Khojasteh, and J. E. McGrath (eds.), Elsevier Science, New York, 193 (1989)

152. C. R. Gautreaux, J. R. Pratt, and T. L. St. Clair, *J. Polym. Sci., Part B: Polym. Phys., 30*, 71 (1992)

153. A. Yamaguchi and M. Ohta in *Proceedings 18th Interna. SAMPE Tech. Conf.*, 229, (1986)

154. S. Tamai, US Patent 5288843 (1994)

155. Mitsui Toatsu Chem., Inc., *Technical Data Sheet/ A00, Tokyo*, Japan.

156. T. H. Hou and R. M. Reddy, *SAMPE Quarterly, 22(2)*, 38 (1991)

157. P. P. Huo and P. Cebe, *Polymer, 34(4)*, 696 (1993)

158. P. P. Huo, J. B. Friler, and P. Cebe, *Polymer, 34(21)*, 4387 (1993)

159. B. S. Hsia, B. B. Sauer, and A. Biswas, *J. Polym. Sci., Part B: Polym. Phys., 32*, 737 (1994)
160. T. Takekoshi and P. R. Anderson, US Patent 4599396 (1986)
161. T. Takekoshi and P. R. Anderson, US Patent 4716216 (1987)
162. T. P. Gannett, R. J. Kassal, and R. S. Rou, US Patent 4725642 (1988)
163. T. P. Gannett, H. H. Gibbs, and R. J. Kassal, US Patent 4485140 (1984)
164. T. P. Gannett and H. H. Gibbs, US Patent 4576857 (1986)
165. M. E. Rogers, M. H. Brink, J. E. McGrath, and A. Brennan, *Polymer, 34(4)*, 849 (1993)
166. M. H. Brink, D. K. Brandom, G. L. Wilkes, and J. E. McGrath, *Polymer, 35(23)*, 5018 (1994)
167. C. C. Fay, J. G. Smith, and T. L. St. Clair, *Polym. Prep., 35(1)*, 541 (1994)
168. F. W. Harris and H. S. Lien, *Polym. Mat. Sci. Eng., 60*, 197 (1988)
169. C. Cururas, Masters Thesis, University of Akron (1987)
170. S. Z. D. Cheng, D. P. Heberer, H. S. Lien, and F. W. Harris, *J. Polym. Sci., Part B: Polym. Phys., 28*, 655 (1990)
171. S. Z. D. Cheng, D. P. Heberer, J. J. Janimak, H. S. Lien, and F. W. Harris, *Polymer, 32(1)*, 2053 (1991)
172. D. P. Heberer, S. Z. D. Cheng, J. S. Barley, H. S. Lien, R. G. Bryant, and F. W. Harris, *Macromolecules, 24(8)*, 1890 (1991)
173. S. Z. D. Cheng, M. L. Mittleman, J. J. Janimak, D. X. Shen, T. M. Chalmers, H. S. Lien, C. C. Tso, P.A. Gabori, and F. W. Harris, *Polym. Int. , 29*, 201 (1992)
174. T. M. Chalmers, A. Q. Zhang, D. X. Shen, H. S. Lien, C. C. Tso, P.A. Gabori, F. W. Harris, and S. Z. D. Cheng, *Polym. Int. , 31*, 261 (1993)
175. S. Z. D. Cheng, T. M. Chalmers, Y. Gu, Y. Yoon, and F. W. Harris, *Macromol. Chem. Phys., 196*, 1439 (1995)
176. H. Ishida and M. T. Huang, *J. Polym. Sci., Part B: Polym. Phys., 32*, 2271 (1994)
177. H. R. Kricheldorf and V. Linzer, *Polymer, 36(9)*, 1893 (1995)
178. T. Inuoe, M. Kakimoto, and Y. Imai, *Macromolecules, 28*, 6368 (1995)
179. K. Itoya, Y. Kumagai, M. Kakimoto, and Y. Imai, *Macromolecules, 27*, 4101 (1994)

180. T. Inuoe, Y. Kumagai, M. Kakimoto, Y. Imai, and J. Watanabe, *Macromolecules*, *30*, 1921 (1997)

181. C. E. Koning, L. Teuwen, A. De Plaen, and J. P. Mercier, *Polymer, 37(25)*, 5619 (1996)

182. Y. Nagata, Y. Ohnishi, T. Kajiyama, *Polym. J., 28(11)*, 980 (1996)

183. M. H. Brink, PhD Dissertation, Virginia Tech (1994)

184. A. L. Endrey, US Patent 3179631 (1965)

185. R. A. Dine-Hart and W. W. Wright, *Makromol. Chem., 143*, 186 (1971)

186. B. Jensen and P. R. Young in *Polyimides: Synthesis, Characterization, and Application*, K. L. Mittal (ed.), Plenum, New York, 1, 417 (1984)

187. F. Helmer-Metzmann, M. Rehahn, L. Schmitz, M. Ballauf, and G. Wegner, *Makromol. Chem., 193*, 1847 (1992)

188. D. Ayala, A. E. Lozano, J. G. de la Campa, and J. de Abajo, *Polym. Prep, 38(2)*, 359 (1997)

189. E. Moyer, D. K. Mohanty, C. A. Arnold, and J. E. McGrath, *Polym. Mater. Sci. Eng., 60*, 202 (1989)

190. D. R. Heath and J. G. Wirth, US Patent 3847867 (1974)

191. F. J. Williams and P. E. Donahue, US Patent 3983093 (1975)

192. T. Takekoshi and J. E. Kochanowski, US Patent 3905942 (1975)

193. J. L. Webb, German Patent DE3212163 A1 (1982)

194. M. Matzner and D. M. Papuga, US Patent 45040748 (1985)

195. E. R. Peters, Eur. Pat. Applic. 0117416 A1 (1984)

196. P. E. Howson, US Patent 4769476 (1988)

197. R. A. Hayes, US Patent 4717394 (1988)

198. T. Matsuura, M. Ishizawa, Y. Hasuda, and S. Nishi, *Macromolecules, 25*, 3540 (1992)

199. M. Langsam in *Polyimides*, M. K. Ghosh and K. L. Mittal (eds.), Marcel Dekker, 697 (1996)

200. F. W. Harris, S. H. Lin, F. Li, and S. Z. D. Cheng, *Polymer, 37(22)*, 5049 (1996)

201. B. C. Auman, D. P. Higley, and K. V. Scherer, *Polym. Prep., 34(1)*, 389 (1993)

202. D. J. Liaw and B. Y. Liaw, *Polym. J., 28(11)*, 970 (1996)

203. D. J. Liaw and B. Y. Liaw, *J. Polym. Sci., Part A: Polym. Chem., 35(8)*, 1527 (1997)

204. H. Yagci and L. J. Mathias, *Polymer, 39(16)*, 3779 (1998)

205. D. J. Liaw, B. Y. Liaw, and M. Q. Jeng, *Polymer*, *39(8)*, 1597 (1998)

206. K. H. Becker and H. W. Schmidt, *Polym. Mater. Sci. Eng., 66*, 303 (1992)

207. W. Chiang and W. Mei, *Angew. Makromol. Chem.*, *214*, 57 (1994)

208. J. Pfeifer and O. Rohde, *Proceedings of the 2nd International Conference on Polyimides*, 130 (1985)

209. A. A. Lin, V. R. Sastri, G. Tesoro, A. Reiser, and R. Eachus, *Macromolecules*, *21*, 1165 (1988)

210. W. Chiang and W. Mei, *J. Polym. Sci.,Part A: Polym. Chem., 31*, 1195 (1993)

211. J. Pfeifer, US Patent 4629777 (1986)

212. O. M. Ekiner and J. W. Simmons, US Patent 5248319 (1993)

213. R. A. Hayes, US Patent 5322549 (1994)

214. R. A. Hayes, US Patent 4932983 (1990)

215. R. A. Hayes, US Patent 4705540 (1987)

216. R.A. Hayes, US Patent 4838900 (1989)

217. R. A. Hayes, US Patent 4717393 (1988)

218. J. Pfeifer and O. Rohde in *Recent Advances in Polyimide Science and Technology*, W. D. Weber and M. R. Gupta (eds.), Society of Plastic Engineers, Poughkepsie, NY, 336 (1987)

219. Y. Li, M. Ding, and J. Xu, *J. Memb. Sci.-Pure Appl. Chem., A34(3)*, 461 (1997)

220. G. C. Eastmond, P. C. B. Page, J. Paprotny, R. E. Richards, and R. Shaunak, *Polymer*, *35(19)*, 4215 (1994)

221. S. M. Korneev and V. A. Nikolev, *J. Org. Chem.*, USSR, 26(8),1493 (1990)

222. M. Konas, T. M. Moy, M. E. Rogers, A. R. Shultz, T. C. Ward, and J. E. McGrath, *J. Polym. Sci. Part B: Polym. Phys., 33*, 1429 (1995)

223. Slade Gardner, PhD Dissertation, Virginia Tech (1998)

224. S. Srinivas, PhD Dissertation, Virginia Tech (1996)

225.G. Odian, *Principles in Polymerization*, 3rd edition, Wiley (1991)

226. D. E. Hirt, J. M. Marchello, and R. M. Baucom, Int. SAMPE Symp., 22, 360 (1990)

227. R. M. Baucom and J. M. Marchello, Int. SAMPE Symp., 36, 175 (1990)

228. T. M. Towell, D. E. Hirt, and N. J. Johnston, Int. SAMPE Symp., 22, 1156 (1990)

229. M. Ohta, S. Tamai, T. W. Towell, N. J. Johnston, and T. L. St. Clair, Int. SAMPE Symp., 25, 1030 (1990)

230. D. F. Hiscock and D. M. Bigg, Polym. Comp., 10, 3 (1989)

231. J. Muzzy, B. Varughese, and P. H. Yang, Int. SAMPE Symp., 36, 1523 (1991)

232.T. L. St. Clair in *Symposium on Recent Advances in Polyimides and Other High Performance Polymers*, Reno, Nevada (1987)

233. H. H. Gibbs, *J. Appl. Polym. Sci.(Appl. Polym. Symp.), 35*, 207 (1979)

234. M. J. Graham, S. Srinivas, A. Ayambem, V. Ratta, G. L. Wilkes, and J. E. McGrath, *Polym. Prep., 38(1)*, 306 (1997)

235. S. Srinivas, M. Graham, M. H. Brink, S. Gardner, J. E. McGrath, R. M. Davis, and G. L. Wilkes, *Polym. Eng. Sci., 36*, 1928 (1996)

236. S. Srinivas, F. E. Caputo, M. Graham, S. Gardner, R. M. Davis, J. E. McGrath, and G. L. Wilkes, *Macromolecules*, *30*, 3012 (1997)

237. M. J. Graham, S. Srinivas, G. L. Wilkes, and J. E. McGrath, *Polym. Prep., 37(1)*, 485 (1996)

238. J. A. Kreuz, B. S. Hsiao, C. A. Renner, and D. L. Goff, *Macromolecules*, *28*, 6926 (1995)

239. J. B. Friler and P. Cebe, *Polym. Eng. Sci., 33*, 587 (1993)

240. M. V. Brillhart and P. Cebe, *J. Polym. Sci., Part B: Polym. Phys., 33*, 927 (1995)

241. S. X. Lu, P. Cebe, and M. Capel, *J. Appl. Polym. Sci., 57*, 1359 (1995)

242. J. J. Dumais, A. L. Cholli, L. W. Jelinski, J. L. Hedrick, and J. E. McGrath, *Macromolecules*, *19*, 1884 (1986)

243. V. Ratta, E. J. Stancik, A. Ayambem, H. Parvatareddy, J. W. McGrath, and G. L. Wilkes, *Polymer*, in press.

244. D. A. Scola, R. A. Pike, J. H. Vontell, J. P. Pinto, and C. M. Brunette in *Polyimides: Materials, Chemistry, and Characterization*, C. Feger, M. M Khojasteh, and J. E. McGrath (eds.), Elsevier Science, New York, 293 (1989)

245. P. J. Halfpenny, P. J. Johnson, M. J. Robinson, and M. G. Ward, *Tetrahedron*, 32(6), 1873 (1976)

VITA

Marvin Jerome Graham was born in Newport News, Virginia on October 14, 1971. In June 1989, he graduated from Denbigh High School. He would begin his studies in chemistry later that year at the University of Virginia. In the summer of 1992, he was able to participate in a summer undergraduate research program at Virginia Polytechnic Institute and State University under the tutelage of Dr. James E. McGrath. While there, he assisted research efforts involving polyimide siloxane copolymers. He graduated with a Bachelor of Science degree in chemistry in May 1993 and was acknowledged as a GEM Fellow by the National Consortium for Graduate Degrees for Minorities in Engineering and Science, Inc.

After graduating, Marvin held a summer internship at Union Carbide in South Charleston, West Virginia. Then in August 1993, he began his advanced degree studies back at Virginia Polytechnic Institute, again under the guidance of Dr. McGrath. The topic of his doctoral research focused on the development of processable semicrystalline polyimides. In the summer of 1996, he served as an intern at BF Goodrich in Brecksville, Ohio. He has recently accepted a position as a senior research chemist at PPG Industries in Monroeville, PA.